REFERENCE ONLY

UNIVERSITY OF LONDON THESIS

Degree **Pho**   Year **2005**   Name of Author **DURGAWI J**

Protein Kinase C -

Binding Partners &

Phosphorylation

Joanne Durgan

This thesis is submitted in partial fulfillment
of the requirements for the degree of
Doctor of Philosophy
Biochemistry

University College London
University of London

September 2005

Cancer Research UK
London Research Institute
44 Lincoln's Inn Fields
London WC2A 3PX

1

UMI Number: U591954

UMI

Dissertation Publishing

UMI U591954

ProQuest

Abstract

Protein Kinase C (PKC) comprises a family of phospholipid-dependent Ser/Thr kinases, implicated in a broad array of cellular processes. PKC activity is subject to a complex network of regulatory inputs, including co-factor binding, phosphorylation and protein-protein interaction. In addition, the chronic activation of PKC frequently leads to its down-regulation; this process may be intrinsic to the tumour promoting activity of the phorbol esters. The aim of this work was to investigate the regulation of the novel PKC-ε isoform by binding partners and phosphorylation, with a particular focus on the process of agonist-induced degradation.

A yeast 2-hybrid screen was performed using a PKC-ε bait and two novel binding partners were identified, both with associations to the ubiquitin/proteasome system; VHL Binding Protein 1 (VBP1) and F-box WD40 protein 7 (Fbw7). Interactions were verified in mammalian cells and mapped to the catalytic domain of PKC-ε. Extensive studies revealed that neither partner influenced the process of PKC-ε down-regulation. However, Fbw7α was demonstrated to represent an *in vitro* PKC substrate. The site of phosphorylation was mapped to Ser-18 and, using phospho-specific antibodies, was shown to be phosphorylated in the cell.

PKC-ε activity is required for its agonist-induced degradation. Studies were therefore undertaken to investigate autophosphorylation, which may be implicated in this process. Serine residues 234, 316 and 368 were identified as novel PKC-ε autophosphorylation sites. Using phospho-specific antibodies, all three sites were shown to be occupied in response to PKC-ε activation. Phosphorylation at these sites was found not to influence agonist-induced PKC-ε down-regulation. However, a critical

2

role was established for phosphorylated Ser-368, in the recruitment of the PKC-ε binding partner, 14-3-3β.

Together these findings provide insight into the mechanisms controlling PKC-ε activity and demonstrate a relationship between regulation through phosphorylation and protein-protein interaction.

Acknowledgements

First and foremost, I'd like to thank Peter for giving me the opportunity to work in his lab and for being such a great boss; his approach to science and endless enthusiasm is really remarkable. I'm also very grateful to Richard, Phil, Tony, Mark and Jo for keeping the lab running so smoothly, and to all of the CR-UK research support staff who have helped during my PhD. In particular, I'd like to mention Nick Totty and his lab for all their assistance.

A big thank you goes to all members of the Parker lab, both past and present, who have made my PhD such a great experience; I've had a brilliant time and learnt a lot by working alongside such fantastic colleagues. I'm especially grateful to Ade for all his advice and encouragement, Xabi for lots of help and entertainment, Johanna for her guidance when I first joined the lab, Angus and Amir, who have been great collaborators and Manu, for reading through my thesis. I'd also like to mention Neil, Amy, Jef, Harold, Shippy, Adele, Sylvie, Steph, Paqui, and Veerle for making the lab such an enjoyable place to be.

My final acknowledgements go to my friends and family; to Oli for lots of love, encouragement and scientific discussion, and to my Mum, Dad and brother Jim for their constant support.

Table of Contents

Table of Figures

CHAPTER 5 Identification of Novel PKC-ε/δ Phosphorylation Sites

CHAPTER 6 Characterisation of PKCε Phospho-Site Mutants

Table of Tables

Abbreviations

Å	angstroms
AD	GAL4 transcriptional activation domain
Ala	alanine
aPKC	atypical PKC
Arg	arginine
Asp	aspartate
ATP	adenosine triphosphate
BIM1	bisindoylmaleimide 1
bps	base pairs
BSA	bovine serum albumin
°C	degrees centigrade
cfu	colony forming units
Ci	curies
CNS	central nervous system
cPKC	classical PKC
cpm	counts per minute
CSM	complete supplemented medium
Da	daltons
DAG	diacylglycerol
DMSO	dimethyl sulphoxide
DNA	deoxyribonucleic acid
DNA-BD	GAL4 DNA binding domain
EDTA	ethylene diamine tetra-acetic acid
EGF	epidermal growth factor
EtOH	ethanol
F	forward
Fbw	F-box WD40 protein
FCS	foetal calf serum
g	grams
g (rcf)	relative centifugal force

GFP	green fluorescent protein
Glu	glutamate
GST	glutathione S-transferase
HIF-1α	hypoxia inducible factor-1α
hrs	hours
IB	immunoblot
IF	immunofluorescence
IP	immunoprecipitation
J	joules
k	kilo
kb	kilobase
l	litres
Lys	lysine
M	molar
m	milli
μ	micro
MBP	myelin basic protein
MEF	mouse embryonic fibroblast
mins	minutes
MAPK	mitogen activated protein kinase
n	nano
nPKC	novel PKC
OD	optical density
ORF	open reading frame
p	pico
PAGE	polyacrylamide gel electrophoresis
PBS	phosphate buffered saline
PCR	polymerase chain reaction
PDGF	platelet derived growth factor
PI-3 Kinase	phosphatidylinositol-3-OH kinase
PKC	Protein Kinase C
PKN	Protein Kinase Novel (formerly referred to as PRK)
PD	pull-down

18

PFD	prefoldin
Pro	proline
PS	phosphatidylserine
R	reverse
RFP	red fluorescent protein
rpm	revolutions per minute
RT	room temperature
s	sedimentation coefficient
SCF	Skp1/Cullin/F-box
secs	seconds
Ser	serine
Thr	threonine
Tm	melting temperature
TPA	12-O-tetradecanoyl-phorbol-13-acetate
U	unit of activity
Ub	ubiquitin
UTR	untranslated region
UV	ultra-violet radiation
V	volts
VBP1	von Hippel-Lindau interacting protein 1
pVHL	von Hippel-Lindau gene product
WB	western blotting
w/v	weight/volume
v/v	volume/volume
x	times

CHAPTER 1

Introduction

1.1 Cell Signalling

1.1.1 Cellular Communication

An essential requirement for all cells is the ability to interpret environmental cues and respond appropriately. Single-celled organisms must be able to sense the availability of nutrients and, in some cases, communicate with other cells to facilitate mating. Within metazoans, bi-directional cellular communication is critical in order to coordinate and control the activities of their diverse and specialised constituent cells, thereby maintaining the organism as a whole.

Cell signalling is the means by which this transfer of biological information is mediated; a complex network of signal transduction pathways operate in order to receive, interpret, integrate and respond to extracellular cues. At a cellular level, signalling controls decisions regarding proliferation, differentiation, migration, senescence and death; in more specialised cells it is also central to processes such as the mounting of the immune response and the transmission of nerve impulses. At the level of the whole organism, signalling contributes to the control of growth and development, as well as aspects of metabolism and behaviour (see (Downward, 2001) for a general review).

Given the fundamental role of cell signalling in the control of numerous physiological processes, it is perhaps not surprising that defects in signal transduction pathways underlie a multitude of human diseases. Components of these pathways represent promising targets for the development of novel therapeutics, and thus further elucidation of the mechanisms of cell signalling is an important goal for research.

1.1.2 General Principles of Cell Signalling

Cell signalling is mediated by a bewildering array of different signal transduction pathways. However, despite the obvious diversity, some common mechanisms have evolved. The following describes the general principles of cell signalling and highlights some of the key features of signal transduction pathways (see Figure 1.1).

1.1.2.1 Signal Transduction

The process of signal transduction is initiated with the recognition of a bioactive ligand, which serves to deliver information from the extracellular milieu. Signalling ligands include soluble growth factors, hormones, nitric oxide (Esplugues, 2002) and nutrients (Meijer and Dubbelhuis, 2004), which may be produced locally, or distally and delivered via the bloodstream, as well as insoluble extracellular matrix components, and other cells. Upon binding to their complementary cell surface or intracellular receptors, these ligands induce a change in conformation and/or activity, which facilitates the transmission of the signal into the cell.

A wide variety of receptors exist in order to detect and respond to these diverse signals. The largest family comprises the G-protein coupled receptors, which exhibit tremendous diversity, responding to ions, organic odorants, amines, peptides, proteins, lipids, nucleotides, and even photons (see (Fredriksson et al., 2003) for a review). The receptor tyrosine kinases, which include the receptors for epidermal growth factor (EGF) and insulin, represent another large family (reviewed by (Blume-Jensen and Hunter, 2001)); and yet other receptors are associated with tyrosine kinases, for instance, the cytokine receptors which couple to the Janus Kinases (JAKs) (see (Ihle and Kerr, 1995)). Another class of receptors possess Ser/Thr kinase activity, such as those which respond to the transforming growth factor-β (TGFβ) family (see for a (Massague, 1998) review). Additionally, there are a class of intracellular receptors which recognise soluble signals, for example, the sex hormone receptors (Mangelsdorf et al., 1995). Others comprise ligand gated ion channels, for instance, the nicotinic acetylcholine receptor (McGehee, 1999).

Finally, the integrins (Hynes, 2002) and the cadherins (Buckley et al., 1998) comprise extracellular matrix and cell adhesion receptors respectively.

A series of intracellular mediators may then be involved in relaying the signal through the cell. These include second messengers, such as cyclic AMP, DAG, IP$_3$ and calcium, small GTP binding proteins, for example, Rac1 and Rho, and adaptor proteins, including Grb2. These components, working in series or in parallel, often serve to regulate a cascade of protein kinases, such as the MAPKs, and/or their antagonistic phosphatases (see (Downward, 2001) for a review). Ultimately, these pathways culminate in the regulation of enzyme activity and/or gene expression, thereby enabling a response to be mounted.

Cells receive inputs from many signalling pathways concurrently, and must interpret them within the context of each other, in order to respond appropriately. Integration involves the process of cross-talk, whereby one pathway influences the activity of another; for example, both PI-3 kinase and PAK feed into the MAPK pathway triggered by activated Ras (Downward, 2001). The spatial control of signalling is also of importance in determining the cellular response, as evidenced by ERK1/2, which act at the nucleus to regulate gene expression, but at the cell periphery to control HGF-induced cell migration (Kermorgant and Parker, 2005). Finally, the regulation of signal amplitude and duration is critical to the final outcome of the pathway. For example, transient activation of the MAPK pathway by EGF causes PC12 cells to multiply slowly, while sustained activation of the same pathway following NGF stimulation leads to neurite outgrowth (Marshall, 1995).
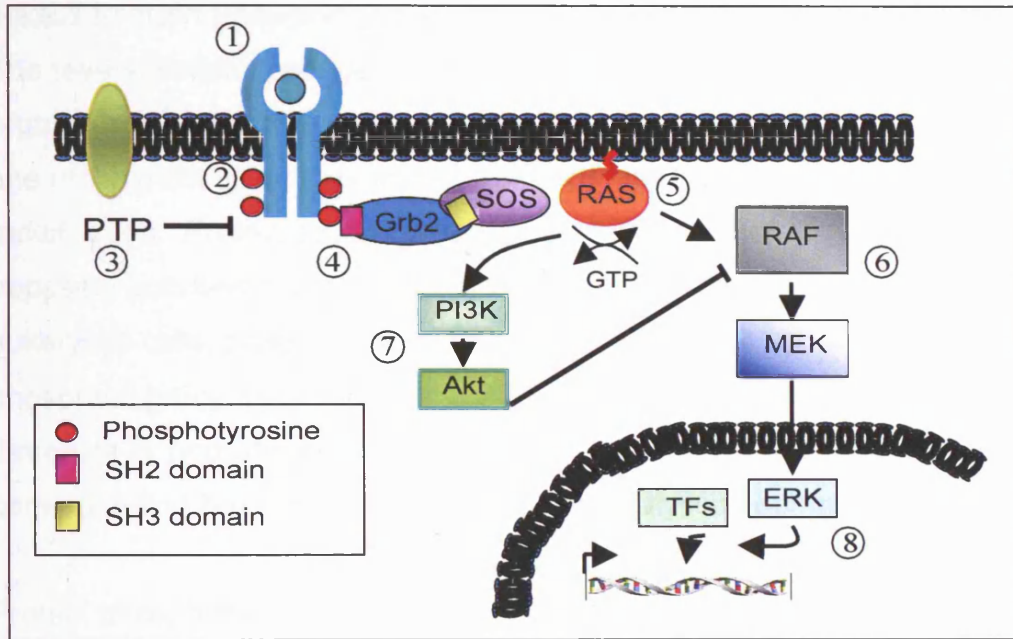
Figure 1.1 Schematic Representation of A Signal Transduction Paradigm. A generalised growth factor responsive signal transduction pathway is represented schematically, illustrating the general principles of signal transduction. 1) Growth factor binding to its complementary cell surface receptor induces receptor dimerisation and 2) autophosphorylation. 3) This signal may be attenuated by an antagonistic phosphatase. 4) A series of adaptor proteins are recruited through protein interaction domains, resulting in 5) the activation of the small GTPase Ras. 6) Ras activates a kinase cascade, from Raf to MEK and MEK to ERK. 7) This cascade is also influenced by information received from a parallel PI3-kinase dependent pathway, thereby integrating cellular information (cross-talk). 8) Ultimately, enzyme activity and/or gene expression is regulated, enabling an appropriate response to be mounted.

1.1.2.2 Protein Phosphorylation

The reversible phosphorylation of proteins plays a pivotal role in the regulation of signal transduction, and many other cellular processes; it is one of the most ubiquitous and well studied forms of post-translational modification. Protein phosphorylation is exquisitely controlled by the opposing activities of protein kinases and protein phosphatases. In eukaryotic cells, protein kinases typically catalyse the transfer of the γ-phosphate group from ATP onto the hydroxyl group of either a serine, threonine or tyrosine residue; this reaction can be antagonised by a corresponding protein phosphatase, which catalyses dephosphorylation.

Protein phosphorylation was first described as the reversible modification of phosphorylase kinase (DeLange et al., 1968; Riley et al., 1968). Subsequently, it has been estimated that as many as one third of cellular proteins are phosphorylated at any one time, with 90% of phosphorylations occurring at serine residues, 10% at threonine residues and just 0.05% at tyrosine residues (reviewed by (Mann et al., 2002)). The near completion of the human genome project has revealed that approximately 2% of the genome encodes proteins involved in this process, with more than 500 kinases (Manning et al., 2002) and over 100 phosphatases (Lander et al., 2001; Venter et al., 2001) identified.

The conventional eukaryotic protein kinases comprise one of the largest groups of homologous proteins (Hanks and Hunter, 1995). The superfamily consists of two main subgroups based on substrate specificity, the protein serine/threonine (Ser/Thr) kinases (which include the dual specificity kinases) and the protein tyrosine kinases; these can be further divided into additional classes (see (Manning et al., 2002) for classification system). Although there is a rich diversity with respect to structure, mode of regulation and specificity, a common catalytic core, of 250-300 residues, is conserved among the superfamily. The bi-lobal structure formed by this region facilitates the three main roles of the kinase, namely the binding and orientation of ATP (complexed with a

24

divalent metal ion), the binding and orientation of the substrate, and the transfer of phosphate (Hanks and Hunter, 1995).

Eukaryotic cells contain a smaller, but nevertheless extensive, complement of antagonistic phosphatases. These too are classified according to substrate specificity, the main subgroups comprising the protein tyrosine phosphatases, the protein Ser/Thr phosphatases, and the dual specificity phosphatases, which can catalyse dephosphorylation of both Ser/Thr and Tyr residues. A fine balance exists between the numbers of tyrosine kinases and tyrosine phosphatases within the cell, facilitating the precise control of tyrosine phosphorylation (Alonso et al., 2004). In contrast, there are relatively few Ser/Thr phosphatases; however, their elegant regulatory mechanisms confer the versatility required to antagonise the diverse activities of the Ser/Thr kinases. The Ser/Thr phosphatases operate as distinct holoenzymes, comprised of various combinations of regulatory and catalytic subunits, such that a myriad of substrate specificities and subcellular localisations are achieved (see (Wera and Hemmings, 1995) for a review).

The combined activities of the protein kinases and protein phosphatases thus serve to control the balance of protein phosphorylation, which in turn contributes to the regulation of cell signalling. The covalent attachment of a phosphate group to a target protein incorporates a bulky negative charge, which can influence the substrate in different ways. In the case of certain enzymes, phosphorylation can regulate activity, facilitating either activation, as illustrated by the activation loop phosphorylation of the AGC kinases (Parker and Parkinson, 2001), or inactivation, as exemplified by phosphorylation of Src at Tyr-527 (Kmiecik and Shalloway, 1987). Phosphorylation can also promote protein-protein interactions, for example, tyrosine phosphorylation of numerous receptor tyrosine kinases, such as the EGF receptor, creates a docking site for SH2 containing proteins (Margolis et al., 1990), and there are numerous other examples of phospho-specific protein interaction domains (see section 1.2.4). Localisation too can be influenced in this manner, as in the case of

the Forkhead transcription factors, whose nuclear import is impaired upon phosphorylation (Datta et al., 1999). Finally, phosphorylation also plays a critical role in targeting certain substrates, such as Sic1, for degradation (Skowyra et al., 1997).

1.1.2.3 Other Post-Translational Modifications

In addition to protein phosphorylation, there are more than 200 other forms of post-translational modification that have been reported to influence signal transduction pathways and other cellular processes (Zhu et al., 2003). Together, these modifications provide additional functional diversity to the proteome, and it has been speculated that the complexity of higher organisms can be attributed in part to such mechanisms (Lander et al., 2001; Venter et al., 2001). Examples of some of the most common, and functionally important, post-translational modifications are given in Table 1.1. The process of ubiquitination is considered in more detail in Section 1.3.3.1.

Post-Translational Modification	Functional Implications
Phosphorylation	activation/inactivation, modulation of protein-protein interactions and localisation, degradation
Sulphation	modulation of protein-protein and receptor-ligand interactions
Proline Hydroxylation	regulation of protein-protein interactions and protein stability
Glycosylation	cell-cell recognition and signalling
Acylation/Fatty acid modification	membrane tethering and modulation of localisation
GPI anchor attachment	membrane tethering
Ubiquitination	degradation, trafficking

Table 1.1 Post-translational Modifications. A selection of common post-translational modifications are summarised with key functional effects indicated (Mann and Jensen, 2003).

1.1.2.4 Protein-Protein Interactions

A characteristic property of many cell signalling proteins is that they contain modular interaction domains, which allow them to assemble into specific multi-protein complexes (Pawson and Nash, 2000). The transfer of information along a signal transduction pathway frequently involves a series of dynamic protein-protein interactions, which recruit and confine the constituent species to appropriate subcellular localisations, exposing them to particular regulators and targets (Faux and Scott, 1996b).

Interaction domains tend to comprise independently folding modules of 35-150 amino acids, and typically recognise specific peptide motifs; many distinguish particular post-translational modifications (see below). These conserved signalling modules tend to occur in multiple proteins, and conversely, a number of different interaction domains may be found within the same protein. The reiterated and combinatorial use of interaction domains provides a common means by which the flow of information can be controlled and integrated (Pawson and Nash, 2003). Protein interaction domains can be divided into different groups based on their ligand binding properties (see (Pawson et al., 2002) for review, and table 1.2). Src homology 2 (SH2) and phospho-tyrosine (PTB) domains, along with the C2-like fold of PKC-δ (Benes et al., 2005), comprise interacting modules which recognise phospho-tyrosine containing motifs. There are more than 100 known SH2 domains, with varying preferences for adjacent residues. A number of other classes of interaction domain bind specifically to phospho-serine/threonine residues, these include the 14-3-3 (see section 1.2.4.1), Forkhead-Associated (FHA) and WD40-repeat domains. Additional post-translational modifications can also be recognised, notably, acetylated and methylated lysine residues are bound by Bromo and Chromo modules respectively. Other groups of interaction domain are not dependent upon protein modifications and tend to interact more stably with targets, these include the Src homology 3 (SH3) and WW domains, which recognise proline-rich motifs, and the PDZ domains, which bind to the extreme C-termini of target proteins. Finally, certain other modules engage specifically in lipid binding, for example Pleckstrin-

homology (PH) domains bind to phosphoinositides such as $PI-4,5-P_2$ and $PI-3,4,5-P_3$, FYVE domains recognise PI-3-P and C1 domains typically bind to DAG and phorbol esters.

Interaction Domain	Recognition Motif
SH2 *e.g. Phospholipase C-γ*	Phospho-tyrosine *e.g. β-PDGF receptor*
PTB *e.g. Shc*	Phospho-tyrosine *e.g. TrkA NGF receptor*
14-3-3 *e.g. 14-3-3*	Phospho-serine/threonine *e.g. cdc25*
WD40 repeat *e.g. G-Protein β-chain*	Phospho-serine/threonine (and certain unphosphorylated motifs) *e.g. G-protein α/γ-chain*
SH3 *e.g. Src*	Proline rich *e.g. PI 3-kinase p85 subunit*
PDZ *e.g. PSD-95*	C-termini *e.g. NMDA receptor B*

Table 1.2 Protein Interaction Domains. The recognition motifs of some prevalent interaction domains are summarised, with examples of interacting pairs provided in italics (Pawson, 2002).

Related to the capacity of signalling proteins to participate in defined protein-protein interactions is the formation of kinase/phosphatase signalling complexes that modulate the phosphorylation of particular target substrates (Smith and Scott, 2002). The building of these complexes is co-ordinated by multivalent scaffolding proteins, which serve as platforms for assembly. This phenomenon is exemplified by the A-kinase anchoring proteins (AKAPs), which direct Protein Kinase A (PKA) activity (see (Faux and Scott, 1996a) for review). Numerous AKAPs have been identified, facilitating diverse PKA functions, for instance mAKAP juxtaposes cyclic AMP responsive PKA and antagonistic cAMP-specific phosphodiesterase, PDE4D3, to maintain a hormonally regulated negative feedback loop (Dodge et al., 2001).

Advances in proteomics have facilitated the detailed analyses of signal transduction pathways. Recently, the dynamic interactions of the transforming growth factor-β (TGFβ) pathway were characterised, providing insights into the mechanism of TGFβ-dependent tight junction dissolution during the epithelial-to-mesenchymal transition (Barrios-Rodiles et al., 2005). Additionally, the large scale mapping of protein-protein interaction networks has been undertaken in yeast (Ito et al., 2001) and Caernorhabditis (Li et al., 2004), and a probabilistic model of the human interactome has been developed (Rhodes et al., 2005). Corresponding advances in bioinformatics and computer modelling will be required in the future to fully integrate and interpret the data gathered (Legrain et al., 2001).

1.1.2.4.1 14-3-3 Proteins

The protein-protein interactions of the 14-3-3 proteins are pertinent to work presented in this thesis, as such, their key features are considered in more detail here.

The 14-3-3 proteins are small (~30kDa), acidic proteins which bind to phospho-serine and phospho-threonine containing motifs, and also to some non-phosphorylated targets (see (Bridges and Moorhead, 2005) for recent review). 14-3-3 proteins are found in all eukaryotes and are highly conserved both across and within species, in mammalian cells there are seven isotypes (β, γ, ϵ, η, σ, τ, ζ). The importance of their function is evidenced by the lethal phenotype derived from simultaneous knock out of both yeast isoforms (Gelperin et al., 1995).

14-3-3 proteins exist primarily as homo- or hetero-dimers in the cell. Crystallographic studies have revealed that 14-3-3 dimers assume a highly helical, cup-shaped conformation. Each subunit of the dimer can bind to one discrete phospho-serine or phospho-threonine containing motif, with the ligands in extended, antiparallel orientations and the phosphate groups 34Å apart (Obsil et al., 2001). Examinations of 14-3-3

interacting partners, and the use of an orientated peptide library, have defined two major consensus motifs for binding: Mode I, RSXpS/TXP and Mode II RXXXpS/TXP (X denotes any amino acid) (Yaffe et al., 1997). Several 14-3-3 binding partners bear more than one 14-3-3 binding site, and the affinity of a protein with two appropriately spaced sites is more than thirty times that of a protein with only one (Yaffe et al., 1997). For most targets it seems that there is a single dominant site, known as the 'gatekeeper', and a second, lower affinity site; once the gatekeeper site is phosphorylated and bound to one 14-3-3 monomer, the secondary site is able to interact with the other subunit by virtue of its close proximity, thereby stabilising the complex (Yaffe, 2002). The presence of one suboptimal site may facilitate a certain degree of dissociation, and thereby confer reversibility to the interaction.

14-3-3 binding typically mediates one of three effects on target proteins: conformational change, steric hindrance or scaffolding (see Figure 1.2). The propensity of 14-3-3 proteins to mediate conformational change is thought to relate to the rigidity of its own structure; it acts as a 'molecular anvil', deforming its ligands while undergoing only minimal adjustment itself (Yaffe, 2002). The anvil effect is illustrated by serotonin-N-acetyltransferase, which is held in an active conformation upon 14-3-3 binding (Obsil et al., 2001). The steric effects of 14-3-3 dimers involve the occlusion of functionally significant sites on the target protein. For instance, 14-3-3 mediated masking of the Cdc25 nuclear localisation signal causes accumulation of Cdc25 in the cytoplasm and thereby allows mitotic entry (Yang et al., 1999). Alternatively, where a 14-3-3 dimer binds to phospho-motifs on two separate proteins, it can facilitate dimerisation; one example of 14-3-3 scaffolding involves glycogen synthase kinase 3β and tau (Agarwal-Mawal et al., 2003).
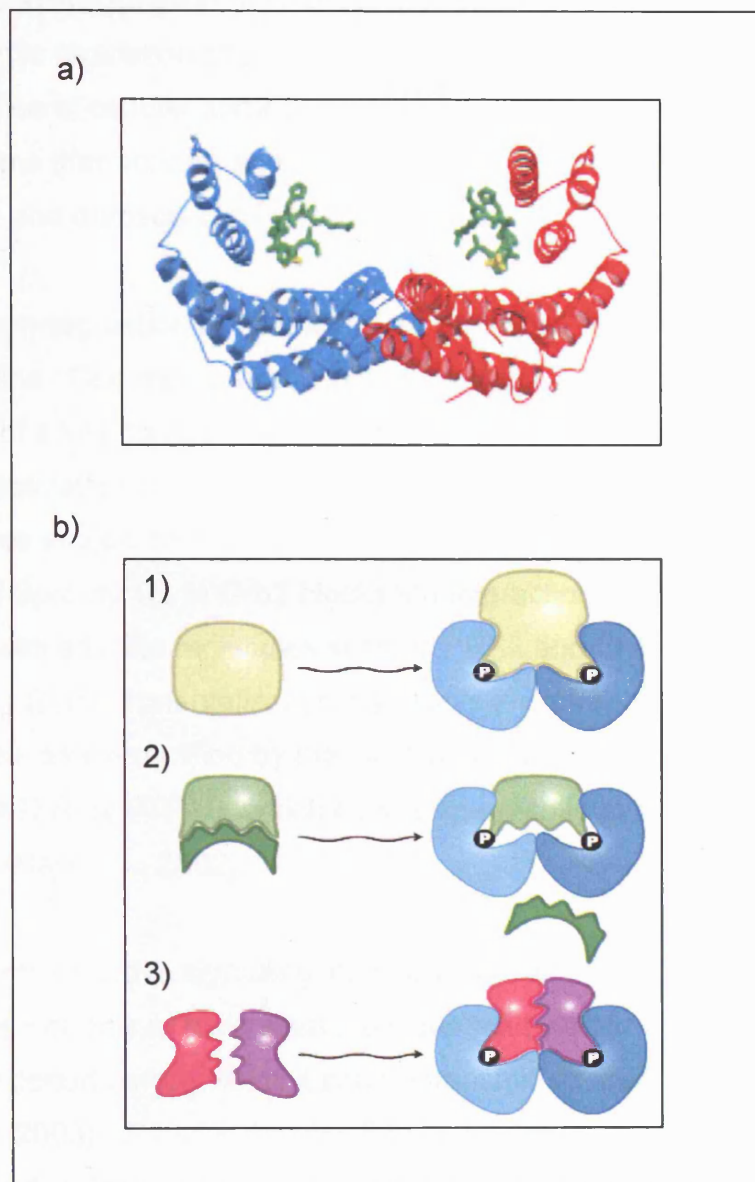
Figure 1.2 14-3-3 Proteins: Structural Features & Modes of Action.
a) Structural representation of a 14-3-3ζ dimer (red/blue ribbons), bound
to two ARSHpSYA phospho-peptide ligands (green, peptide; yellow,
phosphate group). b) The three major effects elicited by 14-3-3 binding
1) conformational change; 2) steric hindrance; 3) scaffolding. (Figures
reproduced from (Bridges and Moorhead, 2005)).

1.1.2.5 Down-regulation of Cell Signalling

The dynamic regulation of signal transduction is critical to the maintenance of cellular homeostasis. A delicate balance exists between mechanisms that activate and inactivate cell signalling, such that signal amplitude and duration can be precisely controlled.

Signal down-regulation can be achieved through a number of different mechanisms. Commonly, pathways are negatively regulated by catalytic inhibition of a key component, for instance, through dephosphorylation of a kinase activation loop (Dikic and Giordano, 2003). Other signalling proteins are subject to inhibition through steric hindrance, for example, binding of Sprouty 1/2 to Grb2 blocks the interaction of the Grb2-SOS complex with adapter molecules such as FRS2 and Shc2 (Hanafusa et al., 2002). Compartmentalisation also plays an important role in signal attenuation, as exemplified by the inactivating dephosphorylation of EGFR/PDGFR by PTP1B, which occurs specifically at the endoplasmic reticulum (Haj et al., 2002).

Longer term 'negative signalling' can be achieved by protein degradation; this serves not only to extinguish the signal, but also to impose a refractory period before which it can be transmitted again (Dikic and Giordano, 2003). A major deactivation pathway involves the ligand induced endocytosis of receptor tyrosine kinases, such as EGFR/PDGFR, followed by their lysosomal degradation; in certain cases this process is directed by Cbl catalysed mono-ubiquitination of the receptor (Levkowitz et al., 1998). However, it is important to note that prior to degradation, important signalling functions persist within this endosomal compartment (Clague and Urbe, 2001).

1.1.3 Aberrant Cell Signalling and Disease

1.1.3.1 Cell Signalling and Cancer

Cancer is a disease of signalling malfunction, which is driven by microevolutionary processes. Tumour development is typically initiated via one of two mutational routes, the hyperactivation of an oncogene,

32

which stimulates cell division, or the inactivation of a tumour suppressor gene, which would normally inhibit proliferation. More than one hundred proto-oncogenes and tumour suppressor genes have been identified, and of these, the vast majority encode components of the signal transduction pathways (Sherr, 1996). Neoplastic cells subsequently tend to undergo further changes, which, by affecting DNA replication, repair and recombination, confer a high mutability rate. Thus a heterogeneous tumour population is formed capable of evolving further properties associated with greater malignancy, characterised by more rapid growth, invasiveness, metastasis and angiogenesis.

A multitude of signalling defects have been associated with different cancers (see (Adjei and Hidalgo, 2005) for a recent review). Key mediators of carcinogenesis include the Ser/Thr kinases Raf (Wellbrock et al., 2004), and Akt (Luo et al., 2003), the small GTPase Ras (Bos, 1989) and numerous tyrosine kinases, including EGFR and HER-2 (Kolibaba and Druker, 1997); given the relatively low level of tyrosine phosphorylation under normal conditions, protein tyrosine kinases play a disproportionate role in tumour progression, contributing to a significant fraction of human cancers (Blume-Jensen and Hunter, 2001).

Since the components of these abnormal signalling pathways are specific to neoplastic cells, they represent highly selective targets for potential anticancer therapies. Typically, only one key component of a given pathway is mutated, such that its inhibition will cause a significant perturbation to the malignant cell, ultimately leading to cell death (Baselga and Arribas, 2004). Where specific mutations can be identified through biomarkers, the response to a given therapy can be predicted; those tumours in which the targeted pathway is critical will be most susceptible to its inhibitory agents. This type of directed therapy is exemplified by the development of Herceptin, a monoclonal antibody specific for HER-2/*neu*, for the treatment of patients with breast cancers that overexpress this receptor (Slamon et al., 2001).

Successful therapeutic interventions have been developed which are directed at various points of the signalling cascade. The initial event, the binding of a ligand to its receptor, can be inhibited, as exemplified by the neutralisation of the vascular endothelial growth factor (VEGF) by bevacizumab (Ferrara et al., 2005). Alternatively, the receptor itself can be blocked as described for HER-2 above. Additionally, the downstream kinases responsible for signal transduction represent key targets which can be suppressed using small molecule inhibitors; Gleevec, an inhibitor of the aberrant bcr-abl tyrosine kinase (and c-kit/PDGFR), has revolutionised the treatment of certain leukaemias and represents a paradigm of this type of rationally designed treatment (Druker, 2004). Detailed analyses of the pathways of cell signalling will be critical to the development of further therapeutics of this kind.

1.1.3.2 Cell Signalling and other diseases

It is important to note that defective cell signalling is implicated in the onset of many other non-infectious diseases in addition to cancer, such that therapeutic developments may also be made outside the field of oncology through the further elucidation of signal transduction pathways. Diabetes, for example, results from the malfunction of the insulin signalling pathway, which normally regulates blood sugar levels (Withers and White, 2000). Similarly, the developmental disorder achondroplasia (genetic, short-limbed dwarfism) is caused by mutation of the fibroblast growth factor (Aviezer et al., 2003). Also, the immunological disease agammaglobulinaemia, which is characterised by a lack of immunoglobulin antibodies in the blood, is in many cases attributed to Bruton tyrosine kinase (Btk) mutation (Vihinen et al., 2000).

1.2 Protein Kinase C

1.2.1 Protein Kinase C

Protein Kinase C (PKC) comprises a family of phospholipid-dependent Ser/Thr kinases with a broad array of cellular substrates and a central role in signal transduction. PKC has been implicated in the regulation of diverse physiological processes from proliferation (Soh and Weinstein, 2003), differentiation (Kashiwagi et al., 2002), migration (Ivaska et al., 2003) and apoptosis (DeVries et al., 2002; Mandil et al., 2001) at the cell autonomous level, to development (Otte et al., 1991) and memory (Birnbaum et al., 2004) at the level of the organism.

PKC was originally discovered, by Nishizuka and colleagues, as a histone kinase activity from rat brain which could be activated by limited proteolysis (Inoue et al., 1977). It was subsequently shown that (c)PKC responds to the second messengers phosphatidylserine (PS) and diacylglycerol (DAG) in a calcium (Ca^{2+})-dependent manner, and may thus act to integrate agonist responses (Takai et al., 1979). Significantly, it was also demonstrated that the tumour-promoting phorbol esters, such as 12-O-tetradecanoylphorbol-13-acetate (TPA), could also directly activate PKC by substituting for DAG, directly implicating PKC in carcinogenesis (Castagna et al., 1982).

1.2.2 The PKC Superfamily

PKC is conserved among eukaryotes, demonstrating both the early origins and fundamental importance of this protein kinase activity. A single PKC isoform, Pkc1p, exists in *Saccharomyces cerevisiae*, with a key role in the maintenance of cell integrity (Perez and Calonge, 2002), while an entire superfamily of PKC isoforms has evolved in mammalian cells to perform more specialised functions (see (Mellor and Parker, 1998) for a review). The first PKC isoforms to be identified were α, β and γ, which were isolated and cloned from bovine brain cDNA libraries (Coussens et al., 1986; Parker et al., 1986). This tissue proved to be a

rich source of PKC isotypes and subsequent low stringency screening with probes derived from thes sequences yielded three additional PKCs: δ, ε and ζ (Ono et al., 1987). A similar approach has also led to the identification of PKC-η (Osada et al., 1990), PKC-θ (Osada et al., 1992), PKC-ι/λ (Selbie et al., 1993) and most recently, the related PKNs: 1, 2 and 3 (Mukai and Ono, 1994; Palmer et al., 1995). Protein Kinase D (PKD/PKCμ) was also originally considered to be a member of the PKC superfamily, however, it has subsequently been shown to possess distinct regulatory and enzymatic properties (Rozengurt et al., 1997); nevertheless, functional links exist between PKD and the PKCs (Matthews et al., 2000; Rey et al., 2001; Yuan et al., 2002; Zugaza et al., 1996).

The mammalian PKC superfamily is divided into subgroups based upon structural differences and related cofactor requirements (see Figure 1.3 and section 1.2.3). The classical PKC isoforms (α, β_I, β_{II}, and γ respond both to Ca^{2+} and DAG, the novel isoforms (δ, ε, θ, η) require only DAG and the atypical PKCs (ι/λ, ζ) are responsive to neither co-factor, they may be activated through protein-protein interactions (Ohno, 2001). The PKNs are subject to regulation by small GTPases (Amano et al., 1996; Watanabe et al., 1996).

Each of the PKC isoforms represents a distinct gene product, with the exception that β_I and β_{II}, are alternatively spliced variants of the same gene (Coussens et al., 1986). Splice variants have also been identified for PKC-δ, which differ in caspase cleavage properties (Sakurai et al., 2001), and PKC-ζ, which vary with respect to kinase activity (Parkinson et al., 2004). Additionally, the PKC-ζ gene bears an internal promoter from which its isolated catalytic domain can be generated, PKMζ (Hernandez et al., 2003).

The different PKC isoforms bear broadly overlapping substrate specificities, and a degree of functional redundancy exists among the

superfamily (Mellor and Parker, 1998). However, there is also substantial evidence for isoform specific functions. Divergence among the PKC superfamily is implied by the marked differences in tissue distribution detected among the isoforms; PKC-$\alpha/\delta/\zeta$ are widespread, while PKC-$\gamma/\eta/\theta$ are more restricted to one or a few tissues (Dekker and Parker, 1994). Differential responses to agonists are also indicative of isoform specific properties, for example, PKC-ε is selectively down-regulated in response to chronic TRH treatment in GH4C1 pituitary cells (Kiley et al., 1991), while PKN1 uniquely is translocated to a vesicular compartment following osmotic stress (Torbett et al., 2003). Consistent with these observations, numerous studies using constitutively active or dominant negative constructs, isoform specific inhibitors, or RNAi knockdowns have demonstrated requirements for particular isoforms in particular processes. For instance, recent work from our laboratory has implicated specific PKC isoforms in the control of distinct c-Met properties downstream of chronic HGF treatment, namely, PKC-α promotes the perinuclear accumulation of c-Met, while PKC-ε controls c-Met endosomal signalling (Kermorgant et al., 2004).

Perhaps most informative with regards to PKC isoform specificity are the knock-out studies which have been undertaken in various laboratories. A number of knock-out phenotypes have been established, which is indicative of certain non-redundant functions. The PKC-β and δ knock-out mice bear deficiencies in B-cell signalling (Leitges et al., 1996; Mecklenbrauker et al., 2002; Miyamoto et al., 2002), the PKC-γ null mutants exhibit defective CNS functions (Abeliovich et al., 1993) and the PKC-ζ knock-outs display impaired NFκB signalling (Leitges et al., 2001). Null mice have also been generated and characterised for PKC-ε, the main focus of this thesis; they show defects in innate immunity (Castrillo et al., 2001), demonstrate hypersensitivity to ethanol (Hodge et al., 1999) and are impaired in their capacity for ischemic preconditioning (Saurin et al., 2002).

37

Significantly, the first double PKC knock-out line has recently been generated (PKC-$\varepsilon^{-/-}$/PKC-$\delta^{-/-}$), and this combination has proved to be embryonic lethal (unpublished data reported by Michael Leitges). As such, we can conclude that although there are numerous PKC-ε and PKC-δ specific functions, there is also a significant degree of redundancy which must be acknowledged. Future studies involving multiple isoform knock-out mice will address the physiological roles of PKC more comprehensively.

1.2.3 PKC Structure

As shown in Figure 1.3, each PKC isoform is composed of a combination of conserved (C) and variable (V) domains, with a well conserved, C-terminal catalytic domain, separated from a more divergent N-terminal regulatory domain, by a flexible hinge region (V3). All of the conserved domains associated with PKC regulation are present within pkc1, the single PKC isoform expressed in *S.cerevisiae*; pkc1 can be considered to represent the archetypal PKC (Mellor and Parker, 1998). Within the mammalian superfamily these domains have been differentially distributed between isoforms. The structural and functional characteristics of these domains have been well characterised as described below.
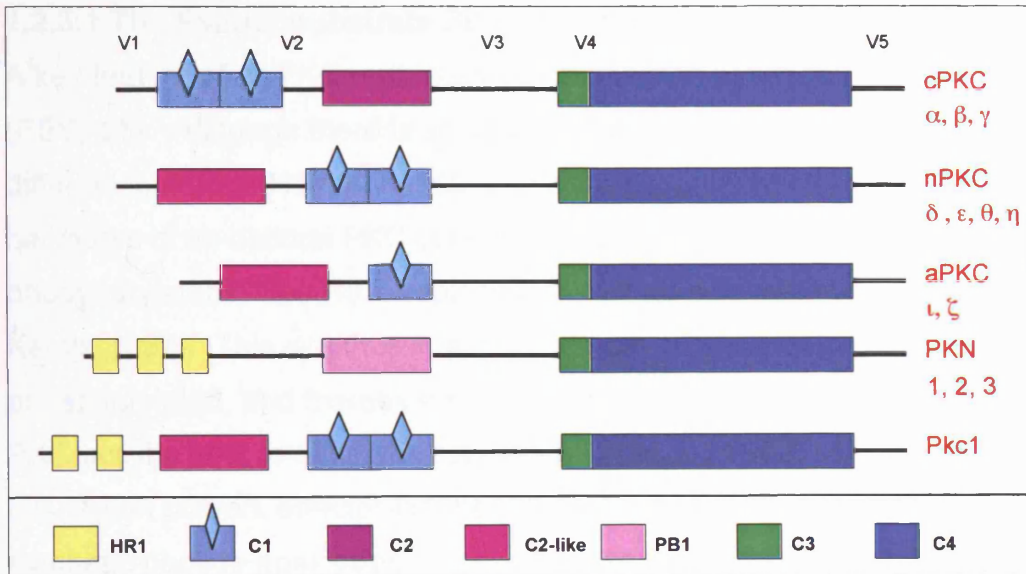
Figure 1.3 The PKC Superfamily. A schematic representation of the PKC superfamily domain structure.

1.2.3.1 The Pseudosubstrate Site

A key feature of all PKC regulatory domains is the pseudosubstrate (PSS) site. Although there is some variation among sequences from different isoforms (Hofmann, 1997), in each case the motif bears all the hallmarks of an optimal PKC consensus, except that the phosphorylatable Ser/Thr is replaced with an alanine residue (House and Kemp, 1987). This site thus interacts with the catalytic domain, but is not phosphorylated, and thereby mediates intramolecular suppression of PKC activity prior to allosteric activation (Orr et al., 1992). Mutation of this region confers effector-independent activity (Pears et al., 1990), and synthetic peptide analogues of these sequences act as potent inhibitors of PKC (House and Kemp, 1987).

1.2.3.2 The C1 Domain

The cPKCs and nPKCs each contain a C1 domain that is composed of two repeated zinc-finger like motifs, C1a and C1b. Each motif bears a conserved series of cysteine and histidine residues ($H-X_{12}-C-X_2-C-X_{13/14}-C-X_2-C-X_4-H-X_2-C-X_7-C$; C; X refers to any amino acid) that are responsible for the co-ordination of two Zn^{2+} ions (Hommel et al., 1994; Quest et al., 1992).

The C1 domain contributes to phosphatidlylserine binding (Bittova et al., 2001) and represents the interface for interaction with DAG and phorbol ester (Ono et al., 1989), which bind competitively to the same site (Sharkey et al., 1984). The crystal structure has been solved for the PKC-δ C1b domain complexed with TPA (Zhang et al., 1995). Ligand binding does not result in a conformational change, but rather 'caps' a hydrophilic site at the top of the domain, thereby forming a contiguous hydrophobic surface that facilitates insertion into the lipid bilayer. The aPKCs contain just a single zinc-finger like motif each, and are not responsive to DAG.

The degree of equivalency between C1a and C1b motifs appears to vary among different PKC isoforms. The C1a and C1b domains in PKC-α (Medkova and Cho, 1999) and PKC-δ have been shown to be non-equivalent, for instance, mutation of a highly conserved Proline residue in the PKC-δ C1a domain has little effect on TPA responsiveness, while alteration of the equivalent amino acid in the C1b domain causes a 125-fold decrease in phorbol ester binding efficiency (Szallasi et al., 1996). Interestingly, the C1a and C1b domains of PKC-δ show opposite affinities towards DAG and TPA (Stahelin et al., 2004). In contrast, these two motifs exhibit comparable affinities for DAG and phorbol ester in PKCs -γ (Ananthanarayanan et al., 2003) and -ε (Stahelin et al., 2005). These data suggest that differences with respect to cofactor binding properties may contribute to isoform specific regulation.

It is important to note that a number of other proteins contain C1 domains and may therefore bind to TPA, including PKD and β2-chimaerin (see (Brose and Rosenmund, 2002) for review). When interpreting experimental results, it is critical to acknowledge that phorbol ester-responsiveness is not solely a property of PKC.

1.2.3.3 The HR1 Domain

The HR1 domain, which is composed of a repeated, conserved motif of approximately 55 amino acids (Palmer et al., 1995), is found in yeast pkc1 (S,cerevisiae) and pck1/2 (S.pombe), and in the PKNs. The HR1 interacts with both Rac1 and Rho (Flynn et al., 1998), thereby mediating activation by small GTPases.

1.2.3.4 The C2/C2-like Domain

The C2 domain is a calcium binding domain found only in the cPKCs, explaining the characteristic calcium-dependence of their phospholipid binding. Calcium binding C2 domains are found in a number of other proteins, including synaptotagmin (Shao et al., 1996), Ras-GAP and PLC-γ (see (Ponting and Parker, 1996) for a review).

41

A classical C2 domain is absent from both the nPKCs and PKNs, such that they are calcium insensitive; they do, however, bear a C2-like domain (Pappa et al., 1998; Ponting and Parker, 1996). The C2 domains of other proteins have been shown to mediate protein-protein interactions, for instance, the C2A and C2B domains of synaptotagmin facilitate binding to syntaxin and clathrin respectively (Li et al., 1995). It has been postulated that the nPKC/PKN C2-like domains may play analogous roles, serving to recruit interacting partners. For instance, the binding interface for GAP43 has been mapped to the C2-like fold of PKC-δ (Dekker and Parker, 1997) and the Receptor for Activated C-Kinase (RACK1) binding site is also located in this domain in PKC-β (Ron et al., 1995).

Most recently, compelling evidence has been obtained which demonstrates that the C2 domain of PKC-δ, and probably PKC-θ too, comprises a novel phospho-tyrosine binding domain (Benes et al., 2005); the crystal structure of this domain complexed with an optimal tyrosine-phosphorylated peptide has been solved. This is the first example documented of a tyrosine binding module occurring within the structure of a protein Ser/Thr kinase, thus linking Tyr-phosphorylation and Ser/Thr phosphorylation. The full functional implications of this newly identified mode of interaction remain to be investigated; notably, it may contribute to PKC isoform-specific functions.

1.2.3.5 The V3 Region

The V3 region represents a flexible hinge domain between the regulatory and catalytic domains, which varies in length between different isoforms. The V3 region has been shown to be proteolytically cleaved by calpain, to yield a co-factor independent catalytic fragment termed PKM (Kishimoto et al., 1989). This region of PKC-δ can also be targeted by caspases for proteolysis during apoptosis; significantly, an alternatively spliced variant of PKC-δ lacks the caspase cleavage site (Sakurai et al., 2001).

1.2.3.6 The Catalytic Domain

PKC is a member of the extended AGC superfamily of kinases, which also includes PKA, PKG, PKB, p70s6K and p90rsk (see The Protein Kinase Resource, www.kinasenet.org). These enzymes exhibit a high degree of homology with respect to their kinase domains, and parallels can be drawn with respect to their structures, and means of regulation by phosphorylation (see next section).

The catalytic domain comprises the highly conserved C3 and C4 domains. The C3 domain largely comprises the ATP binding pocket; a point mutation at the ATP binding site renders the enzyme catalytically inactive (kinase dead) (Ohno et al., 1990). The C4 domain, contains the phosphoryl transfer region and the substrate binding site. Under basal conditions, the pseudosubstrate sequence occupies this site, inhibiting substrate binding in the absence of allosteric activation.

Crystal structures have recently been solved for the PKC-θ (Xu et al., 2004) and PKC-ι (Messerschmidt et al., 2005) kinase domains, to 2Å and 3Å respectively. These structures reveal that the PKC catalytic domain comprises a classical bilobal kinase fold, with a smaller, N-terminal lobe, consisting mainly of β-sheet, and a larger, predominantly α-helical, C-terminal lobe, connected by a linking hinge.

The V5 region, comprised of approximately 50 residues at the extreme C-terminus of PKC, is also a functionally significant part of the protein, containing the key 'TP' and 'FSY' priming phosphorylation sites (see next section). Recent work on PKC-ε has demonstrated that the last 8 amino acids are also critical with respect to catalytic competence, presumably due to their interaction with the catalytic core (Zhu et al., 2005b). Interestingly, the two PKC-β splice variants, PKC-β_I and PKC-β_{II}, vary only in this region, such that any functional differences between them must be attributed to these residues; for example, in U937 monocytic

cells, PKC-β_I localises to the microtubules, whereas PKC-β_{II} is localised in part to secretory granules (Kiley and Parker, 1995).

1.2.4 PKC Activation

As represented in Figure 1.4, the activation of cPKC and nPKC isoforms typically involves their recruitment to the membrane and allosteric activation by DAG, in the presence of phosphatidylserine. Agonist-induced production of DAG may be effected by multiple mechanisms, most prominently, receptor tyrosine kinases, and receptors linked to non-receptor tyrosine kinases, operate through the phosphatidylinositol (4,5)-bisphosphate (PtdIns(4,5)P_2)-specific phospholipases $C\gamma_{1/2}$ (PtdIns-PLC$\gamma_{1/2}$); G-protein coupled receptors activate PtdIns-PLCβ family members; and Ras can target PtdIns-PLCϵ (Parker and Murray-Rust, 2004). For cPKCs, initial membrane recruitment is a calcium sensitive event (Keranen and Newton, 1997), for nPKCs no equivalent mechanism has been elucidated, but protein-protein interactions have been speculated to play a role. In its inactive state, the PKC C1 and C2 domains are tethered, upon calcium dependent/independent binding to phosphatidyserine, the C1 domain is unleashed, allowing its membrane penetration and interaction with DAG (Bittova et al., 2001). DAG binding is associated with a PKC conformational change, which results in the removal of the psuedosubstrate motif from the catalytic domain, thereby relieving autoinhibition.
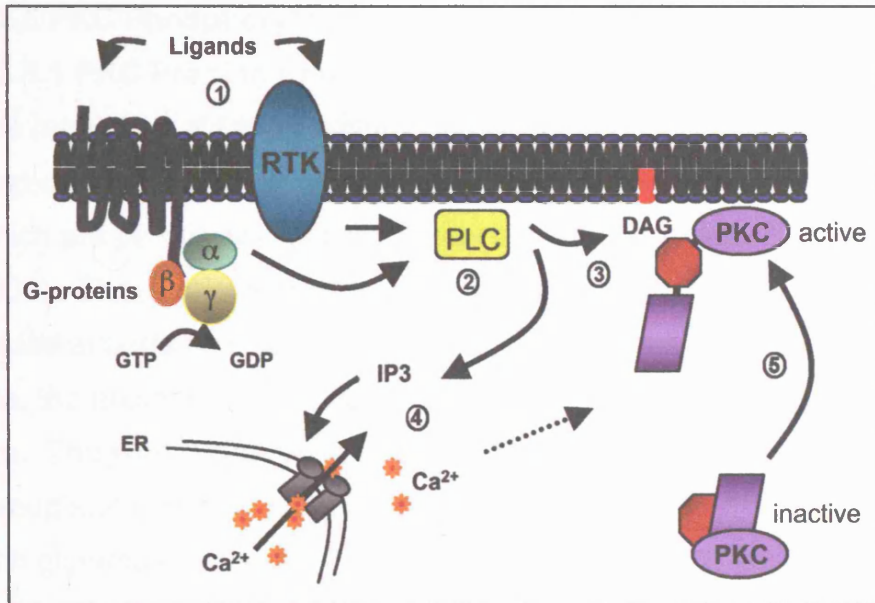
Figure 1.4 Classical Pathway of PKC Activation. A schematic representation of the activation of cPKC/nPKC isoforms. 1) Ligand binding to a receptor tyrosine kinase or G-protein coupled receptor leads to 2) the activation of a phospholipase C isoform, which catalyses the production of 3) DAG and 4) IP3, thereby mediating the release of calcium. 5) Inactive PKC translocates from the cytosol to the membrane for allosteric activation by DAG (in the presence of phosphatdylserine); for cPKCs the initial recruitment event is calcium dependent.

1.2.5 PKC Phosphorylation

1.2.5.1 PKC Priming Phopshorylation sites

The regulation of PKC through co-factor binding is subject to a complex amplitude control via the phosphorylation of three key 'priming' sites, which are permissive for subsequent allosteric activation (Parekh et al., 2000). These priming phosphorylation sites are characteristic of AGC kinase superfamily members and comprise the activation loop (or T-loop) site, the autophosphorylation ('TP') site and the hydrophobic (or 'FSY') site. They are conserved throughout the PKC kinase superfamily, and throughout evolution, with the exception that the FSY site is substituted with glutamate in the aPKCs, and aspartate in the PKNs; these acidic residues may mimic phosphorylation (see Figure 1.5).

Phosphorylation of the T-loop site is critical for PKC activity; catalytic competence is abolished in a PKC-α T-loop T497 mutant (Cazaubon et al., 1994), and impaired in the corresponding PKC-δ T505 mutant (Le Good et al., 1998). Based upon the detailed structural analysis of PKA, the phosphorylated PKC T-loop was predicted to correctly align active site residues for catalytic activity (Cazaubon et al., 1994; Knighton et al., 1991; Orr and Newton, 1994). This prediction has been borne out following the resolution of the PKC-θ structure (Xu et al., 2004).

Phosphorylation of the T-loop site is, in most cases, catalysed by polyphosphoinositide-dependent kinase 1 (PDK1) (Chou et al., 1998; Le Good et al., 1998). However, recent kinetic analyses indicate that the PKC-θ T-loop site may be autophosphorylated (Czerwinski et al., 2005). This is consistent with previous data that showed the kinase dead mutant of PKC-θ not to be phosphorylated at the T-loop (Liu et al., 2002), as well as with the finding that the wild type, but not kinase dead, PKC-θ catalytic domain is phosphorylated in bacteria (Xu et al., 2004). It has been proposed that the sequence surrounding the PKC-θ T-loop site, uniquely, bears attributes of a PKC consensus (Xu et al., 2004).

The 'TP' and 'FSY' priming phosphorylation sites play more subtle roles in maintaining a closed PKC conformer, conferring optimum thermal stability and resistance to proteases and phosphatases (Bornancin and Parker, 1997). The PKC-ι and PKC-θ crystal structures define important intramolecular interactions mediated by the 'TP' and 'FSY' sites respectively, which serve to stabilise PKC conformation (Messerschmidt et al., 2005; Xu et al., 2004).

The 'TP' site has been shown to represent an autophosphorylation site (Flint et al., 1990; Standaert et al., 2001). Removal of the PKC-α 'TP', T638, results in its impaired function, however, mutation of the corresponding PKC-β_{II} residue, T641, can be compensated for through the phosphorylation of other local sites (see (Newton, 1997)).

The phosphorylation of the hydrophobic 'FSY' site has been shown to represent the rate limiting step for the occupation of all three priming phosphorylation sites in PKC-α (Bornancin and Parker, 1997). This is likely to relate to the observation that the "FSY' site is involved in the recruitment of PDK1 (Balendran et al., 2000). Like the 'TP', the 'FSY' site is also phosphorylated through an autocatalytic mechanism in cPKCs ((Behn-Krappa and Newton, 1999; Dutil et al., 1994; Dutil et al., 1998). However, the pathway(s) to the phosphorylation of the hydrophobic motif in nPKCs remain more elusive. Cenni *et al* have presented evidence for autophosphorylation (Cenni et al., 2002), while Parekh and colleagues have shown, under different experimental conditions, that an upstream kinase activity is required (Parekh et al., 1999). Previous data from our laboratory suggests that an aPKC complex may be responsible for phosphorylation of the hydrophobic motif (Ziegler et al., 1999), with a parallel, mTOR regulated, amino acid sensing pathway providing a permissive signal, possibly through control of a protein phosphatase (Parekh et al., 1999).

A significant observation with regards to the PKC priming phosphorylation sites relates to their relative stablility. Unlike PKB, c/nPKC retains its priming phosphorylations following the release of its activator, DAG. In fact, the closed, but phosphorylated, latent PKC conformer is relatively resistant to phosphatases. An important consequence of this behaviour is that an accumulation of phosphorylated PKC isoforms is permitted, which may serve to integrate information over time (Parekh et al., 2000). It is also important to note that the processes of PKC phosphorylation and degradation are intimately linked (see Section 1.3.5).

1.2.5.2 Further Autophosphorylation Sites

In addition to the 'TP'/'FSY' priming phosphorylation sites, a number of other autophosphorylated PKC residues have been reported including T250 in PKC-α (Ng et al., 1999) and multiple sites in PKC-β (Flint et al., 1990). Notably, phospho-specific antibodies which recognise these sites may be applied as markers of active PKC; this can be of use both experimentally, allowing the detection of a specific subpopulation of the enzyme, and clinically, facilitating the analysis of disease tissues for aberrant PKC activation (Ng et al., 1999).

1.2.5.3 Tyrosine Phosphorylation

PKC is also subject to tyrosine phosphorylation. To date this has been most thoroughly studied with respect to the PKC-δ isoform, which is phosphorylated on multiple tyrosine residues in cells transformed with Src or Ras or acutely stimulated with hydrogen peroxide, TPA, EGF or PDGF (see (Steinberg, 2004) for a recent review). The roles of certain of these sites have been characterised, for example, phosphorylation at Tyr-332 creates a docking site for the SH2 domain of Shc, mediating an interaction relevant to mast cell degranulation (Leitges et al., 2002).

T-loop site

```
Pkc1     HIKIADYGLCKDEMWYGNRTSTFCGTPEFMAPE....
PKCα     HIKIADFGMCKEHMMDGVTTRTFCGTPDYIAPE....
PKCδ     HIKIADFGMCKENIFGESRASTFCGTPDYIAPE....
PKCε     HCKLADFGMCKEGILNGVTTTFCGTPDYIAPE....
PKCζ     HIKLTDYGMCKEGLGPGDTTSTFCGTPNYIAPE....
PKN1     YVKIADFGLCKEGMGYGDRTSTFCGTPEFLAPE....
PKB      HIKITDFGLCKEGIKDGATMKTFCGTPEYLAPE....
P70s6k   HVKLTDFGLCKESIHDGTVTHTFCGTIEYMAPE....
          *   *  *  ***        *****      ***
```

'TP' site   'FSY' site

```
Pkc1     FTSAPPTLTPLP-SVLTTSQQE----EFRGFSFMPDDLD
PKCα     FTRGQPVLTPPDQLVIANIDQS----DFEGFSYVNPQFV
PKCδ     FLNEKARLSYSDKNLIDSMDQS----AFAGFSFVNPKFE
PKCε     FTREEPVLTLVDEAIVKQINQE----EFKGFSYFGEDLM
PKCζ     FTSEPVQLTPDDEDAIKRIDQS----EFEGFEYINPLLL
PKN1     FTGEAPTLSPPRDARPLTAAEQ---AAFLDFDFVAGGC-
PKB      FTAQMITITPPDQDDSMECVDSERRPHFPQFSYSASGTA
P70s6k   FTRQTPVDSPDDSTLSESANQV-----FLGFTYVAPSVL
          *                          *   *
```

Figure 1.5 AGC Kinase Priming Phosphorylation Sites. Sequence alignments are shown surrounding the three priming phosphorylation conserved among the AGC kinases. Stars denote residue identity; dots represent a separation of approximately 125 residues between the two stretches of sequence. All sequences are human, with the exception of Pkc1 from *S.cerevisiae*. Accession numbers: pkc1, NP_009445; PKC-α, NP-002728; PKC-δ, AAH43350; PKC-ε NP_005391; PKC-ζ, NP_002735; PKN1, NP_998725; PKB, NP_001014432; p70^{S6K}, NP_003152.

49

1.2.6 PKC Binding Partners

A number of functionally significant PKC interacting proteins have been
identified and characterised. Binding partners have been shown to
influence a variety of PKC properties, including activation, inactivation,
localisation and substrate engagement (Parker et al., 2003).

The Drosophila InaD (Inactivation No-After Potential) protein provides a
compelling example of a binding partner which influences PKC activation.
InaD functions as a multivalent scaffolding protein, its five PDZ domains
facilitate the assembly of a multiprotein signalling complex containing the
transient receptor potential protein, phospholipase C-β, and InaC (eye-
PKC). Juxtaposition with regulators serves to control the activity of InaC
during the visual response (Tsunoda et al., 1997).

Atypical PKCs can also be regulated through protein-protein interactions.
The binding of cdc42/PAR6/PAR3 influences aPKC activity, within a
complex implicated in establishing cell polarity (Ohno, 2001).
Conversely, other partners participate in down-regulation; pVHL, an E3
ubiquitin ligase with activity towards activated atypical PKC-λ, was first
associated with PKC as a binding protein (Okuda et al., 1999; Okuda et
al., 2001).

Perhaps the most thoroughly studied of the PKC binding partners are
those that serve to regulate localisation, as exemplified by the Receptors
for activated c-kinase (RACKs). RACKs bind selectively to activated
PKCs, but do not represent substrates, rather, it is suggested that they
anchor translocated PKCs in specific membrane domains, in close
proximity to appropriate substrates (Mochly-Rosen, 1995). Mapping
studies have revealed that WD40 motifs in isoform specific RACKs for
PKC-β (RACK1, (Mochly-Rosen and Gordon, 1998)) and PKC-ε (β'-COP,
(Csukai et al., 1997)), interact with unique peptide sequences in the PKC
regulatory domains. Other sequences within these PKC isoforms have
been identified which bear homology with the corresponding RACK

(pseudo-RACK motifs); it has been postulated that the RACK binding site and the pseudo-RACK sequence undergo intra-molecular interaction, serving to stabilise an inactive PKC conformation. Synthetic peptides based on the RACK binding site sequence interfere with PKC redistribution, and thereby act as PKC inhibitors; conversely, peptides based on the pseudo-RACK sequence serve to activate the enzyme. Such peptides have been exploited to regulate specific PKC isoforms both experimentally in cellular systems (Ron et al., 1995), and therapeutically in animal models (Tanaka et al., 2005; Tanaka et al., 2004).

Another binding partner that may relate to PKC targeting is actin. PKC-βII (Blobe et al., 1996) and PKC-ε (Prekeris et al., 1996) have been shown to localise with and bind directly to actin; PKC-δ has also been linked to actin in neutrophils (Lopez-Lluch et al., 2001), as has PKC in Aplysia (Nakhost et al., 1998). In the case of PKC-ε, the interaction has been mapped to an actin binding hexapeptide between the C1a and C1b domains (Prekeris et al., 1998); a mutant lacking this motif loses the ability to bind to actin *in vitro* and colocalise with actin in zones of adhesion. It has been postulated that interaction with actin stimulates PKC-ε phosphotransferase activity, while reciprocally, PKC-ε promotes the stablisation and elongation of actin filaments (through a kinase-independent mechanism) (Hernandez et al., 2001). The actin binding site has been shown to be important for neurite outgrowth during neuronal differentiation, however, this would appear to reflect an indirect effect on conformation or localisation, since an actin binding site peptide suppresses outgrowth induced by full length PKC-ε, but not an isolated regulatory domain (Zeidman et al., 2002).

Binding partners can also serve to integrate PKC signalling with inputs from other pathways. For example, by binding to both PKA and PKC, gravin facilitates coordination of signal transduction events in the filopodia of human erythroleukemia cells (Nauert et al., 1997).

A final class of PKC interacting proteins comprise the Substrates That Interact with C-Kinase (STICKs) (Chapline et al., 1993). Substrates are considered further in Section 1.2.7.

1.2.6.1 PKC & 14-3-3

A number of studies have explored the physical and functional relationships between PKC and 14-3-3 families, which are relevant to work presented later in this thesis. Conflicting results have been obtained, and a coherent model of the association between these two proteins has yet to be defined. Disparity is likely to stem in part from the use of different PKC isoforms, cell types and stimuli.

The first study to describe a connection between PKC and 14-3-3 defined a 14-3-3 population isolated from sheep brain as a potent inhibitor of PKC (Toker et al., 1992). Subsequently, direct binding of 14-3-3τ to PKC-θ in Jurkat T cells (Meller et al., 1996), and of 14-3-3ζ to myosin II heavy-chain-specific PKC in Dictyostelium (Matto-Yelin et al., 1997), was shown to correlate with PKC inhibition.

Conversely, work from other groups has implicated 14-3-3 binding in the activation of PKC. Tanji and colleagues demonstrated that 14-3-3 purified from bovine forebrain was able to activate PKC independently of phosphatidylserine and calcium (Tanji et al., 1994). Subsequently, it has been shown that cPKCs, nPKCs and aPKCs can all bind to 14-3-3ζ in rodent brain, and that interaction leads to constitutive activity (Dai and Murakami, 2003). Interaction was shown not to require phosphorylation, and to occur via the C1 domain, in agreement with data from Matto et al (Matto-Yelin et al., 1997). It has been postulated that PKC activation may result rather non-specifically from the charge properties of these proteins, since numerous acidic proteins have been shown to confer the same effects (Van Der Hoeven et al., 2000).

Intriguingly, an element of PKC isoform specificity has been demonstrated in certain assay systems exploring 14-3-3 effects. Both PKC-α and PKC-ε have both been shown to become associated with 14-3-3ζ upon NGF induced neuronal differentiation in PC12 cells (Gannon-Murakami and Murakami, 2002). However, the PKC population immunoprecipitated via 14-3-3 was shown to exhibit constitutive and autonomous nPKC (PKC-ε), but not cPKC (PKC-α), activity. Consistent with this, Acs and colleagues found that recombinant 14-3-3ζ mediated differential activation of PKC isoforms, in a lipid independent manner, with PKC-ε the most strongly activated (Acs et al., 1995). That interaction with 14-3-3 can mediate alternative effects on different PKC isoforms may in part explain the conflicting results obtained in other studies. It also raises interesting questions about the mechanisms and consequences of these differential effects, which remain to be investigated.

1.2.7 PKC Substrates

The PKC superfamily comprises a collection of promiscuous kinases with broadly overlapping specificities. Many *in vitro* substrates have been reported, demonstrating that PKC is a basophilic kinase (reviewed by (Hofmann, 1997)), which strongly disfavours a proline residue at the +1 position (Zhu et al., 2005a). However, the characterisation of physiologically relevant substrates, associated with particular PKC isoforms, has proved more challenging (Parker and Murray-Rust, 2004).

Myristoylated alanine-rich C kinase substrate (MARCKS) was one of the first PKC substrates to be identified, and its sites of phosphorylation conform to a basic consensus (Stumpo et al., 1989). PKC mediated phosphorylation has been shown to bring about dissociation of MARCKS from the membrane (Thelen et al., 1991). Since one function of MARCKS is to sequester PI(4,5)P$_2$, it has been speculated that this serves to increase available PI(4,5)P$_2$, resulting in a dynamic reorganisation of the microfilaments (see (Larsson, 2005) for review).

While the presence of an appropriate PKC consensus sequence is clearly important in defining a PKC substrate, within a cellular setting, the accessibility of the protein to PKC is equally significant. An interesting example in this regard is provided by RasGRP3 in B-cells. As a C1-domain containing protein, RasGRP3 is recruited to the membrane upon DAG production, alongside active PKC, such that phosphorylation at T133 can proceed (Zheng et al., 2005). Similarly, PKD is a PKC substrate that is responsive to DAG (Yuan et al., 2002); the modulation of PKD by PKC plays an important role in antigen receptor signalling in lymphocytes (Matthews et al., 2000).

1.2.8 PKC Down-regulation

A characteristic property of the classical and novel PKC isoforms is that their chronic activation frequently leads to their down-regulation (Ballester and Rosen, 1985; Stabel et al., 1987). This agonist induced inactivation results from an increase in the rate of PKC degradation, rather than from a decrease in its rate of synthesis (Young et al., 1987). The down-regulation of PKC represents an important, yet poorly characterised, phase of its 'life cycle'; it may in fact be intrinsic to the tumour promoting activity of phorbol esters such as TPA (Young et al., 1987).

The multistage process of carcinogenesis has been extensively studied using the development of squamous cell cancers on mouse skin as a model (see (Yuspa, 1998) for a review). In this system, TPA serves as a powerful tumour promoter, increasing sensitivity to papilloma formation in combination with tumour initiators. Identification of PKC as a major cellular target of TPA (Castagna et al., 1982) strongly implicated the enzyme in the process of carcinogenesis; subsequent work demonstrated the involvement of PKC more directly (Dlugosz et al., 1994). Intriguingly, an alternative PKC activator, Bryostatin 1, acts as an inhibitor of TPA-induced tumour promotion in skin (Hennings et al., 1987). Bryostatin 1 has been shown to differentially down-regulate various PKC isoforms (Szallasi et al., 1994). As such, it has been speculated that TPA-induced tumour promotion is dependent upon a particular profile of PKC isoform

activation/inactivation (Hale et al., 2002). Consistent with this, overexpression of PKC-δ has been shown to decrease both the incidence and promotion of skin tumours in mice (Reddig et al., 1999), while overexpression of PKC-ε, under the control of the same promoter, decreased papilloma burden and accelerated progression to carcinoma (Reddig et al., 2000).

The mechanisms that have been implicated to date in the control of PKC degradation are described in section 1.3.5.

1.2.9 PKC and Cancer

There has been considerable interest in the potential role of the PKC superfamily in cancer progression. This stems largely from the fact that the PKC activating phorbol esters also act as potent tumour promoters (see above). In addition, PKC has been directly linked to the control of many cellular processes relevant to neoplastic transformation, carcinogenesis and invasion, including proliferation (Soh and Weinstein, 2003), apoptosis (DeVries et al., 2002; Mandil et al., 2001) and migration (Ivaska et al., 2003).

A number of studies have investigated whether mutations in PKC are associated with certain cancers. A mutation in the PKC-α V3 region, D279G, has been detected in human pituitary (Alvaro et al., 1993), thyroid (Prevostel et al., 1997) and breast (Vallentin et al., 2001) tumours, which may serve to target the protein to cell-cell contacts. Additionally, a rearrangement and amplification of the PKC-ε gene was detected from a thyroid cancer cell line, which resulted in the overexpression of a truncated, dominant negative form of the protein, which protected cells from apoptosis (Knauf et al., 1999).

Other studies have screened for changes in the expression patterns of different PKC isoforms in cancer samples. Increased levels of PKC have been detected in cells derived from carcinomas of the breast (O'Brian et

al., 1989) and lung (Takenaga and Takahashi, 1986). Conversely, major, isoform-specific reductions of PKC-ε, which were shown to occur post-transcriptionally, we detected in certain thyroid papillary carcinomas (Knauf et al., 2002). Interestingly, Mandil and colleagues showed that higher levels of PKC-α, but lower levels of PKC-δ, were detected specifically in malignant gliomas (Mandil et al., 2001).

Since PKC comprises an enzyme activity subject to acute allosteric regulation, it may in fact be more informative to analyse its activation state than its protein concentration in addressing its the potential involvement in disease (Parker, 1999). This strategy was pioneered by Ng and colleagues, who employed a marker of PKC-α activation, the phosphorylation of its Thr-250 site, to screen breast tumour samples. Activated PKC-α was identified in 11 out of 23 specimens, and notably, activation was not shown to correlate with overexpression in all cases (Ng et al., 1999). It will be of interest to exploit a similar approach in order to analyse the roles of other PKC isoforms in disease.

Despite all of this data, the role of PKC in tumour progression is still conjectural. It remains to be established whether an alteration of PKC, either by mutation or dysregulated expression, actually represents the rate-limiting event in any form of cancer (Parker, 1999). It is currently unclear whether the mutations noted above represent causes, or consequences, of malignancy. Nevertheless, it is clear that within the context of an established tumour, PKC may play an important role. PKC-ε has recently been shown to correlate with an aggressive, metastatic phenotype in breast cancer; *in vivo* tumour growth of associated samples was significantly retarded following RNA interference of PKC-ε (Pan et al., 2005).

The resolution of this issue is impeded somewhat by the multiplicity of the PKC isoforms, which have different, and sometimes opposing, functions. The development of isoform selective inhibitors will go some way to

clarifying this matter, and if a correlation is established, will provide an impetus to the development of further such compounds as therapeutics. For instance, a PKC-β selective inhibitor is already under analysis as a treatment for microvascular complications associated with diabetes (Joy et al., 2005).

A number of PKC inhibitors have been assessed as anticancer drugs in clinical trials (see (Mackay and Twelves, 2003) for a review), including the bryostatins, which are thought to function by mediating the down-regulation of certain PKC isoforms (Hale et al., 2002). Although the success of these trials has been limited, there is some evidence that certain of these compounds may have improved therapeutic efficacy when administered in combination with established cytotoxic agents, and may also sensitise cells to ionising radiation.

1.3 Protein Degradation

Most cellular proteins are subject to continuous cycles of synthesis and degradation; their half-lives vary enormously, ranging from a few seconds to many days (Schimke, 1973). Among the numerous functions of intracellular proteolysis are the elimination of abnormal proteins, the maintenance of amino acid pools under conditions of starvation, and the activation of precursor proteins (Varshavsky, 1996). Significantly here, proteolytic pathways also operate to mediate the selective destruction of proteins whose concentrations must vary according to time and/or cellular context. Metabolic instability is a key property of many regulatory proteins, as epitomized by the cyclins (Rechsteiner, 1991).

1.3.1 Proteolysis

Protein degradation is mediated by different proteolytic enzymes, which catalyse the hydrolysis of the peptide bond. Many of the cellular proteases are localised to the lysosomal and proteasomal compartments as described below. Others act at the endoplasmic reticulum (e.g. S2P (Ye et al., 2000)), the mitochondria (e.g. paraplegin (Atorino et al., 2003)) or within the extracellular milieu (e.g. matrix metalloproteinases (Stamenkovic, 2003)).

Additional cytosolic proteases with important cellular functions include the calpains and the caspases. Calpains are calcium-dependent cysteine proteases, which catalyse the limited proteolysis of a range of substrates, to yield often stable fragments whose properties differ from those of the intact protein (see (Sorimachi et al., 1997) for a review). Calpains have been implicated in the regulation of a range of cellular processes, including migration (Franco and Huttenlocher, 2005). The caspases comprise another family of cysteine proteases, which operate as a cascade to coordinate apoptosis; they target a plethora of substrates for limited proteolysis, exhibiting specificity for aspartate residues (reviewed by (Earnshaw et al., 1999)).

1.3.2 Eukaryotic Pathways of Protein Degradation

There are two main routes via which cellular proteins are directed for more complete degradation in mammalian cells, the lysosomal and proteasomal pathways.

The lysosome comprises an acidic compartment, containing a variety of hydrolytic enzymes; the protease complement of the lysosome includes many cathepsins (cysteine proteases), some aspartate proteases and one zinc protease. Extracellular and plasma membrane proteins may undergo lysosomal degradation following internalisation into endosomes, which can then fuse with lysosomes for delivery of their contents. Cytosolic proteins may be targeted to the lysosome non-selectively through autophagic processes, or specifically via the recognition of the KFERQ motif (see (Cuervo and Dice, 1998) for review).

The major extralysosomal proteolytic pathway is mediated via the proteasome; this system is pertinent to work presented later in this thesis and is considered in more detail below.

1.3.3 Ubiquitin/Proteasome System

The ubiquitin/proteasome system is responsible for the regulated proteolysis of many target proteins, and plays a critical role in the control of numerous cellular processes, most notably, the cell cycle (King et al., 1996a). An overview of this degradative pathway is represented in Figure 1.6. Typically, a target protein is flagged for proteolysis with a polyubiquitin chain, and is subsequently degraded at the proteasome (comprehensively reviewed by (Hershko and Ciechanover, 1998)).
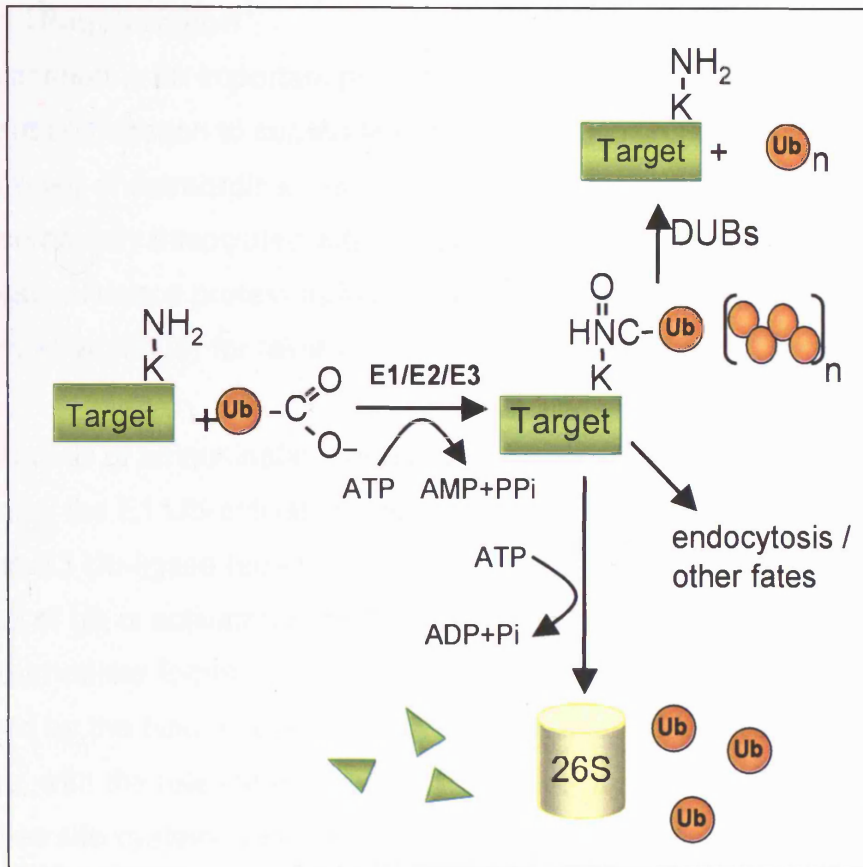
Figure 1.6 The Ubiquitin/Proteasome System. The ubiquitin/ proteasome pathway is represented schematically. A target protein is tagged for degradation via the polyubiquitination of a particular lysine residue. This process is mediated by the sequential activities of E1, E2 and E3 enzymes, and may be antagonised through the action of deubiquitylating enzymes (DUBs). Polyubiquitinated protein is directed to the proteasome for ATP-dependent degradation, generating target protein fragment peptides and recycling ubiquitin (ubiquitination may also target proteins for other fates eg. endocytosis (d'Azzo et al., 2005)).
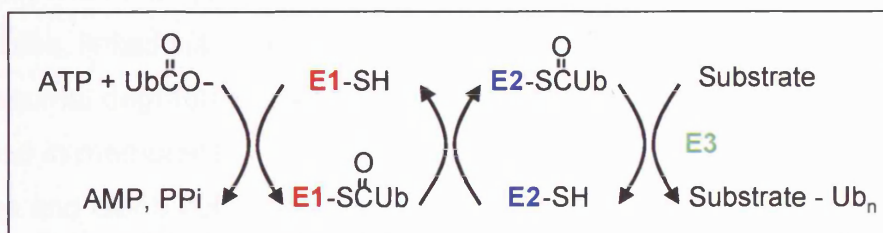
Figure 1.7 Enzymatic Pathway of Ubiquitin Conjugation.
Ubiqutination is mediated by the sequential activities of 3 enzymes. Ubiquitin is activated by E1 in an ATP-dependent fashion, transferred to the active site of an E2 conjugating enzyme and finally linked to a target protein lysine residue in a step catalysed by an E3 ligase.

1.3.3.1 Ubiquitination

Ubiquitination is an important post-translational modification involving the covalent conjugation to substrate proteins of ubiquitin (Ub), a 76 amino-acid protein of extraordinary evolutionary conservation. Ubiquitination is most commonly associated with targeting proteins for degradation, but may also influence protein trafficking and protein-protein interactions (see (d'Azzo et al., 2005) for review).

The process of ubiquitination requires the sequential action of three enzymes, the E1 Ub-activating enzyme, the E2 Ub-conjugating enzyme and the E3 Ub-ligase (see Figure 1.7). Firstly, the C-terminal glycine residue of Ub is activated in an ATP-dependent step by E1; this involves the intermediate formation of ubiquitin adenylate, with the release of PPi, followed by the binding of Ub to a cysteine residue of E1 in a thiolester linkage, with the release of AMP. Activated ubiquitin is next transferred to an active site cysteine residue of the E2 enzyme. In the third step, catalysed by an E3-ligase, ubiquitin is linked by its C-terminus, in an isopeptide linkage, to the ε-amino group of a substrate protein lysine residue (see (Pickart, 2001) for review).

Some substrates are modified with a single Ub moiety, but since Ub itself contains seven lysine residues, repetition of the conjugation reaction can also result in the formation of polyubiquitin chains. The fate of the ubiquitylated protein depends upon the length and the linkage type of the ubiquitin chain. In general, substrates with chains of four or more Ub molecules, linked via lysine 29 or 48, are efficiently targeted for proteasomal degradation, whereas lysine 63-linked chains may be involved in membrane protein endocytosis and kinase activation (see (Strous and Gent, 2002) for review).

1.3.3.2 Proteasomal Degradation

The 26S proteasome is a large (approximately 2.5 MDa), multisubunit, cytosolic protease composed of a 20S catalytic core particle, which is capped on both sides by a 19S regulatory complex (see (Hershko and Ciechanover, 1998) and (von Arnim, 2001) for reviews).

The 20S core complex comprises a cylindrical stack of 4 seven membered rings enclosing a cavity of three compartments. The two outer rings are each composed of 7 α-type proteins, the two inner rings of 7 β-type proteins, 3 of which bear protease activity (chymotrypsin-like, trypsin-like and caspase-like). The proteasomal hydrolases comprise a unique family of threonine protease; proteasome inhibitors target the active site threonine (Lee and Goldberg, 1998).

The 19S cap complex is responsible for recognition and unfolding of polyubiquitinated proteins, threading the substrates into the core complex and removing Ub moieties for recycling. The 'lid' of the cap comprises a ring of 8 proteins, the 'base' includes 6 ATPases, which mediate unfolding. An 11S cap may also be associated with the proteasome, allowing small, non-ubiquitinated proteins to enter the core complex (Glickman, 2000).

Typically, the proteasome mediates the hydrolysis of substrates into 8-11 amino acid peptides, which may be further hydrolysed to amino acids by other peptidases, although occasionally limited processing yields biologically active fragments.

1.3.4 E3 Ubiquitin Ligases

The E3 ligase component of the ubiquitin system is responsible for substrate recognition and therefore confers specificity. As such, the E3s represent a functionally important class of proteins, which have been much studied in recent years; the following provides an overview of their established characteristics.

1.3.4.1 Degrons

The features of a protein that confer metabolic instability are called degrons; they constitute the degradation signals, which are recognised by the E3 Ub-ligases (Varshavsky, 1991).

The first degron to be identified comprises the N-terminal amino acid of the target protein, and forms the basis of the 'N-end rule' (see (Varshavsky, 1996) for a review). This rule relates the *in vivo* half-life of a protein to the identity of its N-terminal residue. Certain N-terminal residues, including arginine, lysine, histidine, phenylalanine, leucine, tryptophan, tyrosine and isoleucine, confer a destabilising effect on the protein, such that its half-life is in the region of 3 minutes. Others, including methionine, are stabilising, such that the protein may persist for days.

Another motif that has been implicated in protein degradation is the PEST sequence (see (Rechsteiner and Rogers, 1996)for a review). The PEST motif is a region enriched in proline (P), glutamate (E), serine (S) and threonine (T), typically flanked by lysine, arginine or histidine, and uninterrupted by positively charged residues. PEST sequences are found in a large number of rapidly degraded proteins, including c-myc, c-jun, and cyclin E, but their mode of action is not well defined. Perhaps significantly, the S/TP phosphodegrons described below are frequently found within PEST motifs (Hershko and Ciechanover, 1998).

The destruction box (D-box) is a degron that plays a key role in the degradation of mitotic cyclins. It is comprised of a 9-amino acid motif with some homology to the following consensus: **RA**ALG**X**IG**N** (where bold indicates invariant residues; and X, any amino acid) (Hershko and Ciechanover, 1998). The D-box is necessary for mitotic cyclin degradation both *in vitro* and *in vivo*, and can mediate cell cycle stage specific degradation of fused reporter proteins via the cyclosome/anaphase-promoting complex (APC) (King et al., 1996b).

63

Additionally, phosphorylated motifs, or phospho-degrons, are critical to the degradation of certain proteasomal targets. For instance, the F-box components of the Skp1/Cullin/F-box (SCF) E3 ligases specifically recognise phosphorylated substrates (Skowyra et al., 1997). As described in Section 1.3.4.4, solution of the Cdc4 crystal structure, in the presence of an optimal phospho-degron, provides a rationale for this preference (Orlicky et al., 2003).

1.3.4.2 Classes of E3 Ubiquitin Ligases

There are four main classes of E3 ubiquitin ligase. The main N-end rule E3, N-recognin, is among the best characterised (see (Varshavsky, 1996) for a review). The other classes include the HECT type E3s, the U-boxes type E3s and the RING-finger type E3s.

The homologous to E6-AP carboxy terminus (HECT) type E3 Ub-ligases are exemplified by E6-AP, which catalyses p53 ubiquitylation in a manner dependent upon the human papilloma virus gene product E6. A characteristic property of this subclass of E3 ligase is that they participate directly in the transfer of Ub to the substrate; Ub is transferred from the E2 to an E3 active site cysteine, and from here it is donated to the substrate (Pickart, 2001).

The U-box type E3 Ub-ligases are typified by yeast Ufd2. These are the most recently identified of the E3 ligases and remain to be thoroughly investigated. It would seem though, that a characteristic feature of E3s of this class is that they mediate unusual patterns of polyubiquitin chain assembly, linking additional Ub moieties to lysines other than the established 29, 48 and 63 sites, and thereby producing heterogeneous branched structures, with distinct biological functions (Hatakeyama and Nakayama, 2003).

The really interesting new gene (RING)-finger type E3s are the final class of Ub-ligase defined to date (see (Pickart, 2001) for a review). They are distinguished by the presence of a RING finger structure, comprising a

64

series of histidine and cysteine residues, with a characteristic spacing that allows for the coordination of two zinc ions in a cross-brace formation. The RING finger serves as a molecular scaffold, recruiting E2s in a specific and catalytically productive manner. There are two main types of RING-type E3s, those comprising a single subunit, the single-polypeptide RING-finger (SPRF) Ub-ligases, such as Cbl (Joazeiro and Weissman, 2000), and those which contain a RING finger protein as part of a multimeric complex, these include the SCF, the Cul2-Elongin B-Elongin C (CBC), and the cyclosome/APC, and are structurally analogous.

1.3.4.3 SCF E3 Ubiquitin Ligases

The SCF complex has three primary subunits: Skp1, Cullin (Cul) and the RING finger protein Rbx1/Roc1/Hrt1 (Deshaies, 1999). This complex can interact with an assortment of modular F-box proteins, which all bind to Skp1 via a conserved N-terminal F-box domain (see Figure 1.8) (Bai et al., 1996). The F-box proteins are responsible for substrate recognition and recruitment, which they mediate through a C-terminal substrate binding domain (Skowyra et al., 1997).

F-box proteins are defined by the nature of their substrate binding domain, which may be based on WD40 domains (Fbw), leucine-rich repeats (Fbl) or other sequences (Winston et al., 1999). Typically, they recognise phospho-degrons, and thereby allow for sophisticated substrate discrimination, which is regulated dynamically by kinase signalling (Skowyra et al., 1997). This mechanism is well defined with respect to the SCF^{Fbw7} E3 Ub-ligase and is considered in more detail below (see Section 1.3.4.4).

Interestingly, the SCF complex itself is also subject to post-translational modification. For instance, the cullin subunit undergoes neddylation, resulting in a dramatic increase in Ub transfer from the associated E2 to target; Nedd8 is a 76-residue protein with homology to ubiquitin (Lammer et al., 1998). It has been speculated that various components of the SCF

complex may also be regulated by phosphorylation, for example, Skp1 is phosphorylated upon expression in insect cells (Deshaies, 1999); to date though, there are no well defined functional consequences associated with a particular phosphorylation event.

1.3.4.4 F-box WD40 Protein 7

The SCF^{Fbw7} complex is one of the best characterised of the E3 Ub-ligases and is relevant to work described later in this thesis. The following provides an overview of the main features of the substrate recognition component, F-box WD40 Protein 7 (Fbw7).

Fbw7 is the apparent mammalian homologue of yeast cdc4. It is comprised of an N-terminal F-box domain and a C-terminal substrate binding domain, the latter is based on 8 WD40 repeats, which fold to form an unusual 8-bladed propeller structure (Orlicky et al., 2003). In mammalian cells, Fbw7 comprises three isoforms: α, β and γ. These isoforms differ only with respect to their extreme N-termini, which possess signals mediating their differential localisation; Fbw7α is nuclear, Fbw7β is cytoplasmic, and Fbw7γ is nucleolar (Welcker et al., 2004).

SCF^{Fbw7} has been shown to mediate the poly-ubiquitination and subsequent proteasomal degradation of numerous substrates, including cyclin E (Moberg et al., 2001; Strohmaier et al., 2001); c-myc (Moberg et al., 2004; Welcker et al., 2004; Yada et al., 2004); c-jun (Nateri et al., 2004); Notch (Gupta-Rossi et al., 2001; Oberg et al., 2001; Wu et al., 2001) and presenilin (Li et al., 2002; Wu et al., 1998). Interestingly, cyclin E degradation has also been demonstrated within the context of a novel E3 Ub-ligase, containing Fbw7, Cul1, and the RING finger protein Parkin (Staropoli et al., 2003). Through the degradation of these target substrates, SCF^{Fbw7} plays a critical role in controlling cell cycle progression (Feldman et al., 1997), cell growth (Welcker et al., 2004) and apoptotic JNK signalling in neurons (Nateri et al., 2004). Fbw7 null mice display elevated levels of both cyclin E and Notch1/4, and die at

approximately day 10 of gestation from multiple defects, including deficiences in hematopoietic and vasular development (Tetzlaff et al., 2004). Significantly, Fbw7 has been identified as a tumour suppressor gene (Mao et al., 2004); it is mutated in a number of cancer cell lines (Moberg et al., 2001; Strohmaier et al., 2001) and its loss of function is associated with genomic instablility (Perez-Losada et al., 2005; Rajagopalan et al., 2004).

Fbw7 recognises and specifically interacts with a phospho-threonine-proline (pTP) based motif, termed the cdc4 phospho-degron (CPD), in all documented substrates (Nash et al., 2001). The resolution of the crystal structure of yeast cdc4 provides a rationale for this mode of recognition, defining a dedicated pThr-Pro binding pocket, as well as a deep groove which exerts a preference for hydrophobic residues N-terminal to the phospho-site (see Figure 1.9). In yeast, phosphorylation of numerous sub-optimal CPDs is required for cdc4 catalysed degradation of Sic1, setting a threshold that influences the onset of DNA replication (Nash et al., 2001). An equivalent mechanism has not been detected in mammalian cells to date and there are clear examples in which a single site is critical. For instance, a mutation in v-jun, which prevents its phosphorylation by GSK3, allows it to escape recognition by Fbw7; it is postulated that its increased stability contributes to its transforming capacity (Wei et al., 2005). Also significant is the fact that additional Fbw7 binding proteins can be recruited using the same mechanism, effectively competing with substrates. For instance, the large T antigen contains a 'decoy' CPD through which it can bind to Fbw7γ and mediate its mislocalisation to the nucleoplasm (Welcker and Clurman, 2005).
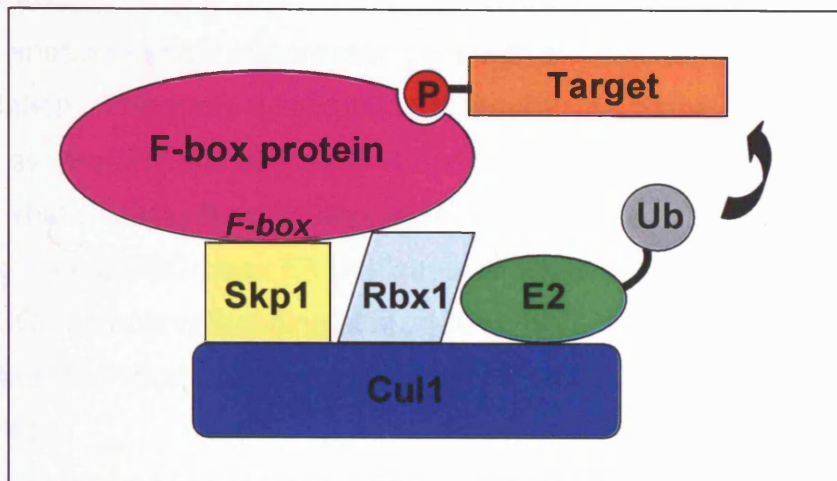
Figure 1.8 Schematic representation of the SCF E3 ligase complex.
The organisation of the SCF E3 ubiquitin ligase is represented
schematically. Skp1, Rbx1 and Cul1 comprise the core components of
the complex. The variable F-box protein binds to Skp1 via its F-box
domain and confers substrate specificity, typically recognising a particular
phospho-degron in its target protein. The SCF complex facilitates the
transfer of ubiquitin from the E2 conjugating enzyme to the target protein.
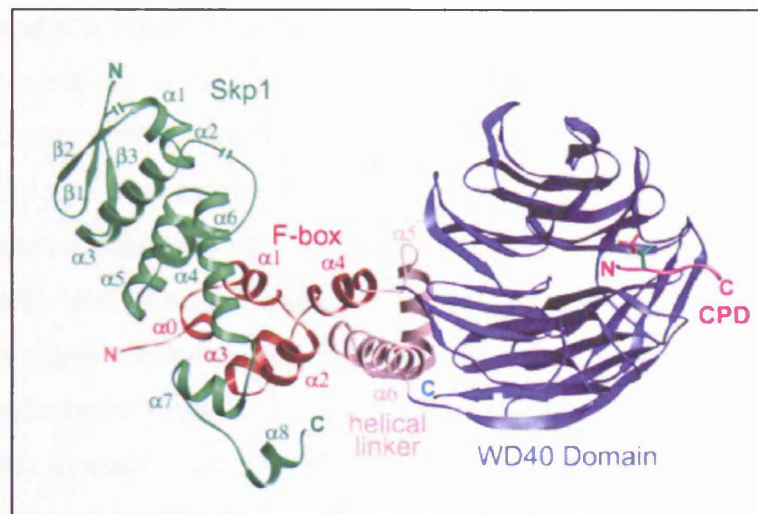
**Figure 1.9 Representation of the Crystal Structure of the SCF^{cdc4}
complex.** The crystal structure of the SCF^{cdc4} E3 ligase in complex with
an optimal phospho-degron peptide (CPD) is represented. Skp1 is
shown in green, the F-box domain of cdc4 in red, and the WD40 based
substrate binding domain of cdc4 in blue. (Figure reproduced from
(Orlicky et al., 2003)).

1.3.4.5 VHL

VHL is another tumour suppressor gene with an important role in protein degradation. This protein is mutated in familial von Hippel-Lindau (VHL) cancer syndrome (Latif et al., 1993) and in the majority of kidney cancers (Shuin et al., 1994). It associates with Elongin C, Elongin B, Cullin-2 and Rbx1 to form a CBC class E3 Ub-ligase, which is structurally analogous to the SCF complex (Stebbins et al., 1999). VHL is a SOCS-box protein, which like the F-box protein component of the SCF, confers substrate recognition.

The most well established substrate for the VHL E3 ligase to date is hypoxia inducible factor-1α (HIF-1α) (Maxwell et al., 1999) (Cockman et al., 2000). Rather than targeting a phospho-degron, VHL specifically recognises this substrate via an hydroxylated proline (Ivan et al., 2001; Jaakkola et al., 2001); the structural basis of this interaction has been defined (Hon et al., 2002). The modification of HIF-1α by proline hydroxylases is a process dependent upon iron and molecular oxygen, and thus the activity of the VHL Ub-ligase is implicated in oxygen sensing. Under normoxic and iron replete conditions, HIF-1α is proline hydroxylated and thus targeted for VHL-mediated degradation. However, under hypoxic conditions, HIF-1α is not modified and therefore not recognised by VHL; under these conditions, the transcription factor accumulates and facilitates induction of hypoxia inducible genes, such as vascular endothelial growth factor (VEGF) and erythropoietin. Loss of VHL function through mutation results in a prolonged accumulation of HIF1α, which can contribute to tumour progression by promoting vascularisation (reviewed by (Ivan and Kaelin, 2001)).

It has been speculated that further targets exist for the VHL/CBC Ub-ligase, including activated aPKCs (Okuda et al., 2001); additional substrates, and their associated degrons, remain to be fully characterised.

1.3.4.5.1 VBP1

VHL Binding Protein 1 (VBP1), the focus of some work presented later in this thesis, was originally identified from a human B-cell cDNA library as a VHL interacting partner, and was shown to colocalise with VHL upon coexpression in mammalian cells (Tsuchiya et al., 1996). This prompted speculation about a potential role for VBP1 in protein degradation (Brinke et al., 1997).

However, VBP1 has also been implicated, and studied much more thoroughly, in another context. The amino acid sequence of VBP1 is identical to that of a protein called prefoldin 3 (PFD3), a component of the prefoldin co-chaperone complex. This complex is involved in the delivery of unfolded clients to the TRiC/CCT chaperone, and has been shown to be responsible for the folding of actin and tubulin (Geissler et al., 1998; Vainberg et al., 1998). Notably, VHL has been shown to be recruited to the TRiC/CCT chaperone complex (Feldman et al., 1999), as such, we could speculate that its interaction with VBP1 reflects this aspect of its life-cycle.

1.3.5 Pathways of PKC Degradation

As described in Section 1.2.8, the chronic activation of cPKC/nPKC isoforms by phorbol esters typically leads to their down-regulation (Ballester and Rosen, 1985; Stabel et al., 1987), mediating an increase in the rate of PKC degradation (Young et al., 1987). The down-regulation of PKC represents an important, yet poorly characterised, phase of its 'life cycle', which may be intrinsic to the tumour promoting activity of the phorbol esters (Young et al., 1987). As such, the further elucidation of this process is an important focus for research in our laboratory.

The degron(s) associated with PKC down-regulation remain to be defined. There is no evidence to suggest that under basal conditions the N-terminal residue is implicated, and this would not be expected to contribute to an agonist-induced pathway. In fact, previous work has suggested that the PKC N-terminus is blocked, such that the protein

would be inherently recalcitrant to the N-end E3 ligases (D.Schaap and P.J. Parker, unpublished data). All PKCs, with the exception of the δ isoform, bear a PEST sequence (Lee et al., 1997), but the significance of this motif is unclear. Yeast pck1/2 are rapidly degraded proteins which can be stabilised by association with rho1; since the rho1 binding site lies close to the PEST sequence, it has been speculated, but not proven, that it may serve to occlude this motif (Arellano et al., 1999). However, since PKC-δ is known to undergo TPA-induced degradation, an intact PEST sequence would not appear to be critical (Srivastava et al., 2002). It is also noteworthy that a D-box like motif has been noted in PKC-ε (RLGLDEFNF, 402-410); again the relevance of this site has not been explored (Prekeris et al., 1998).

Early work implicated calpains in the process of PKC-downregulation (Kishimoto et al., 1989). However, the evidence presented derived from the use of inhibitors of limited specificity (Webb et al., 2000), and Junco *et al* proved subsequently that mutants with differential sensitivities to m-calpain were indistinguishable with respect to profiles of TPA-induced degradation (Junco et al., 1994). Caspase mediated, limited proteolysis of certain PKC isoforms has also been detected, in response to apoptotic stimuli, but evidently operates independently of TPA-induced down-regulation (Koriyama et al., 1999). It is noteworthy, however, that caspase cleavage of PKC-ζ can generate a catalytically active fragment that is subsequently degraded by the ubiquitin/proteasome system (Smith et al., 2000). A role for the lysosomal compartment in TPA-induced PKC degradation has also been excluded, since monensin and NH4Cl, which de-acidify the lysosomal compartment and thereby inhibit its hydrolases, have no effect (Lee et al., 1997).

In contrast, there is a growing body of evidence which supports a role for the ubiquitin/proteasome system in the agonist-induced down-regulation of PKC. Ubiquitination of PKC was first reported following the treatment of renal epithelial cells with Bryostatin 1 (Lee et al., 1996b), and has

subsequently been observed in many other systems. Significantly, proteasomal inhibition in these models mediates the accumulation of PKC (Junoy et al., 2002; Lee et al., 1997; Leontieva and Black, 2004; Lu et al., 1998).

PKC activity has been implicated in the pathway(s) of down-regulation. Studies focussed on different PKC isoforms have shown that kinase dead mutants are down-regulation insensitive (Kang et al., 2000; Ohno et al., 1990), and that PKC inhibition can prevent down-regulation (Junoy et al., 2002). Interestingly, studies of mammalian PKCs expressed in yeast would suggest that this catalytic input can be mediated in trans (Parker et al., 1995).

An intimate association has been established between PKC phosphorylation and down-regulation. Experiments with PKC-α and PKC-ε demonstrated that de-phosphorylation of priming sites is a critical step in the process of down-regulation by the ubiquitin-proteasome system (Hansra et al., 1999; Lee et al., 1996a; Lee et al., 1997). Prevostel and colleagues demonstrated that in the case of PKC-α, this pathway involved the cavaolae-dependent trafficking of the dephosphorylated protein to an endosomal compartment (Prevostel et al., 2000). However, this is clearly cell type and/or context dependent, since another report showed that phosphorylation of PKC-δ was required for its degradation in NIH 3T3 cells (Srivastava et al., 2002). More recent work from Leontieva and colleagues provides support for both of these models (see Figure 1.10), revealing two independent pathways of PKC-α desensitization operating in response to the same stimuli, one involving the ubiquitination and subsequent proteasomal degradation of the mature, fully phosphorylated enzyme, the second, a proteasome-independent mechanism, requiring caveolar trafficking and dephosphorylation (Leontieva and Black, 2004).
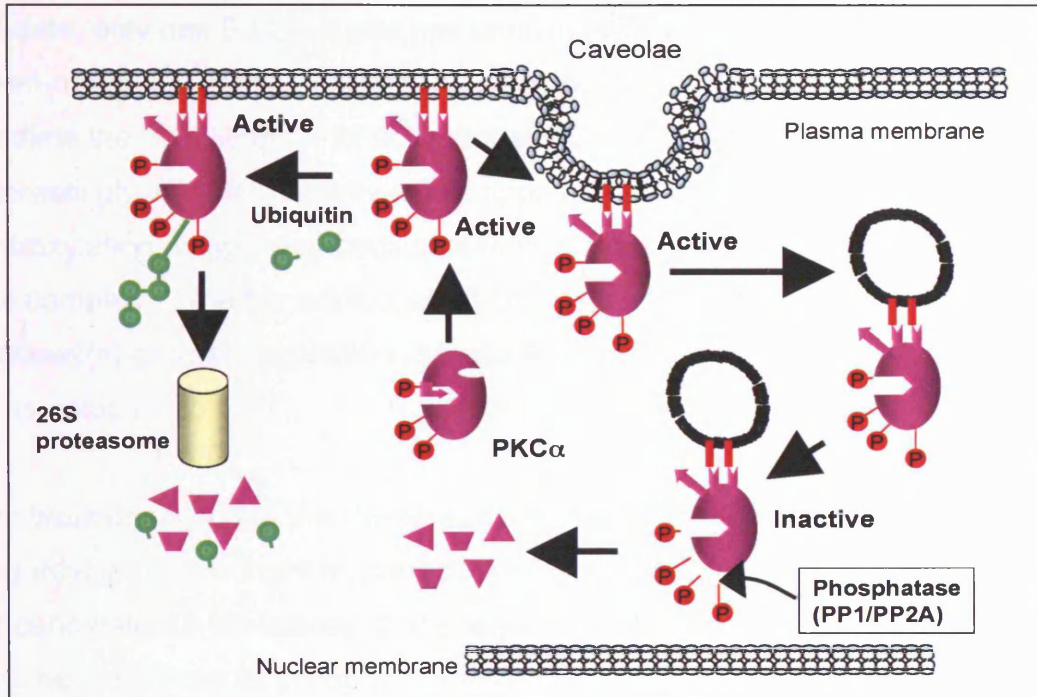
Figure 1.10 Two Pathways of Agonist-Induced PKC-α Downregulation in Intestinal Epithelial Cells. Upon activation with Bryostatin 1, PKC-α is recruited to the plasma membrane. A portion of fully phosphorylated, activated enzyme undergoes ubiquitination within this compartment and is targeted for degradation by the proteasome (26S). A pool of caveolae-associated PKC-α is transported to the perinuclear region, where it undergoes dephosphorylation and eventual degradation, via a proteasome-independent mechanism (figure reproduced from (Leontieva and Black, 2004)).

To date, only one E3 Ub-ligase has been specifically associated with the down-regulation of PKC; the VHL/CBC complex has been shown to mediate the ubiquitination of activated aPKC (Okuda et al., 2001). Interestingly, this VHL activity would appear to be independent of proline hydroxylation, suggesting additional modes of substrate recognition for this complex. Whether additional E3 Ub-ligases participate in the pathway(s) of down-regulation of these PKC isoforms, or others, remains to be established.

The work described in this thesis was motivated by the theme of PKC degradation, and sought to characterise the process further, by screening for candidate E3 Ub-ligases, and analysing phosphorylation sites which may be implicated as phospho-degrons.

CHAPTER 2

Materials and Methods

2.1 Materials

2.1.1 Chemicals and Plasticware

All reagents were obtained from Sigma-Aldrich unless otherwise indicated. Acetic Acid, Ammonium Acetate, Dimethyl Sulphoxide (DMSO), Glycerol, β-Mercaptoethanol, Magnesium Sulphate, Sodium Dodecylsulphate and Triton X-100 were from BDH. Ethanol (EtOH) and Methanol (MetOH) were purchased from Fisher. Optimem was from Gibco, Agarose from Invitrogen, Dithiothreitol (DTT) from Melford and NP-40 was from USB. Plasticware was purchased from Eppendorf, Corning, BD Falcon, Sterilin and Scientific Specialities Inc.

2.1.2 Buffers and Media

Coomassie blue stain

0.1% (w/v) Coomassie-Brilliant Blue, 10% (v/v) acetic acid, 50% (v/v) methanol

Coomassie destain

10% (v/v) acetic acid, 10% (v/v) methanol

CSM drop-out media base (SD-DO base)

0.59g CSM-Ade-His-Leu-Trp-Ura (Bio 101)/l SD media

CSM-Leu

40mg/l Ade, 20mg/l His, 50mg/l Trp, 20mg/l Ura in SD-DO base

CSM-Trp

40mg/l Ade, 20mg/l His, 100mg/l Leu, 20mg/l Ura in SD-DO base

CSM-Trp/Leu

40mg/l Ade, 20mg/l His, 20mg/l Ura in SD-DO base

CSM-Trp/Leu/His

40mg/l Ade, 20mg/l Ura in SD-DO base

CSM-Trp/Leu/His/Ade

20mg/l Ura in SD-DO base

75

CSM-Trp/Leu/His/Ade/X-α-Gal

20μg/ml X-α-Gal (Clontech) in CSM-Trp/Leu/His/Ade

DNA loading buffer

0.25% (w/v) bromophenol blue, 40% (w/v) sucrose in water

ELISA Coating buffer

15mM Na_2CO_3, 34.8mM $NaHCO_3$, pH 9.6

Imidazole elution buffer

50mM Tris, 100mM NaCl, 100-500mM imidazole, 1x protease inhibitor cocktail

Imidazole lysis buffer

50mM Tris, 100mM NaCl, 5mM imidazole, 1x protease inhibitor cocktail

Kinase Assay Mix

20mM Tris pH 7.5, 5mM $MgCl_2$, (+100μM $CaCl_2$ for cPKCs), 1μg/μl phosphatidylserine (Lipid Products), 0.2% Triton X-100, 1ng/μl TPA, 50-100μM ATP, 2.5-5μCi [γ^{32}P]-ATP (added last to start the reaction; Amersham)

3x Kinase Assay Sample Buffer

75% (v/v) 4x LDS Sample Buffer (Invitrogen), 0.2M DTT, 4% (v/v) β-mercaptoethanol, 5mM EDTA

LB (Agar)

10g/l Bacto-Tryptone, 5g/l Yeast Extract, 10g/l NaCl (6g agar/400ml LB); autoclave (provided by CR-UK research services)

LB-I

16mM $MgSO_4$, 10mM KCl, 1.2mM KOH in LB media; filter sterilise

LB^{amp}

100μg/ml ampicillin in LB

LB^{kan}

25μg/ml kanamycin (Melford Labs) in LB

2x LDS Sample Buffer

50% (v/v) 4x LDS Sample Buffer (Invitrogen), 0.2M DTT

Mowiol Mounting Solution

10% (w/v) Mowiol 4-88 (Calbiochem), 25% (v/v) glycerol, 100mM Tris pH 8.5; incubate 50°C, 8hrs

PBS (Ca^{2+}/Mg^{2+} free)

8g/l NaCl, 0.25g/l KCl, 1.43g/l Na_2HPO_4, 0.25g/l KH_2PO4, pH 7.2; autoclave (provided by CR-UK research services)

Ponceau stain

0.1% (w/v) Ponceau S in 5% acetic acid

1x Protease inhibitor cocktail

1 Complete tablet (EDTA-free, Roche) in 50ml specified buffer

SD (agar)

0.67% (w/v) Yeast Nitrogen Base (without amino acids), 2% (w/v) glucose, (8.8g agar/400ml SD) pH 5.8; autoclave (provided by CR-UK research services)

SOC

20g/l Tryptone, 5g/l yeast extract, 0.6g/l NaCl, 0.2g/l KCl, 2g/l $MgCl_2$, 2.5g/l $MgSO_4$, 3.6g/l D-glucose; autoclave (provided by CR-UK research services)

TAE

0.04M Tris, 0.1% glacial acetic acid, 1mM EDTA pH 8

TBS

20mM Tris pH 7.5, 0.9% (w/v) NaCl

TBS-T

0.1% (v/v) Tween-20 in TBS

TCA buffer

20mM Tris pH 8, 50mM ammonium acetate, 2mM EDTA, 1x protease inhibitor cocktail, 100mM PMSF

TCA-Laemmli loading buffer

3.5% (w/v) SDS, 14% (v/v) glycerol, 120mM Tris, 8mM EDTA, 5% (v/v) β-mercaptoethanol, 2mM PMSF, 0.1% (w/v) bromophenol blue, 1x protease inhibitor cocktail

TFBI

30mM KAc, 50mM $MnCl_2$, 100mM $RbCl_2$, 18% (v/v) glycerol; adjust to pH 5.8 with glacial acetic acid; filter sterilise

TFBII

10mM MOPS, 50mM $CaCl_2$, 10mM $RbCl_2$, 18% (v/v) glycerol; adjust to pH 7.0 with 1M NaOH; filter sterilise

Transfer Buffer

10mM Trizma base, 80mM Glycine, 10% (v/v) MetOH

5x Trypsin/Versene

0.25% trypsin in versene, pH 7.2; filter sterilise (provided by CR-UK research services)

Tryptic Digest Mix

0.04 mg/ml modified trypsin (16 000 U/mg), 10mM ammonium bicarbonate, in ice-cold resuspension buffer (supplied with the enzyme, Promega)

Versene

0.2g/l EDTA in PBSA, 1.5ml/l 1% phenol red, pH 7.2; autoclave (provided by CR-UK research services)

Yeast Cracking Buffer

2% (v/v) Triton-X 100, 1% (w/v) SDS, 100mM NaCl, 20mM Tris pH 8, 10mM EDTA pH 8

YP (agar)

11g/l Yeast Extract, 22g/l Bacto-Peptone (8.8g agar/400ml YP); autoclave (provided by CR-UK research services)

YPDA

2% (v/v) Glucose, 0.003% (w/v) Adenine hemisulphate in YP (8.8g agar/400ml)

2.1.3 Pharmacological Agents

Reagent	Source	Solvent	[Stock]	[Working]
BIM1	Calbiochem	DMSO	2mM	1-2μM
Bryostatin	Alexis	EtOH	1mM	1μM
Calyculin A	Calbiochem	EtOH	100μM	100nM
Gö6976	Calbiochem	DMSO	1mM	1μM
MG-132	Calbiochem	DMSO	42mM	30μM (4hrs) 10μM (16hrs)
Staurosporine	Calbiochem	DMSO	1mM	1μM
TPA 12-O-tetradecanoyl-phorbol-13-acetate	Sigma	DMSO	1.6mM	400nM

Table 2.1 Pharmacological Agents. The pharmacological agents used in subsequent experiments are summarised with their sources, solvents and stock and working concentrations ([ ]) indicated.

2.1.4 Antibodies

2.1.4.1 Primary Antibodies

Name	Source	Antigen	Use	Dilution
mouse anti-FLAG M5	Sigma	FLAG	IB	1:1000
rabbit anti-BD living colours full length Av	Clontech	GFP (also recognises YFP/CFP)	IP	1:200
mouse anti-GFP 3E1	CR-UK	GFP	IB	1:1000
mouse anti GFP 4E12/8	CR-UK	GFP	IP	1:300
rabbit anti-GST (z-5) sc-459	Santa Cruz	GST	IB	1:2000
mouse anti-HA 12 CA5	CR-UK	HA	IB	1:1000
rabbit anti-c-jun p-S63	Cell Signalling	c-jun p-S63	IB	1:1000
mouse anti-myc 9E10	CR-UK	myc	IB	1:1000
mouse anti-PKC-α MC5	in house	PKC-α V3 domain	IB	1:1000

rabbit anti-PKC-δ (C-17) sc-213	Santa Cruz	PKC-δ (C-terminus)	IB	1:2000
rabbit anti-PKC-δ p-304	in house (PPA-514)	PKC-δ p-304	IB	1:1000 (+ 1μg/ml blocking de-P peptide)
mouse anti-PKC-ε	BD Transduction Laboratories	PKC-ε (1-175)	IB IP	1:1000 1.25μg
rabbit anti-PKC-ε (C-15) sc-214	Santa Cruz	PKC-ε (C-terminus)	IB	1:5000
rabbit anti-PKC-ε	in house (Ab.130)	PKC-ε C-terminus	IB	1:1000
rabbit anti-PKC-ε p-T566	in house (PPA-204)	PKC-ε p-T566	IB	1:1000 (+ 1μg/ml blocking de-P peptide)
rabbit anti-PKC-ε p-T710	in house (PPA-218)	PKC-ε p-T710	IB	1:1000 (+ 1μg/ml blocking de-P peptide)
rabbit anti-PKC-ε p-S729	Upstate	PKC-ε p-S729	IB	1:1000 (+ 1μg/ml blocking de-P peptide)
rabbit anti-PKC-ε p-234	in house (PPA-501)	PKC-ε p-234	IB	1:1000 (+ 1μg/ml blocking de-P peptide)

rabbit anti-PKC-ε p-316	in house (PPA-503)	PKC-ε p-316	IB	1:1000 (+ 1μg/ml blocking de-P peptide)
rabbit anti-PKC-ε p-368	in house (PPA-505)	PKC-ε p-368	IB	1:1000 (+ 1μg/ml blocking de-P peptide)
mouse anti-tubulin	Sigma	tubulin	IB	1:5000

Table 2.2 Primary Antibodies. Properties of the primary antibodies employed are summarised. IB, immuno-blot; IP, immuno-precipitation.

2.1.4.2 Secondary Antibodies

Name	Source	Use	Dilution
Sheep HRP-conjugated anti mouse	Amersham	WB	1:5000
Donkey HRP-conjugated anti rabbit	Amersham	WB	1:5000
		ELISA	1:2000
Donkey Cy3-conjugated anti mouse	Amersham	IF	1:500

Table 2.3 Secondary Antibodies. Properties of the secondary antibodies employed are summarised. ELISA, enzyme linked immunosorbent assay; IF, immuno-fluorescence; WB, western blotting.

2.2 Methods

2.2.1 Molecular Biology

Standard molecular biology procedures were performed as described (Sambrook et al., 1989).

2.2.1.1 Polymerase Chain Reaction

Polymerase chain reactions (PCRs) were performed using a DNA Engine DYAD (MJ Research). The reaction mix incorporated: 1U Pfu (Stratagene),1x Pfu buffer, 1.5mM $MgCl_2$, 0.4mM ultrapure deoxynucleotide triphosphate mix (0.4mM with respect to each dNTP; Amersham-Pharmacia), 1μM sense primer, 1μM antisense primer (synthesized in house or purchased from Sigma Geno-Sys) and 100ng double stranded DNA (or bacterial colony) template +/- 10% DMSO as required, made up to a final volume of 50μl in sterile filtered (0.22μm filter, Millipore), distilled water. Unless otherwise specified, PCRs were carried out using the following programme:

Step 1:   94°C, 5mins

Step 2:   94°C, 45 secs; denaturation

Step 3:   (lowest primer Tm-3)°C, 45 secs; annealing

Step 4:   72°C, (length of product in bps/500)mins; extension

            → Cycle back to Step 2 x28

Step 5:   72°C, 8 mins

Step 6:   4°C, hold

PCR products were examined by agarose gel electrophoresis and purified using the QIAquick PCR Purification Kit (Qiagen) or by gel extraction.

2.2.1.2 Restriction Digests

Restriction digestions were carried out according to the manufacturer's instructions (NEB).

2.2.1.3 Agarose Gel Electrophoresis and Gel Purification

Samples were diluted 5:1 in 6x DNA loading buffer and separated on a 1% agarose gel in 1x TAE buffer, alongside 1kb ladder DNA markers (Invitrogen). 1μM ethidium bromide was incorporated into the gel to allow visualisation of DNA on a transilluminator. For use in subsequent cloning, bands were excised and DNA was extracted and purified using the QIAquick Gel Extraction Kit (Qiagen).

2.2.1.4 Ligation

Ligation reactions were performed using T4 DNA ligase (NEB). The reaction mix contained: 400U T4 DNA ligase, 1x ligase buffer, 100ng digested vector and an appropriate amount of insert DNA; a 3:1 molar ratio of insert:vector was typically employed with a 'vector only' control carried out in parallel. Ligation reactions were incubated at RT overnight.

2.2.1.5 Preparation of Chemically Competent DH5α for Transformation

High quality chemically competent cells were prepared for transformation by heat shock. A single colony of DH5α cells was inoculated into 5ml LB and incubated overnight at 37°C with shaking. This overnight culture was diluted 1:20 into pre-warmed LB-I and grown to a density of OD_{600}=0.4-0.5. All subsequent manipulations were performed using pre-cooled pipettes and tubes in the cold room. Cells were harvested by centrifugation at 2300g for 20mins at 4°C, resuspended in 30ml pre-chilled TFBI and incubated on ice for 10mins. Cells were then harvested by centrifugation and resuspended in 4ml pre-chilled TFBII. Cells were aliquoted into 500μl volumes in pre-chilled Eppendorf tubes and rapidly frozen on a dry ice/EtOH mix. Cells were stored at -70°C.

2.2.1.6 Transformation of Chemically Competent Escherichia Coli

Chemically competent DH5α or RapidTrans (Active Motif) E. Coli were transformed with purified plasmids or ligation reaction products by heat shock. Chemically competent cells (50μl) were mixed with 100ng plasmid

84

or 5μl ligation reaction in pre-cooled 15ml Falcon tubes on ice for 30mins. Cells were heat shocked at 42°C for 45secs and then placed on ice for 2mins. 1ml LB was added and the transformation mixtures were incubated at 37°C with shaking for 45mins. The bacteria were harvested by centrifugation at 4000rpm in a benchtop microcentrifuge, resuspended in 100μl LB and spread onto an LB$^{amp/kan}$ agar plate for selection. Plates were inverted and incubated overnight at 37°C.

2.2.1.7 Transformation of Competent BL21-CodonPlus Competent Cells

A modified heat shock protocol was employed for the transformation of competent BL21-CodonPlus (DE3)-RIL cells (Stratagene) for protein purification from bacteria. Cells (100μl) were incubated with 2μl 10% XL10-Gold β-mercaptoethanol mix (Stratagene) on ice for 10mins with periodic mixing. 1-50ng plasmid DNA was added and incubated for a further 30mins on ice. Cells were heated shocked at 42°C for 20 secs, placed on ice for 2mins, suspended in 0.9ml warm SOC and incubated at 37°C with shaking for 1hr. Bacteria were pelleted by microcentrifugation at 3000rpm for 2mins, resuspended in 100μl SOC and plated onto a selective plate. Dishes were inverted and incubated overnight at 37°C.

2.2.1.8 Preparation of Electro-competent DH5α for Transformation

For maximum transformation efficiency of plasmid DNA extracted from yeast, high quality competent DH5α were prepared for electroporation. A single colony of DH5α cells was inoculated into 10ml LB and incubated overnight at 37°C with shaking. This overnight culture was diluted into 1l pre-warmed LB and grown to a density of OD$_{600}$=0.6. All subsequent manipulations were performed using pre-cooled pipettes and tubes in the cold room. Cells were incubated on ice for 5mins, pelleted by centrifugation at 2300g for 5mins at 4°C and resuspended in an equal volume ice-cold water. Cells were then washed, first in 500ml ice-cold water, then in 500ml 10% glycerol in ice-cold water. Finally, cells were harvested by centrifugation at 2300g for 5mins at 4°C, resuspended in

2.5ml 10% glycerol in ice-cold water, aliquoted into 50µl volumes in pre-chilled Eppendorf tubes and rapidly frozen on a dry ice/EtOH mix. Cells were stored at -70°C.

2.2.1.9 Transformation of Electro-competent DH5α

Electrocompetent DH5α (50µl) were incubated with 1µl DNA extracted from yeast in a pre-cooled cuvette (0.4cm gap chamber, Equibio) on ice for 30mins. The cuvette was patted dry and transferred to a Biorad Gene Pulser. Cells were pulsed at 2.5kV with settings of 200ohms resistance and 25µFD capacitance and 250µl pre-warmed SOC was immediately added. The suspension was transferred to a 15ml tube and incubated with shaking at 37°C for 1hr. The entire transformation mix was plated on LB^{amp} agar and incubated overnight at 37°C.

2.2.1.10 Plasmid DNA Preparation

A single transformed bacterial colony was inoculated into 5ml $LB^{Kan/Amp}$ selection media and incubated overnight at 37°C with shaking. To prepare a stock for long-term storage at -70°C, 500µl overnight culture was mixed with 500µl 30% glycerol in LB and frozen rapidly on an EtOH/dry ice mix; the remainder was used for plasmid preparation. For small scale DNA purification, the culture was processed using the QIAprep Spin MiniPrep Kit (Qiagen). For larger scale DNA purification the overnight starter culture was diluted into 100ml $LB^{Kan/Amp}$ media, grown for a further 16hrs at 37°C with shaking and processed using the QIAGEN Plasmid Maxi Kit. The concentration of the purified DNA was determined by measuring the OD_{260} and assuming that a DNA concentration of 50µg/ml gives $OD_{260}=1$. The quality of the DNA was considered acceptable if the ratio OD_{260}/OD_{280} was approximately 1.8.

2.2.1.11 DNA Sequencing

DNA sequencing was carried out using the ABI BigDye Terminator v3.1 system in accordance with the manufacturer's protocol. Typically, the reaction mix incorporated 150ng plasmid, 3.2pmol primer and 1x BigDye

Terminator Mix in Sequencing Buffer made up to a final volume of 20µl in filter sterilised, distilled water. Cycle sequencing was performed using the following programme:

Step 1:   Ramp to 96°C at 2.5°C/sec

Step 2:   96°C, 1min; denaturation

Step 3:   96°C, 10secs; denaturation

Step 4:   Ramp to (primer Tm-3)°C at 1°C/sec

Step 5:   (primer Tm-3)°C, 5secs; annealing

Step 6:   Ramp to 60°C at 1°C/sec

Step 7:   60°C, 4mins; extension

      → Cycle back to Step 3 x24

Step 8:   12°C, hold

Reaction products were purified using DyeEx 2.0 Spin Kits (Qiagen) and sequenced by CR-UK research services on an Applied Biosystems 3730 DNA Analyser. Sequencing results were opened with EditView software and analysed using the DNA Strider package and the GeneStream online resource centre (http://www2.igh.cnrs.fr/home.eng.html).

2.2.2 Cloning

2.2.2.1 PKC Constructs

PKC epsilon constructs were cloned by PCR using mouse PKCε cDNA in pMT2 as a template (from Dr. Ben Webb). The Entrez Nucleotide accession number is AF325507; our stock bears 2 silent mutations: A1782G and C1890T.

PKC delta constructs were generated using either rat PKCδ in pCO2 (from Dr Ben Webb; NM_133307) or human PKCδ in pBluebac (Eli Lilly; NM_006254) as the PCR template.

2.2.2.1.1 Yeast 2-Hybrid Constructs

A panel of PKC yeast 2-hybrid bait constructs were cloned into the
pGBKT7 vector (Clontech) as myc-tagged GAL4 DNA binding domain
fusion proteins.

PKC-pGBKT7 Bait Construct	Boundaries within PKC ORF (bps)
Full length ε	1-2214
ε Regulatory domain	1-1197
ε Catalytic domain	892-2214
Full length δ	1-2022
δ Regulatory domain	1-1023
δ Catalytic domain	856-2022

Table 2.4 Yeast 2-Hybrid Bait Constructs. The domain boundaries of
full length PKC-ε/δ, and regulatory and catalytic domain, yeast 2-hybrid
bait constructs are summarised.

Full length PKCε and individual PKCε regulatory and catalytic domains
were introduced in frame into pGBKT7 between the Nco I and BamH I
restriction sites. PKCε sequences were amplified by PCR using primers
which incorporated a 5'-Nco I site and a 3'-Bgl II site (BamH I and Bgl II
yield compatible cohesive ends):

1.	PKCε	F:	5'-cagca**ccatgg**caatggtagtgttcaatggccttc-3'	(**Nco I**, ε)
2.	PKCε	R:	5'-gtgac**agatct**ctcagggcatcaggtcttcacc-3'	(**Bgl II**, ε)
~	ε reg.	F:	see primer 1	
~	ε reg.	R:	5'-gataag**agatct**cctggcctggccggacttcc-3'	(**Bgl II**, ε)
~	ε cat.	F:	5'-cagct**ccatgg**caggaattgccaaagtgctggctg-3'	(**Nco I**, ε)
~	ε cat.	R:	see primer 2	

The resulting products were PCR purified and double digested as
indicated, alongside pGBKT7. Digested vector and insert were gel
purified, ligated and transformed into bacteria, from which plasmid DNA
was purified and sequenced.

Using a similar strategy, full length rat PKCδ and its regulatory and catalytic domains were cloned into the bait vector. PCR primers were used to introduce a 5'-EcoR I and a 3'-BamH I site to the PKCδ sequences to allow ligation into the corresponding restriction sites in pGBKT7:

7.	PKCδ	F:	5'-gagtagaattcatggcaccgttcctgcgc-3'	(EcoR I, δ)
8.	PKCδ	R:	5'-gcacggatcccttccaggaattgctcatatttgg-3'	(BamH I, δ)
~	δ reg.	F:	see primer 7	
ĩ	δ reg.	R:	5'-gagaaggatcctccggttgctcccctcccag-3'	(BamH I, δ)
ĩi	δ cat.	F:	5'-gatcagaattcctcttggctgaggccttgaacc-3'	(EcoR I, δ)
ĩ	δ cat.	R:	see primer 8	

2.2.2.1.2 GST-tagged Constructs

A series of GST-PKC constructs, with boundaries corresponding exactly to those described in 2.2.2.1.1, were created for expression in mammalian cells. The PKC sequences were cloned in frame between the Xma I-Kpn I sites of a modified pMT2 vector (from Dr. Dick Schaap) such that each bears a C-terminal GST tag; stop codons were deleted from full length and catalytic domain constructs, and start codons were added to the latter. The following primers were employed to generate these constructs:

13.	PKCε	F	5'-gaacacacccgggatggtagtgttcaatggccttc-3'	(Xma I, ε)
14.	PKCε	R	5'-catctatggtaccggggcatcaggtcttcaccaa-3'	(Kpn I, ε)
15.	ε reg.	F	see primer 13	
16.	ε reg.	R	5'-catataaggtaccgctggcctggccggacttcc-3'	(Kpn I, ε)
17.	ε cat.	F	5'-catattacccgggatgggaattgccaaagtgctggctg-3'	(Xma I, ε)
18.	ε cat.	R	see primer 14	
19.	PKCδ	F	5'-gataatacccgggatggcaccgttcctgcgc-3'	(Xma I, δ)
20.	PKCδ	R	5'-ctaagcaggtaccgttccaggaattgctcatatttgg-3'	(Kpn I, δ)
21.	δ reg.	F	see primer 19	
22.	δ reg.	R	5'-gatataaggtaccgccggttgctcccctcccag-3'	(Kpn I, δ)
23.	δ cat.	F	5'-gatataacccgggatgctcttggctgaggccttgaacc-3'	(Xma I, δ)
24.	δ cat.	R	see primer 20	

2.2.2.1.3 GFP-tagged Constructs

GFP-tagged mouse PKCε was obtained from Dr. Johanna Ivaska; the PKCε ORF and 3' UTR were cloned into pEGFP-C1 (Clontech) between the Bgl II and Sal I restriction sites (Ivaska et al., 2002). GFP-PKCδ (rat) in pEGFP-C3 was from Dr. Jyoti Srivastava (Srivastava et al., 2002). Bovine PKCα and related phosphorylation site mutants (T497A, T497E, T638A, T638E, S657A and S657E) were cloned into pEGFP-C2 by Dr. Scott Parkinson.

Human PKCδ was introduced into the pEGFP-C1 vector between the EcoR I and BamH I sites using the following PCR primers:

25.	PKCδ	F	5'-atattagaattcaatggcgccgttcctgcgcatcgc -3'	(EcoR I, δ)
26.	PKCδ	R	5'-taatatggatcctcaatcttccaggaggtgctcg-3'	(BamH I, δ)

PKCα was cloned into the pEGFP-C1 vector between Bgl II and Sal I sites. Bovine PKCα in pEGFP-C2 was used as a template with the following primers:

27.	PKCα	F	5'-attataagatctatggctgacgtcttcccggcc-3'	(Bgl II, α)
28.	PKCα	R	5'-taatatgtcgactcataccgcgctctgcaggatgg-3'	(Sal I, α)

2.2.2.1.4 RFP-tagged Constructs

RFP-PKCε was cloned by manipulating the GFP-PKCε construct; the GFP sequence was removed by digestion of the unique, flanking restriction sites, Nhe I and Bgl II, and replaced with RFP (Accession no: AF506027). Monomeric RFP cDNA was obtained from Dr. Veronique Calleja (Campbell et al., 2002) and amplified using the following primers:

29.	RFP	F	5'-aatatagctagcatggcctcctccgaggacg-3'	(Nhe I, RFP)
30.	RFP	R	5'-atataaagatcttgcgccggtggagtggcggccctc-3'	(Bgl II, RFP)

2.2.2.1.5 His-tagged Constructs

His-tagged PKCα, PKCα-T638A and PKCα-T638E in pKS1 were from Dr. Frederic Bornancin (Bornancin and Parker, 1996).

2.2.2.1.6 PKCε and PKCδ Sequencing Primers

All of the PKCε constructs cloned were sequence checked using the following primers to achieve full coverage:

a.   5'-cgcatacgctccctgaacac-3' (436-455, antisense)

b.   5'-cgctgacttggatcggtcg-3' (1023-1041, antisense)

c.   5'-gcagtccacatcatcgtcttg-3' (1336-1356, antisense)

d.   5'-caggccaagcgcttggggc-3' (1195-1213, sense)

e.   5'-ccagattcagcggtcccga-3' (1488-1506, sense)

f.   5'-cgagatgatggctgggcagc-3' (1794-1813, sense)

PKCδ sequences were verified using the following:

g.   5'-ctcgtggttcttgatgtagtg-3' (460-480, antisense)

h.   5'-tcacactttaatccctgtttcacc-3' (762-785, antisense)

i.   5'-gatcgacgatgacgtggagtg -3' (1152-1172, sense)

j.   5'-gcctttgtcctgaatgtggaac-3' (1302-1323, antisense)

k.   5'-cacatcaagattgctgacttc-3' (1450-1471, sense)

l.   5'-gaccctgccaagaggctgg-3' (1750-1768, sense)

PKCα constructs were sequenced using primers from Dr. Angus Cameron.

2.2.2.2 PKCε and PKCδ Mutagenesis

2.2.2.2.1 PKCε Autophosphorylation Site Mutants

A panel of PKCε autophosphorylation site mutants were cloned using a two-step PCR based mutagenesis strategy: S234A, S234D, S316A, S316D, S368A and S368D.
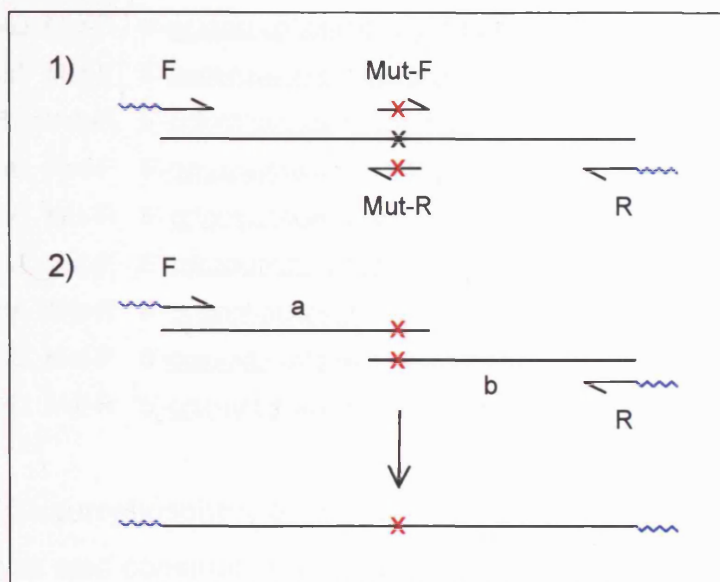
Figure 2.1 Site Directed Mutagenesis. The two-step PCR based strategy employed for the cloning of mutants is summarised diagrammatically. Primers are represented by half arrows; blue zigzags denote non-complementary sequences incorporating restriction sites for subsequent cloning. The codon targeted for mutagenesis is signified by a cross, black corresponds to the wild type sequence, red to the desired mutation.

Briefly, in the first round of PCR, primer F and primer Mut-R were used to amplify product a from a wild type PKCε template, while primer Mut-F and primer R were used to amplify product b; the Mut- primers are antiparallel with respect to one another and harbour the appropriate mutation in the codon of interest (X). Products a and b were separated from the wild type PKCε template by agarose gel electrophoresis, purified by gel extraction and used in combination as a PCR template for step two. The second round of PCR was performed using external primers F and R, which amplify full length, mutated PKCε and incorporate Xma I and Kpn I sites respectively. The primers used to construct these PKCε mutants were as follows:

31.	PKCε F	see primer 13	
32.	PKCε R	see primer 14	
33.	S234A Mut-F	5'-gacgaggtgggcgcccaacggttcagc-3'	(**mutation**, ε)
34.	S234A Mut-R	5'-gctgaaccgttgggcgcccacctcgtc-3'	(**mutation**, ε)
35.	S234D Mut-F	5'-gacgaggtgggcgaccaacggttcagc-3'	(**mutation**, ε)

92

36.	S234D Mut-R	5'-gctgaaccgttggtcgcccacctcgtc-3'	(mutation, ε)
37.	S316A Mut-F	5'-gacaaaatcaccaacgctggccaaaggagg-3'	(mutation, ε)
38.	S316A Mut-R	5'-cctcctttggccagcgttggtgattttgtc-3'	(mutation, ε)
39.	S316D Mut-F	5'-gacaaaatcaccaacgatggccaaaggagg-3'	(mutation, ε)
40.	S316D Mut-R	5'-cctcctttggccatcgttggtgattttgtc-3'	(mutation, ε)
41.	S368A Mut-F	5'-cggaaggccttggcatttgacaaccgagg-3'	(mutation, ε)
42.	S368A Mut-R	5'-cctcggttgtcaaatgccaaggccttccg-3'	(mutation, ε)
43.	S368D Mut-F	5'-cggaaggccttggattttgacaaccgagg-3'	(mutation, ε)
44.	S368D Mut-R	5'-cctcggttgtcaaaatccaaggccttccg-3'	(mutation, ε)

A triple PKCε autophosphorylation site mutant S234A/S316A/S368A
(PKCε^{3A}) was also constructed by sequential cycles of mutagenesis:
S234A was used as the template for S316A cloning and the resulting
S234A/S316A double mutant was used as the template for S368A
alteration.

The PKCε autophosphorylation mutants were ligated into pMT2-GST as
described in the previous section. Subsequently, all were introduced into
pEGFP-C1; PKCε^{3A} was also transferred to pRFP-C1. Subcloning was
achieved by exploiting unique EcoR V (bps 593-598) and EcoR I sites
(2170-2175) within the PKCε ORF. GFP-PKCε and RFP-PKCε were
digested to remove the EcoR V/EcoR I fragment, and following gel
purification, these were replaced by ligation of mutant fragments digested
with the same enzymes.

2.2.2.2.2 PKCδ Autophosphorylation Site Mutants

A set of human PKCδ putative autophosphorylation site mutants were
generated by two-step PCR based mutagenesis: S57A/T58A, T141A, and
S304A. External primers in round 2 incorporated a 5' EcoR I site and a 3'
BamH I site for in frame ligation into pEGFP-C1:

45.	PKCδ	F	see primer 26
46.	PKCδ	R	see primer 27
47.	57A/58A		Mut-F 5'-cctgagtggaaggcggcgttcgatgcccac-3'	(mutation, δ)
48.	57A/58A		Mut-R 5'-gtgggcatcgaacgccgccttccactcagg-3'	(mutation, δ)

49.	T141A	Mut-F	5'-<u>gccaagttcccagcgatgaaccgccgc</u>-3'	(**mutation**, <u>δ</u>)
50.	T141A	Mut-R	5'-<u>gcggcggttcatcgctgggaacttggc</u>-3'	(**mutation**, <u>δ</u>)
51.	T304A	Mut-F	5'-<u>cggagatcagacgcagcctcctcagag</u>-3'	(**mutation**, <u>δ</u>)
52.	T304A	Mut-R	5'-<u>ctctgaggaggctgcgtctgatctccg</u>-3'	(**mutation**, <u>δ</u>)

2.2.2.2.3 F-box WD40 (Fbw) Protein and c-jun Constructs

2.2.2.2.3.1 GFP-tagged Fbw7 C-terminal Clone

The C-terminal region of Fbw7 (encoding amino acids 283-629; F7C) was recovered in pACT2 from positive clone 19 following the yeast 2-hybrid screen described in section 2.2.3. This partial insert was subcloned directly into the mammalian pEGFP-C1 vector by PCR, using primers complementary to the vector sequence adjacent to the library insert (F: 5032-5012, R: 4990-4964; see Appendix A2). The primers incorporated a 5' Kpn I site and a 3' Age I site to facilitate in-frame ligation between the Kpn I/Xma I sites of pEGFP-Cl; Age I and Xma I yield complementary cohesive ends.

| 53. | F7C | F 5'-aatacag**gtacc**<u>ggtcatatggccatggaggcc</u>-3' | (**Kpn I**, <u>pACT2</u>) |
| 54. | F7C | R 5'-ataagaa**accggt**CC<u>cagtatctacgattcatagatctctcg</u>-3' | (**Age I**, <u>pACT2</u>) |

2.2.2.2.3.2 Full length F-box WD40 (Fbw) Protein and c-jun Constructs

FLAG-tagged mouse Fbw1 (Miura et al., 1999), mouse Fbw2 (Miura et al., 1999), zebrafish Fbw4 (Maruyama et al., 2001) and mouse Fbw6/7 (AF391192; referred to subsequently as Fbw7β; (Maruyama et al., 2001)) were obtained from Professor Shigetsugu Hatakeyama. Fbws1, 4 and 7 are in pcDNA3, Fbw2 in pCl-neo. Empty pcDNA3.1 expressing a FLAG-tag alone was provided by Dr. Sylvie Lachmann. FLAG-tagged human Fbw7β in pIRES2-EGFP (NM_018315; (Nateri et al., 2004)), GFP-Fbw7β in pEGFP-C2 (EcoR I/Sal I) and myc-c-jun-FLAG in pCMV were from Anett Jandke. FLAG-tagged Fbw7α (Welcker et al., 2004b) and Fbw7α$^{\Delta BD1}$ (Welcker et al., 2004a) in 3pX-FLAG-myc-CMV-24 were provided by Dr. Bruce Clurman (NM_033632); these constructs contain an amino acid change, A626T, and lack the 2 C-terminal residues.

GFP-tagged Fbw7α was cloned in frame into pEGFP-C1 between Bgl II and Sal I. FLAG-Fbw7α was used as a PCR template with the following; Fbw7α-R was designed to accommodate the C-terminal mutation harboured by this construct:

55.	Fbw7α F	5'-attataagatctatgaatcaggaactgctctctgtgg-3'	(Bgl II, F7α)
56.	Fbw7α R	5'-taatatgtcgactcattccacatcaaagtccagc-3'	(Sal I, F7α)

2.2.2.2.3.3 Fbw7α Mutagenesis

Fbw7α S18A and S18D mutants were generated by two-step PCR. Since the codon for S18 is so close to the N-terminus, the first round of PCR was performed using an external F primer complementary to the vector sequence upstream of Fbw7α paired with the Mut-R primer; this generated a larger product for more convenient subsequent manipulation. In round two, regular external primers were used to incorporate a 5' Bgl II site and a 3' Sal I site for in frame ligation into pEGFP-C1:

57.	Fbw7α F	see primer 65	
58.	Fbw7α R	see primer 66	
59.	round 1 F	5'-cggtgggaggtctatataagc-3'	(vector)
60.	S18A Mut-F	5'-cgaactggaggcgctctgagagg-3'	(mutation,F7α)
61.	S18A Mut-R	5'-cctctcagagcgcctccagttcg-3'	(mutation, F7α)
62.	S18D Mut-F	5'-cgaactggaggcgatctgagagg-3'	(mutation, F7α)
63.	S18D Mut-R	5'-cctctcagatcgcctccagttcg-3'	(mutation, F7α)

The N-terminal domain of Fbw7α (bps 1-204) was also generated as a GFP construct. GFP-wt Fbw7α, S18A and S18D were used as PCR templates with the following primers:

64.	F7α-N F	see primer 65	
65.	F7α-N R	5'-taatatgtcgacgcctccaggtctaggttctactcc-3'	(Sal I, F7α)

Fbw7α constructs were sequenced using the following primers:

l.	5'-cctcatcttgttcaccaga-3'	(antisense)
m.	5'-caggaactgctctctgtgggcagc-3'	(sense)
n.	5'-gccaaaattctccagtagcg-3'	(antisense)
o.	5'-ggggacctcagagcagccaatggc-3'	(sense)
p.	5'-gcagctcagacatgtcgctactgg-3'	(sense)
q.	5'-gtgggacatacaggtggagtatgg-3'	(sense)
r.	5'-ccagagactgaaacctgtctag-3'	(sense)
s.	5'-ggtcccaacaagcatcagagtgc-3'	(sense)

2.2.2.2.4 VHL Binding Protein 1 (VBP1) Constructs

2.2.2.2.4.1 His-tagged VBP1 for protein purification

His-tagged human VBP1 (BC046094), cloned between the EcoR I/Sal I
sites of the bacterial expression vector pET-28a, was provided by Dr.
Chengtao Her (Her et al., 2003). This construct bears two mutations:
A2G and K196E.

2.2.2.2.4.2 GFP-tagged VBP1

Human VBP-1 cDNA (BC046094) was obtained from the IMAGE
consortium (IMAGE no: 6058145) and used as a PCR template with the
following primers to facilitate cloning between the EcoR I and Xma I sites
in pEGFP-C1:

66.	VBP1	F 5'-tcttct**gaattc**Aatggcggccgttaaggacag-3'	(**EcoR I**, VBP1)
67.	VBP1	R 5'-acacaa**cccggg**ttatgctttgttcttggtagagtc-3'	(**Xma I**, VBP1)

2.2.3 Yeast Two-Hybrid Analysis

The MATCHMAKER GAL4 System 3 (Clontech) was employed for yeast two-hybrid analysis according to the manufacturer's recommendations.

2.2.3.1 Yeast Culture

2.2.3.1.1 Yeast Strain AH109

Yeast 2-hybrid analysis was performed using the *Saccharomyces cerevisiae* strain AH109 (Clontech); its genotype is as follows: *MATa, trp1-901, leu2-3, 112, ura3-52, his3-200, gal4Δ, gal80Δ, LYS2 : : GAL1$_{UAS}$-GAL1$_{TATA}$-HIS3, GAL2$_{UAS}$-GAL2$_{TATA}$-ADE2, URA3 : : MEL1$_{UAS}$-MEL1$_{TATA}$-lacZ.*

2.2.3.1.2 Yeast Media and Maintenance

Wild type AH109 were cultured in YPDA liquid media or on YPDA Agar plates. AH109 transformants were maintained using an appropriate SD based nutrient drop-out medium for selection.

CSM-drop-out media	Selection
-TRP	bait vector
-LEU	prey vector
-TRP/LEU	bait/prey cotransfection
-TRP/LEU/HIS	medium stringency interaction
-TRP/LEU/HIS/ADE	high stringency interaction
-TRP/LEU/HIS/ADE/X-α-Gal	high stringency interaction with blue/white verification

Table 2.5 Nutritional Markers for Yeast Selection. The nutritional markers employed for yeast 2-hybrid screening using AH109 yeast, and pGBKT7/pACT2 vectors

Yeast stocks were streaked onto agar plates and incubated at 30°C for 2-6 days. In order to establish an overnight culture, a single colony was picked into 1ml media in an Eppendorf tube and vortexed extensively; this cell suspension was used to inoculate 5ml media and incubated at 30°C with shaking for 16hrs. Glycerol stocks were prepared for long-term

with shaking for 16hrs. Glycerol stocks were prepared for long-term storage at −70°C by diluting 250μl sterile glycerol into 500μl overnight culture and snap freezing on an EtOH/dry ice mixture.

2.2.3.1.3 Yeast Transformation

Yeast transformations were performed according to the Gietz 2-Hybrid TRAFO Protocol (Agatep et al., 1998). For high efficiency co-transformation, yeast were transformed sequentially; the bait construct was introduced into AH109 and the resulting transformants were used to prepare competent cells for the subsequent introduction of prey/library.

The basic protocol for 10 transformations (10x) was as follows. A single colony from a freshly streaked stock plate was picked into 5ml liquid YPDA and incubated with shaking at 30°C overnight. An appropriate volume of this overnight culture was used to inoculate 50ml warm YPDA at 5×10^6 cells/ml. The culture was incubated with shaking at 30°C until the cell density reached 2×10^7 cells/ml (3-5hrs); transformation efficiency is highest when cells have completed 2-4 cycles of division. Cells were harvested by centrifugation at 3000g for 5mins, washed in 25ml sterile water, and harvested again. The yeast were resuspended in 1ml 100mM LiAc, pelleted at 14,000rpm for 15secs in a benchtop microfuge, diluted in 500μl 100mM LiAc and aliquoted into 50μl volumes. Competent cells were then harvested by microcentrifugation at 14,000rpm for 15secs and resuspended in the following: 240μl 50% (w/v) PEG (average MW = 3,350), 36μl 1M LiAc, 50μl 2mg/ml YEASTMAKER carrier DNA (Clontech), 0.1-1μg plasmid DNA made up to a final volume of 360μl in sterile water (ingredients were added in this order). The transformation mix was vortexed vigourously, incubated at 30°C for 30mins and heat shocked at 42°C for 30mins (with gentle shaking every 5mins). Finally, the yeast were harvested by microcentrifugation at 6000rpm for 15sec, resuspended in 1ml distilled, filter sterilised water and plated onto the appropriate CSM-drop out agar (typically 100μl/plate). Plates were inverted and incubated at 30°C for 3-10 days to recover transformants.

For sequential transformation the protocol was essentially the same except that in the initial overnight culture bait transformants were grown in 25ml of the appropriate CSM-drop out media to maintain plasmid expression (yeast were then subcultured in YPDA for two doublings without significant loss of expression). In order to carry out 30 transformations (30x), all volumes were scaled up by a factor of 3 and the heat shock was extended to incubation at 42°C, 40mins.

2.2.3.2 Yeast Two-Hybrid System: Preliminary Characterisation

AH109 were co-transformed with a panel of bait/prey vectors in order to characterise the yeast 2-hybrid system. The pGBKT7-PKC constructs were introduced alongside an empty prey vector (pGADT7, Clontech) to test for bait expression, toxicity and autoactivation of reporter genes. AH109 co-transformed with empty pGBKT7/pGADT7 provided a negative control.

2.2.3.2.1 Test for Bait Expression and Toxicity

Yeast protein extracts were prepared from co-transformed yeast by TCA precipitation to verify bait expression. A single colony was used to inoculate 5ml CSM-TRP/LEU and grown overnight with shaking at 30°C. The overnight culture was vortexed vigorously, diluted into 50ml YPDA and grown to OD_{600}=0.4-0.6 (OD_{600} x total volume = OD units). Cells were chilled rapidly by the addition of 1 volume of ice and harvested by centrifugation at 1000g for 5mins at 4°C. Yeast were then washed in 50ml ice cold water, recovered by centrifugation and snap frozen on an EtOH/dry ice mixture. The pellet was thawed on ice for 20mins and resuspended in 100μl ice-cold TCA buffer/7.5 OD units. The cell suspension was then transferred to a screw cap microfuge tube containing 100μl glass beads (425-600μm) and 100μl 20% TCA/7.5 OD units. Cells were disrupted using a bead-beater at the highest setting 3x30secs (FastPrep FP120, Bio101); this process was followed under a light microscope, successfully ruptured yeast appear as darkened

'ghosts'. The supernatant was removed to a fresh tube and the beads were resuspended in a mixture of 250μl TCA and 250μl 20% TCA for another round of agitation. The second supernatant was pooled with the first and proteins were pelleted by microcentrifugation at 14,000rpm for 10mins at 4°C. Protein extracts were solubilised in 10μl TCA-Laemmli buffer/OD unit, boiled at 100°C, 10mins, cleared by centrifugation at 14,000rpm for 10mins at RT and analysed by Western blotting.

5ml cultures were established from the same co-transformed AH109 and incubated overnight at 30°C with shaking. Growth was assayed by measuring OD_{600} in order to determine whether bait expression conferred toxicity.

2.2.3.2.2 Test for Bait Autoactivation of Reporter Genes

AH109 co-transformed with pGBKT7/PKCs and pGADT7 were plated on selective media to test for autoactivation of reporter genes; additionally, pGBKT7-p53/pGADT7-T antigen expressing yeast were used as a robust positive control for protein-protein interaction (vectors from Clontech). Single colonies were picked and streaked onto CSM-TRP/LEU, CSM-TRP/LEU/HIS or CSM-TRP-LEU/HIS/ADE/X-α-gal agar plates for selection at increasing stringency. Following incubation at 30°C for 6 days plates were photographed by the CR-UK Photographic Department.

2.2.3.3 GAL4 cDNA Library Preparation

A mouse brain MATCHMAKER cDNA library of 3.5×10^6 independent clones was obtained from Clontech. This library is constructed in the pACT2 vector and provided in *E.Coli* BNN132.

Serial dilutions of the library were spread onto LB^{amp} plates and incubated at 37°C for 20hrs. Colonies were counted and the library titre was determined to be 1.28×10^8 cfus/ml. The library was then amplified to obtain enough plasmid for screening in yeast; 3x coverage of the library was considered sufficient (1.05×10^7 cfus, 82μl library). In order to plate

the library at near confluency, *E.coli* were spread at a density of 140 000 cfus/245mm square plate; 82μl library was mixed with 37.5ml LB and distributed at 500μl/plate over 75 245mm square LB^{amp} plates using ColiRoller Plating Beads (Novagen). The plates were inverted and incubated at 37°C for 20hrs. 10ml 25% (v/v) glycerol/LB was added to each plate and colonies were harvested by shaking the beads and then scraping with a sterile spreader. Cell suspensions were pooled and shown to be equivalent to 10l of a regular overnight bacterial culture by OD$_{600}$. Plasmid DNA from 500ml cell suspension was isolated and purified over 6 Megaprep columns (Qiagen) for screening by yeast 2-hybrid. The remainder was aliquoted (5x1mls and 10x50mls) and frozen at −70°C for future use.

2.2.3.4 Yeast Two-Hybrid Screen
2.2.3.4.1 Library Transformation

pGBKT7-PKCε bait was transformed into AH109 as described. Fresh transformant colonies were then used to prepare competent cells for subsequent introduction of the cDNA library; screening of 10^6 independent clones was judged to be a suitable target for 2-hybrid analysis.

A small scale test run was performed to optimise conditions and estimate transformation efficiency: yeast were co-transformed with PKC-ε bait and a dilution series of the library. The aim was to determine the lowest concentration of DNA required to screen 10^6 cfus in an effort to circumvent the problem of introducing >1 library plasmid into a given cell. A dilution series of co-transformants was plated on CSM–TRP/LEU and incubated at 30°C for 4 days. Colonies were counted and the transformation efficiency was estimated at 10^{4}cfu/μg when a 1x transformation was carried out using 0.5μg library DNA.

In order to screen 10^{6}cfus in the final yeast 2-hybrid screen, this protocol was scaled up 120x using a total of 60μg library DNA. This was achieved

could be readily handled and efficiently heat shocked. In the final step, pellets were each resuspended in 15ml distilled, filter sterilised water and pooled; the suspension was plated at 2ml/plate over 30 245mm square CSM-TRP/LEU/HIS plates and incubated at 30°C for 5 days. A dilution series was plated onto CSM-TRP/LEU in parallel, colonies were counted and it was determined that a total of 1.4×10^5 cfus had been screened.

2.2.3.4.2 Sequential Rounds of Yeast Two-Hybrid Screening

Positive clones recovered following incubation on CSM-TRP/LEU/HIS plates (medium stringency) were screened for interaction at higher stringency. Colonies were restreaked onto 22x22 grids on 245mm square CSM-TRP/LEU/HIS/ADE plates alongside a pGBKT7-p53/pGADT7-T antigen positive control and incubated at 30°C for 3 days. Positive colonies were then subjected to a final round of selection; yeast were restreaked onto CSM-TRP/LEU/HIS/ADE/X-α-gal agar plates and incubated for a further 5 days at 30°C.

2.2.3.4.3 Plasmid Rescue and Purification

A single colony of AH109 co-transformed with pGBKT7-PKCε/pACT2-putative interacting library clone was picked from the final CSM-TRP/LEU/HIS/ADE/X-α-gal selection plate and used to inoculate 4ml CSM-TRP/LEU/HIS. The culture was grown at 30°C with shaking for 1-3 nights until $OD_{600} \geq 0.8$. 1ml was removed to establish a glycerol stock, the remainder was split between 2 screw cap tubes and microcentrifuged at 13,000rpm for 2mins. The yeast were washed in 500µl water, pooled, and recovered by microcentrifugation. The pellets were resuspended in 200µl yeast cracking buffer, glass beads (425-600µm) were added up to the meniscus and 200µl phenol:chloroform:isoamylalcohol was introduced. The mix was vortexed 3x30secs, with 30secs incubation ice in between, and microcentrifuged at 13,000rpm for 10mins at 4°C. 150µl aqueous layer was removed to a tube containing 500µl 85% (v/v) EtOH, 1M ammonium acetate, mixed with 10 inversions and microcentrifuged at 13,000rpm for 30mins at 4°C. Precipitated plasmid DNA was washed in

250μl 70% EtOH and resuspended in 50μl distilled, sterile filtered water. Extracted plasmid DNA (1μl) was electroporated into competent DH5α and plated onto LB^{amp} plates to select for the library vector.

DH5α colonies transformed with the positive library vectors were inoculated into 5ml LB^{amp} overnight cultures. 500μl of each was used to establish a glycerol stock and plasmid DNA was purified from the remainder by mini-prep.

2.2.3.4.4 Sequence analysis

Recovered library vectors from positive AH109 colonies were sequenced using the following primers:

t. 5'-taccactacaatggatg-3' (pACT2 5153-5137, sense)
u. 5'-agatggtgcacgatgcacag-3' (pACT2 4939-4920, antisense)

2.2.4 Protein Purification

His-tagged VBP1 was expressed in bacteria and purified using Ni-NTA agarose according to the manufacturer's instructions (Qiagen). Briefly, pET-VBP1 was transformed into BL21-CodonPlus bacteria and plated onto LB^{kan} agar. A single colony was used to inoculate a 50ml overnight starter culture, this was subsequently diluted into 1l LB^{kan} and grown to OD$_{600}$=0.5. An aliquot of this culture (1ml) was removed (non-induced control) and expression was induced in the remainder with the addition of 0.4mM IPTG; cells were incubated overnight at 16°C with shaking. After the removal of 1ml (post-induction control) the culture was harvested by centrifugation at 4000g for 20mins. The pellet was resuspended in 20ml Imidazole Lysis Buffer and sonicated 6x10secs with 30sec intervals on ice. Lysates were cleared at 55 000rpm for 1hr at 4°C using a 70Ti rotor in an XL70 ultracentrifuge (Beckman) and the supernatant was decanted. The pellet was resuspended in 20ml 8M urea (insoluble extract). 1ml of the supernatant was removed (protein expression control) and the remaining 20ml soluble extract was subjected to a native protein purification protocol. Ni-NTA agarose (1ml) was washed in 5ml Imidazole

purification protocol. Ni-NTA agarose (1ml) was washed in 5ml Imidazole Lysis Buffer x3 and the final slurry was transferred to the soluble protein extract; this mix was tumbled at 4°C for 1hr. The beads were washed 6x in 5ml Imidazole Lysis Buffer and the purified protein was eluted using step gradients of imidazole. Ni-NTA agarose was recovered by centrifugation in a benchtop centrifuge at 1000 rpm for 1min. Beads were resuspended in 100mM Imidazole Elution Buffer and recovered again by centrifugation; the supernatant containing eluted protein was transferred to a fresh tube. The same procedure was repeated using 200mM, 300mM, 400mM and finally 500mM Imidazole Elution Buffers. Samples of all controls and eluted fractions were subjected to SDS-PAGE and protein expression was visualised by Comassie staining. The eluate containing the majority of the purified protein was then dialysed against 50mM Tris pH 7.5, 100mM NaCl and stored at 4°C.

2.2.5 Mammalian Cell Culture

2.2.5.1 Cell lines

COS7 (african green monkey kidney), 293 (human embryonic kidney), HeLa (human cervical carcinoma) and NIH3T3 (mouse embryonic fibroblast) cells were obtained from CR-UK research services, RCC (renal carcinoma) cells were from Dr. Xavier Iturrioz. PKCε knock out MEFs ($\varepsilon^{-/-}$) and $\varepsilon^{-/-}$ MEFs re-expressing PKCε (clone 5) were established by Richard Whelan (Ivaska et al., 2002). $\varepsilon^{-/-}$ MEFS re-expressing GFP-ε, and GFP-ε 234A/316A/368A (ε^{3A}) were generated by Dr. Angus Cameron; $\varepsilon^{-/-}$ MEFS were stably transfected with pBABE GFP-PKCε constructs to generate polyclonal cell lines from which subpopulations expressing similar levels of GFP were isolated by 3 successive rounds of Fluorescent Activated Cell Sorting (FACS).

2.2.5.2 Cell culture and transfection

All cells, with the exception of NIH3T3, were maintained in Dulbecco's modified Eagle's medium (DMEM, provided by CR-UK Research Services) supplemented with 10% foetal calf serum (PAA laboratories;

10% E4) in a humidified 5% CO_2 incubator at 37°C. Where serum starvation was necessary, media was typically replaced with 0.1% E4 for 16 hrs. NIH3T3 were cultured in DMEM with 10% donor calf serum (PAA laboratories). $\epsilon^{-/-}$ MEFs and clone 5 cells were supplemented with 100µg/ml hygromycin, GFP/PKC expressing $\epsilon^{-/-}$ MEFs with 5µg/ml puromycin.

Transient transfections were performed using Lipofectamine 2000 (Invitrogen) following the manufacturer's instructions for the appropriate cell lines. Typically, DNA/lipofectamine in Optimem was added directly to the culture media, incubated for 6hrs and then replaced with warm E4 10%. Subsequent manipulations were typically performed 24hrs post-transfection.

2.2.6 Preparation of total cell extracts

Cells seeded in 24 well dishes were washed with PBS and harvested by scraping into 100µl boiling 2x LDS sample buffer. Extracts were boiled at 100°C for 5mins and briefly sonicated to shear genomic DNA.

2.2.7 GST Pull down and Immunoprecipitation
2.2.7.1 GST Pull-Down

Cells seeded in 6 well dishes were washed in ice-cold PBS and harvested in 400µl pre-chilled lysis buffer containing: 50mM Tris pH 7.5, 150mM NaCl, 0.5% (v/v) NP40, 0.1mM Na_3VO_4, 10mM NaF, 1x protease inhibitor cocktail. Cells were resuspended thoroughly by pipetting, incubated on ice for 10mins and subjected to microcentrifugation at 14 000rpm for 10mins at 4°C. The resulting pellet was stored at -20°C and resuspended in 2x LDS sample buffer by sonication where the insoluble fraction was of interest, and a 50µl aliquot of the supernatant was diluted in 2x LDS sample buffer (total cell lysate); the remainder was used for GST pull-down. The cell lysate was pre-cleared by tumbling with 25µl Sepharose 4B (Amersham) pre-equilibrated in lysis buffer for 30mins at 4°C. Beads were pelleted by pulsing at 4 000rpm in a microcentrifuge

and the cleared lysate was transferred to a fresh tube containing 25μl pre-equilibrated Glutathione Sepharose 4B (Amersham) and incubated for a further 2hrs on a rotating wheel at 4°C. The beads were washed by tumbling 3x10mins in lysis buffer and then boiled in 2x LDS sample buffer (typically 50μl) at 100°C for 5mins.

GST pull downs performed to analyse 14-3-3β protein-protein interactions were carried out using a similar protocol with the following modifications. The lysis buffer comprised: 50mM Tris pH 7.5, 150mM NaCl, 0.5% (v/v) Triton X-100, 0.1mM Na_3VO_4, 10mM NaF, 1x protease inhibitor cocktail and 10nM Calyculin. Glutathione Sepharose 4B bearing GST or GST-tagged, bacterially expressed 14-3-3β was used in place of Glutathione Sepharose 4B (prepared by Dr. Adrian Saurin and stored at 4°C), and beads were tumbled overnight at 4°C with cell lysates; where included, competing phosphopeptides were used at 1μg/ml.

2.2.7.2 Native Immunoprecipitation

All immunoprecipitations were performed under non-denaturing conditions unless otherwise stated. The protocol followed was the same as that for GST-pull downs with the following modifications. Cell lysates were pre-cleared using 25μl Protein A/G (CR-UK research services) equilibrated in lysis buffer. Immuno-complexes were typically captured using pre-equilibrated 25μl Protein A/G and 1μg antibody. For immunoprecipitation of FLAG-tagged proteins, anti-FLAG M2-agarose affinity gel (Sigma) was employed instead.

2.2.7.3 Denaturing Immunoprecipitation of PKCε from Clone 5 cells

Enrichment of PKCε from clone 5 cells was achieved by immunoprecipitation under denaturing conditions. In this case, confluent clone 5 cells were harvested from 15cm dishes into 2ml denaturing lysis buffer containing: 1% SDS, 20mM Tris pH 7.5. Cell lysates were boiled at 100°C for 10mins, sonicated and then diluted 1:10 into lysis buffer containing: 50mM Tris pH 7.5, 150mM NaCl, 1% (v/v) Triton X-100,

0.1mM Na_3VO_4, 10mM NaF, 1x protease inhibitor cocktail. Pre-clearing was performed as above with volumes scaled up proportionally. Cleared lysates were then tumbled overnight at 4°C with 1.25μg anti PKC-ε (BD Transduction Laboratories). Immuno-complexes were recovered by incubation with Protein A on a rotating wheel for 1hr at 4°C and processed as described above.

2.2.8 Polyacrylamide Gel Electrophoresis (PAGE)

Unless otherwise indicated, polyacrylamide gel electrophoresis was performed using the NuPAGE system as recommended by the manufacturer (Invitrogen). Samples were loaded onto 4-12% Bis-Tris Gels and run at 200V (constant) in NuPAGE MOPS SDS Running Buffer. All samples were run alongside RPN800 Full Range Rainbow Markers (Amersham). Protein bands were then visualised either by Coomassie staining or Western blotting.

2.2.9 Coomassie blue staining

NuPAGE gels were submerged in Coomassie blue stain and incubated at RT for 30mins with shaking. Gels were then destained in Coomassie destain at RT with shaking until clear bands were visible against a clean background (2-16hrs). Images were captured using an Epson Expression 1680 Pro scanner and Adobe Photoshop CS software.

2.2.10 Western Blotting

Proteins separated on NuPAGE gels were transferred electrophoretically onto polyvinylidene difluoride (PVDF) membranes (Millipore) pre-soaked in MetOH. A wet transfer system was employed (Biorad) with all components pre-equilibrated in cold transfer buffer. Unless otherwise specified, transfers were carried out at constant voltage and 400mA/hour at 4°C; the efficiency of transfer was verified by Ponceau S staining. All subsequent incubations were performed with shaking. Membranes were first blocked with 2% (v/v) BSA/TBS-T for 1hr at RT and then incubated with primary antibody diluted in TBS-T either for 1hr at RT or overnight at

4°C. Where primary antibodies were phospho-specific, 1µg/ml of the corresponding blocking dephospho-peptide was included in this incubation. Membranes were washed 3x10mins in TBS-T, incubated with HRP-conjugated secondary antibody in TBS-T for 1hr at RT and then washed again 3x10mins. Blots were developed by enhanced chemiluminescence (ECL) according to the manufacturer's guidelines (Amersham) and exposed to Hyperfilm (Amersham). For quantitative analysis, an image of a film was captured using an Epson Expression 1680 Pro scanner and Adobe Photoshop CS; densitometry was performed using NIH image software (ImageJ 1.34).

2.2.11 Ubiquitination assays

Ubiquitination assays were performed using over-expressed proteins. The candidate ubiquitin ligase and the putative substrate were co-expressed in the presence of HA-tagged ubiquitin. The putative substrate was then isolated by immunoprecipitation, and probed for ubiquitin by western blotting against the HA epitope. The protocols employed were modified to optimise the detection of high molecular weight, ubiquitinated proteins.

2.2.11.1 Cell transfection and lysis

293 cells were transfected with a FLAG-tagged ubiquitin ligase, GST-tagged PKC and HA-tagged ubiquitin at a ratio of 2:2:1. The cells were incubated for 24hrs post-transfection and treated +/- 10µM MG132 overnight. Cells were processed by GST pull-down as described in Section 2.2.7.1, using the following modified lysis buffer: 50mM Tris pH 7.5, 150mM NaCl, 1% NP40, 2mM EDTA, 2mM EGTA, 10mM N-ethylmaleimide (NEM, Sigma), 50µM ALLN (Calbiochem), 2mM $NaVO_3$, 50mM NaF, 1x protease inhibitor cocktail.

2.2.11.2 SDS-PAGE of poly-ubiquitinated protein

Poly-ubiquitinated proteins were separated by SDS-PAGE using Hoefer Pharmacia Biotech gel apparatus as recommended (Sambrook et al.,

1989). To facilitate the resolution of high molecular weight species, 6% running gels were prepared: 6% (v/v) AcrylaGel (National Diagnostics), 0.16% (v/v) Bis-AcrylaGel (National Diagnostics), 0.1% (w/v) SDS, 0.375M Tris pH 8.8, 0.03% (v/v) TEMED, 0.1% ammonium persulphate; with 3% stacking gels: 3% (v/v) AcrylaGel (National Diagnostics), 0.08% (v/v) Bis-AcrylaGel (National Diagnostics), 0.1% (w/v) SDS, 0.125M Tris pH 6.8, 0.1% (v/v) TEMED, 0.1% ammonium persulphate. Gels were run at 18mA overnight in SDS-PAGE running buffer: 0.025M Trizma base, 0.192M Glycine, 0.1% SDS.

2.2.11.3 Western blotting of poly-ubiquitinated protein

Poly-ubiquitinated proteins were processed for Western blotting as described in Section 2.2.10, with the following modified transfer buffer: 25mM Trizma base, 0.15% (w/v) SDS, 200mM Glycine, 20% (v/v) MetOH (not pH adjusted).

2.2.12 *In Vitro* Kinase Assays

2.2.12.1 PKC Autophosphorylation

Recombinant human PKCε and PKCδ purified from insect cells (Calbiochem) were tested for autophosphorylation. Reaction mixes were prepared in screw cap tubes and typically comprised 50µl kinase assay mix and 25ng-1µg PKCε/δ. Reactions were started with the addition of ATP, and incubated at 30°C with shaking (Microtherm incubator, Camlab) over the indicated timecourses. Reactions were stopped with 25µl 3x kinase assay sample buffer, boiled for 5mins at 100°C and resolved by PAGE. Gels were stained by Coomassie, scanned, and then exposed to a pre-blanked phosphor screen overnight; analysis was performed using the Storm 860 PhosphorImaging System (Molecular Dynamics). Subsequently, PKC bands were removed into sterile tubes using a clean scalpel. These bands, alongside a dilution series of the ATP stock, were counted using a 2min Cerenkov programme in a Beckman LS6000IC scintillation machine in order to calculate ^{32}P incorporation and stoichiometry.

2.2.12.2 VBP1 Phosphorylation

PKCε/α catalysed phosphorylation of purified VBP1 was assayed using the same basic protocol described above (Section 2.2.12.1). Typically, reactions were performed in 50μl kinase assay mix, with 25-250ng PKCε/α and 250ng-5μg purified His-VBP1 (or an MBP control) for 0-2hrs. Proteins were resolved by SDS-PAGE, using a 14% running gel and a 9% stacking gel. Phosphorylation was visualised using the PhosphorImager as described in Section 2.2.12.1. Following autoradiography, VBP1 bands were excised and counted.

2.2.12.3 Fbw7α Peptide Phosphorylation

The following Fbw7α derived peptides (prepared by the CR-UK Peptide Synthesis Laboratory) were assayed as PKC substrates:

Fbw7α 6-22:	N-LSVGSKRRRTGGSLRGN-C
Fbw7α wt 11-22:	N-KRRRTGGSLRGN-C
Fbw7α S18A 11-22:	N-KRRRTGGALRGN-C

A PKCζ pseudosubstrate sequence (Ala→Ser) was also employed as a control:

PKCζ PSS:	N-RKRQGSVRRRV-C (bold = Ala in PKCζ)

Reactions were performed using 50μl standard kinase assay mix with 0.2mM peptide substrate and the following PKC isoforms: 25ng α (produced by Phil Whitehead), 15ng δ, 12.5ng ε or 250ng ζ (produced by Phil Whitehead). Assays were incubated at 30°C for the indicated timepoints, and stopped by spotting 15μl onto P81 paper (Whatman) and washing 3x5mins in 30% acetic acid. P81 strips were then counted alongside the ATP stock mix in order to quantitate ^{32}P incorporation (see Section 2.2.12.1).

2.2.12.4 Fbw7α Peptide Array Assays

A peptide array representing the N-terminal region of Fbw7α was produced on a cellulose membrane using the Intavis Multipep peptide synthesizer (prepared by the CR-UK Peptide Synthesis Laboratory). The array comprised 20x12-mer peptide spots, which walked along the Fbw7α sequence from residue 1-31, one amino acid at a time.

Kinase assays were performed in 15ml falcon tubes, with the peptide array cellulose strip laid along the length of the tube. All incubations were performed at RT, with the tube positioned on a rocking shaker such that the strip was constantly covered by moving buffer. The strip was blocked in 3ml of the following buffer for 30mins: 20mM Tris pH7.5, 5mM $MgCl_2$, 0.2% Triton X-100, 0.5% Tween-20. The blocking mix was decanted and replaced with an equal volume of equilibration buffer for a further 30mins: 20mM Tris pH7.5, 5mM $MgCl_2$, 0.2% Triton X-100, 1μg/μl phosphatidylserine (Lipid Products), 1ng/μl TPA, 100μM ATP, 0.5% Tween-20. This buffer was removed and the strip was finally incubated in 2ml full kinase assay mix, with either no enzyme, 10μg purified PKC-α or 100μg purified PKC-α. The reaction was started with the addition of [$γ^{32}P$]-ATP and incubated for 15mins. To stop the reaction, the kinase assay mix was removed and the strip was washed 2x15mins in 15ml 30% acetic acid, 3x15mins in TBS-T and 3x5mins in water. Phosphorylation was visualised using the PhosphorImager as described in Section 2.2.12.1.

2.2.12.5 F-box WD40 Immuno-complex Assays

COS7 cells were plated onto 10cm dishes and transfected with a series of FLAG-tagged F-box WD40 protein constructs (and an empty FLAG vector control). 24hrs post-transfection, Fbw fusion proteins/associated partners were recovered by anti-FLAG immunoprecipitation. Washed beads were incubated in 60μl kinase assay mix with 50ng PKCε for 30mins at 30°C with shaking. Reactions were stopped with 30μl 3x kinase assay sample buffer and boiled at 100°C for 5mins. Proteins were

resolved by PAGE and phosphorylation was visualised using the PhosphorImager as described in Section 2.2.12.1.

2.2.12.6 Immuno-complex Activity Assays

COS7 cells were plated and transfected on 6-well dishes with a panel of GFP-PKCε wild type/mutants constructs. Transfected cells were treated in the presence or absence of 400nM TPA for 45mins, and GFP-PKCε fusions were captured by immunoprecipitation, using standard lysis buffer plus 10nM Calyculin A, with Protein A/anti-GFP (4E12/8). Washed PKCε-bearing beads were incubated in 50μl kinase assay mix with either 5μg MBP, 10μg Protamine Sulphate or 10μg pseudosubstrate peptide (N-RKRQGSVRRRV-C). Reactions were started with the addition of ATP and incubated at 30°C with shaking over the indicated timecourse. In order to assess the lipid dependency of these activities, a second set of reactions were performed in the absence of phosphatidylserine/TPA, using the pseudosubstrate peptide as substrate.

MBP assays were stopped with 25μl kinase assay sample buffer, boiled at 100°C for 5mins and resolved in duplicate by PAGE. One gel was stained by Coomassie and MBP phosphorylation was visualised using the PhosphorImager (see Section 2.2.12.1), and quantified by excising and counting the bands, alongside a dilution series of the ATP stock (see Section 2.2.12.1). The other gel was analysed by western blotting for GFP. Relative activity was determined as a function GFP-PKCε expression. MBP assays are representative of 3 separate experiments; relative specific activity is plotted with error bars to denote standard deviation.

Protamine and pseudosubstrate peptide assays were divided into two aliquots. One aliquot (12.5μl) was removed to 6.25μl kinase assay sample buffer, boiled at 100°C for 5mins, resolved by PAGE, and analysed by western blotting against GFP. The other aliquot (25μl) was spotted onto P81 paper (Whatman) and washed 3x5mins in 30% acetic

acid. P81 strips were then counted alongside the ATP stock in order to quantitate ^{32}P incorporation (see Section 2.2.12.1). Relative activity was determined as a function of PKC-ε expression.

2.2.13 Phosphopeptide Mapping

Putative PKC-ε/δ *in vitro* autophosphorylation sites were analysed by phosphopeptide mapping by the Protein Analysis Laboratory, CR-UK. The samples tested correspond to the PKC-ε/δ gel pieces described in Section 2.2.12.1.

2.2.13.1 Tryptic Digests

PKC-ε/δ samples were subjected to in-gel tryptic digestion as follows. Excised bands were destained using 25mM ammonium bicarbonate/acetonitrile (Rathburn Chemicals) and washed with water for 20 mins. They were then equilibrated with 25 mM ammonium bicarbonate (10mins), dehydrated with acetonitrile (10 mins) and dried in a SpeedVac (10 mins); this process was repeated, this time with a longer drying period (45 min). Gel pieces were next rehydrated in 5µl tryptic digest mix (200ng modified trypsin) and incubated on ice for 45 min. 30µl of 25mM ammonium bicarbonate was added and samples were incubated for a further 4hrs at 37°C; digestions were stopped by placing the tubes on dry ice. Samples were defrosted and the supernatant was decanted to a 0.2 ml siliconized, thin walled tube (Bioquote). Two further rounds of extraction were performed, using 30µl of 5% (v/v) formic acid in water, with a 15min incubation in a sonicating water bath. Peptides from the three extractions were pooled and dried in a SpeedVac. Finally, the peptides were twice resuspended in 50µl water and dried to completion in a SpeedVac to remove all volatile salts.

2.2.13.2 Reverse Phase High Performance Liquid Chromatography

Tryptic peptide extracts were fractionated by reverse-phase high performance liquid chromatography using an ABI 130A Separation System with a Vydac 1mm x 150mm C8 reverse phase column, run at

$50\mu l/min$. Fractions were counted using a 2min P^{32} programme in a Beckman LS6000IC scintillation machine, and those containing radiolabelled peptides were analysed by mass spectrometry and Edman degradation.

2.2.13.3 Matrix-Assisted Laser Desorption Ionization Time-Of-Flight Mass Spectrometry

An aliquot (5%) of each radiolabelled fraction was analysed by Matrix-Assisted Laser Desorption Ionization Time-Of-Flight (MALDI-TOF) mass spectrometry. All mass spectra were recorded with an Applied Biosystems 4700 Proteomics Analyzer in MS Reflector Positive mode, with a fixed laser intensity of 4488, and a focus mass of 1800Da. α-cyano-4-hydroxycinnamic acid ($10\mu g/\mu l$ in 50% (v/v) acetonitrile, 0.1% (v/v) trifluoacetic acid) was used as the matrix. Spectra were internally calibrated with 20fmols of angiotensin 1, or a trypsin autolysis peptide. The peptide masses were searched against the National Center for Biotechnology Information (NCBI) non-redundant database using the Protein Prospector MS-FIT or Mascot programs. One missed cleavage per peptide and an initial mass tolerance of 10 ppm were used in all searches.

2.2.13.4 Edman Degradation

The remainder of each radiolabelled fraction (95%) was subjected to solid-phase Edman degradation using an ABI Procise Sequencer and sequelon acrylamine membranes. Fractions were stored in the dark over night, and then scintillation counted using a 10min P^{32} programme in a Beckman LS6000IC scintillation machine; this relatively long count time was employed to reduce standard error.

114

2.2.14 Raising Phosphospecific Antibodies

Polyclonal phospho-specific antibodies were raised against the following sites: PKCε (mouse) p-S234, p-S316, p-S368; PKCδ (human) p-S304; Fbw7α (human) p-S18.

2.2.14.1 Peptide Synthesis

The following 9/10-mer phospho-peptides were synthesized by the CR-UK Peptide Synthesis Laboratory for use as immunising antigens:

PKCε p-S234: N-DEVGpSQRFS-C
PKCε p-S316: N-KITNpSGQRR-C
PKCε p-S368: N-RKALpSFDNR-C
PKCδ p-S304: N-SRRSDpSASSE-C
Fbw7α p-S18: N-RTGGpSLRGN-C

Equivalent dephospho-peptides were also prepared for each site for use as blocking peptides.

2.2.14.2 Peptide Coupling

Phospho-peptides were coupled to Keyhole Limpet Haemocyanin (KLH) prior to immunisation. Typically, 10mg KLH was dialysed against PBS overnight at 4°C and mixed with 10mg phospho-peptide in a total of 980μl PBS. Where peptide solubility was not complete (PKCε p-S234), 5μl Triton X-100 was added and the solution was sonicated. Coupling was initiated with the addition of 5μl 50% glutaraldehyde (BDH) and incubated at RT for 15mins. A further 2.5μl 50% glutaraldehyde was added and the mix was incubated for 15mins at RT. The reaction was then quenched with 200μl 1M Glycine, made up to 20ml in PBS and aliquoted 6x3.3ml for immunisation. In the case of PKCε p-S368, the protocol was modified to account for the presence of an internal lysine which could couple to KLH and potentially affect the antibodies generated; in this case 8mg of glutaraldehyde coupled peptide was combined with 2mg uncoupled peptide for immunisation.

2.2.14.3 Immunisation

Antibodies were raised against KLH-coupled phopsho-peptides by Harlan Sera-Lab. Three rabbits were immunised with each antigen and test bleeds were collected at day 35 (TB1), 49 (TB2) and 63 (TB3) post-immunisation, the terminal bleed-out (TBO) was harvested at day 77.

Phospho-Site	Rabbits Immunised
PKCε p-S234	PPA-499,500,**501**
PKCε p-S316	PPA-502,**503**,504
PKCε p-S368	PPA-**505**,506,507
PKCδ p-S304	PPA-513,**514**,515
Fbw7α p-S18	PPA-525,526,**527**

Table 2.6 Phosphospecific Antibodies. The phosphospecific antibodies raised are summarised. The optimal antibody for each antigen, which was used in the experiments presented in subsequent results chapters, is indicated in bold.

2.2.14.4 Antibody Characterisation by ELISA

Fbw7α p-S18 second test bleeds were characterised by ELISA prior to use in Western blotting. Plates were prepared bearing either the phospho-S18 peptide or corresponding dephospho-S18 peptide coupled to BSA, and incubated with a dilution series of each test bleed +/- blocking peptide.

1mg phospho/dephospho-S18 peptide was mixed with 1mg BSA in a total of 1ml TBS. Coupling was initiated with the addition of 5μl 50% glutaraldehyde and incubated at RT for 15mins. A further 2.5μl 50% glutaraldehyde was added and left for 15mins at RT. The reaction was then quenched with 200μl 1M Glycine. BSA-coupled peptides were diluted to 10μg/ml in ELISA Coating Buffer and aliquoted at 100μl/well over a plastic 96-well plate; coating was allowed to proceed overnight at 4°C. Wells were washed with 3x200μl 0.5% Tween-20/TBS, blocked with 200μl 1% BSA/TBS for 1hr at 37°C and washed again with 3x200μl 0.5%

Tween-20/TBS. Plates were then incubated overnight at 4°C with a dilution series of each test bleed (10^{-3},10^{-4}, 10^{-5}, 10^{-6}) +/- 1µg/ml blocking peptide in 200µl/well TBS; de-phosphopeptide was used to block in phospho-peptide wells and vice versa. Wells were washed with 3x200µl 0.5% Tween-20/TBS, incubated with 200µl/well 1:2000 HRP-conjugated anti-rabbit secondary antibody in TBS for 1hr at 37°C, and washed again with 3x200µl 0.5% Tween-20/TBS. Finally SIGMAFAST o-phenylendiamine dihydrochloride substrate was prepared according to the manufacturer's instructions and incubated at 100µl/well; the reaction was stopped in the linear range with 100µl 2N H_2SO_4 and quantified at 490nm using a plate reader (Dynatech).

2.2.15 Immunofluorescence
2.2.15.1 Coverslip preparation
Cells were seeded on acid washed glass coverslips (provided by CR-UK research services) and transfected/stimulated as indicated in figure legends. Carrier controls were performed in parallel for each solvent. Cells were washed in PBS and fixed in 4% (w/v) paraformaldehyde/PBS for 10mins at RT. For visualisation of GFP/RFP-tagged proteins, coverslips were then washed and mounted as described below. Where staining was required, cells were first permeablized and blocked by incubation in 0.2% Triton X-100/2% BSA/PBS for 10mins at RT. Cells were then incubated either with primary antibody or 1:200 Alexa Fluor 546 Phalloidin (Molecular Probes) diluted in 2% BSA/PBS for 45mins at RT. Cells were washed 3x10mins in PBS with shaking and for antibody staining incubated in the dark with fluorescent dye-conjugated secondary antibody for 45mins at RT. Coverslips were washed 3x10mins in PBS, once in water and mounted onto glass slides (Western Laboratory Services) using Mowiol mounting media; slides were incubated for 1hr at 37°C to allow the mountant to set and then stored at 4°C.

2.2.15.2 Confocal Microscopy

Images were acquired as recommended by the CR-UK Light Microscopy Laboratory using an upright laser scanning confocal microscope (LSM 510, Carl Zeiss Jena) equipped with a 63x/1.4 Plan-Apochromat Oil Ph3 objective. GFP was excited with the 488nm line of an Argon laser, Cy3 with a 543nm HeNe laser; individual channels were scanned sequentially line by line with averaging set at 8. Each image represents a single 1.0μm 'Z' optical section with a pixel size of approximately 0.1μm. Each confocal image is representative of at least 3 separate experiments.

CHAPTER 3

PKC-ε Yeast 2- Hybrid Analysis

3.1 Introduction

Cellular behaviour is controlled by complex networks of proteins, which signal, integrate and interpret environmental and internal cues. These proteins rarely act as single, isolated species, but rather assemble into dynamic complexes in which they regulate and support each other. Protein-protein interactions influence many aspects of protein function, binding partners can direct association with upstream regulators and downstream targets, mediate recruitment to an appropriate cellular location or impose integration with other signalling systems. As such, one valuable means of characterising a protein is by identifying those other proteins with which it interacts.

A number of functionally significant PKC binding proteins have been defined to date, including activators (*e.g.* cdc42/PAR6/PAR3 complex (Ohno, 2001)), inactivators (e.g. pVHL (Okuda et al., 1999)), substrates (*e.g.* MARCKS (Stumpo et al., 1989)), anchors (*e.g.* InaD (Tsunoda et al., 1997)) and scaffolds which may facilitate cross-talk (*e.g.* gravin (Nauert et al., 1997)). These examples illustrate the importance of protein-protein interactions in the regulation and function of PKC, but by no means constitute an exhaustive list of binding partners.

In order to further develop our understanding of the novel PKC isoform PKC-ε, we therefore resolved to screen for additional interacting proteins. This was undertaken with a particular interest in the detection of binding partners which might relate to the down-regulation of PKC, an important yet poorly characterised process, which represents a focus of ongoing research in our laboratory. To date, only one ubiquitin ligase, pVHL, has

been identified with activity towards PKC (Okuda et al., 2001), and as noted above, pVHL was in fact first linked to PKC as a binding partner.

Advances in the field of proteomics have led to the development of many methods for identifying binding partners. Interaction between proteins can be inferred from genetic interaction or mRNA co-expression, detected by recovery of protein complexes followed by identification by mass spectroscopy, or screened for by phage display or a variation of the yeast 2-hybrid system. We chose to exploit the yeast 2-hybrid approach (Fields and Song, 1989) in order to identify PKC binding partners. This technique is well established, relatively straightforward and shows high sensitivity. The interactions detected are direct, and the isolated putative binding partners are immediately available as cDNAs. Also, once a system has been established, it is amenable to screening with numerous different baits, a feature exploited in our laboratory.

This chapter describes the preparation and characterisation of a yeast 2-hybrid system, the screens that were performed to detect PKC-ε binding partners and the putative interacting proteins which were identified.

3.2 Results

3.2.1 MATCHMAKER SYSTEM 3

Yeast 2-hybrid analysis was performed using MATCHMAKER System 3 (Clontech, 1999) as summarised in Figure 3.1. In this system, a bait protein is expressed as a fusion with the GAL4 DNA-binding domain (DNA-BD), alongside a cDNA library in which each clone is constructed as a fusion with the GAL4 activation domain (AD). Where the bait and the library proteins interact, the DNA-BD and the AD are brought into close proximity, thus activating transcription from the GAL4 promoter. Three separate reporter genes are under the control of this promoter in the yeast strain AH109: *HIS3, ADE2* and *MEL1*, which code for essential genes in the biosynthetic pathways for histidine and adenine, and for α-galactosidase respectively. As such, protein-protein interactions can be detected by nutritional selection using media lacking His or Ade, and/or by blue/white screening using X-α-Gal indicator plates.
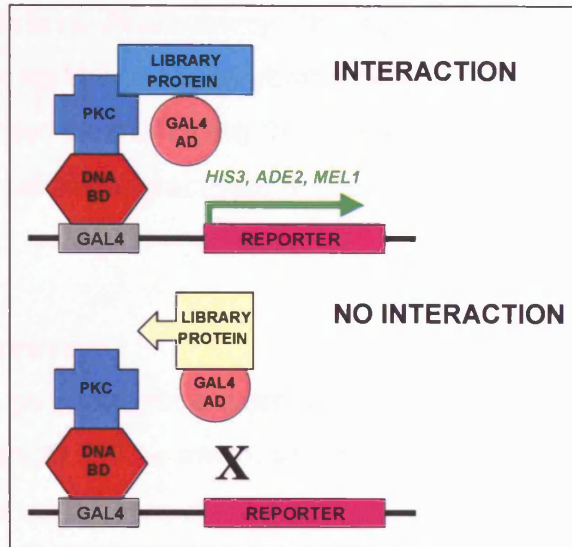
Figure 3.1 MATCHMAKER System 3. Yeast 2-hybrid analysis was performed using MATCHMAKER System 3 (Clontech). In this system, a bait protein, such as PKC, is expressed as a fusion with the GAL4 DNA-binding domain (DNA-BD), alongside a cDNA library in which each clone is constructed as a fusion with the GAL4 activation domain (AD). Where the bait and the library proteins interact, the DNA-BD and the AD are brought into close proximity, thus activating transcription from the GAL4 promoter. Three separate reporter genes are under the control of this promoter in the yeast strain AH109: *HIS3, ADE2* and *MEL1*.
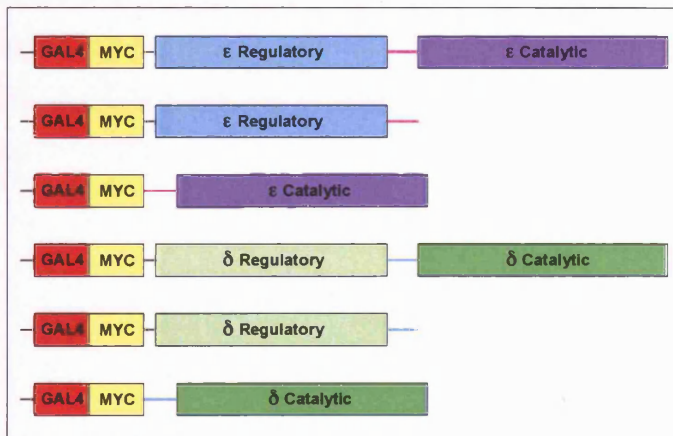
Figure 3.2 PKC Yeast 2-Hybrid Bait Constructs. A panel of PKC yeast 2-hybrid baits were cloned into pGBKT7 as myc-tagged GAL4 DNA binding domain fusion proteins. Full length mouse PKC-ε was prepared as a bait, alongside its individual regulatory and catalytic domains, which bear an overlapping sequence derived from the hinge region. Corresponding rat PKC-δ constructs were generated in parallel.

3.2.2 Yeast 2-Hybrid: Preliminary Characterisation

Prior to undertaking the yeast 2-hybrid screen, it was first necessary to validate the system by confirming that the bait constructs could be expressed and did not autoactivate the reporter genes used to detect interactions.

3.2.2.1 Bait Expression

A panel of PKC bait constructs were generated for yeast 2-hybrid analysis. Full length PKC-ε and δ, as well as their individual regulatory and catalytic domains, were cloned as myc-tagged, GAL4 DNA-BD fusion proteins (see Figure 3.2).

Bait expression in yeast was confirmed by Western blotting, as shown in Figure 3.3. Although each of the constructs bears a myc tag, not all were readily detectable by Western blotting against the myc epitope. Full length PKC-ε and δ, and the PKC-δ catalytic domain, were not visualised using the 9E10 antibody under the conditions employed; they could, however, be detected with PKCε/δ specific primary antibodies. This suggests that the expression level of these bait constructs is relatively low, a conclusion supported by a comparative blot in which PKC-ε and PKC-ε catalytic domain baits are probed alongside each other (see Figure 3.3vii).
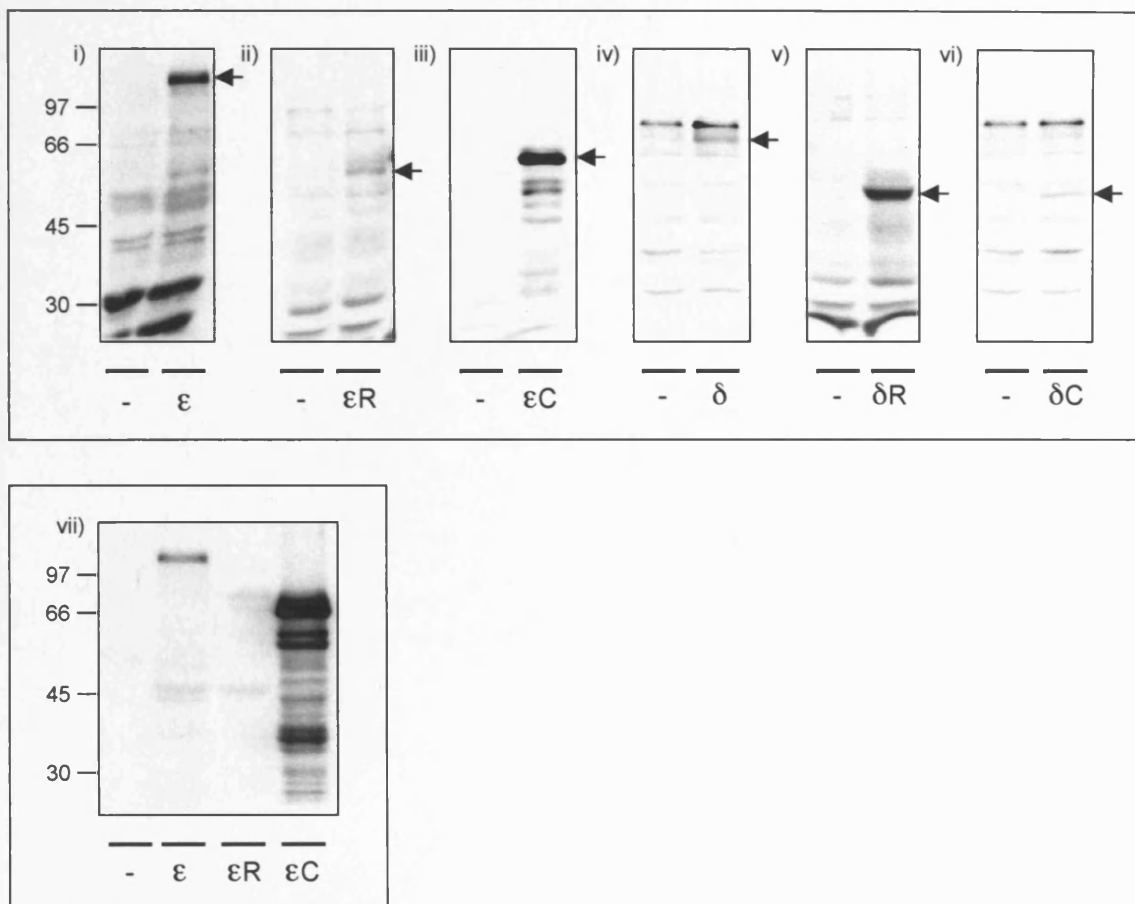
Figure 3.3 PKC Bait Expression in AH109 Yeast. Yeast were co-transformed with a PKC bait, or empty pGBKT7 negative control, and empty pGADT7 prey vector. Protein extracts were prepared by TCA precipitation and bait expression was analysed by western blotting; extracts were probed as follows: i) PKC-ε bait (ε), anti-PKCεPPA-130; ii) PKC ε-regulatory domain bait (εR), anti-myc 9E10 (30min exposure); iii) PKC ε-catalytic domain bait (εC), anti-myc 9E10 (5min exposure); iv) PKC-δ bait (δ), anti-PKCδC-17; v) PKC δ-regulatory domain bait (δR), anti-myc (5 min exposure); vi) PKC δ-catalytic domain bait (δC), anti-PKCδ C-17; vii) PKC ε bait comparison, anti-PKCεPPA-130.

124

3.2.2.2 Bait Toxicity

As interacting partners are detected according to growth on selective media in the yeast 2-hybrid system, it was also important to establish that bait expression did not confer toxicity. This was investigated by comparing the growth rates of yeast transformed with bait constructs to yeast transformed with an empty bait plasmid. Growth in liquid media was followed, by measuring the OD_{600} of the culture (see Figure 3.4). None of the bait constructs proved to be lethal, however all slowed down the growth rate of the yeast to a certain extent.

3.2.2.3 Bait Autoactivation of Reporter Genes

Since the detection of protein-protein interactions by yeast 2-hybrid analysis relies on the specific up-regulation of reporter genes, it was necessary to verify that the bait constructs did not have any intrinsic DNA binding and/or transcriptional activating properties. This was achieved by plating yeast co-transformed with bait plasmids/empty library plasmid on selective media at increasing stringency (see Figure 3.5). Yeast expressing empty bait plasmid/empty library plasmid were used as negative controls, while yeast co-expressing murine p53 bait and SV40 large T-antigen prey provided a robust positive control for protein-protein interaction (Li and Fields, 1993).

The *TRP1* and *LEU2* genes are the selective markers for the bait and prey vectors respectively. Since all of the yeast tested were transformed with both vectors, all grow on the -TRP/LEU drop-out plates. However, *HIS3*, *ADE2* and *MEL1* represent the reporter genes for protein-protein interaction. As such, while the positive controls are able to grow on -HIS and -HIS/ADE nutritional selection plates and are positive for blue/white screening in the presence of X-α-gal, the negative controls do not survive. Yeast expressing the PKC bait constructs behave like the negative control, indicating that they are unable to autoactivate reporter gene transcription and are therefore amenable to yeast 2-hybrid analysis using this system.
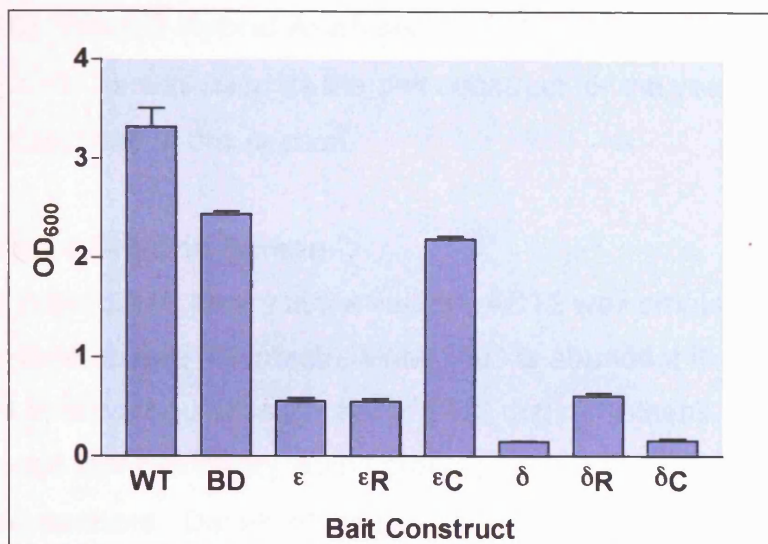
Figure 3.4 PKC Bait Transformant Growth Assays. AH109 yeast were co-transformed with a PKC bait, or empty pGBKT7 negative control (BD), and empty pGADT7 prey vector. 5ml cultures were established in triplicate in -TRP/LEU media and incubated for 24hrs at 30°C with shaking. Untransformed yeast (WT) were grown in fully supplemented SD media in parallel. Proliferation was assayed by measuring OD_{600} in order to determine whether bait expression affects growth rate; error bars denote standard deviation. ε, PKC-ε; δ, PKC-δ; R, regulatory domain; C, catalytic domain.
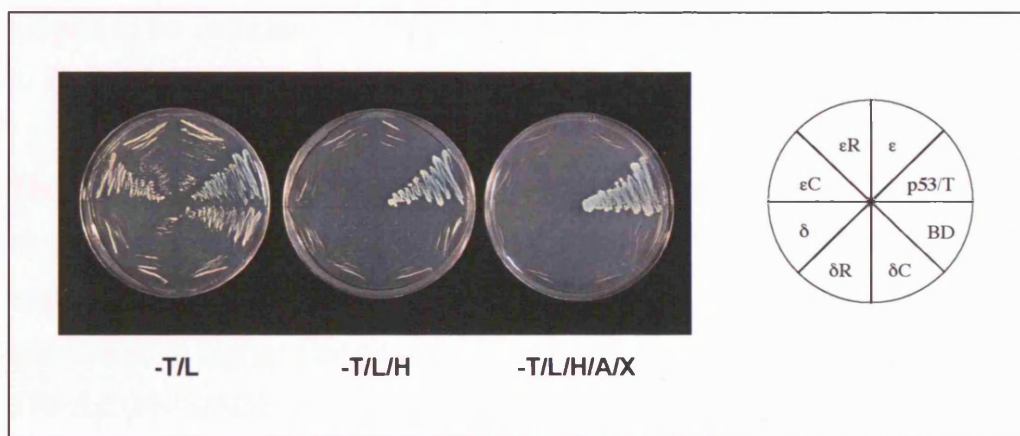
Figure 3.5 PKC Bait Reporter Gene Autoactivation Assay. AH109 yeast co-transformants expressing PKC bait/empty pGADT7 were plated onto media selective for the vectors (-T/L), for medium stringency interaction (-T/L/H) and for high stringency interaction (-T/L/H/A/X) to test for autoactivation of reporter genes. pGBKT7-p53/pGADT7-T Ag were co-transformed as positive controls, pGBKT7/pGADT7 as negative controls. Plates were incubated at 30°C for 6 days and photographed. ε, PKC-ε; δ, PKC-δ; R, regulatory domain; C, catalytic domain.T, Tryptophan; L, Leucine; H, Histidine; A, Adenine; X, + X-α-gal.

3.2.3 PKCε Yeast 2-Hybrid Analysis

Full length PKC-ε was used as the bait construct for the yeast 2-hybrid analysis described in this section.

3.2.3.1 Yeast 2-Hybrid Screen

A mouse brain cDNA library in the vector pACT2 was employed in this yeast 2-hybrid screen (Clontech); since PKC is abundant in the brain, and is subject to downregulation in cells of CNS origin (Kotsonis et al., 2001), we reasoned that this library would prove an appropriate source of PKC-ε interacting partners. Details of the pACT2 vector and of the library's construction are given in Appendix A1.

The PKC-ε bait and the mouse brain cDNA library were transformed sequentially for yeast 2-hybrid analysis with the aim of screening 10^6cfus. A total of 1.4×10^5 cfus were in fact screened, it is likely that the process of scaling up to the volumes required for a library screen reduced the efficiency of transformation. A large number of putative positive binding partners were nevertheless identified and the range of the screen was judged to be sufficient. The screening process employed is summarised in Figure 3.6.

The first round of yeast 2-hybrid screening was performed at medium stringency by plating co-transformed yeast onto -TRP/LEU/HIS media; a total of 980 colonies were recovered. In order to screen these clones for interaction at higher stringency, colonies were re-streaked onto -TRP/LEU/HIS/ADE as shown in Figure 3.6b. 129 colonies demonstrated robust protein-protein interaction on this selection media; the remaining transformants appeared as small, pink colonies because adenine deficiency results in the accumulation of a red oxidized, polymerized derivative of 5-aminoimidazole ribotide in yeast vacuoles (Clontech, 1999). The positive clones were subjected to a final round of selection; colonies were re-streaked onto CSM-TRP/LEU/HIS/ADE/X-αgal agar plates to test for the activation of the third reporter gene by blue/white

selection (see Figure 3.6c). All 129 colonies displayed growth and blue colouration on the highest stringency selection media and were considered to express putative PKC-ε binding proteins.

Following this final round of selection, pACT2 library vectors were recovered from the 129 positive AH109 colonies. Isolated plasmids were reintroduced into yeast expressing PKC-ε bait to confirm the interactions detected; the data obtained is summarised as part of Table 3.2. The level of reproducibility was generally poor (see Discussion), and subsequent analyses were therefore performed in mammalian cells, as described in Chapter 4.

a)   Transform yeast: 1.4 x 10^5 cfus   b)

↓ -HIS

Medium stringency: 980 colonies

↓ -HIS/ADE

c)

High stringency: 129 colonies

↓ -HIS/ADE/X-α-gal

High stringency (blue/white): 129 colonies
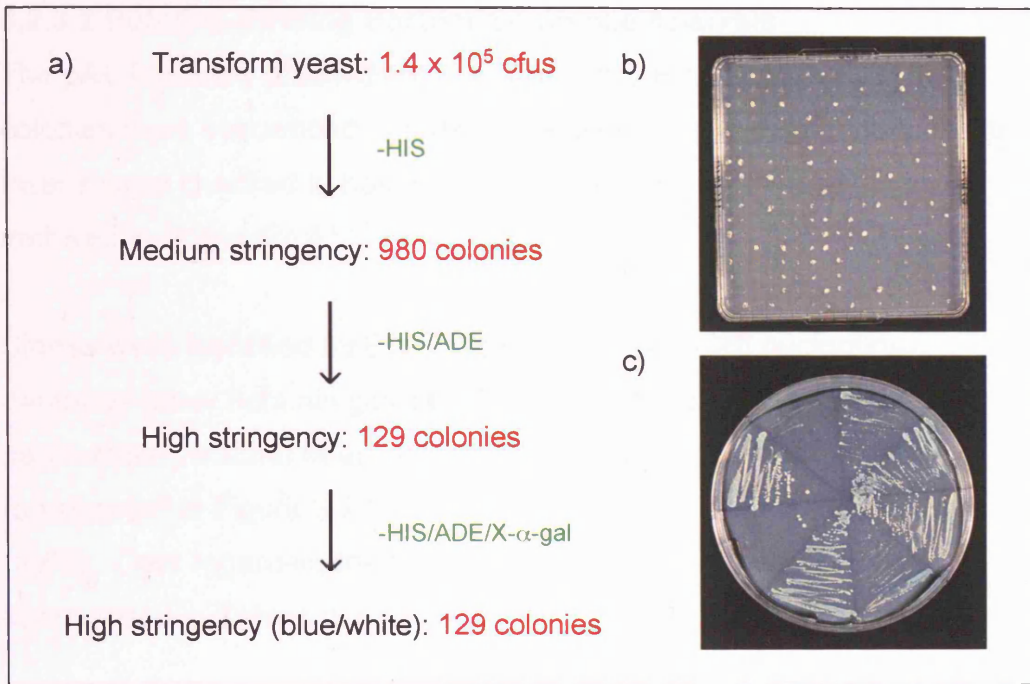
Figure 3.6 Sequential Rounds of Yeast 2-Hybrid Screening with a PKC-ε bait and a mouse brain cDNA library. AH109 yeast were co-transformed sequentially with pGBKT7-PKCε bait, followed by 1.4x10^5 mouse brain cDNA library cfus. Transformants were plated directly onto medium stringency plates and incubated at 30°C for 5 days. Positive colonies from this round of selection were then replated onto higher stringency plates and incubated at 30°C for a further 3 days (b). The remaining positive clones were restreaked onto high stringency media + X-α̃gal for a final round of screening with blue/white selection and incubated for 5 days at 30°C (c).

3.2.3.2 Putative Binding Partner Sequence Analysis

The pACT2 library plasmids recovered from the 129 positive AH109 colonies were sequenced in order to identify the clones encoded. Library inserts were checked in both directions, the raw sequencing data are archived in Appendix A1.

Clones were identified by BLAST searching the NCBI nucleotide database (www.ncbi.nih.gov/BLAST/), using the default search parameters (Altschul et al., 1997). The results of one such search are represented in Figure 3.7 to illustrate the information provided by this facility. Data regarding the highest scoring match for each clone is summarized in Tables 3.1 and 3.2.

In most cases, the library insert represented a coding sequence and the accession number of the top scoring mRNA match was used to retrieve the full length sequence from the Entrez Nucleotide database. However, in some cases, the library insert was best aligned with non-coding sequence and was disregarded for subsequent analyses. This approach was undertaken as a means of avoiding false positives and of reducing the clones studied to a practical number, however, as addressed in Section 3.3, there are circumstances under which such clones may in fact represent valid interacting partners.

Where the library insert comprised coding sequence, an alignment was performed against the corresponding full length cDNA using the GeneStream online resource (www2.igh.cnrs.fr/home.eng.html) in order to determine which part of the ORF was represented in the library vector. A number of clones were identified which lacked the 5' portion of the cDNA, presumably due to inefficient library construction by oligo (dT) priming. The frame of any such partial insert was confirmed with respect to its N-terminal GAL4 AD/HA fusion; frame-shifted clones were not pursued in subsequent studies. It was important to perform these analyses carefully, since there were a small number of cases in which the library vector contained a mutation which had to be accounted for in

130

designating the reading frame; for example, clone 19 contained an adapter sequence deletion (see Appendix A1.3).

a)

Distribution of 61 Blast Hits on the Query Sequence

Mouse-over to show defline and scores, click to show alignments
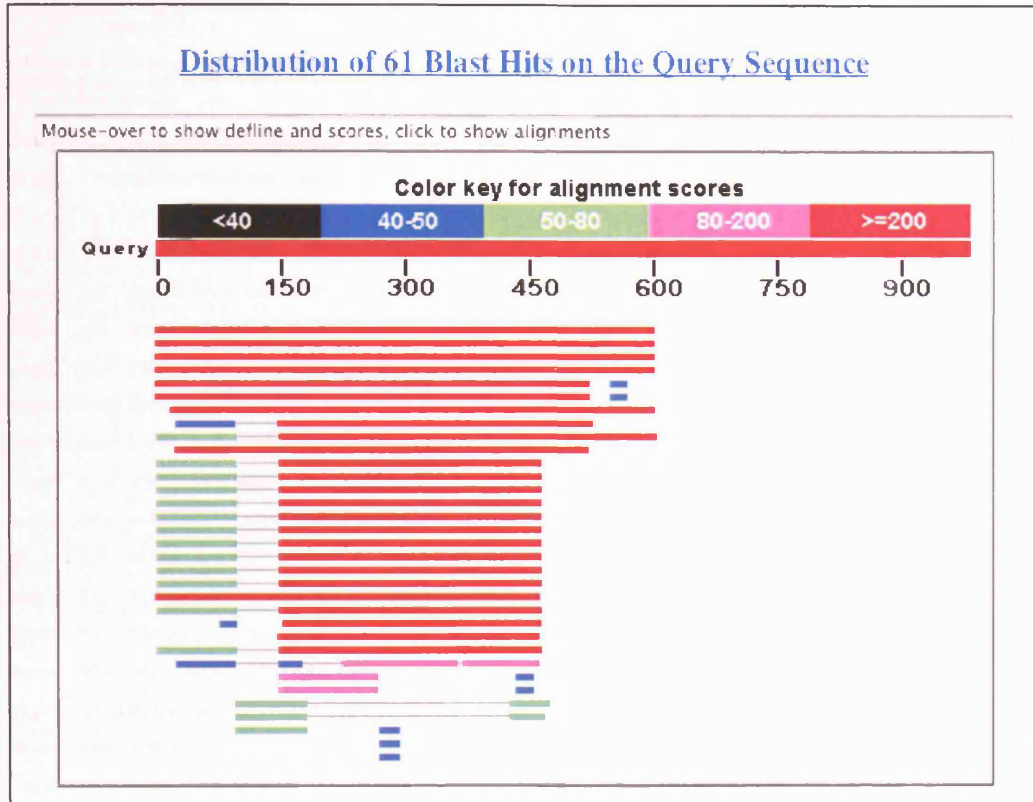
b)

Sequences producing significant alignments:	Score (Bits)	E Value	
gi|20149753|ref|NM_138668.1| Mus musculus RIKEN cDNA 1810047C23	1061	0.0	U E
gi|13529583|gb|BC005503.1| Mus musculus RIKEN cDNA 1810047C23...	1061	0.0	U E
gi|26347130|dbj|AK078309.1| Mus musculus adult male olfactory...	1061	0.0	U
gi|26344629|dbj|AK075795.1| Mus musculus 10 day old male panc...	1061	0.0	U
gi|62079018|ref|NM_001014142.1| Rattus norvegicus similar to ...	664	0.0	
gi|53734271|gb|BC083771.1| Rattus norvegicus similar to RIKEN...	664	0.0	U
gi|61806999|gb|AC114558.18| Mus musculus chromosome 8, clone RP2	385	2e-103	
gi|67970334|dbj|AB169428.1| Macaca fascicularis testis cDNA, ...	287	3e-74	
gi|55727343|emb|CR858199.1| Pongo pygmaeus mRNA; cDNA DKFZp46...	278	3e-71	
gi|57098018|ref|XM_540023.1| PREDICTED: Canis familiaris simi...	268	3e-68	
gi|21750052|dbj|AK091635.1| Homo sapiens cDNA FLJ34316 fis, clon	250	6e-63	U
gi|14714702|gb|BC010493.1| Homo sapiens hypothetical protein ...	250	6e-63	U E
gi|50503627|emb|CR622820.1| full-length cDNA clone CS0DN004YB...	250	6e-63	U
gi|50503376|emb|CR622569.1| full-length cDNA clone CS0DI010YB...	250	6e-63	U
gi|50496548|emb|CR615741.1| full-length cDNA clone CS0DM009YA...	250	6e-63	U
gi|50493993|emb|CR613186.1| full-length cDNA clone CS0DF002YF...	250	6e-63	U
gi|50491062|emb|CR610255.1| full-length cDNA clone CS0DI005YA...	250	6e-63	U
gi|50485053|emb|CR604246.1| full-length cDNA clone CS0DJ005YK...	250	6e-63	U
gi|66884887|gb|DQ033678.1| Homo sapiens FLJ11200 gene, VIRTUA...	250	6e-63	
gi|48146672|emb|CR457278.1| Homo sapiens full open reading fr...	250	6e-63	U
gi|55623583|ref|XM_517560.1| PREDICTED: Pan troglodytes simil...	248	3e-62	
gi|7023716|dbj|AK002062.1| Homo sapiens cDNA FLJ11200 fis, clone	242	2e-60	U E
gi|50483298|emb|CR602491.1| full-length cDNA clone CS0DC013YL...	242	2e-60	U
gi|66884888|gb|DQ033679.1| Pan troglodytes FLJ11200 gene, VIR...	242	2e-60	
gi|8922937|ref|NM_018359.1| Homo sapiens hypothetical protein FL	242	2e-60	U E
gi|21291658|gb|AC106897.5| Homo sapiens BAC clone RP11-27909 fro	119	2e-23	

c)

```
>gi|20149753|ref|NM_133668.1|  [U][image] Mus musculus RIKEN cDNA 1810047C23 gene (1810047C23Rik), mRNA
         Length=1556

 Score = 1061 bits (535), Expect = 0.0
 Identities = 588/600 (98%), Gaps = 3/600 (0%)
 Strand=Plus/Plus

Query  1    AAAAAGTTAACTGACACGCAACAGATAGTAAATATAGACCTCATGCTGGAGATATCGACC  60
            |||||||||||  ||||| |  ||  | |  | | ||| || | |||| || ||| |||||
Sbjct  377  AAAAAGTTAACTGACACGCAACAGATAGTAAATATAGACCTCATGCTGGAGATATCGACC  436

Query  61   CCTCTGGGAGCCGTAACCCCCATCCTGGAGAGGGAAAATGAAGAGCACCACTACATTAAC  120
            ||||||||||||||||||  ||| |||||||| ||||| ||||||||||||| ||||||||
Sbjct  437  CCTCTGGGAGCCGTAACCCCCATCCTGGAGAGGGAAAATGAAGAGCACCACTACATTAAC  496

Query  121  ATGAGCTTGCCAATTGACGCCGTTGTGTCTGTTGCTCCAGAGGAATCATGGGGAAAAGTG  180
            |||||||||||| | | | | || ||||||||||||||||| | |||| || | ||| ||
Sbjct  497  ATGAGCTTGCCAATTGACGCCGTTGTGTCTGTTGCTCCAGAGGAATCATGGGGAAAAGTG  556

Query  181  CGCAAACTTCTAGTGGATGCAATTCTCAGGCAGCTAGTTGATGTGGAAAAATGCATCCTG  240
            ||||||||||||||||||||||||||||||||||||||||||||||||||||||||||||
Sbjct  557  CGCAAACTTCTAGTGGATGCAATTCTCAGGCAGCTAGTTGATGTGGAAAAATGCATCCTG  616

Query  241  AGATATATGAAAGGAACGTCTATTGTGGTCCCCGAGCCACTGCACTTTCAATTGCCAGGG  300
            |||||||||||||||||||||||||||||||||||||||||||||| ||||||||||||
Sbjct  617  AGATATATGAAAGGAACGTCTATTGTGGTCCCCGAGCCACTGCACTTTCAATTGCCAGGG  676

Query  301  AAAAGAATCTTGTAACGGTTTTATATCCATCAGGAATCCCAGATGATCAGCTCCAAGCC  360
            ||||||||||||||||| |||||||| ||||||||||| ||||||||||||||||||||
Sbjct  677  AAAAGAATCTTGTAACGGTTTTATATCCATCAGGAATCCCAGATGATCAGCTCCAAGCC  736

Query  361  TATCGAAAGGAGTTACATGATCTCTTCAATCTGCCTCATGACAGACCTTATTTCAAAAGG  420
            |||||||||||||||||| ||| |||||| |||||||||||||||| ||||||||||||
Sbjct  737  TATCGAAAGGAGTTACATGATCTCTTCAATCTGCCTCATGACAGACCTTATTTCAAAAGG  796

Query  421  ATCAATGCTTATCACTTTCCAGATGAACTATATAAAGATGGCTATATCAG-AACCCACAT  479
            |||||||||||||||| ||||||||||||| | |||||||||||||||||   ||||| |
Sbjct  797  ATCAATGCTTATCACTTTCCAGATGAACTATATAAAGATGGCTATATCAGAAACCCACAT  856

Query  480  ACTTATCTGAAGTCCCCCTAACATAAGGGTAGTATGATTTGTGTGGCCAAGGGCACCTA  539
            ||||||||| |||||  |||||||| |||||||||| |||||||| | | |||||||||
Sbjct  857  ACTTATCTG-AGTCCACCTAACATAGAGGGTAGTATGATTTGTGTGGTCCAGGGCACCTA  915

Query  540  TGCTTAATCATCATTTATATGCCAAGATCGGATTGATGANAATGGTTNGGGCTTTGCTTA  599
            ||||| |||||| |||||||| ||||||||||||||| || ||||| ||||| ||| |||
Sbjct  916  TGCTT-ATCATCA-TTATATG-CAAGATCGGATTGATGACAATGGTTGGGGCTGTGCTTA  972
```

Figure 3.7 Positive Yeast 2-hybrid Clone 1 Forward Sequence BLAST Search Results. Following the final round of PKC-ε yeast 2-hybrid screening, mouse brain library plasmids were recovered from positive clones and sequenced. Clones were identified by BLAST searching the NCBI nucleotide database (http://www.ncbi.nih.gov/BLAST/), using the default parameters. The results obtained with the clone 1 forward sequence are presented. a) top portion of results screen, states the number of database hits and represents their alignment with the input sequence on a colour coded diagram; b) middle portion of results screen, lists the accession numbers and identities of the database hits and indicates the score of the alignment (in bits) and the E value, which estimates the statistical significance of the match; c) the results for the highest scoring database entry, displays the alignment between the input sequence and top hit.

Table 3.1 Forward sequence data for putative positive yeast 2-hybrid clones. 129 mouse brain cDNA clones were recovered from positive yeast colonies following three rounds of yeast 2-hybrid screening with a PKC-ε bait. Library insert sequence data was obtained, using a pACT2 forward primer, and the sequence immediately following the library adapter was analysed using the NCBI BLAST database.

x, no good quality sequence data obtained; N/H no sequences with significant homology identified; N/I CDS boundaries not indicated in mRNA sequence; clone no. underlined, different results obtained with forward and reverse sequences; shaded row, clone meets all of selection criteria required to be considered for further analysis (see text).

Clone	Score	Accession No.	Name	Insert Start (base no.)	mRNA Start (base no.)	CDS?	In Frame?	Alignment From (amino acid no.)
1	1061	NM_138668.1	RIKEN:1810047C23	1	377	Y	Y	98 (of 461)
2	817	BC047068.1	RIKEN:2810432D09	1	40	Y (+60bps 5')	Y	1 (of 163) (+20aa N-)
3	1197	AC127259.3	BAC:RP24304A20 (chr.9)	1	105051	-	-	-
4	543	BC009091.1	zinc finger protein 162	1	2266	N (3'UTR)	-	584-90/608-653
5	46.1	AC129777.4	BAC:RP23281H23 (chr.8)	195	78014	-	-	-
6	971	BC040338.1	autocrine motility factor receptor	1	441	Y	N	-
7	801	AK011889.1	RIKEN:2610205H19 0-44 protein homologue	1	16	Y (+185bp 5')	N	-
8	x	x	x	x	x	x	x	x
9	1068	BC065790.1	sorcin	1	5	Y	N	-
10	N/H	-	-	-	-	-	-	-
11	718	AC123791.4|	BAC:RP24304L14(chr.15)	29	134173	-	-	-
	341	NM_011244.2|	retinoic receptor gamma	1	556	Y	Y	102 (of 458)
12	829	AC087558.13|	C57BL/6J clone rp23-282p18 (chr.2)	1	193091	-	-	-
13	908	AY339599.2	mitochondrial genome; NADH dehydrogenase subunit1 gene	1	2894	Y	N	-

135

14	x	x	x	x	x	x	x	x
15	638	AC149283.2	BAC:RP23-233O21(chr.7)	1	203904	-	-	-
16	x	x	x	x	x	x	x	x
17	771	NM_033561.1	Williams-Beuren syndrome region 1 homologue; wbscr1	1	1467	N (3'UTR)		
18	230	AC025669.19	RP235O16 (chr.14)	1	77762	-	-	-
19	492	NM_080428.2	F-box and WD-40 domain protein 7	1	1008	Y	Y	283 (of 629)
20	733	BC051999.1	amyloid beta precursor-like protein 2	1	2834	N (3'UTR)	-	-
21	805	AK028350.1	RIKEN:3732426M05 Na+/H+ exchanger 6 homologue	1	1166	N/I	-	-
22	331	NM_029929.2	Vacuolar protein sorting 33A	1	2593	N (3'UTR)	-	-
23	422	NM_029929.2	Vacuolar protein sorting 33A	1	2593	N (3'UTR)	-	-
24	x	x	x	x	x	x	x	x
25	973	XM_134593.4	RIKEN:4932417I16	1	513	Y	N	-
26	498	NM_009182.2	ST8 alpha-N-acetyl-neuraminide alpha-2,8-sialyltransferase3	9	3615	N (3'UTR)	-	-

136

27	432	NM_146200.1	eukaryotic translation initiation factor 3, subunit 8	1	2004	Y	Y	649 (of 911)
28	x	x	x	x	x	x	x	x
29	387	NM_019722.3|	ADP-ribosylation factor-like 2	1	4	Y (+33bps 5')	Y	1 (of 184) (+11 aa N-)
30	525	AC102892.9	RP24-362B10 (chr.5)	1	97972	-	-	-
31	224	AY339599.2	mitochondrial genome; cox2	2	7587	Y	N	-
32	x	x	x	x	x	x	x	x
33	103	BC079561.1	N-deacetylase/N-sulfotransferase 1	5	4678	N (3'UTR)	-	-
34	167	BC057207.1	tetratricopeptide repeat domain 3	1	2212	Y	N	-
35	688	NM_030225.3	dihydrolipoamide S-succinyltransferase (E2 component of 2-oxo-glutarate complex)	1	1933	N (3'UTR)	-	-
36	541	AL831750.8	RP23-37L2 (chr.x)	1	112295	-	-	-
37	624	AC153860.4	BAC:RP23170C11	1	54028	-	-	-
	418	NM_011844.3	monoglyceride lipase	105	1	N (5'UTR)	-	-
38	624	AC153860.4	BAC:RP23170C11	1	54028	-	-	-
	418	NM_011844.3	monoglyceride lipase	105	1	N (5'UTR)	-	-

137

39	x	x	x	x	x	x	x	x
40	708	NM_138599.2	translocase of outer mitochondrial membrane 70 homologue	1	1626	Y	Y	493 (of 611)
41	684	AC122022.4	BAC:RP24-372J5 (chr.5)	1	7755	-	-	-
42	936	NM_080635.1	eukaryotic translation initiation factor 3, subunit 3 (gamma)	1	8	Y	Y	2 (of 352)
43	781	AK034899.1	expressed in non-metastatic cells 1 protein (NM23A/nme1/nucleoside diphosphate kinase	1	210	Y	Y	56 (of 152)
44	x	x	x	x	x	x	x	x
45	839	AC115744.9	RP23-479M19 (chr.12)	1	154016	-	-	-
46	835	BC060066.1	TBC1 domain protein 22B	1	2037	N (3'UTR)	-	-
47	x	x	x	x	x	x	x	x
48	513	NM_001001566.1	D1Bwg1363e; chondroitin polymerizing factor	1	2738	N (3'UTR)		
49	932	AC084069.28	rp23-257b17 (chr.13)	1	124011	-	-	-
50	955	AY339599.2	mitochondrial genome; cox1 gene	1	5486	Y	N	-
51	224	XM_132762.6	Predicted: RasGEF domain protein 1a	16	2149	N (3'UTR)	-	-

138

52	x	x	x	x	x	x	x	x
53	1055	NM_138584.1	spastic paraplegia 21 homologue (spg21)	1	187	Y (+23bps 5')	N	-
54	490	BC031782.1	engulfment and cell motility 1	1	1973	N (3'UTR)	-	-
55	315	NM_024227.2	mitochondrial ribosomal protein L28	1	34	Y	Y	2 (of 257)
56	52	AC120549.21	RP23-172L16 (chr.1)	2	68214	-	-	-
57	511	XM_225630.3	rat acyl-Coenzyme A binding domain containing 5 (Acbd5)	1	361	Y	Y	121 (of 705)
58	486	NM_175212.2	RIKEN: 4930438D12	1	421	-	-	-
59	x	x	x	x	x	x	x	x
60	646	BC096426.1	IMAGE:2615937	1	209	Y (+91bps 5')	N	-
61	x	x	x	x	x	x	x	x
62	813	BC060998.1	DNA polymerase beta	1	764	Y	N	-
63	x	x	x	x	x	x	x	x
64	270	BC037027.1	glutathione peroxidase 3	1	36	Y (+24bps 5')	Y	1 (of 226) (+8aas N-)
65	460	MUSGABAAS	GABA-a/benzodiazepine receptor alpha-1 subunit	1	373	Y (+81bps 5')	Y	1 (of 455) (+ 27aas N-)
66	194	AF144695	ERO1L	1	2088	N	-	-

139

67	632	AC109280.9	RP23400B7(chr.18)	1	115172	-	-	-
68	x	x	x	x	x	x	x	x
69	x	x	x	x	x	x	x	x
70	x	x	x	x	x	x	x	x
71	182	AL845502.5	RP23395A21 (chr.4)	1	145946	-	-	-
72	620	AC125179.4	RP23321N8 (chr.16)	1	182977	-	-	-
73	686	NM_011034.2	peroxiredoxin 1 (prdx1)	1	16	Y (+59bp 5')	N	-
74	716	BC094421.1	IMAGE:6413494	1	19	-	-	-
	404	Y13832.1	GT12	1	21	?	-	-
	151	NM_019161.1	rat pb-cadherin	245	2522	Y	?	?
75	656	NM_028325.1	zinc finger CCHC domain 12 (zcchc12)	1	647	Y	Y	90 (of 402)
76	563	AL683822.8	RP2394I24 (chr.x)	1	33043	-	-	-
77	452	AY339599.2	LA9 mitochondrion	1	16168	-	-	-
78	276	AC129314.4	RP23365D12 (chr.1)	18	14474	-	-	-
79	x	x	x	x	x	x	x	x
80	375	BC064081.1	RIKEN: 1500031H01	1	494	-	-	-
81	111	XM_344970.2	rat Ser/Thr kinase 32C	1	2083	N (3'UTR)	-	-
82	833	AB003304.1|	beta-type 20S proteasome subunit X (psmb5)	1	263	Y	Y	86 (of 264)

140

83	266	AC099860.13	RP235C23 (chr.1)	2	163902	-	-	-
84	x	x	x	x	x	x	x	x
85	301	AK122387.1	mKIAA0844	1	2545	N (3'UTR)	-	-
86	605	NM_010250.2	GABA-A receptor, subunit alpha 1	1	2785	N (3'UTR)	-	-
87	x	x	x	x	x	x	x	x
88	359	NM_011983.1	homer homologue 2	1	1141	N (3'UTR)	-	-
89	218	AK075620.1	ferritin light chain 1	42	67	Y (+143bps 5')	N	-
90	670	NM_133206.2	zinc and ring finger 1	1	463	Y	N	-
91	539	BC003794.1	stress-induced phosphoprotein 1	22	1762	N (3'UTR)	-	-
92	708	NM_007727.1	contactin 1	1	3091	Y	Y	948 (of 1020)
93	904	BC064825.1	importin 7	20	3564	N	-	-
94	500	AC124461.3	RP24-144C5 (chr.7)	1	54983	-	-	-
95	x	x	x	x	x	x	x	x
96	x	x	x	x	x	x	x	x
97	414	BC036961.1	IMAGE:4505120	2	838	-	-	-
98	615	AL645625.15	RP23183L1 (chr.4)	1	149634	-	-	-
99	751	BC094422.1	eukaryotic translation initiation	1	999	Y	Y	327 (of 407)

141

			factor 4A2					
100	226	AF041861	synaptojanin 2, zeta isoform	2	1258	Y	N	-
101	x	x	x	x	x	x	x	x
102	163	NM_031037.2	rat guanine nucleotide binding protein, beta 2	1	82	N (5' UTR)	-	-
103	434	NM_013494.2	carboxypeptidase E	1	890	Y	Y	267 (of 476)
104	850	BC052462.1	protein tyrosine phosphatase, receptor type, S	1	4192	Y	Y	1344 (of 1500)
105	969	BC094421.1	IMAGE:6413494	1	19	-	-	-
	613	MMU320506	Gt12 gene	181	97056	-	-	-
106	874	NM_009721.2	ATPase, Na$^+$/K$^+$ transporting, beta 1 polypeptide (Atp1b1)	1	944	Y	Y	149 (of 304)
107	440	NM_010324.1	glutamate oxaloacetate transaminase 1 (got1)	1	7	Y (+48bp 5')	Y	1 (of 413) (+16bps N-)
108	313	NM_016743.1	Nel-like 2 (Nell2)	1	92	Y	Y	306 (of 819)
109	545	NM_027782.1	potassium channel tetramerisation domain containing 6 (kctd6)	1	743	Y	Y	169 (of 237)
110	571	AC124745.4	BAC clone RP23-236O12 (chr.14)	1	24910	-	-	-
111	765	NM_007422.2	adenylosuccinate synthetase (adss)	1	194	Y	Y	67 (of 456)

142

112	x	x	x	x	x	x	x	x
113	x	x	x	x	x	x	x	x
114	515	NM_172624.1	dipeptiylpeptidase 9 (dpp9)	1	2555	Y	Y	792 (of 862)
115	x	x	x	x	x	x	x	x
116	333	BC025165.1	glycoprotein m6b	1	48	Y (+104bps 5')	N	-
117	163	AC126430.3	BAC RP24-406F17	1	45579	-	-	-
118	x	x	x	x	x	x	x	x
119	240	AK077923.1	von Hippel-Lindau binding protein 1	2	32	Y	Y	2 (of 196)
120	x	x	x	x	x	x	x	x
121	305	AK077923.1	von Hippel-Lindau binding protein 1	7	36	Y	N	-
122	684	BC027319.1	ATPase, Na$^+$/K$^+$ transporting, beta 1 polypeptide	1	1756	N (3'UTR)	-	-
	224	BC049225.1 (minus strand)	protein expressed in non-metastatic cells 7 (nme7)	273	1668	-	-	-
123	176	NM_007438.3	aldolase 1, isoform A (Aldoa)	1	590	Y	Y	144 (of 364)
124	444	NM_173446.1	clone AW121567	53	1984	N (3' UTR)	-	-
<u>125</u>	161	AC154237.1	BAC RP24-162018 (chr.17)	77	100662	-	-	-
126	902	AK043846.1	RIKEN:A830039K17	1	150	-	-	-

143

127	x	x	x	x	x	x	x	x
128	430	BC025597.1	calcium/calmodulin-dependent protein kinase II gamma	10	1820	N (3'UTR)	-	-
129	x	x	x	x	x	x	x	x

144

Table 3.2 Reverse sequence data for putative positive yeast 2-hybrid clones. 129 mouse brain cDNA clones were recovered from positive yeast colonies following three rounds of yeast 2-hybrid screening with a PKC-ε bait. Library insert sequence data was obtained, using a pACT2 reverse primer, and the sequence immediately following the Xho I site was analysed using the NCBI BLAST database.

Isolated library plasmids were reintroduced into yeast expressing a PKC-ε bait in four separate experiments, the number of times the original interaction was detectably reproduced is indicated (each * denotes 1 reproduction).

x, no good quality sequence data obtained; N/H no sequences with significant homology identified; N/I CDS boundaries not indicated in mRNA sequence; clone no. underlined, different results obtained with forward and reverse sequences; shaded row, clone meets all of selection criteria required to be considered for further analysis (see text).

Clone	Score	Accession No.	Name	Insert Start (base no.)	mRNA Start (base no.)	CDS?	Reproducibility
1	704	NM_138668.1	RIKEN:1810047C23	26	1540	N (3'UTR)	✳
2	N/H	x	x	x	x	x	✳
3	1150	AC127259.3	RP24304A20 (chr.9)	40	102074	-	✳
4	N/H	-	-	-	-	-	✳
5	436	AC109233.10	RP23219N5 (chr.16)	92	108799	-	✳
6	825	BC040338.1	autocrine motility factor receptor	21	3274	N (3'UTR)	✳✳✳
7	676	AK011889.1	RIKEN:2610205H19 0-44 protein homologue	26	764	Y	✳✳✳✳
8	x	x	x	x	x	x	x
9	714	AC140364.4	RP2475K5 (chr.5)	52	105797	-	✳✳✳
10	N/H	-	-	-	-	-	✳✳✳
11	718	AC123791.4|	RP24304L14 (chr.15)	30	133362	-	✳✳✳
12	N/H	-	-	-	-	-	✳✳
13	908	AY339599.2	mitochondrial genome; NADH dehydrogenase subunit 1 gene	30	3705	Y	✳
14	x	x	x	x	x	x	x

146

15	638	AC149283.2	RP23-233O21(chr.7)	20	199549	-	*
16	x	x	x	x	x	x	x
17	N/H	-	-	-	-	-	*
18	848	AC025669.19	RP235O16 (chr.14)	46	76099	-	*
19	920	NM_080428.2	F-box and WD-40 domain protein 7	43	2117	Y	***
20	x	x	x	x	x	x	*
21	1005	AK028350.1	RIKEN:3732426M05 Na+/H+ exchanger 6 homologue	48	2755	N/I	*
22	x	x	x	x	x	x	*
23	x	x	x	x	x	x	*
24	163	AC124598.5	BAC:RP2322P3	19	87372	-	-
25	581	XM_134593.4	RIKEN:4932417I16	82	2924	N (3'UTR)	-
26	N/H	-	-	-	-	-	**
27	x	x	x	x	x	x	*
28	x	x	x	x	x	x	*
29	x	x	x	x	x	x	*
30	x	x	x	x	x	x	*
31	N/H	-	-	-	-	-	*
32	x	x	x	x	x	x	x

147

33	708	BC079561.1	N-deacetylase/N-sulfotransferase 1	18	6072	N (3'UTR)	✳
34	763	BC057207.1	tetratricopeptide repeat domain 3	24	3571	Y	✳
35	x	x	x	x	x	x	✳
36	779	BC022960.1	BC022960	139	1118	Y	✳
37	724	NM_011844.3	monoglyceride lipase	21	1354	Y	✳
38	581	NM_011844.3	monoglyceride lipase	21	1354	Y	✳
39	954	NM_011844.3	monoglyceride lipase	1	1354	Y	✳✳
40	N/H	-	-	-	-	-	✳
41	706	AC122022.4	BAC:RP24-372J5 (chr.5)	19	7394	-	-
42	x	x	x	x	x	x	✳
43	N/H	-	-	-	-	-	✳✳
44	x	x	x	x	x	x	✳
45	815	AC115744.9	RP23-479M19 (chr.12)	116	154486	-	✳
46	N/H	-	-	-	-	-	✳
47	x	x	x	x	x	x	-
48	248	NM_001001566.1	D1Bwg1363e; chondroitin polymerizing factor	50	3012	N (3'UTR)	✳
49	1108	AC084069.28 (plus strand)	rp23-257b17 (chr.13)	19	122345	-	✳✳
50	955	AY339599.2	mitochondrial genome; cox1	19	6941	Y	✳✳

148

51	155	XM_132762.6	Predicted: RasGEF domain protein 1a	40	2260	N (3'UTR)	*
52	x	x	x	x	x	x	x
53	706	NM_138584.1	spastic paraplegia 21 homologue (spg21)	21	1640	N (3'UTR)	*
54	434	BC031782.1	engulfment and cell motility 1	218	2306	N (3'UTR)	*
55	315	NM_024227.2	mitochondrial ribosomal protein L28	19	1034	Y (+3'UTR)	**
56	x	x	x	x	x	x	x
57	654	AL845257.2	clone:RP23280K4	20	54344	-	*
58	x	x	x	x	x	x	*
59	x	x	x	x	x	x	x
60	N/H	-	-	-	-	-	*
61	325	BC020992.1	similar to DEAD/H box polypeptide 26	39	852	N/I	*
62	854	BC060998.1	DNA polymerase beta	19	1197	Y	*
63	751	NM_133694.1	F-box and leucine-rich repeat protein 15 (fbxl15)	31	1315	Y	*
64	x	x	x	x	x	x	*
65	157	AC133618.3	BAC:CH230-71N8	19	71193	-	*
66	833	AC154575.2	RP23-248E1 (chr.14)	19	70958	-	*

149

67	N/H	x	x	x	x	x	✳
68	827	AC113285.9	clone:RP2340716	19	213772	-	✳✳
69	N/H	x	x	x	x	x	✳
70	x	x	x	x	x	x	x
71	478	AL845502.5	RP23395A21 (chr.4)	24	143637	-	-
72	841	AC125179.4	RP23321N8 (chr.16)	47	185111	-	-
73	x	x	x	x	x	x	x
74	642	BC028971.1	GTL2, imprinted maternally expressed untranslated mRNA	19	1190	-	-
75	x	x	x	x	x	x	x
76	973	AL683822.8	RP2394I24 (chr.x)	19	35595	-	-
77	452	BC002052.1	H3 histone 3A mRNA	29	1077	-	-
78	x	x	x	x	x	x	x
79	714	XM_622593.1	RIKEN: 1500031H01	22	1331	-	-
80	745	BC064081.1	RIKEN: 1500031H01	26	1327	-	-
81	x	x	x	x	x	x	x
82	628	AB003304.1|	beta-type 20S proteasome subunit X	152	874	Y	-
83	474	AC099860.13	RP235C23 (chr.1)	29	161449	-	✳
84	x	x	x	x	x	x	x
85	x	x	x	x	x	x	✳

150

86	605	NM_010250.2	GABA-A receptor, subunit alpha 1	19	4062	N (3'UTR)	✳
87	x	x	x	x	x	x	x
88	458	NM_011983.1	homer homologue 2	19	1655	N (3'UTR)	✳
89	139	AK075620.1	ferritin light chain 1	21	922	N (3'UTR)	-
90	335	NM_133206.2	zinc and ring finger 1	54	2366	N (3'UTR)	✳✳
91	335	BC003794.1	stress-induced phosphoprotein 1	30	2070	N (3'UTR)	✳
92	761	NM_007727.1	contactin 1	20	3829	N (3'UTR)	✳
93	283	BC064825.1 (plus strand)	importin 7	18	2286	N (3'UTR)	✳✳
94	934	AC124461.3 (plus strand)	RP24-144C5 (chr.7)	30	53689	-	✳
95	x	x	x	x	x	x	✳
96	599	NM_028815.3	leucine-rich repeats and IQ motif containing 2 (Lrriq2)	29	5492	N (3'UTR)	✳
97	492	BC036961.1	IMAGE:4505120	19	2346	N (3'UTR)	✳

151

98	x	x	x	x	x	x	✳
99	652	BC094422.1	eukaryotic translation initiation factor 4A2	21	1879	N (3'UTR)	✳
100	484	AC092480.27 (plus strand)	rp23-387f2 (chr.17)	1	129048	-	-
101	x	x	x	x	x	x	x
102	163	NM_031037.2	rat guanine nucleotide binding protein, beta 2	96	1552	N (5'UTR)	-
103	434	NM_013494.2	carboxypeptidase E	1	890	Y	✳✳
104	650	BC052462.1	protein tyrosine phosphatase, receptor type, S	1	5561	N (3'UTR)	✳
105	620	BC024818.1	GTL2, imprinted maternally expressed untranslated mRNA, with apparent retained intron	19	1338	-	✳
	135	BC094421.1	IMAGE:6413494	350	1356	-	
	131	MMU320506	Gt12 gene	352	103392	-	
106	993	NM_009721.2	ATPase, Na$^+$/K$^+$ transporting, beta 1 polypeptide (Atp1b1)	19	1614	Y N (+3'UTR)	✳✳
107	640	NM_010324.1	glutamate oxaloacetate transaminase 1 (got1)	18	1890	N (3'UTR)	✳✳

152

108	313	BC051968.1	Nel-like 2 (Nell2)	26	3125	N (3'UTR)	**
109	406	NM_027782.1	potassium channel tetramerisation domain containing 6 (kctd6)	54	1584	N (3'UTR)	**
110	952	AC124745.4	BAC clone RP23-236O12 (chr.14)	21	22262	-	*
	369	NM_025832.2	NMDA receptor regulated 1-like (Narg1l)	328	3875	N (3'UTR)	
111	525	NM_007422.2	adenylosuccinate synthetase (adss)	22	2553	N (3'UTR)	*
112	x	x	x	x	x	x	x
113	609	BC080776.1	ubiquitin-activating enzyme E1C	18	2091	N (3'UTR)	**
114	396	NM_172624.1	dipeptiylpeptidase 9 (dpp9)	149	3332	N (3'UTR)	*
115	x	x	x	x	x	x	x
116	523	BC025165.1	glycoprotein m6b	19	1460	N (3'UTR)	*
117	569	AC126430.3	BAC RP24-406F17	75	46746	-	*
118	x	x	x	x	x	x	x
119	478	AK077923.1	von Hippel-Lindau binding	28	1575	N	**

153

			protein 1			(3'UTR)	
120	x	x	x	x	x	x	x
121	305	AK077923.1	von Hippel-Lindau binding protein 1	144	1575	N (3'UTR)	*
122	640	BC027319.1	ATPase, Na$^+$/K$^+$ transporting, beta 1 polypeptide	23	2216	N (3'UTR)	*
	381	BC049225.1 (plus strand)	protein expressed in non-metastatic cells 7 (nme7)	20	1477	N (3'UTR)	-
123	285	NM_007438.3	aldolase 1, isoform A (Aldoa)	21	1438	N N (3'UTR)	-
124	773	NM_173446.1	clone AW121567	131	3140	N (3'UTR)	-
<u>125</u>	357	AL451076.14	RP2343020 (chr.X)	19	7299	-	*
126	x	x	x	x	x	x	x
127	x	x	x	x	x	x	*
128	x	x	x	x	x	x	x
129	x	x	x	x	x	x	x

154

3.2.3.3 Elimination of Commonly Occurring False Positives

Following sequence analysis, the remaining putative positive clones were checked against a table of commonly occurring potential false positives (listed at www.fccc.edu:80/research/labs/golemis/main_false.html; see Table 3.3); any clones corresponding to these classes of protein were disregarded for further analysis.

Commonly Occurring Yeast 2-Hybrid False Positives	Corresponding Clones
Heat Shock Proteins	-
Ribosomal proteins	55
Cytochrome Oxidase	-
Mitochondrial proteins	40
Proteasome Subunits	82
Ferritin	-
tRNA synthase	-
Collagen-related proteins	-
Zinc Finger Proteins	4, 75
Vimentin	-
Inorganic pyrophosphatase	-
Proliferating Cell Nuclear Antigen	-
Elongation Factors	-
Lamin	-
Ubiquitin	-

Table 3.3 Commonly Occurring Yeast 2-Hybrid False Positives.
Putative positive mouse brain cDNA clones, isolated after three rounds of yeast 2-hybrid screening with a PKC-ε bait, were sequence analysed. Any clone representing an in-frame coding sequence was checked against a list of commonly occurring potential false positives (www.fccc.edu:80/research/labs/ golemis/main_false.html).

3.2.3.4 Putative Binding Partners: Protein Degradation

Following multiple rounds of high stringency screening, selection based on sequence characteristics, and elimination of commonly occurring potential false positives, 23 candidate PKC-ε binding partners remained (highlighted in bold on Tables 3.1 and 3.2). Since the primary aim of this screen was to identify candidate proteins on the pathway(s) of PKC down-regulation, it was striking that two of these clones* had established associations with the ubiquitin/proteasome system: clone 119, von-Hippel Lindau binding protein 1 (VBP1) (Tsuchiya et al., 1996); and clone 19, the C-terminal region of F-box WD40 Protein 7 (Fbw7) (Maruyama et al., 2001). These clones were therefore selected for further investigation.

Clones 119 and 19 were re-streaked onto selective media alongside negative and positive controls (see Figures 3.8 and 3.9). When co-transformed with PKC-ε bait, both of these clones reproducibly facilitate growth on high stringency drop-out media and allow for positive blue/white selection, and therefore represent putative PKC-ε interacting proteins.

* At the time that this work was undertaken, the database entry corresponding to clone 63, F-box and leucine-rich repeat protein 15, had not been submitted (the sequence was identified only as 'Similar to hypothetical protein MGC11279'). This match was made in a more recent re-analysis of the data. If in frame, clone 63 would represent a good candidate for further analysis, but it was not pursued in this project.
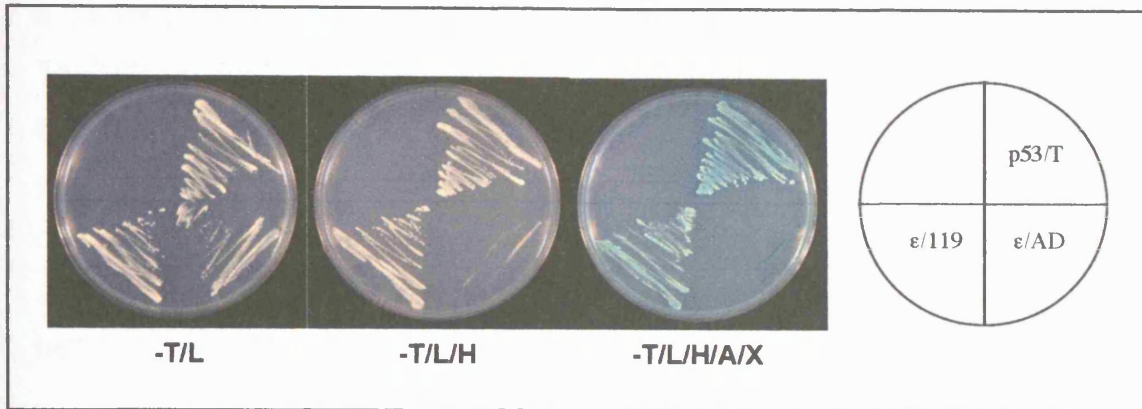
Figure 3.8 PKC-ε/Clone 119 Yeast 2-Hybrid Interaction. AH109 yeast co-transformed with PKC-ε bait/positive yeast 2-hybrid clone 119 (VBP1) were plated onto media selective for the vectors (-T/L), for medium stringency interaction (-T/L/H) and for high stringency interaction (-T/L/H/A/X). pGBKT7-p53/pGADT7-T Ag co-transformants were used as positive controls, pGBKT7/pGADT7 co-transformants as negative controls.
T, Tryptophan; L, Leucine; H, Histidine; A, Adenine; X, + X-α-gal.
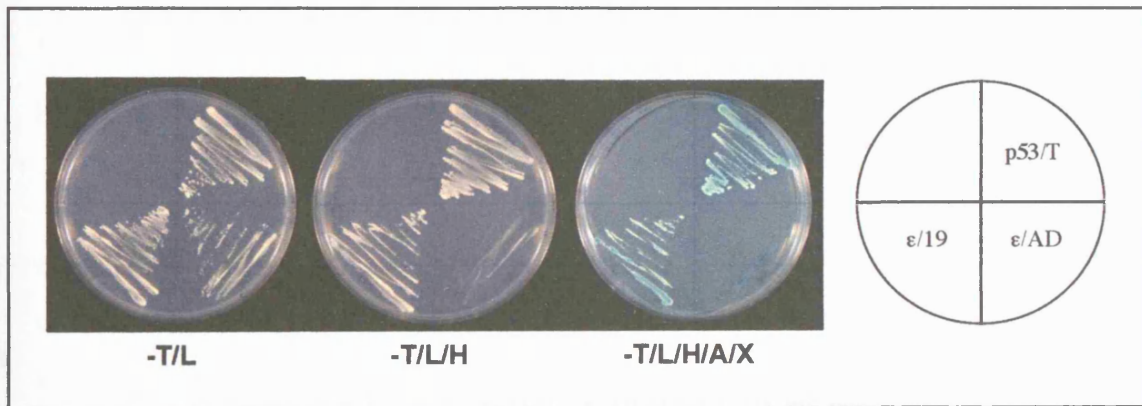
Figure 3.9 PKC-ε/Clone 19 Yeast 2-Hybrid Interaction. AH109 yeast co-transformed with PKC-ε bait/positive yeast 2-hybrid clone 19 (C-terminal portion of Fbw7) were plated onto media selective for the vectors (-T/L), for medium stringency interaction (-T/L/H) and for high stringency interaction (-T/L/H/A/X). pGBKT7-p53/pGADT7-T Ag co-transformants were used as positive controls, pGBKT7/pGADT7 co-transformants as negative controls.
T, Tryptophan; L, Leucine; H, Histidine; A, Adenine; X, + X-α-gal.

3.2.4 PKCε-Regulatory Domain and PKCε-Catalytic Domain Screens

The PKC-ε regulatory and catalytic domain bait constructs described in Section 3.2.2.1 were employed in parallel yeast 2-hybrid screens performed in our laboratory by Dr. Adrian Saurin. These screens were carried out using a human cardiac cDNA library as PKC-ε has a well established role in the phenomenon of ischaemic preconditioning in the heart (Saurin et al., 2002).

It is important to note that among the putative binding partners identified with the PKC-ε regulatory domain bait was 14-3-3β; the relationship between PKC-ε and 14-3-3 is relevant to work presented in Chapter 6.

3.3 Discussion

A yeast 2-hybrid system was established with which to screen a mouse brain cDNA library for PKC-ε interacting proteins, and subsequently, a human cardiac library for PKC-ε regulatory/catalytic domain binding partners.

The system was characterised prior to the screen. All of the bait constructs tested were expressed in yeast, and although full length PKC-ε was expressed at a lower level than its individual domains, it was detectable and judged to be suitable for screening.

The yeast survived transformation with all of the baits, although the growth rate was impaired to a certain extent by each of the constructs. This is an important consideration given that detection of binding partners is based upon growth on selective media in the 2-hybrid system. The negative influence of PKC-δ on growth rate deterred us from attempting a counter-screen of PKC-ε binding partners in yeast.

Inhibition of yeast growth is consistent with a degree of bait toxicity, but may alternatively reflect a functional effect of mammalian PKC in yeast; overexpression of PKC-ε is known to extend the doubling time in

Schizosaccharomyces pombe (Goode et al., 1994). Notably, the PKC constructs that were expressed at the lowest levels were those with the most profound effects on growth rate, suggesting that a bait's expression may be restricted by the capacity of the yeast to tolerate its effects.

Full length PKC-ε bait was employed to conduct a yeast 2-hybrid screen in which 1.4×10^5 mouse brain cfus were examined as potential PKC-ε interacting partners. Although this was not as comprehensive as the intended 10^6 cfus, it was deemed to be sufficiently extensive. The yeast were subjected to numerous rounds of selection, with increasingly stringent criteria, as the requirements of the screen evolved. We sought to find a balance between successfully eliminating false positives and avoiding the generation of false negatives, while confining the study to a manageable size.

The initial screen was conducted at medium stringency, utilizing only the *HIS3* reporter gene for protein-protein interactions in order to include even weak or transient partners. However, because such a large number of clones were isolated using this approach (980), subsequent rounds of selection were focussed towards the rejection of false positives.

Positive colonies were plated first onto -HIS/ADE, and then onto -HIS/ADE/X-α-gal media. Since the three corresponding reporter genes are under the control of distinct GAL4 upstream activating sequences in the MATCHMAKER 3 system, the use of them all eliminated false positives interacting either with sequences surrounding the GAL4 binding site, or with transcription factors bound to specific TATA boxes. As successive rounds of screening were employed, during which extraneous plasmids could be lost, this method also addressed the issue of multiple library vectors occurring in positive clones and complicating results. Ultimately, all but 129 clones were rejected; however, it is important to acknowledge that a number of false negatives are likely to have been sacrificed under these more rigorous conditions.

Following the final round of selection, library plasmids from the surviving yeast were recovered, retested and sequenced. The level of reproducibility achieved was disappointing and it was therefore necessary to confirm interactions carefully in mammalian cells, as described in Chapter 4. However, poor reproducibility is a well documented drawback of the yeast 2-hybrid approach (Ashman et al., 2001). Variation in plasmid copy number among separate experiments has been proposed as one source of disparity (Stephens and Banting, 2000). Since PKC-ε seems to confer some negative effects on yeast growth, it is possible that there was a degree of selection against the bait which contributed to this problem.

Sequence analysis of the isolated library vectors facilitated the identification and preliminary characterisation of the putative positive clones. In order to validate the screen, the compiled results were first examined for known PKC interacting partners. One previously characterised PKC interacting partner was represented by clone 108, NEL-like protein 2 (NELL2). NELL2 is a cytoplasmic, thrombospondin-1 like protein with 6 EGF-like repeats which is strongly expressed in neural tissues (Kuroda and Tanizawa, 1999). It was originally isolated as a PKC-β interacting partner by yeast 2-hybrid analysis with a regulatory domain bait (Kuroda et al., 1999), but was subsequently shown also to interact strongly with PKC-ε and PKC-ζ, and to be phosphorylated by PKC (Kuroda and Tanizawa, 1999). The PKC binding site was mapped to the EGF-like domains of NELL2; consistent with this, clone 108, which starts from residue 306, contains this region (EGF-like repeats begin at residue 399).

The detection of the same binding partner from multiple, separate clones is another good indicator that a screening process has been effective. One such example is provided in this screen by clones 74 and 105; although identified as mRNAs with different accession numbers, the inserts encode sequences corresponding to Gtl2, with different but

overlapping insert boundaries. While this observation is encouraging in terms of reproducibility, the functional significance of Gtl2 as an interacting partner is questionable since this sequence is thought to act as an RNA (Schuster-Gossler et al., 1998).

There are other examples of proteins detected more than once in this screen which are potentially physiologically relevant, for example clones 37,38 and 39 all correspond to the 5'UTR and CDS for monoglyceride lipase. However, in this case, the duplicates encode exactly the same region of sequence and thus represent identical, rather than independent, copies of the same clone. This occurrence could be explained by the fact that an amplified library was employed for the screen. Alternatively, it could be the result of contamination; the fact that the clone numbers are consecutive indicates that they were picked from the same area of the original screen plate, which would be consistent with this latter interpretation.

Among the other yeast 2-hybrid hits were numerous classes of positive clones: uncharacterised and characterised cDNAs; coding and non-coding regions; full length and partial inserts; and in frame and frame-shifted sequences with respect to GAL4. Only clones expressing identifiable, in-frame, coding sequences immediately after the library adaptor sequence were followed up in further studies, however, as touched upon in Section 3.2.3.2, yet more true positives may have been wrongly excluded by these criteria due to the capacity of yeast to permit unconventional transcriptional and translational processes. Firstly, positive clones can occasionally be transcribed in the reverse orientation from a cryptic promoter, such that the protein expressed does not correspond to the sequence encoded after the library adapter (Chien et al., 1991). Secondly, yeast are capable of permitting translational read-through. Therefore, where there appears to be just 5' UTR or a short peptide represented by an insert, there may be a second ORF beyond the stop codon which could be expressed. Finally, yeast can sometimes accommodate translational frameshifts (Clontech, 1999). In a number of

cases a large ORF was identified but was in the wrong reading frame with respect to the GAL4 AD, it is possible that some such clones may have represented true positives. This possibility could have been tested by western blotting for the HA-epitope harboured by all preys, and analysing the sizes of the proteins encoded.

Clones expressing in-frame, coding sequence were next checked against a list of well-documented and commonly occurring false positives, these proteins seem to be inherently adhesive and undergo 'irrelevant' interactions with many baits (Stephens and Banting, 2000). A number of such clones were detected in this screen, and were not pursued further.

For the remaining putative positives, it was important to establish which part of the corresponding protein was encoded by a partial clone, and whether this was likely to be accessible to PKC in a mammalian cell. For example, F3/contactin (clone 92) is a GPI-anchored, cell-surface neural recognition molecule (Gennarini et al., 1989). As such, the region of F3/contactin represented by clone 92 is unlikely to be exposed to PKC in the context of the full length protein, and this interaction is unlikely to have any physiological relevance.

Following three rounds of yeast 2-hybrid screening, selection based on sequence features, elimination of commonly occurring false positives and rejection of partial sequences deemed to be of uncertain physiological significance, a collection of putative PKC-ε binding partners remained. Since the primary aim of this screen was to identify binding proteins with potential relevance to PKC degradation, it was striking that two of these clones have established associations with the ubiquitin/proteasome system: clone 19, the C-terminal region of F-box WD40 Protein 7 (Fbw7) and clone 119, von-Hippel Lindau binding protein 1 (VBP1). Notably, the VBP1 sequence was also represented by clone 121, however, an insertion at base 6 renders almost the entire sequence out of frame. It is conceivable that the yeast were able to accommodate this frameshift, as

described above, in order to translate the wild type protein, but this possibility was not tested.

Clones 19 and 119 were selected for further analysis in the context of PKC down-regulation. It was beyond the scope of this project to investigate any of the other putative PKC-ε binding partners, but many of them remain as potentially interesting candidates for investigation in the future; this is discussed further in Chapter 7.

In conclusion, yeast 2-hybrid analysis identified two putative PKC-ε binding partners, Fbw7 and VBP1, with potential roles in PKC down-regulation. In the following chapter, the interactions between these proteins and PKC are investigated in mammalian cells, and their functional relationships are explored. Additionally, a parallel 2-hybrid screen, performed with the regulatory domain bait, identified 14-3-3β as a PKC-ε binding protein; this interaction is explored further in Chapter 6.

CHAPTER 4

PKC & Protein Degradation:
F-box WD40 Protein 7 & VBP1

4.1 Introduction

A characteristic property of the classical and novel PKC isoforms is that their chronic activation frequently leads to their inactivation and/or degradation (Ballester and Rosen, 1985; Stabel et al., 1987). This process of down-regulation is an important, yet poorly characterised, part of the 'life cycle' of PKC, and may in fact be intrinsic to the tumour promoting activity of the phorbol esters (Young et al., 1987). As such, the elucidation of the PKC degradation pathway(s) represents an important goal for research, and the focus of ongoing work in our laboratory. As described in Chapter 3, yeast 2-hybrid screening with a PKC-ε bait identified two interacting partners with links to the ubiquitin proteasome system, von Hippel-Lindau (pVHL) Binding Protein 1 (VBP1) and F-box WD40 Protein 7 (Fbw7); these proteins represent strong candidates for further investigation in this context.

VBP1 was originally identified from a human B-cell cDNA library by Tsuchiya and colleagues (Tsuchiya et al., 1996), and has subsequently been shown to be highly conserved, and therefore likely to perform an important function (Brinke et al., 1997). Although its precise role remains elusive, VBP1 has been implicated in the activity of the prefoldin co-chaperone complex (Geissler et al., 1998), (Vainberg et al., 1998), and demonstrated to interact with pVHL (Tsuchiya et al., 1996). VHL is a tumour suppressor gene which is mutated in familial VHL cancer syndrome (Latif et al., 1993) and in the majority of kidney cancers (Shuin et al., 1994). pVHL associates with Elongin C, Elongin B, Cullin-2 and

164

Rbx1 to form a ubiquitin ligase complex (Stebbins et al., 1999) in which pVHL confers substrate recognition. Its best established substrate to date is hypoxia inducible factor-1α (HIF-1α) (Maxwell et al., 1999) (Cockman et al., 2000), but significantly, pVHL has been also been connected to the degradation of activated aPKC-λ (Okuda et al., 2001). Since VBP1 interacts both with PKC and pVHL, it constitutes an interesting candidate for further analysis with respect to this pathway.

Fbw7 is the substrate recognition component of a well characterised Skp1/Cullin1/F-box (SCF) class E3 ubiquitin ligase. In mammalian cells, Fbw7 is represented by three isoforms: α, β and γ (Welcker et al., 2004a). SCF^{Fbw7} has been shown to mediate the poly-ubiquitination of numerous substrates, thereby targeting them for proteasomal degradation. In each case, the substrate binding domain of Fbw7 recognises and specifically interacts with a phospho-threonine/proline (pTP) based motif termed the cdc4 phospho-degron (CPD) (Nash et al., 2001). Established SCF^{Fbw7} substrates include: cyclin E (Moberg et al., 2001; Strohmaier et al., 2001); c-myc (Moberg et al., 2004; Welcker et al., 2004a; Yada et al., 2004); c-jun (Nateri et al., 2004); Notch (Gupta-Rossi et al., 2001; Oberg et al., 2001; Wu et al., 2001) and presenilin (Li et al., 2002; Wu et al., 1998). The ubiquitin ligase activity of SCF^{Fbw7} plays a critical role in controlling cell cycle progression (Feldman et al., 1997), cell growth (Welcker et al., 2004a) and apoptotic JNK signalling in neurons (Nateri et al., 2004). Significantly, Fbw7 has been identified as a tumour suppressor gene (Mao et al., 2004) and is found to be mutated in a number of cancer cell lines (Moberg et al., 2001; Strohmaier et al., 2001).

This chapter describes the examination of the functional relationships between PKC and VBP1/Fbw7. Data is presented which validates the interactions detected by yeast 2-hybrid analysis in Chapter 3. VBP1 and Fbw7 are then investigated as candidate proteins on the PKC down-regulation pathway(s), and conversely, as downstream PKC targets.

4.2 Results

4.2.1 PKC Protein-Protein Interactions in Mammalian Cells

4.2.1.1 VBP1/PKC Protein-Protein Interactions

VBP1 was identified as a PKC-ε interacting protein by yeast 2-hybrid analysis. Before the functional significance of this interaction could be explored, it was first important to confirm that binding could also be detected in the context of a mammalian cell.

GFP-VBP1 was cloned and tested for interaction with PKC-ε by GST pull-down in COS7 cells. Preliminary mapping data was also obtained using GST-tagged PKC-ε domain constructs. Figure 4.1 demonstrates that the interaction between PKC-ε and VBP1 is reproducible in mammalian cells and maps to the catalytic domain of PKC-ε. (see Figure 6.13 in Chapter 6 for an example of a similar experiment, performed in the opposite orientation).
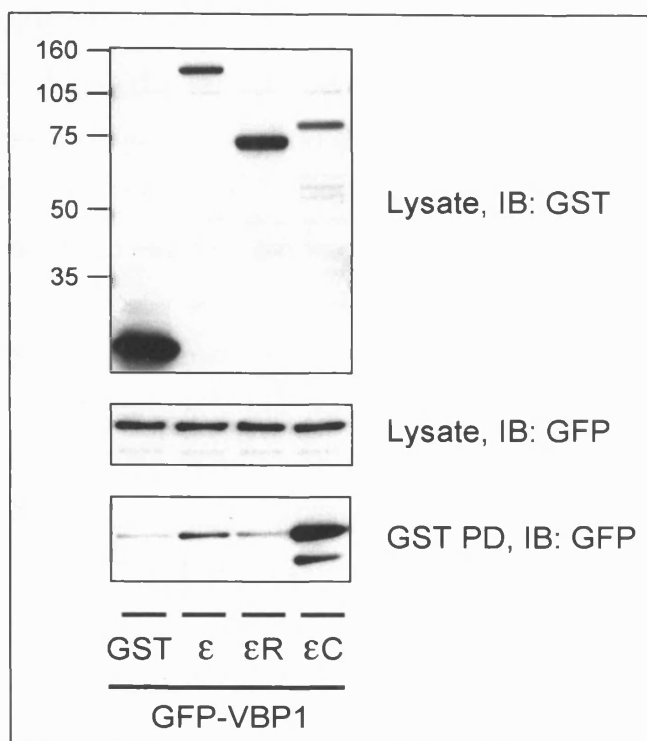
Figure 4.1 Detection and Mapping of the Interaction Between PKC-ε/VBP1 in Mammalian Cells by GST Pull-down. COS7 cells were seeded on 6-well plates and co-transfected with GST/GST-PKC-ε constructs and GFP-VBP1. 24hrs post-transfection, lysates were prepared and subjected to GST pull down. Samples were resolved by SDS-PAGE and analysed by Western blotting with anti-GST and anti-GFP 3E1 antibodies. ε, full length PKC-ε; R, regulatory domain; C, catalytic domain. This data is representative of three independent experiments.

4.2.1.2 Fbw7/PKC Protein-Protein Interactions

The substrate binding domain of Fbw7 was identified as a PKC-ε

interacting protein by yeast 2-hybrid analysis. As was the case for VBP1,

prior to investigating the functional consequences of this interaction, it

was first necessary to validate binding in a mammalian system.

Yeast 2-hybrid clone 19 represents the C-terminal portion of Fbw7. As

shown in Figures 4.2 and 4.3, this region comprises the WD40 domain

responsible for substrate recognition and is shared among all isoforms of

Fbw7. The sequence encoded by clone 19 was sub-cloned directly from

the library vector pACT2, to the mammalian expression vector pEGFP-

C1, and tested for interaction with PKC-ε by GST pull-down in COS7

cells. Figure 4.4 reveals that the interaction between PKC-ε and the

substrate binding domain of Fbw7 is reproducible in mammalian cells

and, as was the case for VBP1, requires the catalytic domain of PKC-ε.

Fbw7α   (NM_033632)

MNQELLSVGS**KRRR**TGGSLRGNPSSSQVDEEQMNRVVEEEQQQQLRQQEEEHTARNGEVVGVEPRPGGQNDSQQGQLEENNNRFISVDEDSSGNQE
EQEEDEEHAGEQDEEDEEEEMDQESDDFDQSDDSSREDEHTHTNSVTNSSSIVDLPVHQLSSPFYTKTTK–

Fbw7β   (NM_018315)

MCVPRSGLILSCICLYCGVLLPVLLPNLPFLTCLSMSTLESVTYLPEKGLYCQRLPSSRTHGGTESLKGKNTENMGFYGTLKMIFYK–

Fbw7γ   (NM_001013415)

MSKPGKPTLNHGLVPVDLKSAKEPLPHQTVMKIFSISIIAQGLPFCRRR–

Conserved region

–M**KRKL**DHGSEVRSFSLGKKPCKVSEYTSTTGLVPCSATPTTFGDLRAANGQGQQRRRITSVQPPTGLQEWLKMFQSWSGPEKLLALDELIDSCEPT
QVKHMMQVIEPQFQRDFISLLPKELALYVLSFLEPKDLLQAAQTCRYWRILAEDNLLWREKCKEEGIDEPLHIKRRKVIKPGFIHSPWKSAYIRQH
RIDTNWR | RGELKSPKVLKGHDDHVITCLQFCGNRIVSGSDDNTLKVWSAV | TGKCLRTLVGHTGGVWSSQMRDNIIISGSTDRTLKVWNAE | TGE
CIHTLYGHTSTVRCMHLHEKRVVSGSRDATLRVWDIE | TGQCLHVLMGHVAAVRCVQYDGRRVVSGAYDFMVKVWDPE | TETCLHTLQGHTNRVYS
LQFDGIHVVSGSLDTSIRVWDVE | TGNCIHTLTGHQSLTSGMELKDNILVSGNADSTVKIWDIK | TGQCLQTLQGPNKHQSAVTCLQFNKNFVITS
SDDGTVKLWDLK | TGEFIRNLVTLESGGSGGVVWRIRASNTKLVCAVGSRNGTEETKLLVLDF | DVDMK

Figure 4.2 Human Fbw7 isoforms and Clone 19 Protein Sequences. The protein sequences of the three Fbw7 isoforms were retrieved from the NCBI Entrez Nucleotide database using the accession numbers indicated. The isoform specific N-termini are represented separately, and the conserved C-terminal region is shown with the following features highlighted (Orlicky et al., 2003): F-box domain (red text); 8 WD40 repeats of the substrate binding domain (green); residue 1 of positive yeast 2-hybrid clone 19 (blue). Nuclear localisation sequences are shown in bold.

169
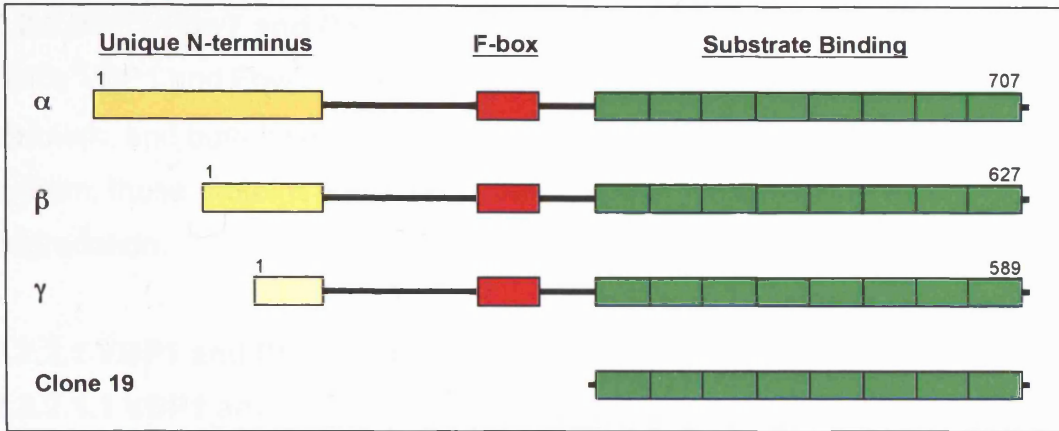
Figure 4.3 Domain Structure of Human Fbw7 Isoforms and Clone 19.
The three human Fbw7 isoforms (α, β and γ) and positive yeast 2-hybrid clone 19 are represented to scale with the following features highlighted (Orlicky et al., 2003): isoform specific N-termini (shades of yellow), conserved linker regions (black), F-box domain (red); 8 WD40 repeats of the substrate binding domain (green).
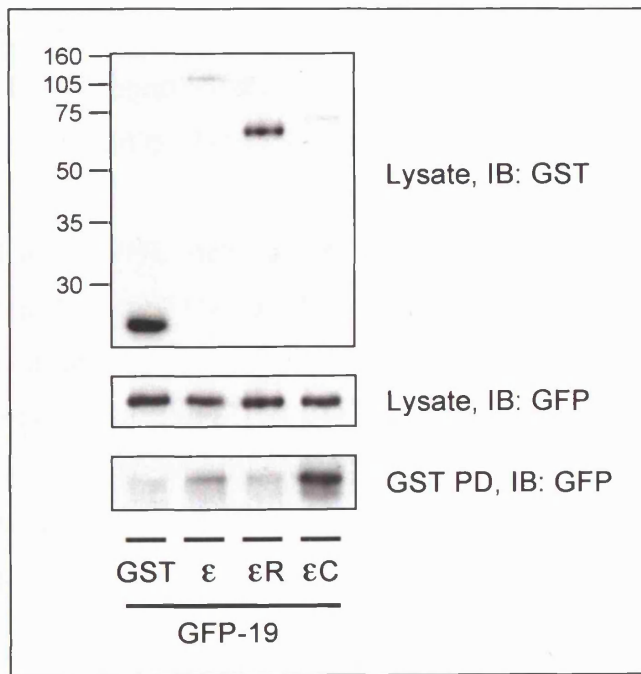
Figure 4.4 Detection and Mapping of the PKC-ϵ/clone 19 Interaction in Mammalian Cells by GST Pull-down. COS7 cells were seeded on 6-well plates and co-transfected with GST/GST-PKC-ϵ constructs and GFP-19 (substrate binding domain of Fbw7). 24hrs post-transfection, lysates were prepared and subjected to GST pull down. Samples were resolved by SDS-PAGE and analysed by Western blotting with anti-GST and anti-GFP 3E1 antibodies. ϵ, full length PKC-ϵ; R, regulatory domain; C, catalytic domain. This data is representative of three separate experiments.

170

4.2.2 VBP1/Fbw7 and PKC Degradation

Since VBP1 and Fbw7 were shown to represent valid PKC-ε binding partners, and both have established links to the ubiquitin-proteasome system, these proteins were next investigated in the context of PKC degradation.

4.2.2.1 VBP1 and PKC Down-Regulation

4.2.2.1.1 VBP1 and TPA Induced PKC Down-Regulation

We sought to investigate whether VBP1 could influence the down-regulation of PKC, either under basal conditions, or in response to a chronic phorbol ester treatment.

NIH3T3 cells were transfected with RFP-PKC-ε, +/- GFP alone or GFP-VBP1. The influence of VBP1 on PKC levels was assessed both under basal conditions, and over a timecourse of TPA treatment. Figure 4.5 shows that, under the conditions employed, there is no detectable effect of VBP1 overexpression on TPA induced PKC degradation.

4.2.2.1.2 VBP1 and pVHL Induced PKC Down-Regulation

We originally hypothesized that VBP1 might participate in the process of PKC down-regulation because of its association with pVHL, a known PKC E3 ubiquitin ligase (Okuda et al., 2001). As such, Dr Xavier Iturrioz endeavoured to establish whether VBP1 might play a role specifically in the VHL-mediated pathway of PKC degradation, which he was studying in our laboratory.

There was no discernable influence of VBP1 on the interaction detected between pVHL and PKC-δ by GST pull-down in COS7 cells. Similarly, no significant co-localisation could be observed between VBP and pVHL/PKC-δ positive structures in COS7 by immunofluorescence. All other experiments relating to pVHL mediated PKC down-regulation were performed on the endogenous proteins in renal carcinoma cells; these

these cells are poorly transfectable and so it was not possible to test the effect of VBP1 over-expression in this system.

The observations here and those of Dr Iturrioz were not consistent with a role for VBP1 in PKC degradation. Subsequent work was therefore focussed on the investigation of Fbw7 as a candidate PKC E3 ubiquitin ligase, and as described in section 4.2.3, on both proteins as potential PKC substrates.
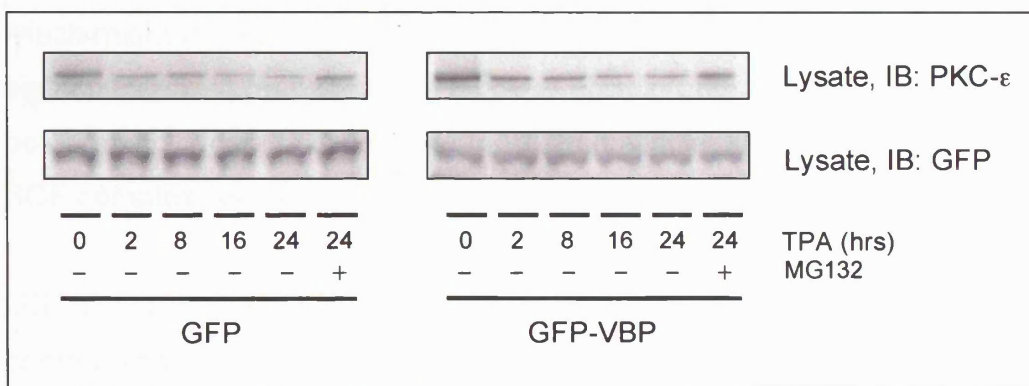
Figure 4.5 TPA Induced Degradation of PKC-ε in the presence or absence of VBP-1. NIH3T3 cells were transfected with RFP-PKC-ε +/- GFP/GFP-VBP1. 24hrs post-transfection cells were treated +/- 400nM TPA over a timecourse of a further 24hrs. Samples were harvested simultaneously in sample buffer, resolved by SDS-PAGE and analysed by western blotting with anti-PKC-ε and anti-GFP 3E1 antibodies.

4.2.2.2 Fbw7 and PKC down-regulation

4.2.2.2.1 PKC Interaction with Full Length Fbw7 and Fbw Isoform Specificity

The results presented in Section 4.2.1.2 confirm that the interaction between PKC-ε and the Fbw7 C-terminal region can be detected in mammalian cells. However, in order to begin to study the functional relationship between the two proteins, it was necessary to determine whether PKC-ε could also interact with the full length Fbw7 protein. The presence of the Fbw7 N-terminal region could potentially affect conformation, localisation and/or other protein-protein interactions, all of which might influence PKC binding. Also, this region is of particular significance with respect to the study of protein degradation, as it is the F-box domain, which is lacking in clone 19, that links Fbw7 to the rest of the SCF complex (Bai et al., 1996).

GST-pull down experiments were performed using GST-PKC-ε, or a GST control, and FLAG-tagged, full length Fbw7 (Fbw7β). The isoform specificity of the interaction, with respect to Fbw7, was also investigated in this experiment. Other members of the F-box WD40 family, Fbws1, 2, and 4, were counter-screened for interaction with PKC-ε. All of these proteins possess an F-box domain and a substrate recognition domain which is based on WD40 repeats, however, other parts of the proteins are variable and the WD40 domains target different motifs and therefore confer differential substrate specificities (Maruyama et al., 2001; Miura et al., 1999).

Figure 4.6 demonstrates that full length Fbw7β is able to bind to PKC. The use of a FLAG-tagged fusion reinforces the finding that the interaction is not artefactually dependent on a GFP tag. However, this data also reveals that the interaction is not isoform specific with respect to the Fbw protein family.

The central panel of Figure 4.6 shows that the Fbw proteins are differentially expressed, with the level of Fbw7β so low as to be undetectable in the lysate under these conditions. Consequently, it is important to consider the efficiency of the pull-down rather than the actual amount of Fbw protein recovered. For example, Fbw4 is expressed at a comparable level as Fbw1, as judged from the lysate, but is represented by a more intense band in the pull down; the efficiency of the interaction can therefore be concluded to be significantly higher, and Fbw4 concluded to be preferred as a PKC binding partner. As such, although the Fbw7β pull down band is relatively weak in intensity, it may represent a significant enrichment given the low level of Fbw7β expression. In subsequent experiments FLAG-Fbw7 was immunoprecipitated using an anti-FLAG antibody, and immunoblotted for anti-FLAG, to facilitate detection and enable more accurate comparison.
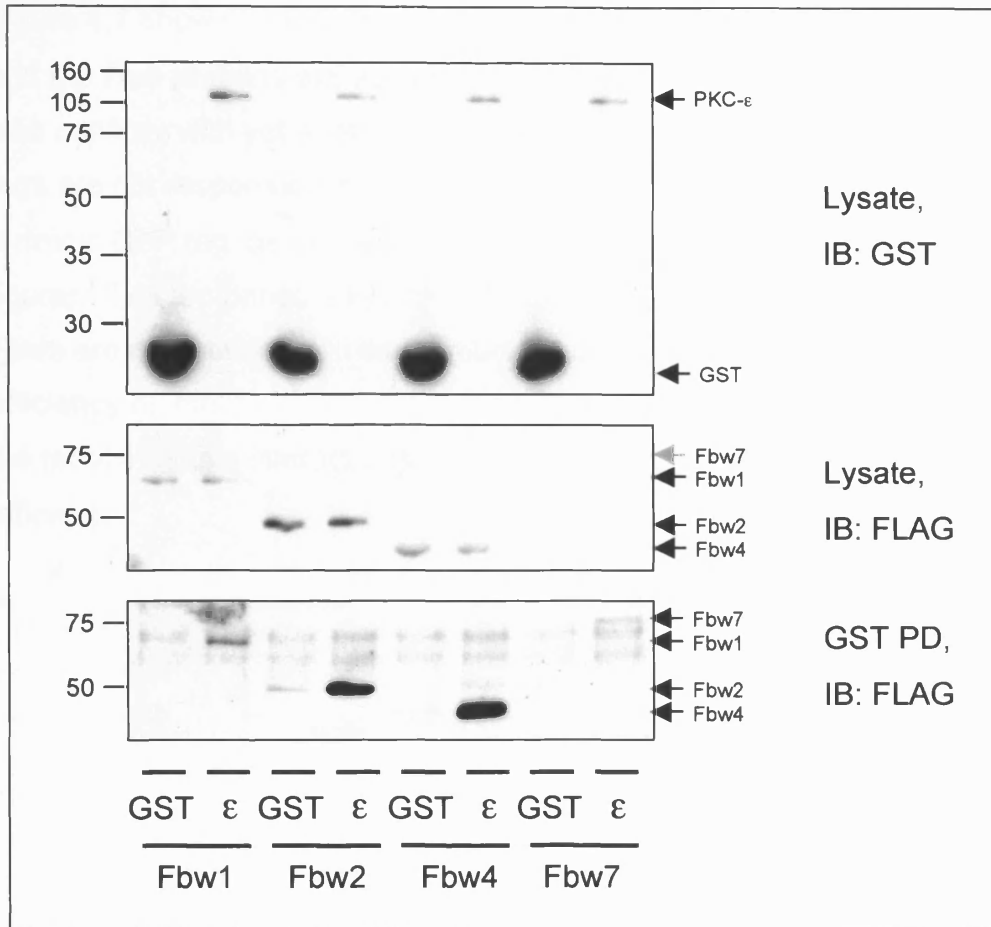
Figure 4.6 Detection of the Interaction Between PKC-ε and Full Length Fbw7 by GST Pull-down, and Counter-screening for Fbw Protein Isoform Specificity. COS7 cells were seeded on 6-well plates and co-transfected with GST/GST-PKC-ε and FLAG-Fbw constructs (indicated with black arrows; the grey arrow signifies that Fbw7 was not detectable in the lysate). 24hrs post-transfection, lysates were prepared and subjected to GST pull down. Samples were resolved by SDS-PAGE and analysed by Western blotting with anti-GST and anti-FLAG antibodies. This data is representative of two separate experiments.

Figure 4.7 shows an experiment, in which the interactions between PKC-ε and the Fbw proteins are verified in the reverse orientation. These blots also confirm, with yet another combination of fusion constructs, that the tags are not responsible for the interactions (here, PKC-ε bears an N-terminal GFP tag, as opposed to the C-terminal GST tag in the previous figure). The top panel of Figure 4.7 illustrates that all of the FLAG-tagged Fbws are detectable from the immunoprecipitated material, and so the efficiency of interaction can be directly compared. Fbws 4 and 7 undergo the most effective interactions with PKC-ε, with Fbw1 significantly less efficient.
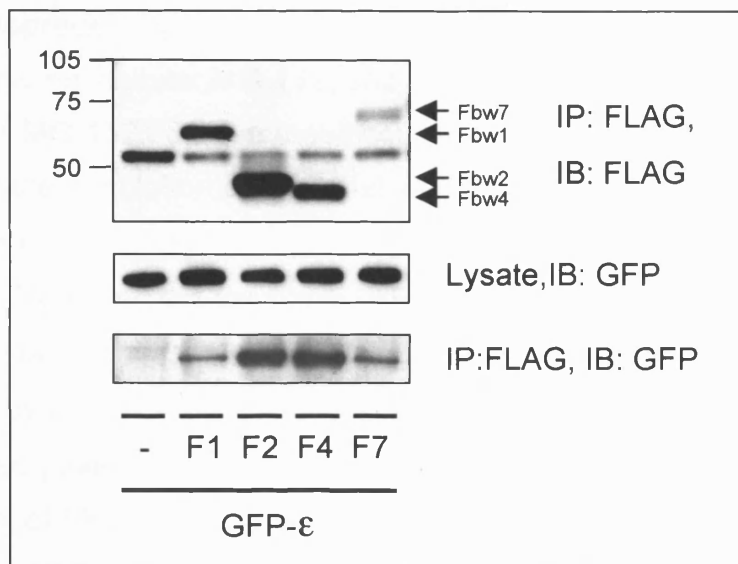
Figure 4.7 PKC-ε/Fbw Protein Interactions Detected in the Reverse Orientation by Coimmunoprecipitation. COS7 cells were seeded on 6-well plates and co-transfected with FLAG-Fbw (F1/2/4/7) constructs (indicated by black arrows) and GFP-PKC-ε. 24hrs post-transfection, lysates were prepared and coimmunoprecipitation was performed using anti-FLAG M2-agarose affinity gel. Samples were resolved by SDS-PAGE and analysed by Western blotting with anti-FLAG and anti-GFP 3E1 antibodies. This data is representative of three independent experiments.

4.2.2.2.2 Interaction with Fbw7: PKC Isoform Specificity +/- MG-132

The isoform specificity of the PKC/Fbw interaction was next investigated with respect to PKC. At least one member of each subgroup of the PKC superfamily was counter-screened for interaction with Fbw7β (classical: α, β_I, β_{II}; novel: δ, ϵ; atypical: ζ). Figure 4.8 reveals that all isoforms tested bind to Fbw7β; this is perhaps not surprising considering that the interaction maps to the well conserved catalytic domain of PKC. The PKC catalytic domain contains the 'TP' phosphorylation site. This site and the surrounding sequence, in at least some of the PKC isoforms, aligns well with the CPD motif which is recognised by Fbw7 (Figure 4.9).

Co-immunoprecipitations were performed in the presence or absence of the proteasome inhibitor MG-132, and an enhanced recovery of PKC was achieved + MG-132. Such a result could indicate that under normal conditions the population of PKC that interacts with Fbw7β is targeted for degradation, supporting the hypothesis that SCF^{Fbw7} represents a PKC E3 ligase. However, the top panel of Figure 4.8 indicates that MG-132 stabilizes Fbw7β itself; as such, the increased recovery of PKC may be explained by the availability of a larger pool of Fbw7β with which to immunoprecipitate. It is noteworthy though, that the augmented enrichment of PKC-ζ in the presence of MG-132 seems to exceed the stabilization of Fbw7β.

Somewhat surprisingly, there is a reduction in the level of PKC-ϵ detected in the lysate following treatment with MG-132, which would be expected to protect proteins from down-regulation. However, this is consistent with observations made by Dr. Amir Faisal in our laboratory, who has demonstrated that MG-132 stimulates caspase-dependent proteolysis of PKC-ϵ in RAW264.7 cells (unpublished data).
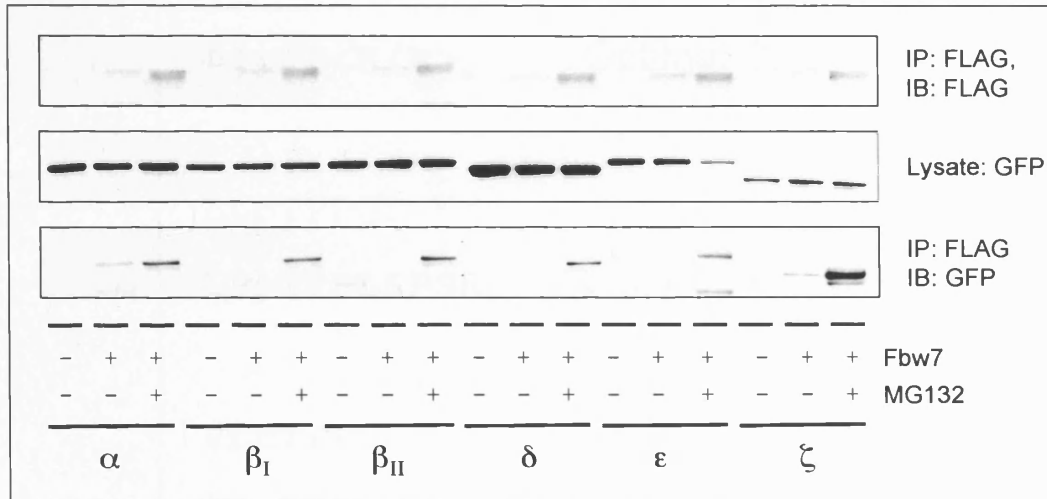
Figure 4.8 Detection of the Interactions Between Fbw7β and the PKC family by Coimmunoprecipitation, in the Presence and Absence of MG132. COS7 cells were seeded on 6-well plates and co-transfected with FLAG-Fbw7 and GFP-PKC (α, βI, βII, δ, ε, ζ) constructs. 32hrs post-transfection, cells were treated +/- 30μM MG-132 for a further 16hrs. Lysates were prepared and coimmunoprecipitation was performed using anti-FLAG M2-agarose affinity gel. Samples were resolved by SDS-PAGE and analysed by Western blotting with anti-FLAG and anti-GFP 3E.

ΦΦpTP<K/R>$_4$	Optimal CPD
LLpTPPQSGKK	cyclin E T380
LPpTPPLSPSR	c-myc T58
VLpTPPDQLVI	PKC-α
ELpTPTDKLFI	PKC-β$_I$
VLpTPPDGQEV	PKC-β$_{II}$
RLpSYSDKNLI	PKC-δ
VLpTLVDEAIV	PKC-ε
QLpTPDDEDAI	PKC-ζ

Figure 4.9 Fbw7 Substrate Recognition Motifs and PKC 'TP' Sites.
Nash *et al* (Nash et al., 2001) defined a high affinity consensus
phosphopeptide binding motif for Fbw7 termed the cdc4 phospho-degron
(CPD). This sequence is shown with hydrophobic residues (Φ) and
disfavoured residues (<>) indicated. CPDs from established Fbw7
substrates are shown, aligned with the 'TP' phosphorylation sites of
different PKC isoforms. The critical phospho-threonine residue of the
CPD is indicated (red); and the amino acid in the +4 position relative to
this is highlighted (blue).

4.2.2.2.3 Fbw7 and PKC Ubiquitination

In order to address the possibility that Fbw7 can facilitate PKC degradation more directly, cell based ubiquitination assays were performed (Figure 4.10). In this system, the putative PKC substrate (or GST control) is expressed in the presence or absence of a FLAG-tagged F-box protein, with or without HA-tagged ubiquitin. PKC is then isolated by GST-pull down, and probed for ubiquitin by immunoblotting against the HA epitope. An adapted Western blotting protocol is employed, to facilitate the detection of high molecular weight, poly-ubiquitinated protein, which manifests as a ladder of differently sized species.

Enhanced ubiquitination is detected from the precipitated material only in the presence of PKC-ε, and only where HA-Ub was included in the transfection. Co-expression of an Fbw protein is also shown to be required, but ubiquitination was not mediated in an isoform specific manner. The experimental design assumes that the HA-immunoreactive protein detected must correspond to ubiquitinated PKC, following partial purification by GST pull-down. However, we cannot exclude the possibility that the assay is in fact detecting a ubiquitinated PKC interacting protein. Examination of the lysates probed for FLAG-Fbw reveals a significant ladder of products, suggesting that the Fbws may themselves be poly-ubiquitinated. Since the Fbws are known to bind to PKC under these conditions, it is feasible that they represent at least a fraction of the ubiquitinated material detected following the pull-down.
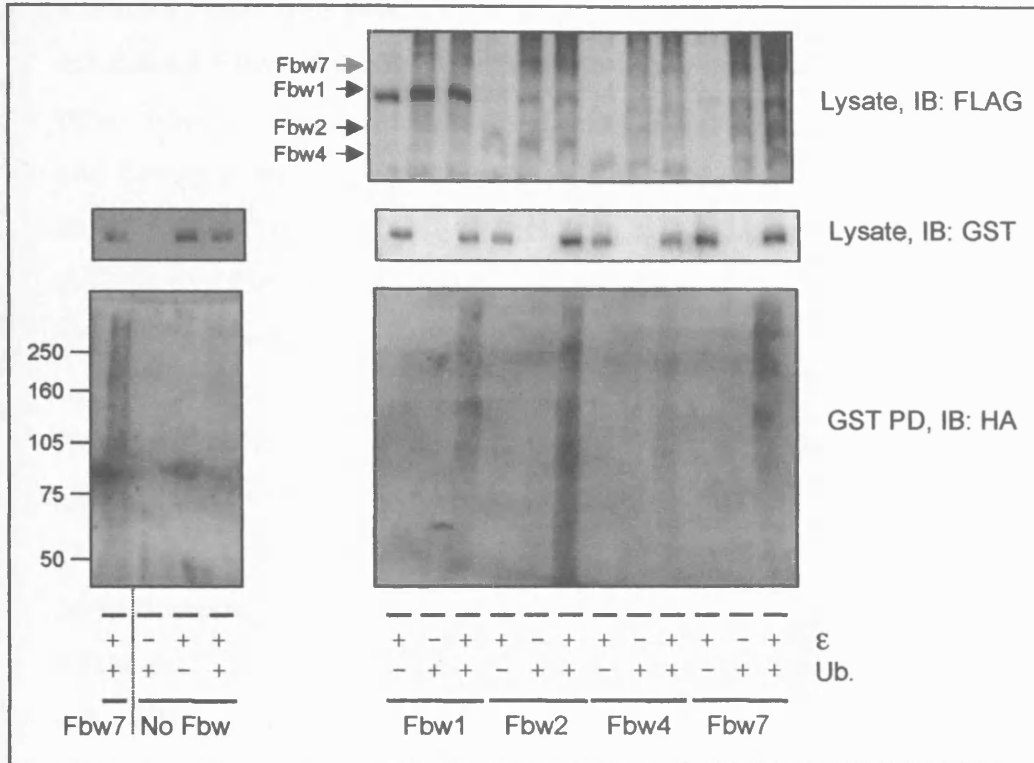
Figure 4.10 Fbw/PKC-ε Ubiquitination assays. 293 cells were seeded on 6-well plates and transfected with GST/GST-PKC-ε (–ε represents GST control) +/- FLAG-Fbw constructs and +/- HA-ubiquitin (Ub.). 48hrs post-transfection, lysates were prepared in ubiquitination assay lysis buffer and subjected to GST pull-down. Samples were resolved by SDS-PAGE and analysed by Western blotting with anti-FLAG, anti-GST and anti-HA antibodies. GST pull-downs were processed using modified protocols to facilitate resolution and transfer of any high molecular weight, poly-ubiquitinated proteins (see Materials and Methods). This data is representative of two separate experiments. (The Fbws are indicated with black arrows; the grey arrow signifies that Fbw7 is not detectable in the lysate).

4.2.2.2.4 Fbw7 and PKC Down-regulation

4.2.2.2.4.1 Fbw7 and Depletion of Phospho-c-jun and PKC-ε

When Fbw7 is co-expressed with an established substrate, such as c-jun and c-myc, a depletion of the substrate can be observed by Western blotting (Nateri et al., 2004), (Welcker et al., 2004b). We therefore tested the effect of Fbw7 co-expression on PKC levels in different cell lines, alongside a c-jun control.

Figure 4.11 shows the optimisation of this co-expression assay with the c-jun control. In Figure 4.11a, c-jun was co-transfected with FLAG/FLAG-Fbw7β in 293 cells; Fbw7β mediated c-jun degradation has previously been demonstrated in this system (Nateri et al., 2004). However, c-jun depletion in the presence of Fbw7β is not apparent in this experiment, even following a UV treatment, which clearly enhances the level of phospho-c-jun, the species specifically recognised by Fbw7. The same test was next performed in a different cell line. As shown in Figure 4.11b, an Fbw7β dependent reduction of c-jun could be detected in HeLa cell lysates; this effect was more evident when lysates were probed for phospho-S63 than for total c-jun.
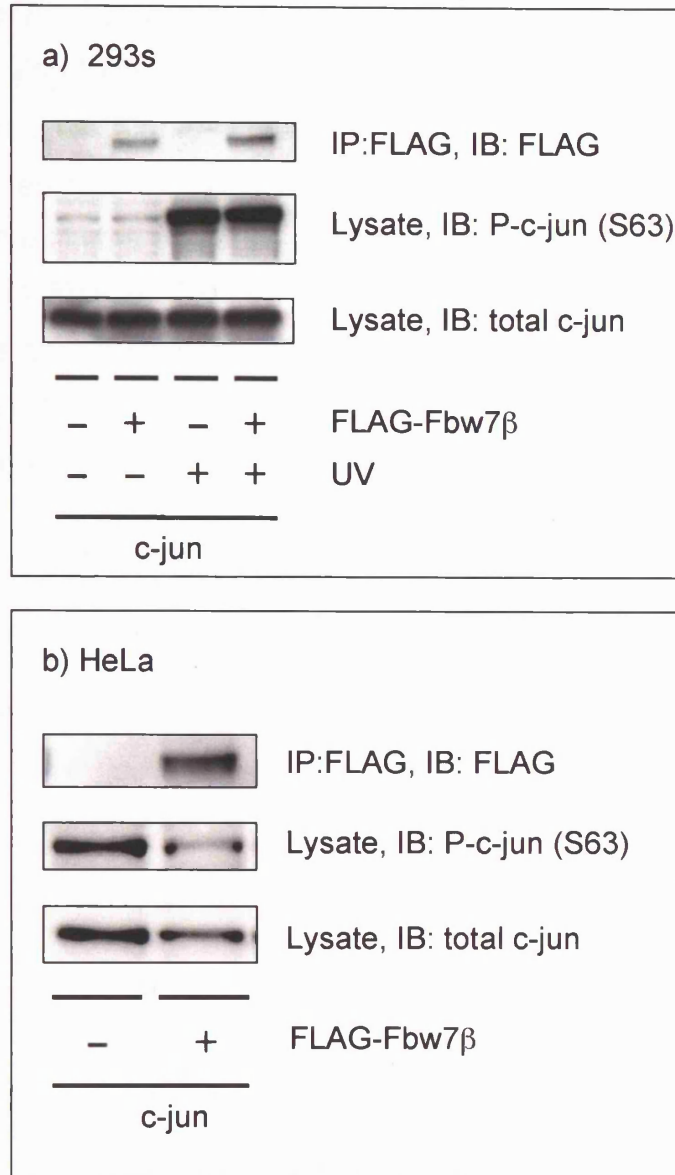
Figure 4.11 Fbw7β and Phospho-c-jun Depletion. a) 293 cells were seeded onto poly-lysine coated 6-well plates and tranfected with FLAG/FLAG-Fbw7 (Nateri et al., 2004) and myc-c-jun-FLAG. 24hrs post-transfection, cells were treated +/- 40J/m^2 UV and incubated for a further hour. Lysates were prepared and immunoprecipitation was performed using anti-FLAG M2-agarose affinity gel. Samples were resolved by SDS-PAGE and analysed by Western blotting with anti-FLAG (Fbw7 and total c-jun) and anti-phospho-c-jun Ser-63 antibodies. b) HeLa cells were seeded onto 6-well plates and tranfected with FLAG/FLAG-Fbw7 (Nateri et al., 2004) and myc-c-jun-FLAG. 24hrs post-transfection, lysates were prepared and immunoprecipitation was performed using anti-FLAG M2-agarose affinity gel. Samples were resolved by SDS-PAGE and analysed by Western blotting with anti-FLAG (Fbw7 and total c-jun) and anti-phospho-c-jun Ser-63 antibodies.

The effect of Fbw7β co-expression on PKC levels was therefore tested in HeLa cells, alongside this c-jun control; Fbw7α and Fbw1 were also studied in parallel. Figure 4.12a again demonstrates the Fbw7β dependent depletion of phospho-c-jun, and reveals that this phenomenon is not observed in the presence of Fbw1, or even with the alternative Fbw7 isoform, Fbw7α. Figure 4.12b shows that the same pattern of behaviour is detected when PKC-ε is expressed as the putative substrate, with a parallel tubulin blot confirming equal loading, suggesting that PKC-ε may also represent an Fbw7 client. The effect of TPA on this process was analysed since TPA can induce PKC down-regulation, however, there was not a substantial difference apparent between treated/untreated cells. Notably, TPA induced an increase in phospho-c-jun levels.
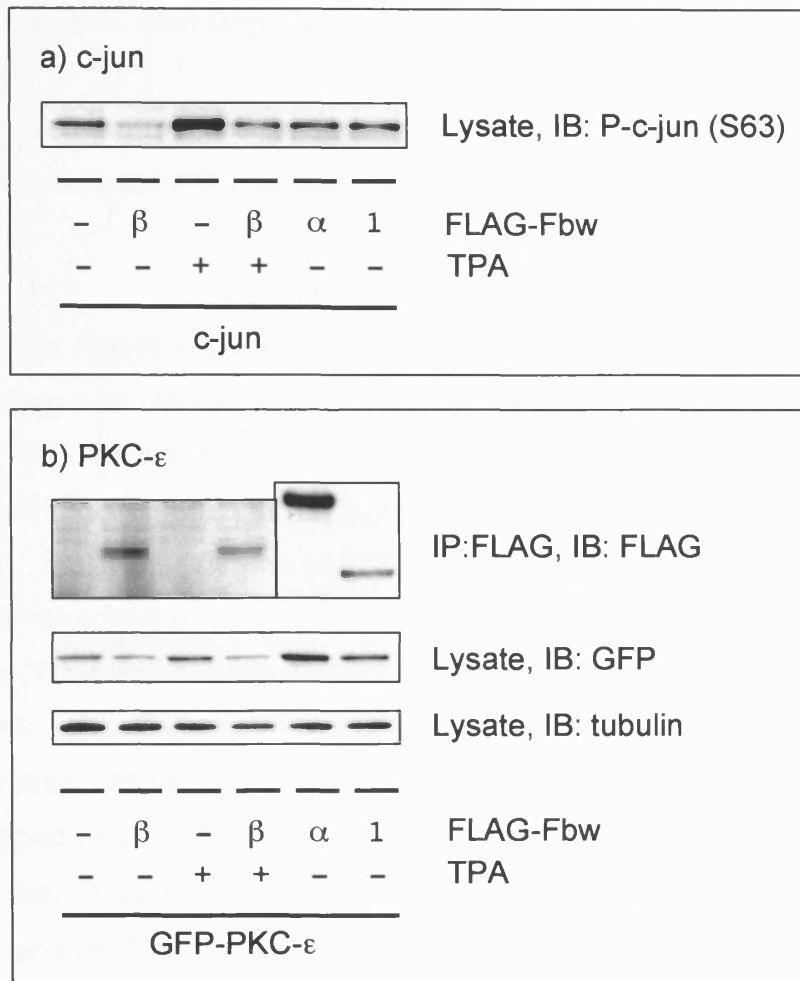
Figure 4.12 Fbw7β and Depletion of Phospho-c-jun and PKC-ε. a) HeLa cells were seeded onto 6-well plates and transfected with FLAG/FLAG-Fbw7 constructs (-, FLAG control; β, Fbw7β; α, Fbw7α; 1, Fbw1) and myc-c-jun-FLAG. 24hrs post-transfection, cells were treated +/- 400nM TPA for 1hr and then harvested in sample buffer. Samples were resolved by SDS-PAGE and analysed by Western blotting with anti-FLAG (Fbw7 and total c-jun) and anti-phospho-c-jun Ser-63 antibodies. b) HeLa cells were seeded onto 6-well plates and transfected with GFP-PKC-ε and FLAG/FLAG-Fbw constructs (-, FLAG; β, Fbw7β; α, Fbw7α; 1, Fbw1). 24hrs post-transfection, cells were treated +/- 400nM TPA for 1hr. Lysates were prepared and immunoprecipitation was performed using anti-FLAG M2-agarose affinity gel. Samples were resolved by SDS-PAGE and analysed by Western blotting with anti-FLAG and anti-GFP 3E1 antibodies. This data is representative of two separate experiments.

4.2.2.2.4.2 Fbw7 and Depletion of PKC 'TP' Phosphorylation Site Mutants

This same co-expression assay was used to determine the requirements of Fbw7β mediated PKC depletion with respect to PKC phosphorylation status.

As shown in Figure 4.9, the PKC 'TP' phosphorylation site bears a degree of homology with the CPD motif recognised by Fbw7. We hypothesized that the PKC 'TP' site may therefore be necessary for this apparent down-regulation to occur, such that a corresponding alanine mutant may be resistant. Since the 'TP' site of PKC-α represents an almost optimal CPD, we reasoned that a potential difference in stability between a wild type and 'TP'-alanine mutant might be best detected using this isoform.

Co-expression experiments were performed using both His-tagged and GFP-tagged PKC-α wild type and 'TP' mutants (Figure 4.13). These blots confirm that, like PKC-ε, PKC-α is depleted in an Fbw7β dependent manner and confirm that the fusion tag has no bearing on this effect. However, it is also revealed that a phosphorlyated 'TP' site is not required for this process to be observed; no difference in depletion is detectable between wild type PKC-α and either its 'TP'-alanine or 'TP'-glutamate mutants.
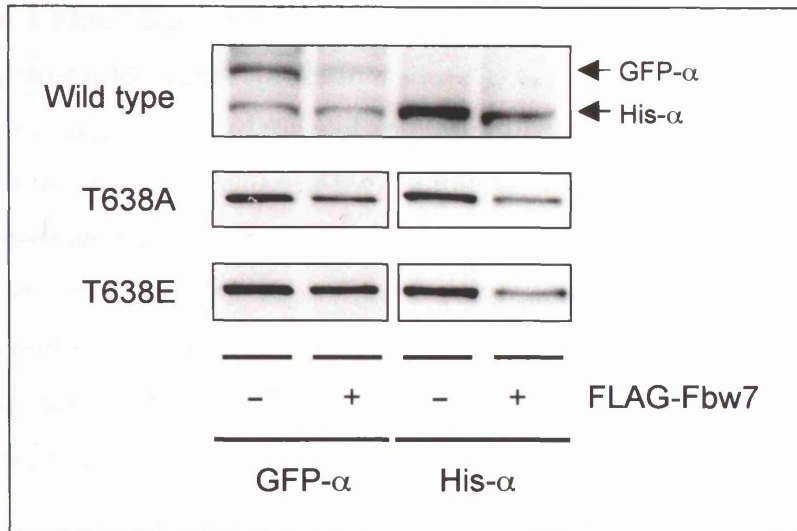
Figure 4.13 Fbw7β and Depletion of PKC-α 'TP' Mutants. a) HeLa cells were seeded onto 6-well plates and co-transfected with FLAG/FLAG-Fbw7β and PKC constructs. His-PKC-α and GFP-PKC-α were examined, and wild type constructs were compared to 'TP' site (T638) mutants. 24hrs post-transfection, cells were harvested in LDS sample buffer. Samples were resolved by SDS-PAGE and analysed by Western blotting with anti-PKCα MC5 antibodies.
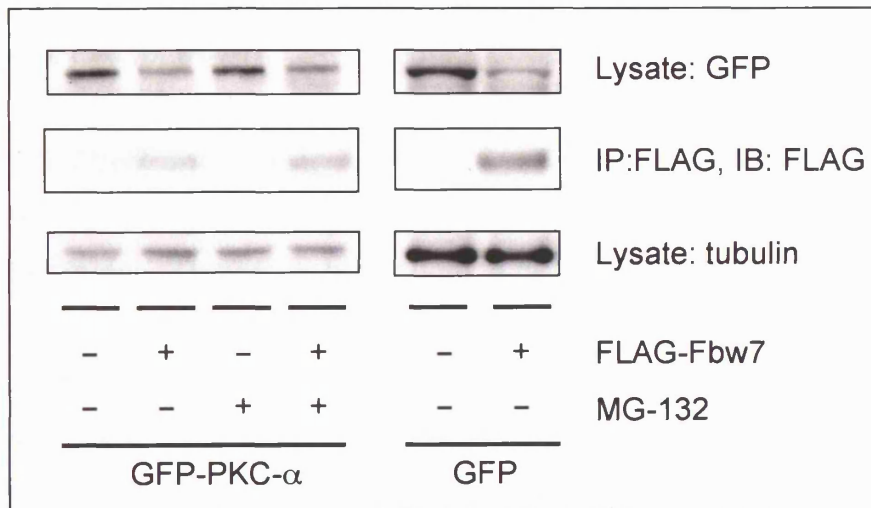
Figure 4.14 Fbw7β and Depletion of PKC-α: Proteasomal Dependence and Specificity. HeLa cells were seeded onto 6-well plates and co-transfected with FLAG/FLAG-Fbw7β and GFP/GFP-PKC-α. 24hrs post-transfection, cells were treated +/- 30μM MG-132 for 4hrs. Lysates were prepared and immunoprecipitation was performed using anti-FLAG M2-agarose affinity gel. Samples were resolved by SDS-PAGE and analysed by Western blotting with anti-FLAG, anti-GFP 3E1 and anti-tubulin antibodies.

4.2.2.2.4.3 Fbw7 Dependent PKC Depletion is not Mediated by the Proteasome and is not Specific

SCF^{Fbw7} mediated degradation of its substrates occurs via the proteasome. As such, where Fbw7 is functioning as a ubiquitin ligase, substrate down-regulation should be blocked by treatment with the proteasome inhibitor MG-132. Fbw7β dependent depletion of PKC-α was investigated +/- MG-132. As shown in Figure 4.14, treatment with MG-132 does not prevent PKC-α depletion in this system, indicating that this effect is not mediated by the ubiquitin-proteasome system.

A further co-expression experiment was performed using GFP in place of a putative Fbw7 substrate. Figure 4.14 reveals that a reduced level of the GFP control is also detectable in the presence Fbw7β.

Since the apparent depletion of PKC in the presence of Fbw7β is neither proteasome-dependent, nor a specific event, we must conclude that this result represents an experimental artefact and that our data does not support a role for Fbw7 in PKC degradation under basal conditions.

4.2.2.2.5 Fbw7 and TPA induced PKC-ϵ Degradation

As noted earlier, PKC degradation can be promoted by chronic phorbol ester treatment. Therefore, we sought to determine whether Fbw7 might play a role in TPA-induced degradation of PKC. We reasoned that the protection of PKC from TPA induced degradation by a dominant negative ubiquitin ligase would be more clearly detected than an augmentation of its down-regulation by a wild-type protein. Since clone-19 corresponds to the Fbw7 substrate binding domain, but lacks the F-box domain required for its association with the rest of the SCF ubiquitin ligase complex, it represents a putative dominant negative and was used as such.

NIH3T3 cells were transfected with RFP-PKC-ϵ, +/- GFP or GFP-19. Cells were treated with TPA and incubated over a 24hr time course.

Figure 4.15 shows that, under the conditions employed, there is no detectable effect of clone-19 on TPA induced PKC degradation.

As was the case for VBP1, our data regarding Fbw7 was not consistent with a role in PKC degradation. Consequently, we pursued an alternative working hypothesis, and investigated whether, VBP1/Fbw7 might represent downstream targets for PKC.

Figure 4.15 TPA Induced Degradation of PKC-ε in the presence or absence of dominant negative Fbw7. NIH3T3 cells were transfected with RFP-PKC-ε +/- GFP/GFP-Fbw7 substrate binding domain (SBD). 24hrs post-transfection cells were treated +/- 400nM TPA over a timecourse of a further 24hrs. Samples were harvested simultaneously in sample buffer, resolved by SDS-PAGE and analysed by western blotting with anti-PKC-ε and anti-GFP 3E1 antibodies.

4.2.3 VBP1/Fbw7 as candidate PKC targets

In order to address the possibility that PKC may influence the function of VBP1 or Fbw7, these proteins were analysed as candidate PKC substrates. There is a precedent for proteins identified as PKC binding partners to also behave as substrates (Chapline et al., 1993; Hyatt et al., 1994); such proteins represent a subgroup of PKC interacting proteins, referred to as STICKs (Substrates That Interact with C-Kinase).

4.2.3.1 VBP1 as a candidate PKC substrate
4.2.3.1.1 VBP1 purification

In order to test VBP1 as a potential PKC substrate it was first necessary to prepare purified protein for use in an *in vitro* kinase assay. His-VBP1 was produced in bacteria and purified using Ni-NTA agarose. Aliquots were removed at each stage of the purification process (Figure 4.16). Clear induction of VBP1 expression was observed following induction with IPTG. After lysis and ultracentrifugation, the majority of the protein was detected in the insoluble fraction, consistent with previous reports that VBP1 occurs in inclusion bodies when expressed in bacteria (Simons et al., 2004). Nevertheless, there was also a significant amount of VBP1 present in the supernatant and this was judged to be sufficient for our requirements. We therefore carried out a native purification protocol on Ni-NTA agarose using the soluble extract. His-VBP1 was eluted with step gradients of imidazole, with the bulk of the protein eluting at 200mM and above. Precipitation of purified VBP1 was observed upon prolonged storage, as such, fresh batches were prepared routinely.

| Pre IPTG | Post IPTG | Pellet | SN | 100mM Elution | 200mM Elution |
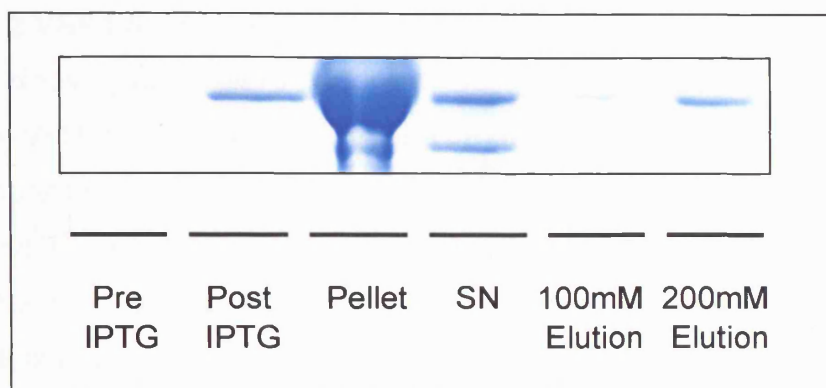
Figure 4.16 Purification of His-VBP1. His-tagged VBP1 was produced and purified from BL21-CodonPlus bacteria (see Materials and Methods). Aliquots of the culture were removed before and after induction with 0.4mM IPTG overnight at 16°C (Pre/Post IPTG). Post-lysis, the insoluble fraction was resuspended in 8M urea for analysis (Pellet), and an aliquot of the supernatant was removed (SN). The remainder of the soluble extract was subjected to a native protein purification protocol using Ni-NTA agarose. The purified protein was eluted with step gradients of imidazole (100mM/200mM). The samples shown are loaded such that pairs are comparable: Pre/Post, 1/200,000 culture volume; Pellet/SN, 1/4000 total fraction; 100mM/200mElution, 1:400 total fraction.

4.2.3.1.2 VBP1 *In Vitro* Kinase Assays

In vitro kinase assays were performed using recombinant human PKC-ε and His-VBP1 as a putative substrate. Figure 4.17a shows that phosphorylation of His-VBP1 is dependent upon PKC-ε, increasing over time, and with increasing substrate concentration. In a similar experiment, enhanced phosphorylation was also detected with increasing enzyme concentration (figure 4.17b). In both panels of this figure, it is apparent that VBP1 undergoes a bandshift over the course of the assay, with at least 2 upper bands emerging (see Discussion).

It is noteworthy that autophosphorylation of PKC-ε is detected using this assay; this phenomenon is investigated further in the next chapter.

4.2.3.1.3 VBP1 & MBP *In Vitro* Kinase Assays

The efficiency of PKC catalysed VBP1 phosphorylation was explored, using a well characterised substrate, myelin basic protein (MBP), as a control (Figure 4.18);.

Both PKC-ε and PKC-α were shown to phosphorylate VBP1, although a difference in substrate specificity was apparent between the two enzymes, with PKC-ε catalysing VBP1 phosphorylation relatively more effectively. However, the stoichiometry of VBP1 phosphorylation, with either isoform, was poor in comparison to MBP. As such, VBP1 was concluded to represent a relatively poor substrate for PKC and was not investigated further.
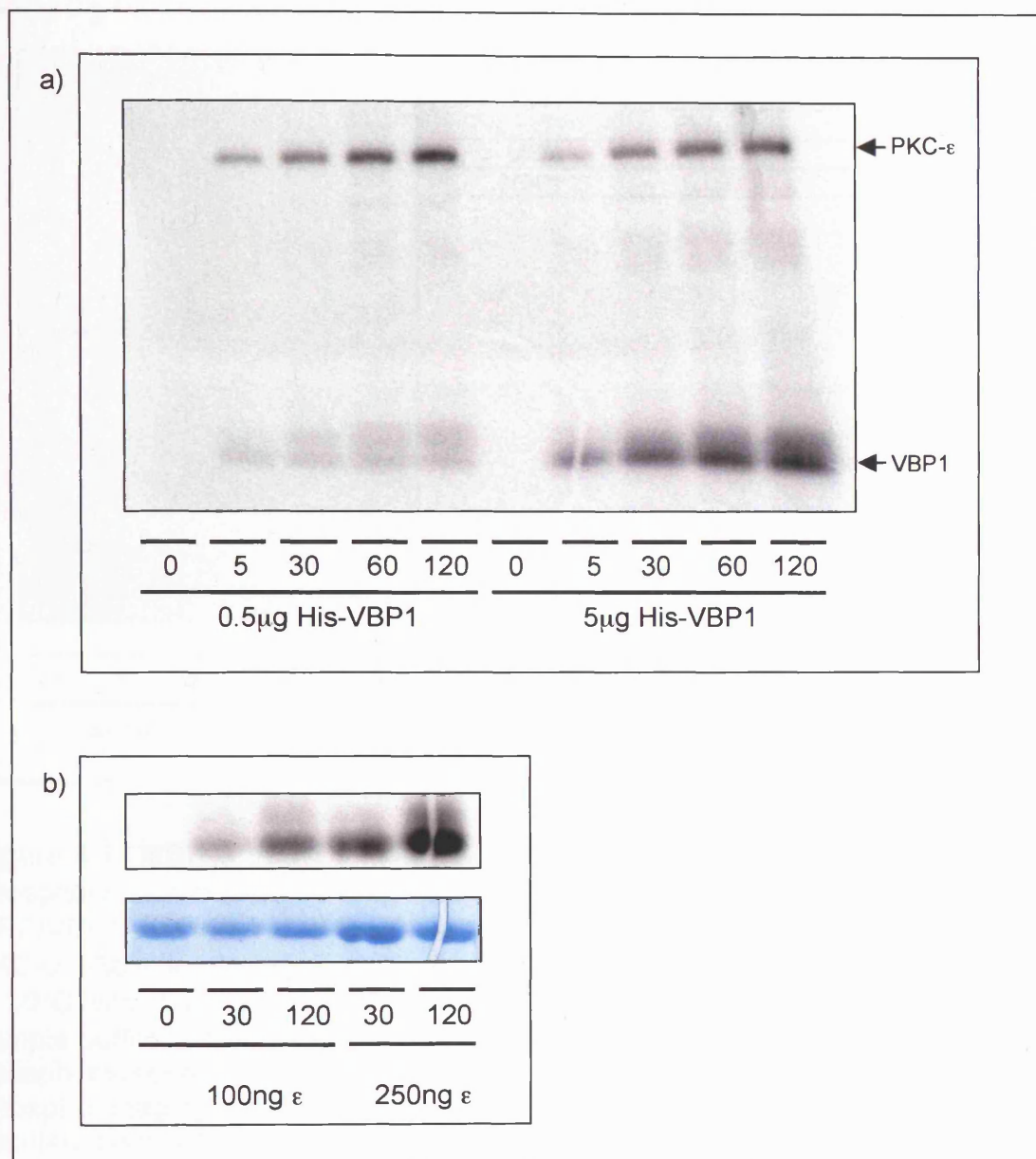
Figure 4.17 VBP1 *In Vitro* Kinase Assays. a) PKC-ε catalysed phosphorylation of VBP1 was assayed at varying substrate concentration. 0.5μg/5μg His-VBP1 was incubated in kinase assay buffer with 25ng PKC-ε. Reactions were started with $[\gamma^{32}P]$-ATP, incubated for 0-2hrs at 30°C with shaking, and stopped with the addition of kinase assay sample buffer. Samples were resolved by SDS-PAGE and exposed to a phosphor screen; phoshorylation was visualised using the Storm 860 PhosphorImaging System. b) PKC-ε catalysed phosphorylation of VBP1 was assayed at varying enzyme concentration. 0.2μg His-VBP1 was incubated in kinase assay buffer with 25/250ng PKC-ε. Reactions were started with $[\gamma^{32}P]$-ATP, incubated for 0-2hrs at 30°C with shaking, and stopped with the addition of kinase assay sample buffer. Samples were processed as described in a). This data is representative of three independent experiments.

Substrate	pmol ATP/pmol substrate	
	PKC-ε	PKC-α
MBP	0.18	0.72
VBP1	0.03	0.02
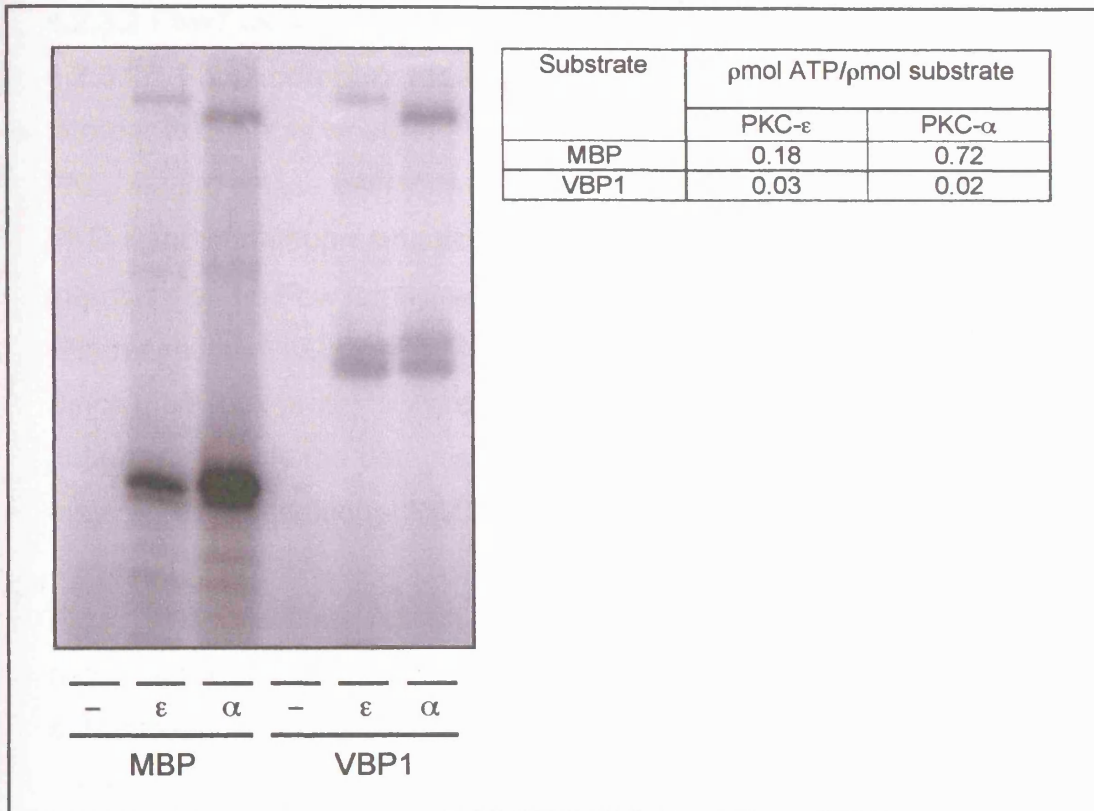
Figure 4.18 MBP & VBP1 *In Vitro* Kinase Assays. PKC-ε/α catalysed phosphorylation of purified MBP/VBP1 was assayed *in vitro*. 5μg MBP/VBP1 was incubated in kinase assay buffer with 25ng PKC-ε/150ng PKC-α. Reactions were started with [γ^{32}P]-ATP, incubated for 0/30mins at 30°C with shaking, and stopped with the addition of kinase assay sample buffer. Samples were resolved by SDS-PAGE and exposed to a phosphor screen; phoshorylation was visualised using the Storm 860 PhosphorImaging System. The MBP/VBP1 bands were excised and counted alongside the ATP stock to allow calculation of stoichiometry. These results are representative of two separate experiments.

4.2.3.2 Fbw7 as a candidate PKC substrate

4.2.3.2.1 Fbw7 complex kinase assays

In order to address whether Fbw7 may represent a downstream target of PKC, *in vitro* kinase assays were performed using recombinant human PKC-ε and immunoprecipitated Fbw7β as a putative substrate. The other members of the Fbw family, which were characterised in section 4.2.2.2.1 with respect to PKC binding, were analysed in parallel (See Figure 4.19). Since the F-box proteins were immunoprecipitated, this assay would potentially enable the detection of any Fbw-associated proteins which may represent additional PKC substrates.

Figure 4.19b confirms that all of the Fbw proteins were expressed and recovered by immunoprecipitation. Figure 4.19a reveals that again, autophosphorylation of PKC-ε is detectable by *in vitro* kinase assay, and thereby confirms that the assay conditions employed facilitated activity. There is a general elevation of phosphorylation apparent in the material immunoprecipitated via Fbw1, regardless of PKC-ε; presumably an active kinase is recruited within this complex. However, there is very little evidence of PKC-ε dependent substrate phosphorylation detected using this approach. There is a just single, subtle difference apparent between samples incubated +/- PKC-ε; interestingly, the size of the putative substrate is approximately the same as the size of FLAG-Fbw7β itself.
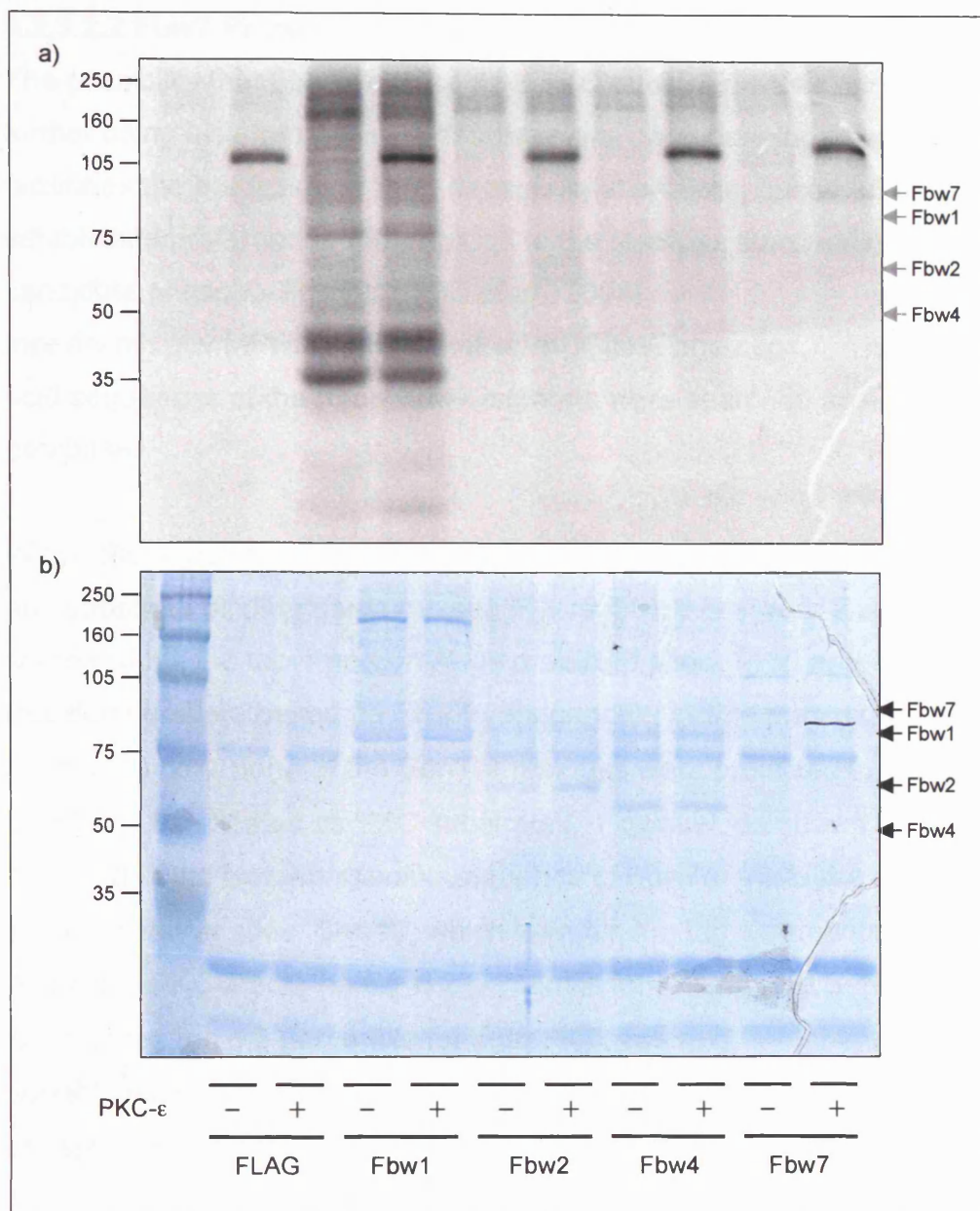
Figure 4.19 Fbw Immuno-complex *In Vitro* Kinase Assays. COS7 cells were plated onto 10cm dishes and transfected with FLAG/FLAG-tagged Fbw constructs (Fbw1/2/4/7). 24hrs post-transfection, Fbw fusion proteins, and associated partners, were recovered by anti-FLAG immunoprecipitation. Washed beads were incubated in kinase assay mix +/- 50ng purified PKCε, reactions were started with [γ^{32}P]-ATP, incubated for 30mins at 30°C with shaking and stopped with the addition of kinase assay sample buffer. Proteins were resolved by SDS-PAGE, Comassie stained and scanned (b). Phoshorylation was then visualised using the Storm 860 PhosphorImaging System (a). Fbws detected by Coomassie are denoted with black arrows, grey arrows indicate the equivalent positions on the PhosphorImage.

4.2.3.2.2 Fbw7 Phosphorylation Site Prediction.

The possibility that Fbw7 represents a PKC substrate was explored further using bioinformatics. A database has been developed which facilitates the prediction of PKC phosphorylation sites, based on its established preferences with regards to the residues surrounding a candidate phospho-Ser/Thr ((Fujii et al., 2004); mpr.nci.nih.gov/MPR/ScanProteinForPKCSitesPage.aspx,). The amino acid sequences of the three Fbw7 isoforms were searched against this database.

Within the region common to all Fbw7 isoforms, encompassing the F-box and substrate binding domains (see Figure 4.3), there were 2 sites which scored within the top 1 percentile as predicted sites: T165 and T226 (residue numbers based on Fbw7α sequence). Within the unique regions of Fbw7β and γ, none of the Ser/Thr residues were predicted to represent significant candidates as PKC substrates. However, as shown in Figure 4.20, within the isoform specific sequence of Fbw7α, there are two highly scoring putative sites: Ser-10, which is within the top 1 percentile with respect to PKC-δ and the top 0.2 percentile for PKC-ζ; and Ser-18, which is within the top 0.2 percentile for both PKC isoforms. We therefore sought next to test whether this region of Fbw7α constitutes a true PKC phosphorylation site.

Predicted Phosphorylation Sites in fbw7α

Citation: Fujii K. Zhu G. Liu Y. Hallam J. Chen L. Herrero J. Shaw S. Kinase Peptide Specificity: Improved Determination and Relevance to Protein Phosphorylation. Proc Natl Acad Sci U S A. 2004 in press.

Site Num	Sequence	P0 Position	Hydrophobicity	Prediction Percentile PKC-delta	PKC-zeta
1	--MNQELL-S-VGSKRRRT	7	0.04	66	58
2	NQELLSVG-S-KRRRTGGS	10	-0.04	1	0.06
3	SVGSKRRR-T-GGSLRGNP	15	-0.11	13	21
4	SKRRRTGG-S-LRGNPSSS	18	-0.19	0.1	0.2
5	GGSLRGNP-S-SSQVDEEQ	24	-0.04	30	16
6	GSLRGNPS-S-SQVDEEQM	25	0.04	53	54
7	SLRGNPSS-S-QVDEEQMN	26	0.00	76	85
8	LRQQEEEH-T-ARNGEVVG	53	-0.05	72	51
9	PRPGGQND-S-QQGQLEEN	72	-0.12	61	49
10	EENNNRFI-S-VDEDSSGN	86	-0.13	75	90
11	RFISVDED-S-SGNQEEQE	91	-0.09	94	69
12	FISVDEDS-S-GNQEEQEE	92	-0.06	90	83
13	EEEEMDQE-S-DDFDQSDD	122	-0.31	99	97
14	QESDDFDQ-S-DDSSREDE	128	-0.37	99	98
15	DDFDQSDD-S-SREDEHTH	131	-0.29	84	83
16	DFDQSDDS-S-REDEHTHT	132	-0.23	90	92
17	DSSREDEH-T-HTNSVTNS	138	-0.17	54	57
18	SREDEHTH-T-NSVTNSSS	140	-0.13	46	41
19	EDEHTHTN-S-VTNSSSIV	142	0.11	27	32
20	EHTHTNSV-T-NSSSIVDL	144	0.25	64	75
21	THTNSVTN-S-SSIVDLPV	146	0.39	72	20
22	HTNSVTNS-S-SIVDLPVH	147	0.38	34	20
23	TNSVTNSS-S-IVDLPVHQ	148	0.36	56	65
24	VDLPVHQL-S-SPFYTKTT	158	0.52	61	95
25	DLPVHQLS-S-PFYTKTTK	159	0.39	68	38

Figure 4.20 Predicted PKC Phosphorylation Sites in Fbw7α. The amino acid sequence of Fbw7α was searched against the Mammalian Phosphorylation Resource database for prediction of PKC phosphorylation sites (Fujii et al., 2004). The results for the isoform specific sequence of Fbw7α (1-167) are shown. The orange box indicates a prediction score within the top 1 percentile, the red box indicates a score within the top 0.2 percentile.

4.2.3.2.3 Fbw7α Peptide Array Kinase Assay

PKC catalysed phosphorylation of the Fbw7α N-terminal region was first investigated using a peptide array. As illustrated in Figure 4.21, the array comprises 20x12-mer peptide spots, which walk along the Fbw7α sequence from residue 1-31, one amino acid at a time. Kinase assays had to be performed in a large enough volume to completely immerse the cellulose strip upon which the peptide array was spotted, as such, pilot studies were carried out using PKC-α, which is purified in-house and therefore available in relatively large quantities, with the view to repeating the assay with PKC-ε, and other isoforms, subsequently.

Figure 4.21a shows that although there is a degree of background under the conditions employed, PKC-dependent phosphorylation of the array is evident. Elevated phosphorylation can be detected broadly across array; it does not correspond unequivocally with the presence of a particular residue. As such, the array does not identify a particular site of phosphorylation, but it does highlight the importance of the context in which a residue is placed.

Since the results obtained using the peptide array kinase assay were ambiguous, it was not repeated using other PKC isoforms, instead an alternative approach was employed as described below.

a)

No PKC

10µg PKC-α

100µg PKC-α

1 2 3 4 5 6 7 8 9 10 11 12 13 14 15 16 17 18 19 20

b)

```
     M N Q E L L S V G S K R R R T G G S L R G N P S S S Q V D E E

1    M N Q E L L S V G S K R

2      N Q E L L S V G S K R R

3        Q E L L S V G S K R R R

4          E L L S V G S K R R R T

5            L L S V G S K R R R T G

6              L S V G S K R R R T G G

7                S V G S K R R R T G G S

8                  V G S K R R R T G G S L

9                    G S K R R R T G G S L R

10                     S K R R R T G G S L R G

11                       K R R R T G G S L R G N

12                         R R R T G G S L R G N P

13                           R R T G G S L R G N P S

14                             R T G G S L R G N P S S

15                               T G G S L R G N P S S S

16                                 G G S L R G N P S S S Q

17                                   G S L R G N P S S S Q V

18                                     S L R G N P S S S Q V D

19                                       L R G N P S S S Q V D E

20                                         R G N P S S S Q V D E E
```

Figure 4.21 Fbw7α Peptide Array Kinase Assays. A peptide array representing the N-terminal region of Fbw7α was synthesized on a cellulose membrane. a) 3 identical arrays were blocked and equilibrated in kinase assay buffer (-PKC/[γ^{32}P]-ATP). Kinase assays were performed with no enzyme, 10µg purified PKC-α or 100µg purified PKC-α. Reactions were started with [γ^{32}P]-ATP, incubated for 15mins, and washed 2x15mins 30% acetic acid, 3x15mins TBS-T and 3x5mins in water. Phosphorylation was visualised using the Storm 860 PhosphorImaging System. b) The array comprises 20x12-mer peptide spots, which walk along the Fbw7α sequence from residue 1-31, one amino acid at a time. Red text indicates S18, the predicted phosphorylation site. Other candidate Ser/Thr residues are highlighted in blue.

4.2.3.2.4 Fbw7α S18 Peptide Kinase Assays

A panel of peptides were synthesized with which to further analyse the Fbw7α N-terminal region as a PKC substrate *in vitro*. Fbw7α 6-22 includes both highly scoring predicted sites (S10 and S18): LSVGSKRRRTGGSLRGN, while Fbw7α wt 11-22: KRRRTGGSLRGN includes just S18; a S18A mutant peptide corresponding to the latter was also synthesized. A peptide based on the PKC-ζ pseudosubstrate sequence, in which the alanine residue is replaced by a phosphorylatable serine, was employed as a positive control.

Figure 4.22 shows that the Fbw7α derived peptides are phosphorylated in a PKC dependent manner over time, and that there are some subtle isoform specific variations in catalytic behaviour towards this substrate. All of the PKC isoforms phosphorylate peptides 6-22 and 11-22 with similar efficiency, indicating that S10 cannot represent the single site of phosphorylation. Since phosphorylation is diminished in the S18A mutant, we can conclude that S18 represents the single site of phosphorylation in this peptide.
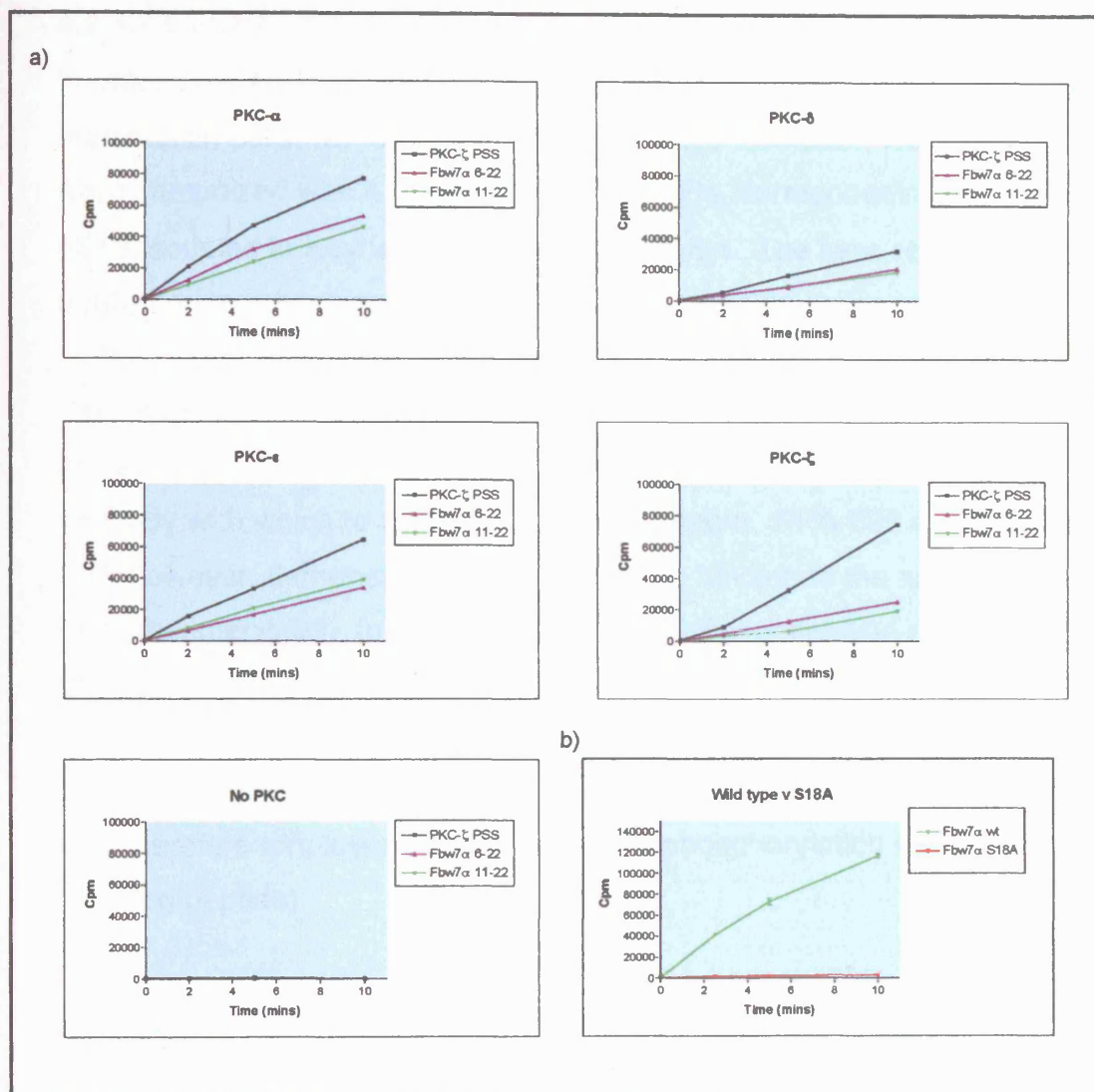
Figure 4.22 Fbw7α Peptide *In Vitro* Kinase Assays. a) Reactions were performed in 50μl kinase assay mix, with 0.2mM peptide substrate* and the following PKC isoforms: 25ng α, 15ng δ, 12.5ng ε or 250ng ζ. Assays were started with [γ^{32}P]-ATP, incubated at 30°C over the indicated timecourse, and stopped by spotting 15μl onto P81 paper and washing 3x5mins in 30% acetic acid. P81 strips were then counted.
* Peptide substrates: PKC-ζ 'PSS': RKRQGSVRRRV; Fbw7α 6-22: LSVGSKRRRTGGSLRGN, Fbw7α wt 11-22: KRRRTGGSLRGN. b) Reactions were performed in 50μl kinase assay mix, with 50ng PKC-ε and 0.2mM peptide substrate: Fbw7α wt 11-22, or Fbw7α 11-22 S18A. Assays were started with the addition of [γ^{32}P]-ATP, incubated at 30°C over the indicated timecourse, and stopped by spotting 15μl onto P81 paper and washing 3x5mins in 30% acetic acid. P81 strips were then counted. These assays were performed in triplicate; error bars denote standard deviation.

4.2.3.2.5 Fbw7α S18 Phospho-specific antibody

In order to investigate whether Fbw7α S18 is phosphorylated in mammalian cells, we raised phospho-specific antibodies. Three rabbits were immunized with a 9-mer phospho-peptide, corresponding to Fbw7α pS18, coupled to Keyhole Limpet Haemocyanin. The sera obtained were analysed for antigen recognition by ELISA as shown in Figure 4.23.

Serum PPA-525 binds to the Fbw7α antigen in a quantitative manner, however, it does not show phospho-specificity; it may represent a useful antibody with which to detect total Fbw7α protein. PPA-526 and PPA-527, however, demonstrate both quantitative binding to the antigen and phospho-specificity. In both cases, non-specific recognition of the de-phospho antigen can be reduced by incubation with the blocking de-phosphopeptide. PPA-527 shows the most significant differential between interaction with phospho- and de-phosphopeptides, this serum was therefore employed to screen for S18 phosphorylation in cells (+ blocking peptide).
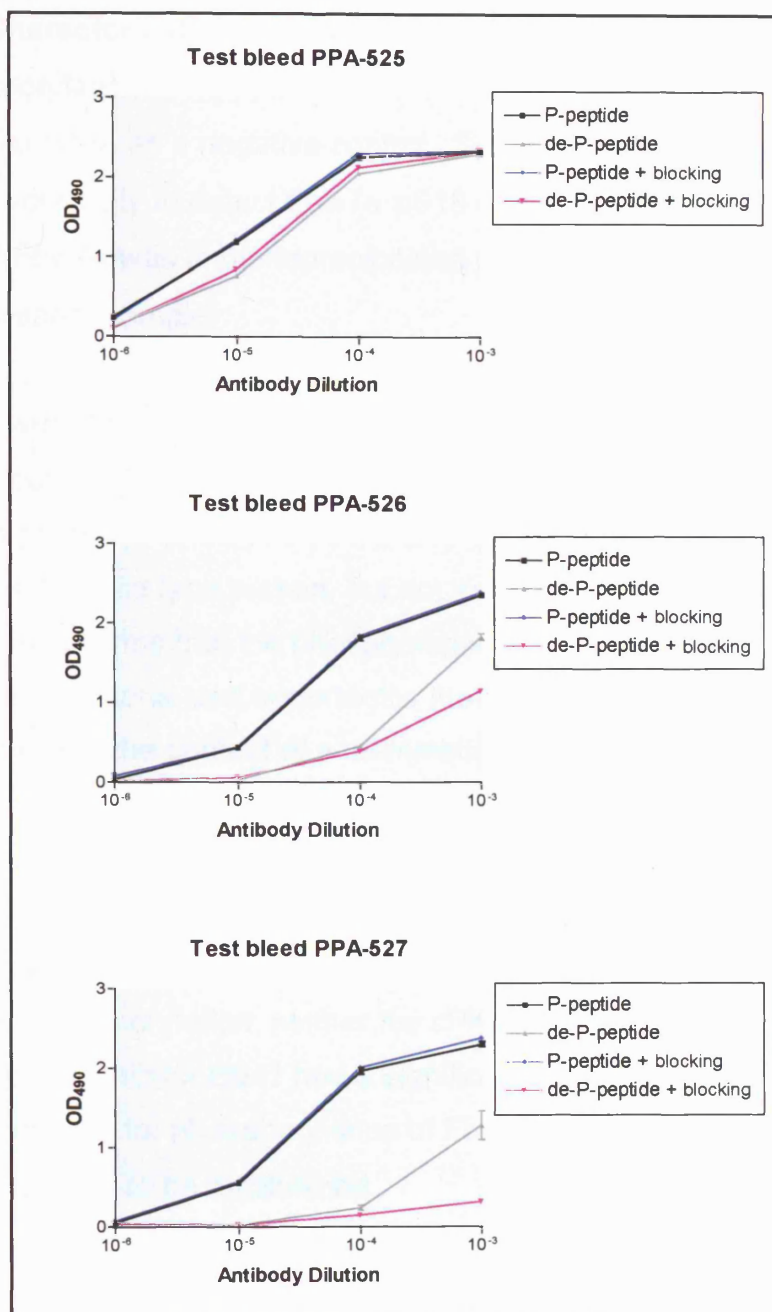
Figure 4.23 Fbw7α S18 Phosphospecific Antibody Characterisation.
3 rabbits (PPA-525/526/527) were immunised with a KLH-coupled 9-mer phospho-peptide corresponding to Fbw7α p-S18: N-RTGGpSLRGN-C. The 2nd test bleed was collected at day 49 and assayed by ELISA for binding to the antigen (P-peptide), or the corresponding de-phosphopeptide control (de-P peptide). Assays were performed using a dilution series of the test bleed +/- blocking peptide. ELISAs were developed using OPD substrate, stopped within the linear range with 2N H_2SO_4 and quantified at 490nm using a plate reader. Assays were performed in triplicate; error bars denote standard deviation.

4.2.3.2.6 Characterisation of Fbw7α S18 Phosphorylation in cells.

The phosphorylation of Fbw7α S18 in mammalian cells was investigated, using Fbw7α S18A as a negative control. Serum PPA-527 lacked the necessary specificity to detect Fbw7α pS18 uniquely within a lysate, as such, GFP-Fbw7α was immunoprecipitated prior to Western blotting to provide a cleaner sample.

HeLa cells were transfected with GFP-Fbw7α/Fbw7α S18A and treated with or without the phosphatase inhibitor Calyculin A. As shown in Figure 4.24, in the presence of Calyculin A, phosphorylation of S18 is clearly detectable in the wild type protein, but not in the corresponding alanine mutant. This confirms that the phospho-specific antibody is effective under these conditions, and importantly, that this site can indeed become phosphorylated in the context of a mammalian cell.

In order to test whether PKC is responsible for this phosphorylation event in cells, a panel of inhibitors were tested in the same experiment. While the broad specificity kinase inhibitor, staurosporine, completely suppressed phsophorylation, neither the cPKC/PKD inhibitor Gö6976, nor the cPKC/nPKC inhibitor BIM1 had a significant effect. The identity of the kinase responsible for phosphorylation of Fbw7α S18 under these conditions remains to be established.
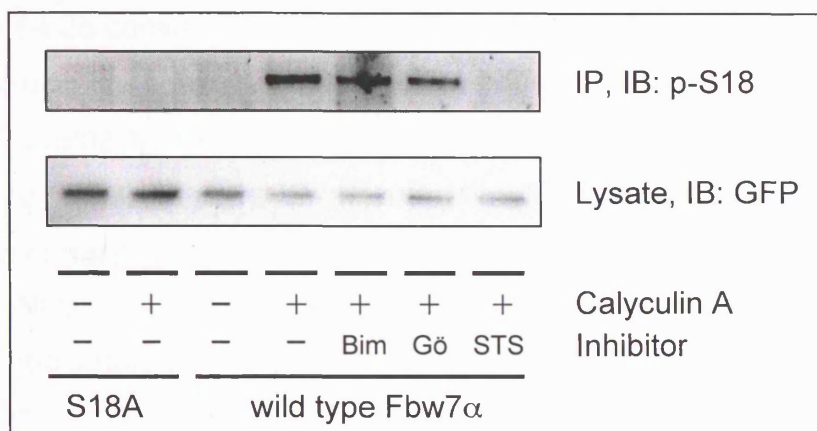
Figure 4.24 Phosphorylation of Fbw7α S18 in Mammalian Cells.
HeLa cells were plated onto a 24-well plate and transfected with GFP-
Fbw7α or Fbw7α S18A control. 24hrs post-transfection, cells were pre-
treated +/- a panel of kinase inhibitors for 15mins: BIM1 (Bim), 2μM;
Gö6976 (Gö), 1μM; Staurosporine (STS), 1μM. The media was then
supplemented +/- 100nM Calyculin A and cells were incubated for a
further 45mins. Lysates were prepared and subjected to
immunoprecipitation with anti-GFP 4E12/8. Samples were analysed by
Western blotting using anti-GFP 3E1 and anti-pS18 (PPA-527, + 0.1μg/ml
dephosphopeptide).

4.2.3.2.7 Fbw7α S18 Phosphorylation and localisation.

The three isoforms of Fbw7 display different patterns of localisation;
Fbw7α resides in the nucleus, Fbw7β is cytoplasmic, and Fbw7γ
nucleolar. The sequence determinants, within the isoform specific N-
termini, which dictate these localisations have been investigated by
Welcker and colleagues (Welcker et al., 2004a).

As indicated in Figure 4.2 there are two nuclear localisation signals
(NLSs) within Fbw7α (11-14 and 169-172). It has been shown that either
is sufficient to facilitate Fbw7α nuclear localisation, but it remains to be
established whether these sites are differentially regulated in cells. Since
it is well established that phosphorylation can influence the function of
NLSs (Jans and Hubner, 1996), we sought to explore whether occupation
of S18 would affect the nearby NLS 11-14, and perhaps affect Fbw7α
localisation in the absence of a second functional site.

Figure 4.25 confirms that the localisations of our GFP-Fbw7α/β

constructs are consistent with previous reports, and demonstrates that

Fbw7α remains in the nucleus even when co-expressed with PKC-ε

(Figure 4.25b). A panel of truncated Fbw7α constructs were generated,

which correspond to amino acids 1-68; these constructs would be reliant

upon NLS 11-14 for nuclear localisation. This region was cloned as a

wild type sequence, with an alanine mutation at Ser-18 (S18A), to abolish

any potential phosphorylation, or with the corresponding aspartate

mutation, to mimic phoshorylation with a negative charge (S18D). Figure

4.25 shows that neither mutation drastically alters localisation under

these conditions. Work is ongoing to explore the effect of this

phosphorylation event more extensively.

a)

GFP-Fbw7α   GFP-Fbw7β

b)

GFP-Fbw7α   RFP-PKC-ε   merge

c)

GFP-Fbw7α 1-68   GFP-Fbw7α 1-68   GFP-Fbw7α 1-68
Wild type   S18A   S18D
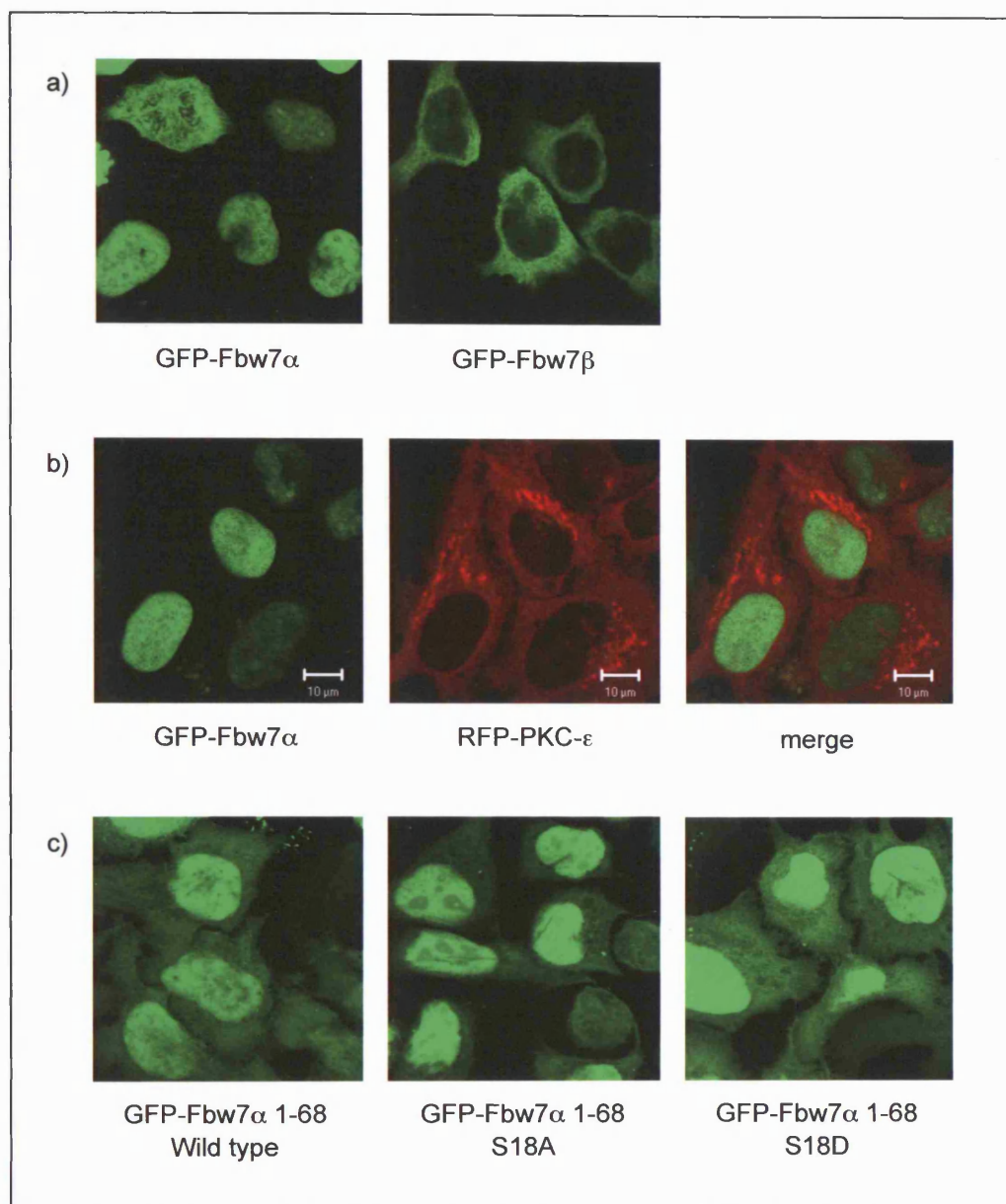
Figure 4.25 Fbw7α/β Localisation in HeLa Cells. HeLa cells were seeded on glass coverslips in 24-well dishes and transfected with a) GFP-Fbw7α or Fbw7β; b) GFP-Fbw7α + RFP-PKC-ε; c) GFP-Fbw7α 1-68 wildtype, S18A or S18D. Cells were washed in PBS, fixed in 4% (w/v) paraformaldehyde/PBS for 10mins at RT, washed 3x10mins in PBS and once in water, and finally mounted onto glass slides using Mowiol mounting media. Images were acquired using an upright laser scanning confocal microscope (LSM 510, Zeiss) equipped with a 63x/1.4 Plan-Apochromat Oil Ph3 objective. GFP was excited with the 488nm line of an Argon laser, Cy3 with a 543nm HeNe laser; individual channels were scanned sequentially line by line with averaging set at 8. Each image represents a single 1.0μm 'Z' optical section with a pixel size of approximately 0.1μm.

208

4.3 Discussion

Yeast 2-hybrid screening with a PKC-ε bait identified two interacting partners with links to the ubiquitin-proteasome system: VBP1 and Fbw7. Since PKC down-regulation is an important yet poorly characterised process, and a focus of ongoing research in our laboratory, these proteins represented interesting candidates for further investigation.

The protein-protein interactions detected by the yeast 2-hybrid system take place within the yeast cell nucleus and as such lack physiological context. It was therefore important to test whether these interactions could be detected in mammalian cells prior to studying their functional consequences. PKC binding to VBP1/Fbw7 was explored by in COS7 cells using over-expressed proteins. GST pull-downs were performed both with full length PKC-ε and its individual regulatory (εR) and catalytic (εC) domains; it was revealed that the VBP1 and Fbw7 binding sites mapped to PKC-ε catalytic domain. Further studies were carried out by co-immunoprecipitation, such that the interactions were tested in both orientations, with different combinations of tags; the binding partners were shown to associate with PKC under all conditions tested. It would have been preferable to further validate these findings by testing the interactions between endogenous proteins; however, at the time of the experiments, antibodies were not available against either VBP1 or Fbw7. It was therefore concluded that both proteins had been shown to interact with PKC-ε as effectively as possible. The yeast 2-hybrid screen described in Chapter 3 was judged to have successfully identified valid binding partners, and these proteins were pursued in further studies.

Investigations were initiated to study the functional significance of the PKC/VBP1 and PKC/Fbw7 interactions. These binding partners were first explored as candidates on the PKC degradation pathway(s), with the most detailed studies focussed on Fbw7.

Fbw7 is the substrate recognition component of a well characterised SCF
E3 ubiquitin ligase, whose substrates include cyclin E (Moberg et al.,
2001; Strohmaier et al., 2001), c-myc (Moberg et al., 2004; Welcker et al.,
2004a; Yada et al., 2004) and c-jun (Nateri et al., 2004). Fbw7 mediates
substrate recognition within this complex, interacting with specific
phosphorylated pTP motifs via its C-terminal, WD40 repeat based
substrate binding domain (Orlicky et al., 2003). Since yeast 2-hybrid
screening revealed that PKC interacts directly with this C-terminal
domain, PKC represented a strong candidate as an additional Fbw7 client
protein.

The isoform specificity of the PKC/Fbw interaction was investigated, firstly
with respect to the F-box WD40 protein. Three other members of the
Fbw family (Fbw1/2/4) were tested for interaction, and PKC-ε was shown
to bind to them all. Since Fbw-mediated ubiquitination is a process
executed with a high degree of selectivity, this promiscuity is not
consistent with the notion that PKC may represent an Fbw substrate.
Using the same panel of Fbw proteins, Yada *et al* were able to
demonstrate an impressive specificity for Fbw7 binding using phospho-c-
myc, a validated Fbw7 substrate (Yada et al., 2004).

PKC isoform specificity was also explored. Fbw7 was shown to interact
with all of the members of the PKC superfamily tested, this is likely to
relate to the fact that the interaction maps to the well conserved PKC
catalytic domain. Notably, all of the PKC isoforms bear some variation of
the conserved 'TP' phosphorylation site within this region, a feature which
bears some similarity to the Fbw7 pTP substrate recognition motif. While
it is tempting to speculate that this site may confer Fbw7 binding, and as
such direct subsequent ubiquitination and degradation by the
proteasome, the data do not support this conclusion. If an optimal pTP
motif was required to mediate recognition by Fbw7, PKC-δ, which has the
most poorly conserved 'TP' site, would be predicted to bind less efficiently
than PKC-α, which bears many of the optimal features (hydrophobic

residues at -1 and -2, phospho-threonine, which is favoured over phospho-serine, and a proline reside at +1). Although PKC-δ perhaps binds less efficiently, the difference is not substantial. It would have been worthwhile to test this assumption using TP site mutants.

Fbw7/PKC co-immunoprecipitations were performed in the presence or absence of the proteasome inhibitor MG-132, and an enhanced recovery of PKC was achieved +MG-132. Such a result could indicate that under normal conditions, the population of PKC that interacts with Fbw7 is targeted for degradation, and thus support the hypothesis that SCF^{Fbw7} represents a PKC E3 ligase. However, MG-132 appears to stabilize Fbw7, and as such it seems more likely that the enrichment of PKC is explained by the availability of a larger pool of Fbw7 with which to immunoprecipitate. It is noteworthy however, that there is a more significant increase in the recovery of PKC-ζ +MG-132, which exceeds the stabilisation Fbw7. It therefore remains possible that in this case, an additional effect on Fbw7 mediated turnover is conferred by the proteasome inhibitor. However, there is not a corresponding depletion of PKC-ζ from the lysate detectable in the presence of Fbw7 and absence of MG-132.

PKC down-regulation was explored further using cell-based ubiquitination assays. These assays were performed using the same panel of Fbw proteins described above (Fbw1/2/4/7), and elevated ubiquitination was detected in the presence of each of them. If this ubiquitinated protein corresponds to PKC, the implication is that, at least under these conditions, the PKC/Fbw interaction has a functional consequence. As noted with regards to the protein-protein interaction data, a greater degree of specificity may be expected from a true PKC E3 ubiquitin ligase, but given its relatively low expression level, the stoichiometry of ubiquitination mediated by Fbw7 may be significant. However, this interpretation of the data is flawed because it is not possible to distinguish whether the high molecular weight species in the pull-down represent

ubiquitinated PKC, ubiquitinated Fbw protein associated with PKC, or another ubiquitinated PKC binding partner. F-box proteins are known to autoubiquitinate (Galan and Peter, 1999) and immunoblotting of the lysates suggests that there may be a ladder of FLAG-immunoreactive products consistent with such a process. As such this experiment is not conclusive. These assays were not optimised further, but one possibility would be to repeat the process, incorporating differential stringengy washes of precipitated material prior to SDS-PAGE; this would be likely to dissociate bound (Fbw) proteins from the PKC, while leaving any covalently attached ubiquitin unaffected. Here though, alternative studies were undertaken instead to establish whether Fbw7 has a detectable effect on PKC down-regulation.

Fbw7 mediated turnover of its substrates has often been explored through co-expression studies, in which the presence of Fbw7 causes a detectable and specific depletion of a steady state client protein such as c-jun (Nateri et al., 2004), or c-myc (Welcker et al., 2004b). This system was employed to test PKC as a potential substrate, using phospho-c-jun, as a positive control.

The depletion of phospho-c-jun in the presence of Fbw7 was shown to be cell type specific, apparent in HeLa, but not 293s. The effect of Fbw7 on PKC was therefore tested in HeLa cells, and a similar reduction in protein level was detected. This finding initially suggested that Fbw7 may indeed mediate PKC down-regulation. However, subsequent experiments revealed that this effect was neither specific, nor dependent on the proteasome. As such, we had to conclude that this result represented an experimental artefact.

Since this artefactual protein depletion was not observed when Fbw1 or Fbw7α controls were co-transfected with PKC/c-jun, it seems unlikely to reflect a general flaw in the design of the experiment. Neither is it caused by the influence of a particular fusion protein, as both GFP- and His-tagged proteins were tested. It therefore remains that this effect is either

212

caused indirectly, through an effect on an additional Fbw7 substrate, or reflects an unusual property of the Fbw7β construct.

We reasoned that the protection of PKC from TPA induced degradation by a dominant negative ubiquitin ligase may be more clearly detectable than an augmentation of its down-regulation by a wild-type protein. Since yeast 2-hybrid clone-19 corresponds to the Fbw7 substrate binding domain, but lacks the F-box domain required for its association with the rest of the SCF ubiquitin ligase complex, it represents a putative dominant negative. We used GFP-19 to further investigate whether Fbw7 might play a role in PKC-degradation, either under basal conditions, or in response to a chronic phorbol ester treatment. No protection was afforded to PKC by co-transfection with GFP-19 under these conditions.

The effects of Fbw7 on PKC-downregulation in response to other stimuli were not explored in this work. Previous data from our laboratory has described a cell cycle dependent pathway of PKC-δ/ε degradation (Olivier et al., 1996). Given the role of Fbw7 in the control of the cell cycle, this would have been a relevant context in which to explore its relationship with PKC (Moberg et al., 2001), (Strohmaier et al., 2001).

The experiments undertaken to investigate Fbw7 as a candidate PKC specific E3 ubiquitin ligase proved problematic, and were not conclusive. While none of the data supports a role for Fbw7 in PKC degradation, it does not convincingly disprove this possibility either. It would perhaps have been more informative to study the effects of Fbw7 by pulse chase, to avoid the artefactual results detected when assessing overall expression; or by using RNAi to knock-down Fbw7 and studying the endogenous proteins.

The investigation of VBP1 as a candidate on the pathway of PKC degradation was more limited. VBP1 showed no discernable effect on either steady state levels of PKC, or on the profile of TPA-induced

degradation. Neither was there a detectable effect of VBP1 on the interaction between PKC and the established E3 ubiquitin ligase pVHL.

VBP1 was first identified as a pVHL interacting protein, prompting speculation about a potential role for VBP in protein degradation (Brinke et al., 1997). However, VBP1 has also been implicated, and studied much more thoroughly, in another context. The amino acid sequence of VBP1 is identical to that of a protein called prefoldin 3 (PFD3), a component of the prefoldin co-chaperone complex. This complex is involved in the delivery of unfolded clients to the TRiC/CCT chaperone, and has been shown to be responsible for the folding of actin and tubulin (Geissler et al., 1998; Vainberg et al., 1998). Since protein-protein interactions are inherent to the biological activity of VBP1/PFD3, it is conceivable that it may represent the type of 'inherently sticky' protein which will be commonly isolated by yeast 2-hybrid screening; the TRiC/CCT γ-subunit was also identified as a PKC-ε catalytic domain interacting protein by Adrian Saurin in our laboratory (unpublished data). It is also feasible that VBP1 may play a role in PKC folding, rather than in PKC degradation; we did not investigate this possibility. Notably, VHL is known to be recruited to the TRiC/CCT chaperone complex (Feldman et al., 1999), as such, we could speculate that its interaction with VBP1 reflects this aspect of its life-cycle.

A major aim of this chapter was to further characterise the elusive mechanism of PKC down-regulation. However, neither Fbw7 nor VBP1 was positively associated with this process by the experiments undertaken. There were clear limitations to the approaches which were employed, but due to a lack of any supporting data, we did not pursue alternative strategies in this work. Instead, we explored the converse relationship between PKC and VBP1/Fbw7, addressing whether these proteins might represent downstream targets for PKC.

VBP1 was tested as a potential PKC substrate. Firstly, VBP1 was purified for use in kinase assays. Although the bulk of the protein was

insoluble in bacteria, we were able to obtain enough soluble VBP1 to carry out a non-denaturing purification, and thereby increase our chances of recovering native protein. This purified VBP1 behaved as a typical substrate, with PKC-catalysed phosphorylation increasing over time, and with increasing enzyme/substrate concentrations.

However, when analysed alongside Myelin Basic Protein (MBP), an established PKC substrate, VBP1 phosphorylation was shown to occur with a relatively inefficient stoichiometry. It could be argued that this may reflect the fact that MBP bears multiple PKC consensus sequences (Ramwani and Moscarello, 1990), such that more than one phosphorylation event may occur per molecule. However, the bandshift observed during a timecourse of phosphorylation suggests that this may also hold true for VBP1.

It is important to acknowledge that the purified VBP1 employed as a kinase assay substrate may not have existed in a native conformation; this protein has a propensity to aggregate (Simons et al., 2004), and a certain amount of precipitation was observed during prolonged storage. Therefore, we cannot exclude the possibility that a small population of correctly folded VBP1 is acting as a high stoichiometry substrate. An additional consideration to bear in mind is that under physiological conditions, VBP1 forms part of the prefoldin complex; perhaps within this context, it would be held in a conformation more conducive to phosphorylation. Work was undertaken to try to isolate the prefoldin complex from mammalian cells for use as an *in vitro* kinase assay substrate. Antibodies specific for different prefoldin subunits were obtained (from Dr. Nick Cowan) to facilitate the immunoprecipitation of the complex, however, they proved to be of insufficient specificity for this purpose, under the conditions employed. Dr. Cowan's group have demonstrated that it is possible to assemble a functional prefoldin chaperone using bacterially expressed constituent subunits; it would be of interest to test this complex as a potential substrate.

Fbw7 was next investigated as a candidate PKC substrate. Kinase assays performed using immuno-precipitated Fbw1/2/4/7β revealed negligible PKC-dependent phopshorylation of either the Fbw proteins themselves, or of any associated proteins. However, there was a subtle increase detected in the phosphorylation of Fbw7β immuno-precipitated material in the presence of PKC, with the putative substrate running at approximately the same size as Fbw7β itself. Since the concentration of the corresponding protein was relatively low, as judged by Comassie staining, it is possible that this phosphorylation event is occurring at a reasonable stoichiometry.

The amino acid sequences of the three Fbw7 isoforms were submitted to a database which predicts the capacity of any given Ser/Thr residue to behave as a PKC substrate, based on the established preferences of PKC with respect to adjacent residues (Fujii et al., 2004). The sequence common to all of the Fbw proteins was predicted to bear two reasonably scoring PKC phosphorylation sites. These sites are not optimal, but could perhaps account for the low level phosphorylation of an Fbw7β sized protein observed in Figure 4.19.

Phosphorylation within a unique region of one of the Fbw7 proteins could potentially contribute to isoform specific behaviours. These regions were therefore also analysed. While the distinct regions of the β and γ isoforms do not bear any highly scoring predicted sites, the Fbw7α isoform specific N-terminus possesses two: S10 and S18. In a series of kinase assays using Fbw7α derived peptides as substrates, we were able to demonstrate *in vitro* that at least one of these sites, S18, is effectively phosphorylated by a number of PKC isoforms. If the phosphorylation of the Fbw7α derived peptides is compared to the phosphorylation of the positive control in these experiments, then PKC-ζ shows the lowest relative activity towards this substrate. However, this may in fact reflect a preference for the control peptide, rather than against the test peptides,

since the control is based on PKC-ζ's own pseudosubstrate sequence, and is therefore "naturally" optimised for this isoform.

Fbw7α S10 remains to be further investigated as a candidate phospho-acceptor. It would have been more informative in this regard had we synthesized the S18A mutation within the context of the Fbw7α 6-22 peptide, and/or included a S10A mutation. In order to resolve this issue, kinase assays could be carried out again using the Fbw7α 6-22 and Fbw7α 11-22 peptides and this time incubated to completion; if greater ^{32}P- incorporation was detected in the longer peptide, we could surmise that more than one site was being phosphorylated. Alternatively, in vitro phosphorylated Fbw7α 6-22 peptide could be analysed by Edman degradation; N-terminal amino acids could be removed sequentially from the peptide and scintillation counted, to establish the positioning of the phosphate group(s).

A parallel study of PKC-catalysed Fbw7α phosphorylation was carried out using a peptide array; phosphorylation of the array was shown to occur in an unexpectedly broad manner. There is clearly a degree of specificity, for example, there is negligible phosphorylation of peptides 19 and 20, despite the presence of three serine residues. However, across the rest of the array, phosphorylation does not correspond clearly to the presence or absence of a particular residue. Since there is a certain amount of PKC-dependent phosphorylation detected on spots 2-6, S18 does not appear to be the sole phospho-residue under these conditions; phosphorylation of S10 could potentially account for this result. Meanwhile, the presence of S18 could account for the elevation of counts at spots 9/10 and 14. This observation is perhaps informative with respect to the importance of context to PKC activity. Spots 9/10 bear both an intact KRRR sequence, and a C-terminal arginine residue; these sequence features are perhaps important in directing PKC mediated phosphorylation, as PKC is a basophilic kinase.

A phospho-specific antibody was raised against Fbw7α S18 in order to test whether this site can be phosphorylated in cells; the anti-sera was characterised by ELISA and a S18A mutant was cloned for use as a negative control. Using this phospho-specific antibody, it was revealed that Fbw7α S18 is indeed phosphorylated in mammalian cells, as treatment with the Ser/Thr phosphatase inhibitor Calyculin A, enabled its detection on wild type, but not S18A protein. It will be informative in the future, in terms of dissecting the potential function of this site, to try to stimulate its phosphorylation with different treatments, rather than merely protecting it from dephosphorylation.

A panel of inhibitors were screened for their capacity to attenuate the effect of Calyculin A, thereby addressing the identity of the kinase responsible in cells. Phosphorylation of Fbw7α S18 was clearly blocked by pre-treatment with the broad specificity kinase inhibitor, staurosporine. However, neither the cPKC/PKD inhibitor Gö6976, nor the cPKC/nPKC inhibitor BIM1 had a significant effect. As such, we have yet to confirm whether PKC represents a kinase responsible for cellular phosphorylation of Fbw7α S18. It will be interesting to follow up this experiment by testing a broader selection of inhibitors. It remains possible that an aPKC, or related PKN, could catalyse phosphorylation of this site. Alternatively, within the context of the cell, perhaps another basophilic kinase performs this function.

It is noteworthy that Fbw7α is a nuclear protein. Consequently, one working hypothesis would be that the S18 kinase can also localise to the nucleus. In this respect it may be significant that PKCδ/ε catalytic domains are known to translocate to the nucleus during apoptosis; as such, it will be important to analyse S18 phosphorylation in response to apoptotic stimuli. An alternative possibility is that Fbw7α is phosphorylated in the cytoplasm, perhaps directly after translation, during a phase of the cell cycle when the nuclear envelope is not intact, or following hypothetical nuclear export; there is currently no evidence of

Fbw7 nuclear shuttling. All of the PKC/Fbw interaction studies were performed using cytoplasmic Fbw7β; it may be informative to test whether Fbw7α binding to PKC can be detected by co-immunoprecipitation, to assess whether these proteins are exposed to one another. Immunofluorecence data would suggest not.

.

The localisation of Fbw7α is likely to be an important factor in controlling the phosphorylation of S18, however, the converse may also be true. We began to address the functional consequences of S18 phosphorylation by focussing on its potential influence on the Fbw7 specific nuclear localisation signal (NLS 11-14); it is well established that phosphorylation close to a NLS can alter its ability to direct nuclear localisation (Jans and Hubner, 1996). The experiments conducted to date, in which phospho-specific mutations have been incorporated into a truncated form of Fbw7α, do not support this hypothesis. However, it may be more meaningful to examine the effect of S18 phosphorylation on nuclear localisation within the context of the full length protein. This experiment would need to be performed using an Fbw7α mutant, which lacks the second NLS (169-172), which may otherwise compensate for any effects. It is reasonable to assume that there may be conditions under which one or the other NLS functionally dominates, for example binding partners or other post-translational modifications could mask either NLS. As such, any regulatory input controlling the other site would have detectable effects. It will also be of interest to determine whether S10 can be phosphorylated too; additional occupation of this site would flank the NLS with phosphate groups and potentially mediate more profound effects.

In summary, VBP1 and Fbw7 were identified as PKC-ε binding partners and selected for further study as candidates on the PKC degradation pathway(s); however, the data presented in this chapter did not support such a role for either protein. Nevertheless, at least in the case of Fbw7, evidence for a functional interaction with PKC was obtained. PKC was shown to phosphorylate Fbw7α S18 *in vitro*, and this site was shown to

be occupied in mammalian cells; the PKC dependence of the latter remains to be established. While there is currently limited data on the phosphorylation of F-box proteins, the potential importance of such post-translational modifications has been commented upon in the literature (Gao and Karin, 2005). The functional significance of this particular Fbw7α phosphorylation event remains to be determined, but it is possible that this site may play an important regulatory role, in an isoform specific manner, adding another level of complexity to the function of this key tumour suppressor.

The theme of post-translational modification is explored further in the remainder of this work. The phosphorylation of PKC itself has been shown to play an important role in regulating its down-regulation (Hansra et al., 1999; Lee et al., 1996; Leontieva and Black, 2004; Srivastava et al., 2002). As such, we reasoned that the characterisation of PKC phosphorylation sites may provide further insights into this elusive process. The following chapter provides an account of the mapping of novel PKC-ε and PKC-δ autophosphorylation sites undertaken to this end.

CHAPTER 5

Identification of Novel
PKC-ε/δ Phosphorylation Sites

5.1 Introduction

PKC activity is controlled by a complex network of regulatory inputs. Seminal work in the field determined that cPKC/nPKC isoforms are subject to acute allosteric control by diacylglycerol (Hug and Sarre, 1993; Nishizuka, 1986), and possibly other bioactive lipids (Nishizuka, 1995), which facilitate PKC activation in the presence of phosphatidylserine (and Ca^{2+} in the case of the cPKCs). However, subsequent studies have revealed that this basic level of regulation is fine-tuned by a number of other modulatory inputs, including the phosphorylation of three key 'priming' sites, permissive for subsequent allosteric activation (Parekh et al., 2000).

The three PKC priming phosphorylation sites comprise the activation loop (or T-loop) site, the autophosphorylation (or 'TP') site and the hydrophobic (or 'FSY') site. These phospho-residues are conserved throughout the PKC superfamily, and throughout evolution, with the exception that the FSY site is substituted with glutamate in the aPKCs, and aspartate in the PKNs; these acidic residues may mimic phosphorylation.

Phosphorylation of the T-loop site is catalysed by polyphosphoinositide-dependent kinase 1 (PDK1) (Chou et al., 1998; Le Good et al., 1998). This phosphorylation is predicted to correctly align active site residues and is critical for catalytic activity (Cazaubon et al., 1994; Orr and Newton, 1994). The two other priming sites play more subtle roles in

maintaining a closed PKC conformer, with optimum thermal stability and resistance to proteases and phosphatases (Bornancin and Parker, 1997). The 'TP' site has been shown to represent an autophosphorylation site (Flint et al., 1990; Standaert et al., 2001), as has the hydrophobic motif in cPKCs ((Behn-Krappa and Newton, 1999; Dutil et al., 1994; Dutil et al., 1998). However, the pathway(s) leading to the phosphorylation of the hydrophobic motif in nPKCs remain more elusive. Cenni et al have presented evidence for autophosphorylation (Cenni et al., 2002), while Parekh and colleagues have shown, under different experimental conditions, that an upstream kinase activity is required (Parekh et al., 1999). Previous data from our laboratory suggests that an aPKC complex may be responsible for phosphorylation of the hydrophobic motif (Ziegler et al., 1999), with a parallel, mTOR regulated, amino acid sensing pathway providing a permissive signal, possibly through control of a protein phosphatase (Parekh et al., 1999). Work is ongoing to resolve the identity of the nPKC hydrophobic site kinase.

In addition to these priming phosphorylation sites, a number of other PKC phospho-residues have been reported including Thr-250 in PKC-α (Ng et al., 1999), multiple PKC-β autophosphorylation sites (Flint et al., 1990), and numerous phospho-tyrosines within PKC-δ (see (Steinberg, 2004) for recent review). The influences of certain of these phosphorylation events on PKC activity have been defined, as discussed in the following chapter, while others remain to be characterised.

PKC phosphorylation status is well documented to influence its TPA-induced degradation. Experiments with PKC-α and PKC-ε demonstrated that de-phosphorylation of priming phosphorylation sites is a critical step in the process of down-regulation by the ubiquitin-proteasome system (Hansra et al., 1999; Lee et al., 1996; Lee et al., 1997). However, this is clearly cell type and/or context dependent, since data from our laboratory showed that phosphorylation of PKC-δ was required for its degradation in NIH 3T3 cells (Srivastava et al., 2002). More recent work from Leontieva

and colleagues provides support for both of these models, revealing two independent pathways of PKC-α desensitization operating in response to the same stimuli, one involving the ubiquitination and subsequent proteasomal degradation of the mature, fully phosphorylated enzyme, the second, a proteasome-independent mechanism, requiring caveolar trafficking and dephosphorylation (Leontieva and Black, 2004). Since phosphorylation plays such a key role in determining PKC down-regulation, we hypothesized that analysis of PKC phosphorylation sites may provide further insights into this process, and as PKC activity has also been implicated in PKC down-regulation (Goode et al., 1995; Kang et al., 2000; Lu et al., 1998; Ohno et al., 1990; Srivastava et al., 2002), sites of autophosphorylation were of particular interest.

This chapter describes the identification of novel phosphorylation sites within PKC-ε, and also PKC-δ, by phosphopeptide mapping and the subsequent analysis of these sites within mammalian cells using phospho-specific antibodies.

5.2 Results

5.2.1 *In Vitro* Phosphorylation & Phosphopeptide Mapping

Phosphopeptide mapping studies were performed in collaboration with the Protein Analysis Laboratory (CR-UK); the approach employed is summarised in Figure 5.1. PKC is first incubated in an *in vitro* kinase assay with $[\gamma^{32}P]$-ATP, to yield radiolabelled, phosphorylated protein. Following resolution by SDS-PAGE and staining by Coomassie, the PKC band is excised and subjected to in-gel tryptic digestion. The tryptic peptides are fractionated by reverse phase high performance liquid chromatography (HPLC), and fractions are counted to locate ^{32}P-labelled phosphopeptides. Radiolabelled fractions are then analysed by both mass spectrometry and Edman degradation.

Mass spectrometry facilitates the identification of the peptides present within a hot fraction; peptide masses are matched against an *'in silico'* tryptic digest of the whole protein. Additionally, spectral features characteristic of phosphopeptides are searched for: phosphorylation adds 80Da to the mass of the de-phosphopeptide, and post source decay of the phosphopeptide in the mass spectrometer flight tube, which releases phosphoric acid, causes a loss of 98Da, which is detected as a broad peak.

Edman degradation then enables the identification of the residue number of the phosphorylation site within a phosphopeptide. Amino acids are sequentially removed from the N-terminus of the tryptic peptide and scintillation counted, elevated counts indicate the presence of an ^{32}P-labelled residue.

By combining the data obtained from mass spectrometry and Edman degradation, it is therefore possible to identify a given phosphopeptide, and locate the phosphorylation site within it.

PKC *In Vitro* Kinase Assay with [γ³²P]-ATP

↓

PAGE, Coomassie staining, excision of PKC band

↓

In gel tryptic digest

↓

Fractionation of peptides by HPLC

↓

Identification of [γ³²P]-labelled peptides by counting

Mass Spectrometry

↓

Identification of
phospho-peptide

Edman degradation
& scintillation counting

↓

Identification of phospho-site
residue number
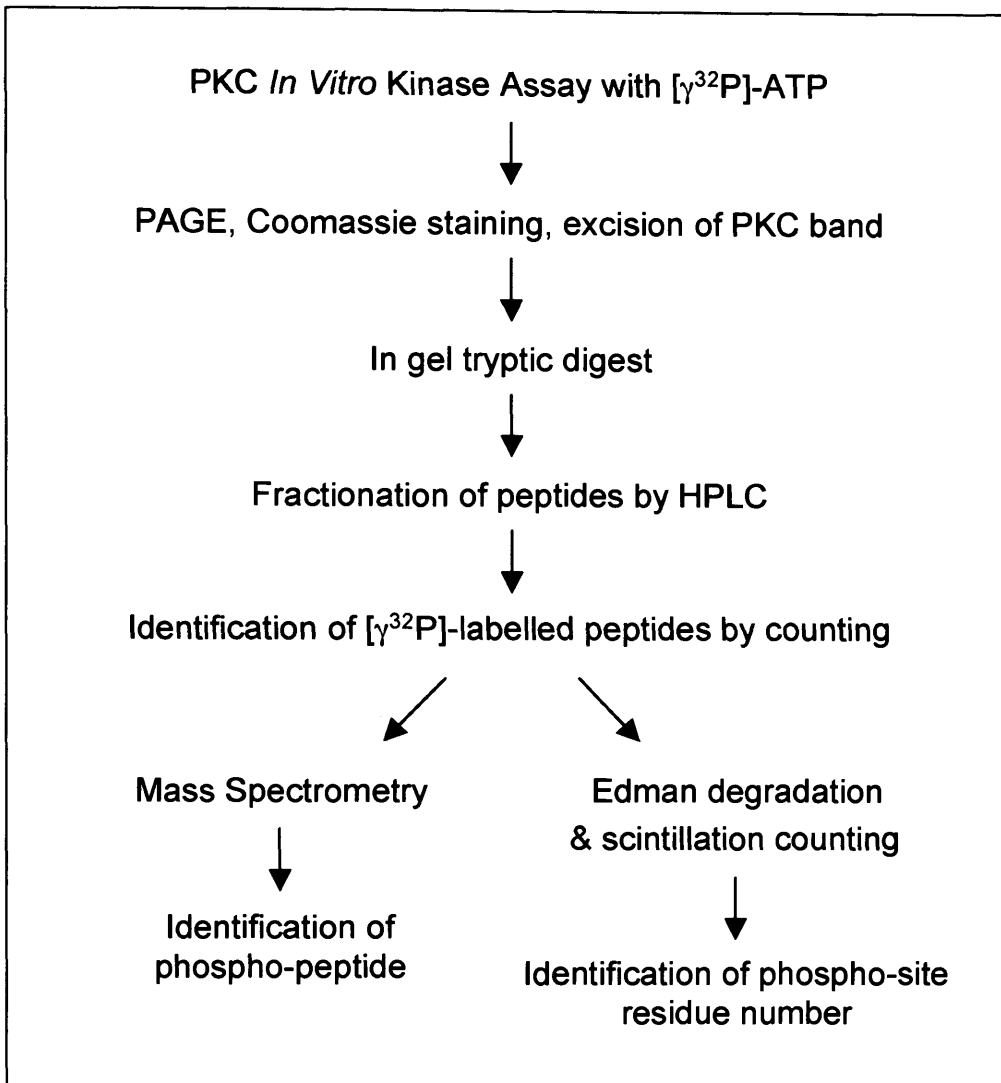
Figure 5.1 PKC Phosphopeptide Mapping. PKC phosphorylation sites were identified by phosphopeptide mapping. In this system, PKC is first incubated in an *in vitro* kinase assay with [γ³²P]-ATP. The kinase assay mix is resolved by SDS-PAGE, the gel is stained using Coomassie and the PKC band is excised and counted. An in-gel tryptic digest is performed to generate a set of peptides, which are then fractionated by reverse phase high performance liquid chromatography (HPLC). Fractions are counted, and those containing [γ³²P]-labelled peptides are analysed both by mass spectrometry, to identify the phosphorylated peptide, and Edman degradation, to locate the phospho-site within the peptide.

5.2.1.1 PKC-ε *In Vitro* Phosphorylation & Phosphopeptide Mapping

5.2.1.1.1 PKC-ε *In Vitro* Phosphorylation

In vitro kinase assays were performed using recombinant human PKC-ε, commerically purified from insect cells. As shown in Figure 5.2, increased phosphorylation was detected with increasing enzyme concentration and incubation time. The stoichiometry of phosphorylation was calculated from four separate experiments at 0.775 ± 0.106 pmol PO_4/pmol PKC-ε.

The requirements for PKC-ε phosphorylation were also investigated, alongside an MBP substrate control. *In vitro* kinase assays were performed in the presence or absence of phosphatidylserine/TPA mixed micelles, with or without the cPKC/nPKC inhibitor BIM1. Phosphorylation was significantly reduced in the absence of lipids, and was inhibited by BIM1 in a dose dependent manner (Figure 5.3); PKC-ε phosphorylation was inhibited to a lesser extent than MBP phosphorylation (see discussion).
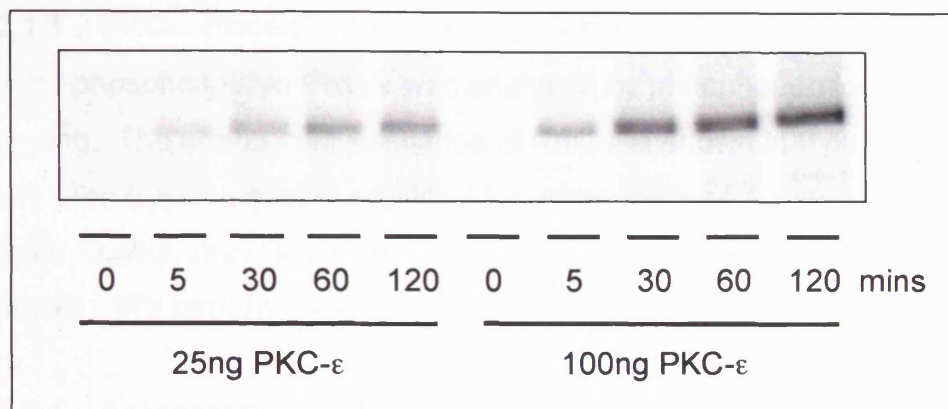
Figure 5.2 Phosphorylation of PKC-ε *In Vitro*. PKC-ε phosphorylation was assayed by *in vitro* kinase assay. 25-100ng of purified recombinant human PKC-ε was prepared in kinase assay buffer. Reactions were started with $[\gamma^{32}P]$-ATP (50μM ATP, 5μCi; 40Ci/mmol), incubated for 0-2hrs at 30°C with shaking, and stopped with the addition of sample buffer. The whole reaction mix was resolved by SDS-PAGE and phoshorylation was visualised using the Storm 860 PhosphorImaging System. Data is representative of 3 separate experiments.
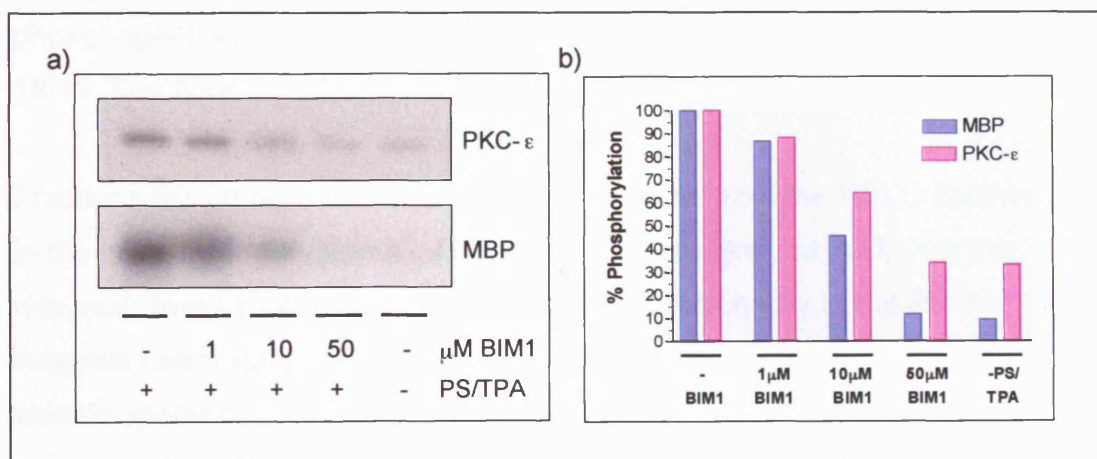
Figure 5.3 Lipid Dependence of MBP/PKC-ε Phosphorylation & Inhibition by BIM1. *In vitro* kinase assays were performed using 50ng of purified recombinant human PKC-ε, either alone or with 5μg of MBP substrate. Reactions were prepared in kinase assay buffer +/- phosphatidylserine/TPA mixed micelles (PS/TPA), and +/- BIM1. Reactions were started with $[\gamma^{32}P]$-ATP (50μM ATP, 5μCi; 40Ci/mmol), incubated for 30mins at 30°C with shaking, and terminated with the addition of sample buffer. Samples were resolved by SDS-PAGE, gels were stained with Coomassie and phosphorylation was visualised using the Storm 860 PhosphorImaging System (a). Bands were excised and counted (b); phosphorylation is expressed as a percentage of the uninhibited control.

5.2.1.1.2 PKC-ε Phosphopeptide mapping

In vitro phosphorylated PKC-ε was analysed by phosphopeptide mapping. The amino acid sequence of PKC-ε is shown in Figure 5.8, and an *in silico* tryptic digest is provided for reference (see Appendix A2.1). Tryptic digests, reverse phase HPLC, mass spectrometry and Edman analysis were performed by the Protein Analysis Laboratory (CR-UK).

5.2.1.1.2.1 Generation & Fractionation of Phosphorylated PKC-ε Tryptic Peptides

Purified recombinant human PKC-ε was incubated in an *in vitro* kinase reaction with $[\gamma^{32}P]$-ATP. ^{32}P-labelled, phosphorylated protein was resolved by SDS-PAGE, stained using Coomassie and subjected to in-gel tryptic digest. Tryptic peptides were fractionated by reverse phase HPLC and each fraction was counted. As shown in Figure 5.4, there were four major peaks in ^{32}P detection, corresponding to four or more phosphopeptides of differing hydrophobicity: Fractions 6/7, Fractions 18/19, Fractions 27/28 and Fractions 35/36.

Fractions 6/7 correspond to peptides which elute from the HPLC column in the breakthrough volume. These peptides are likely to fall below the minimum mass routinely scanned by mass spectrometry in the Protein Analysis Laboratory (<800Da), and to be contaminated with any non-volatile species carried over from peptide processing (eg. SDS-PAGE gel components, salts); as such, these fractions were not analysed further. However, fractions 18/19, 27/28 and 35/36 were all investigated by both mass spectrometry and Edman degradation as described below.
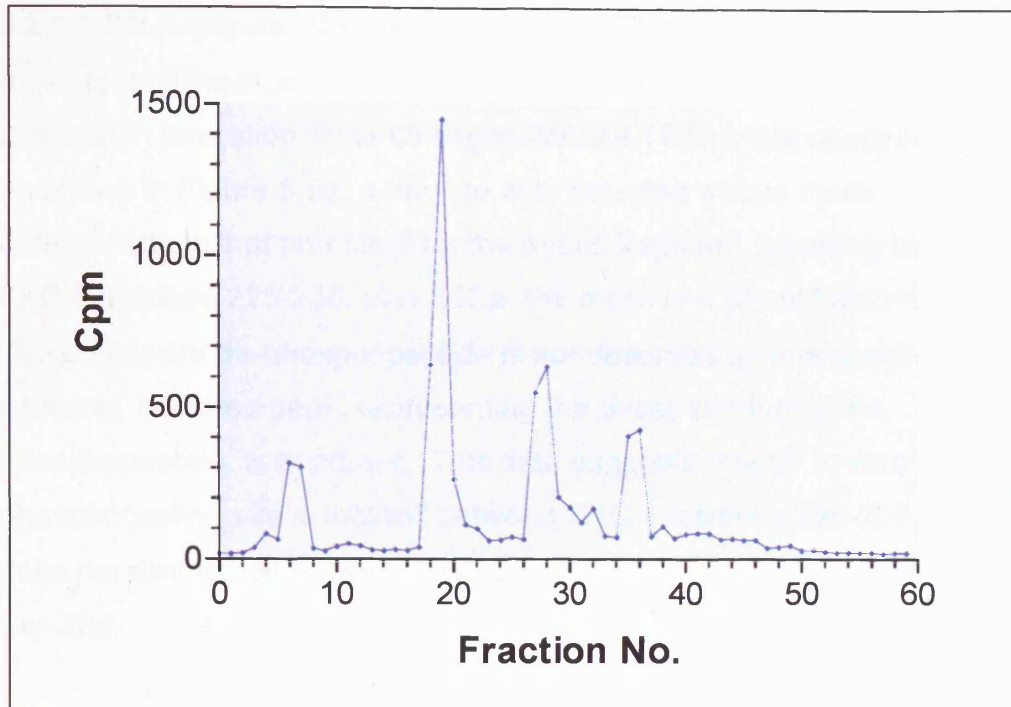
Figure 5.4 Phosphorylated PKC-ε Tryptic Peptide Fractionation.
An *in vitro* kinase assay was performed using 1μg of purified recombinant
human PKC-ε. The reaction was started with [γ^{32}P]-ATP (50μM ATP,
5μCi; 40Ci/mmol), incubated for 2hrs at 30°C with shaking, and stopped
with the addition of sample buffer. Following resolution by SDS-PAGE
and staining by Coomassie, PKC-εwas excised and subjected to in-gel
tryptic digestion at 37°C for 4hrs. Peptides were extracted and
fractionated by reverse phase high performance liquid chromatography,
using an ABI 130A Separation System, with a Vydac 1mm x 150mm C8
reverse phase column at 50μl/min. Fractions were counted and those
containing [γ^{32}P]-labelled phospho-peptides were retained for further
analysis.

5.2.1.1.2.2 Analysis of Phosphorylated PKC-ε Fraction 18

An aliquot of Fraction 18 was analysed by Matrix-Assisted Laser Desorption Ionization Time-Of-Flight (MALDI-TOF) mass spectrometry. As shown in Figure 5.5a, a peptide was detected whose mass corresponds to that predicted for the tryptic fragment occurring between PKC-ε residues 225-236, plus 80Da, the mass of a phosphate moiety. The equivalent de-phosphopeptide is not observed on this spectrum, however, a related peak, representing the decay product of the phosphopeptide, is apparent. This data suggests that an *in vitro* phosphorylation site is located between PKC-ε residues 225-236, but does not distinguish between the two candidate residues: Thr-228 and Ser-234.

The remainder of Fraction 18 was analysed by Edman degradation; N-terminal residues were derivatized, sequentially released and scintillation counted. As shown in Figure 5.5b, the major peak in ^{32}P detection occurs at residue 10, which corresponds to Ser-234 within the phosphopeptide identified by mass spectrometry. Counts are also somewhat elevated in the two fractions adjacent to residue 10. It is likely that the increased radioactivity detected at position 11 results from the inefficient removal of Pro-229 by Edman degradation, and the subsequent staggering of ^{32}P-Ser-234 detection. Ser 234 would occur at position 9 in the event that trypsin digests C-terminal to Lys-225 as indicated in grey. There are no counts above background at either residue 3 or 4, and there is thus no evidence for phosphate incorporation at Thr-228.

Mass spectrometric analysis and Edman degradation of Fraction 18 therefore provide complementary data sets which together unequivocally identify Ser-234 as an *in vitro* PKC-ε phosphorylation site.

a)

231
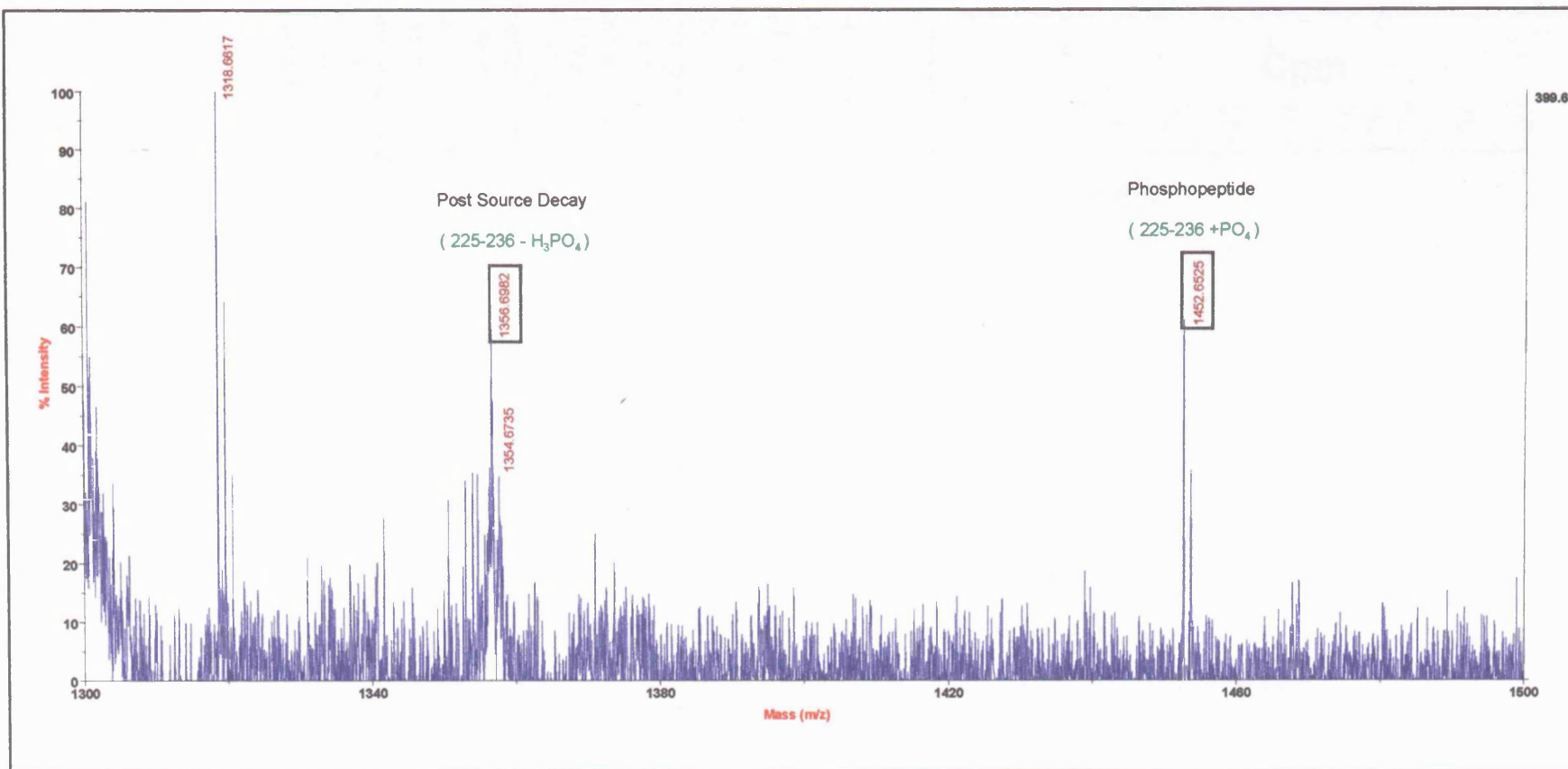
Figure 5.5 Analysis of Phosphorylated PKC-ε Fractions 18 by Mass Spectrometry and Edman Degradation. PKC-ε was *in vitro* phosphorylated in the presence of [γ^{32}P]-ATP (50μM ATP, 5μCi; 40Ci/mmol), isolated and digested with trypsin. Tryptic peptides were fractionated by reverse phase HPLC and counted. ^{32}P-labelled phosphopeptides were detected in Fraction 18 and analysed by mass spectrometry and Edman degradation. a) An aliquot (5%) of fraction 18 was analysed by Matrix-Assisted Laser Desorption Ionization Time-Of-Flight (MALDI-TOF) mass spectrometry using an Applied Biosystems 4700. Peptide masses were searched against an 'in silico' digest (Protein Prospector, UCSF) and assigned as indicated. Phosphorylation increases peptide mass by 80Da (+PO$_4$) and phosphopeptide post source decay decreases this mass by 98Da, detected as a broad peak (-H$_3$PO$_4$). b) The remainder of Fraction 18 (95%) was subjected to solid-phase Edman degradation using an ABI Procise Sequencer. Residue number is shown (in blue) and the sequence of the peptide identified by mass spectroscopy is indicated (an alternative digest is shown in grey). Fractions corresponding to individual residues were scintillation counted.

5.2.1.1.2.3 Analysis of Phosphorylated PKC-ε Fractions 27/28

Samples from Fractions 27 and 28 were analysed by MALDI-TOF mass spectrometry. A peptide corresponding in mass to PKC-ε residues 365-377 was identified in Fraction 27 (Figure 5.6a), and a peptide from 366-377 was detected in Fraction 28 (Figure 5.6b), reflecting an alternative digestion product; the additional lysine present in the former peptide must confer an effect on hydrophobicity which decreases retention time on the column. Both spectra reveal the characteristic peaks associated with the corresponding phosphopeptides: an 80Da increase in mass due to phosphorylation, and a related 98Da loss from this due to phosphopeptide post source decay.

This data indicates that an *in vitro* phosphorylation site is located between PKC-ε residues 365-377. There is only one Ser/Thr residue within this region: Ser-368. Edman degradation is consistent with this observation (Figure 5.6c), with ^{32}P-labelled residues detected at positions 3 and 4; these would correspond to phospho-Ser-368 when trypsin digests either C-terminal to Lys-365 or Arg-364 respectively.

Mass spectrometric analysis and Edman degradation of Fractions 27/28 thereby identify Ser-368 as an *in vitro* PKC-ε phosphorylation site.
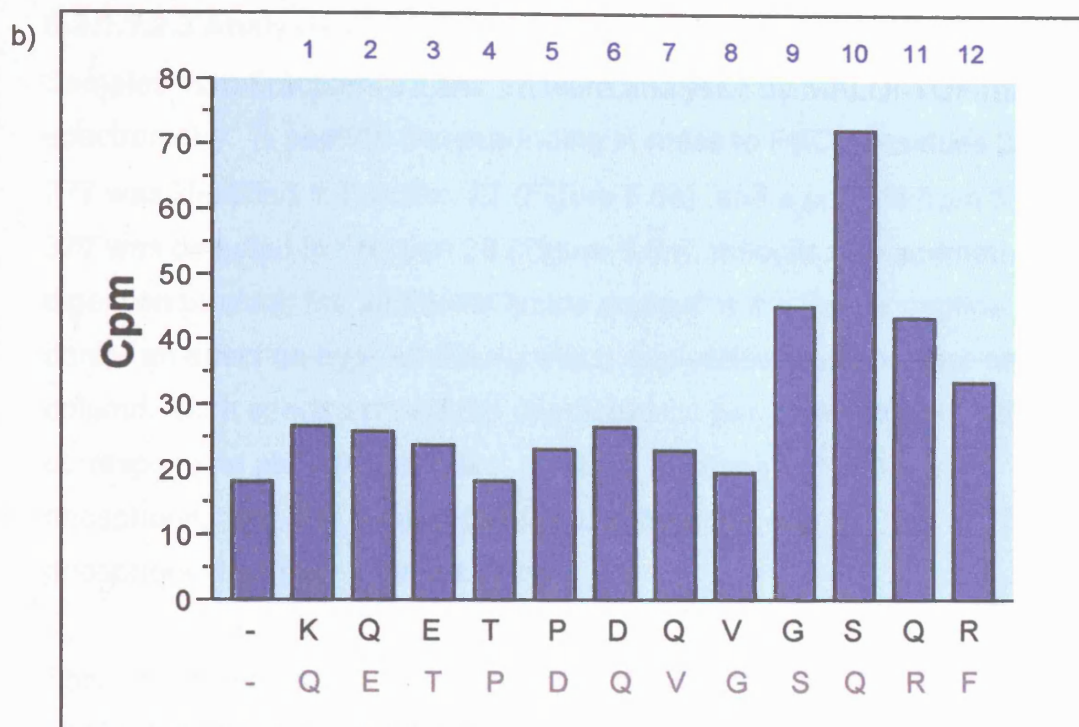
a)

b)

235
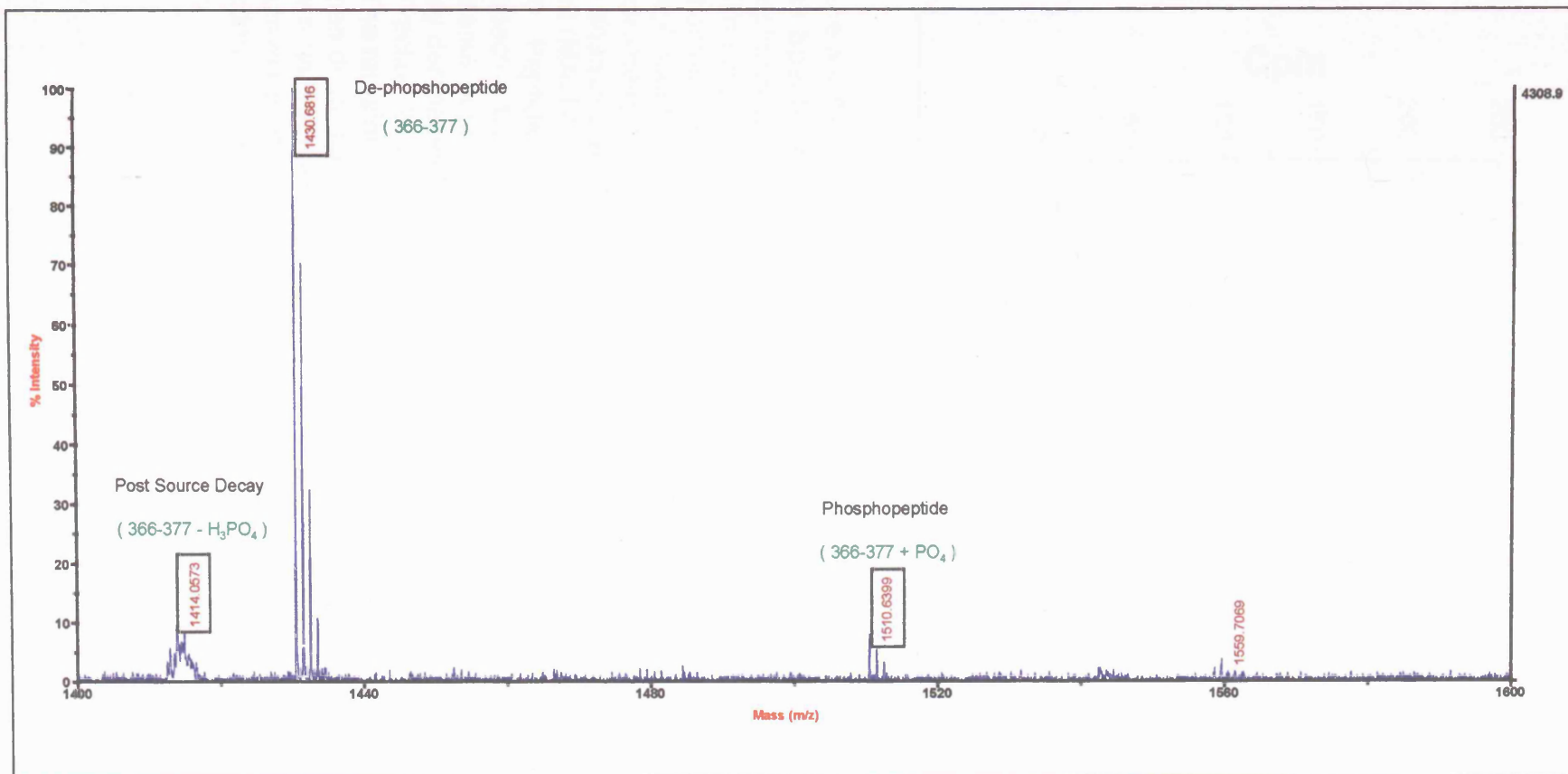
Figure 5.6 Analysis of Phosphorylated PKC-ε Fractions 27/28 by Mass Spectrometry and Edman Degradation. PKC-ε was *in vitro* phosphorylated in the presence of $[\gamma^{32}P]$-ATP (50μM ATP, 5μCi; 40Ci/mmol), isolated and digested with trypsin. Tryptic peptides were fractionated by reverse phase HPLC and counted. ^{32}P-labelled phosphopeptides were detected in Fractions 27/28 and analysed by mass spectrometry and Edman degradation. a) An aliquot (5%) of fraction 27 was analysed by Matrix-Assisted Laser Desorption Ionization Time-Of-Flight (MALDI-TOF) mass spectrometry using an Applied Biosystems 4700. Peptide masses were searched against an *'in silico'* digest (Protein Prospector, UCSF) and assigned as indicated. Phosphorylation increases peptide mass by 80Da (+PO_4) and phosphopeptide post source decay decreases this mass by 98Da, detected as a broad peak (-H_3PO_4). b) Fraction 28 was analysed by mass spectrometry as described in a). c) The remainder (95%) of fraction 28 was subjected to solid-phase Edman degradation using an ABI Procise Sequencer. Residue number is shown (in blue) and the sequence of the peptide identified by mass spectroscopy is indicated (an alternative digest is shown in grey). Fractions corresponding to individual residues were scintillation counted.
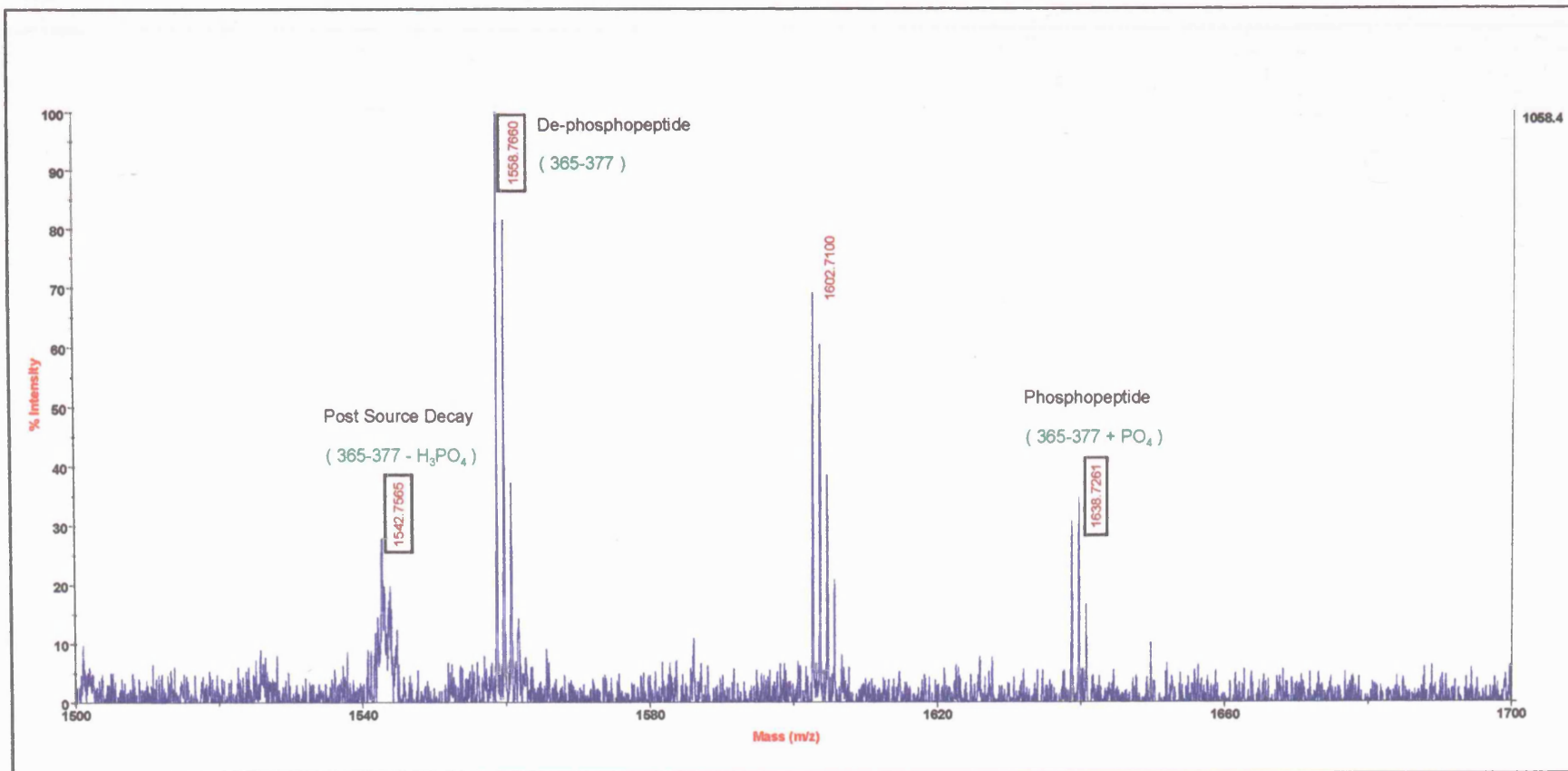
5.2.1.1.2.4 Analysis of Phosphorylated PKC-ε Fraction 36

An aliquot of fraction 36 was analysed by MALDI-TOF mass spectrometry. As shown in Figure 5.7a, a peptide of the same mass as PKC-ε residues 302-319 was detected. There was direct evidence for phosphorylation of this peptide, since one peak was apparent at a mass 80Da greater, corresponding to the addition of PO_4, and another peak was observed at a mass 98Da less than this, representing post source decay of phosphoric acid from the phosphopeptide. This data suggests that an *in vitro* phosphorylation site is located between PKC-ε residues 302-319, which could correspond to either Thr-309, Thr-314 or Ser-316.

The remainder of Fraction 36 was analysed by Edman degradation. There is a single major peak in ^{32}P detection at residue 15, corresponding to Ser-316 within the phosphopeptide identified by mass spectrometry. Together, the data identify Ser-316 as an *in vitro* PKC-ε phosphorylation site.
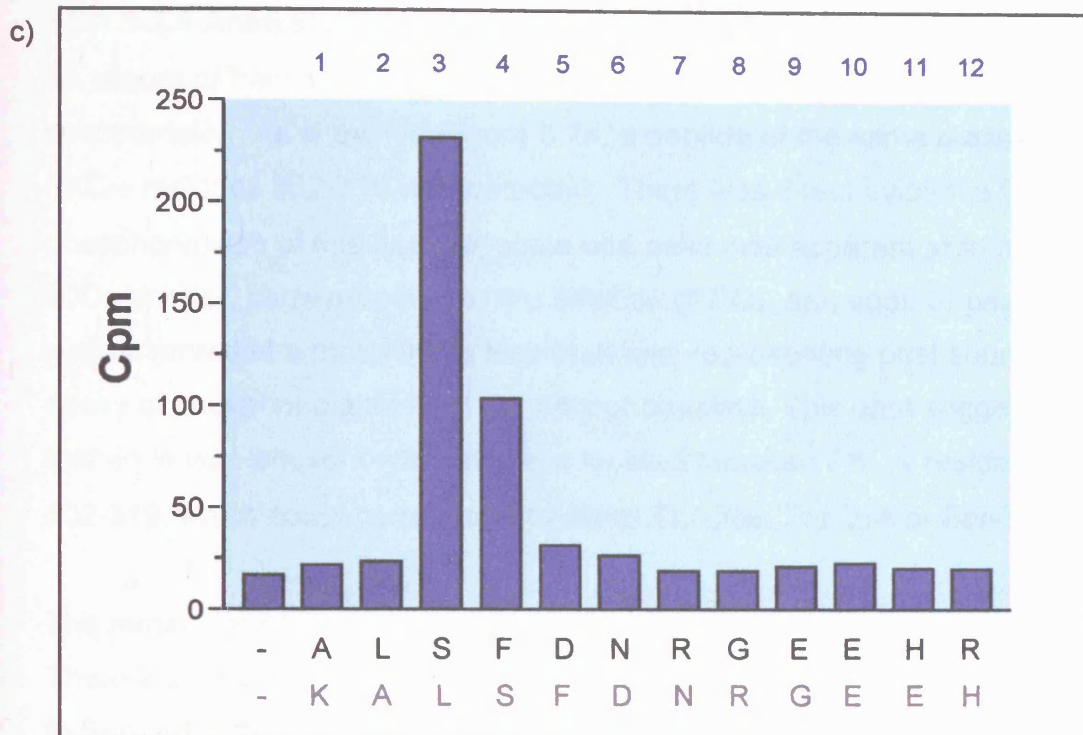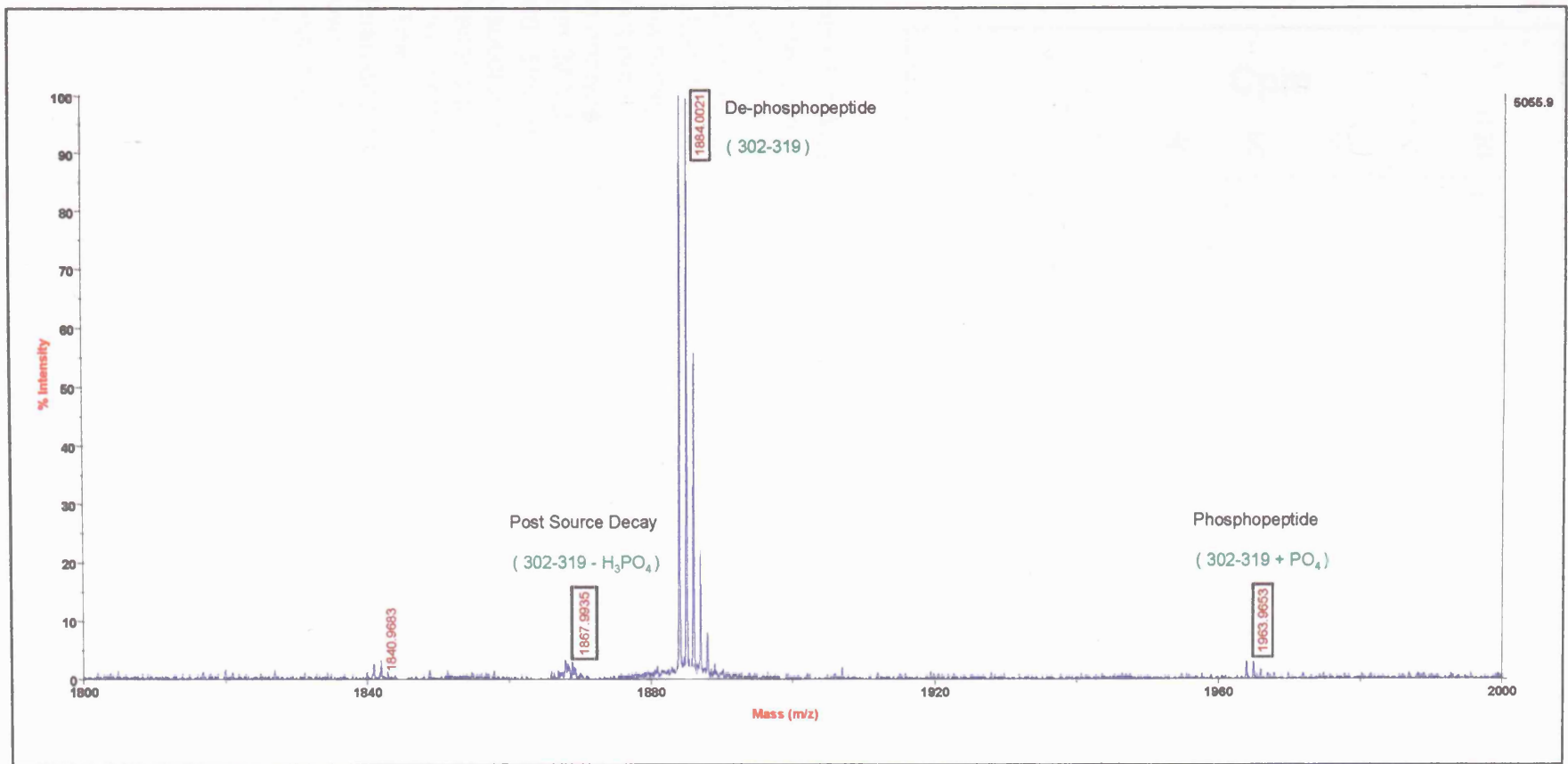
a)

238

b)
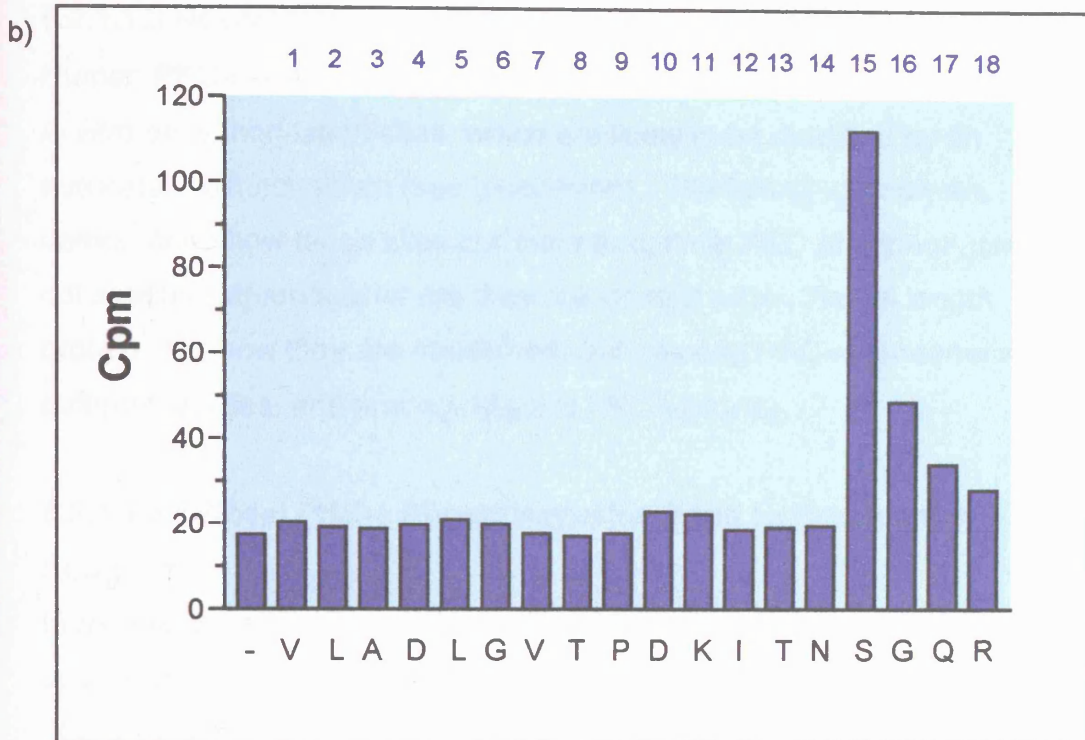
Figure 5.7 Analysis of Phosphorylated PKC-ε Fraction 36 by Mass Spectrometry and Edman Degradation. PKC-ε was *in vitro* phosphorylated in the presence of [γ^{32}P]-ATP (50μM ATP, 5μCi; 40Ci/mmol), isolated and digested with trypsin. Tryptic peptides were fractionated by reverse phase HPLC and counted. ^{32}P-labelled phosphopeptides were detected in Fraction 36 and analysed by mass spectrometry and Edman degradation. a) An aliquot (5%) of fraction 36 was analysed by Matrix-Assisted Laser Desorption Ionization Time-Of-Flight (MALDI-TOF) mass spectrometry using an Applied Biosystems 4700. Peptide masses were searched against an *'in silico'* digest (Protein Prospector, UCSF) and assigned as indicated. Phosphorylation increases peptide mass by 80Da (+PO$_4$) and phosphopeptide post source decay decreases this mass by 98Da, detected as a broad peak (-H$_3$PO$_4$). b) The remainder (95%) of fraction 36 was subjected to solid-phase Edman degradation using an ABI Procise Sequencer. Residue number is shown (in blue) and the sequence of the peptide identified by mass spectroscopy is indicated. Fractions corresponding to individual residues were scintillation counted.

5.2.1.1.3 Novel PKC-ε *In Vitro* Phosphorylation Sites

Human PKC-ε residues Ser-234, Ser-316 and Ser-368 were identified as *in vitro* phosphorylation sites, which are likely to be modified by an autocatalytic mechanism (see discussion). The following analyses demonstrate how these sites compare to optimal PKC phosphorylation consensus sequences, where they are located within the full length protein, and how they are conserved, both among PKC-ε sequences from different species, and among different PKC isoforms.

5.2.1.1.3.1 Novel PKC-ε Phosphorylation Sites as Consensus Sequences

In the previous chapter, a database predictive for PKC consensus sequences was employed to screen for substrates *in silico* (Fujii et al., 2004). The newly identified, putative PKC-ε autophosphorylation sites were analysed retrospectively using this tool, to test their potential as phospho-acceptors in relation to established substrates (Table 5.1). With the exception of Ser-368, these sites score relatively poorly, however, this is also the case for the 'TP' autophosphorylation site T710. It should be noted however, that these scores are based upon PKC-δ preferences, and so are indicative, but not be wholly representative, of PKC-ε behaviour.

Phospho-Site	Protein Scan Score	Percentile
Ser-234	40	Bottom 95
Ser-316	20	Bottom 95
Ser-368	2	Top 5
Thr-710	76	Bottom 95

Table 5.1 Predicted PKC Phosphorylation Sites in PKC-ε. The amino acid sequence of human PKC-ε was searched against the Mammalian Phosphorylation Resource database for prediction of PKC phosphorylation sites. The scores obtained for selected phosphorylation sites (as PKC-δ phospho-acceptors) are shown, and the percentile in which this score falls is indicated. Residues scoring below the fifth percentile have been classed as unlikely to represent substrates (Fujii et al., 2004).

5.2.1.1.3.2 Positioning of Novel PKC-ε Phosphorylation Sites

Figures 5.8 and 5.9 illustrate the positioning of the PKC-ε *in vitro* phosphorylation sites within the full length protein. Ser-234 falls between the C1a and C1b diacylglycerol/phorbol ester binding domains, in close proximity to the PKC-ε actin binding site, while both Ser-316 and Ser-368 are located within the variable V3 region.

5.2.1.1.3.3 Conservation of Novel PKC-ε Phosphorylation Sites

Figure 5.10a reveals that PKC-ε Ser-234, Ser-316 and Ser-368 are all conserved among mammalian species, and are also found in the PKC-ε sequence from the pufferfish, although the residues N-terminal to 'S316' are variable in the latter. However, corresponding residues were not identified in the ε-type PKC isoforms from Drosophila (PKC98E), Caenorhabditis (pkc-1, TTX-4), Aplysia (Apl II), nor in the yeast PKCs.

An alignment was performed between human PKC-ε and human PKC-η, the most closely related member of the PKC superfamily. None of the three PKC-ε phosphorylation sites are conserved in PKC-η, and the surrounding sequences are relatively divergent. It is notable though, that within the loosely conserved region between the C1a and C1b domains, there is a glutamate residue in PKC-η equivalent to PKC-ε Ser-234 (Figure 5.10b); acidic glutamate/aspartate residues can behave as 'mimics' for phosphorylated residues in certain contexts.

MVVFNGLLKIKICEAVSLKPTAWSLRHAVGPRPQTFLLDPYIALNVDDSRIGQTATKQKT

NSPAWHDEFVTDVCNGRKIELAVFHDAPIGYDDFVANCTIQFEELLQNGSRHFEDWIDLE

PEGRVYVIIDLSGSSGEAPKDNEERVFRERMRPRKRQGAVRRRVHQVNGHKFMATYLRQP

TYCSHCRDFIWGVIGKQGYQCQVCTCVVHKRCHELIITKCAGLKKQETPDQVGSQRFSVN

MPHKFGIHNYKVPTFCDHCGSLLWGLLRQGLQCKVCKMNVHRRCETNVAPNCGVDARGIA

KVLADLGVTPDKITNSGQRRKKLIAGAESPQPASGSSPSEEDRSKSAPTSPCDQEIKELE

NNIRKALSFDNRGEEHRAASSPDGQLMSPGENGEVRQGQAKRLGLDEFNFIKVLGKGSFG

KVMLAELKGKDEVYAVKVLKKDVILQDDDVDCTMTEKRILALARKHPYLTQLYCCFQTKD

RLFFVMEYVNGGDLMFQIQRSRKFDEPRSRFYAAEVTSALMFLHQHGVIYRDLKLDNILL

DAEGHCKLADFGMCKEGILNGVTTTTFCGTPDYIAPEILQELEYGPSVDWWALGVLMYEM

MAGQPPFEADNEDDLFESILHDDVLYPVWLSKEAVSILKAFMTKNPHKRLGCVASQNGED

AIKQHPFFKEIDWVLLEQKKIKPPFKPRIKTKRDVNNFDQDFTREEPVLTLVDEAIVKQI

NQEEFKGFSYFGEDLMP

Figure 5.8 Annotated PKC-ε Amino Acid Sequence. The amino acid sequence of human PKC-ε (NP_005391) is presented with the following features highlighted: C2-like domain, pink; pseudosubstrate sequence, red; C1 domains, turquoise; actin binding motif, maroon; V3, underlined; ATP binding site, green; kinase domain, blue; priming phosphorylation sites, grey (T-loop, T566; 'TP',T710; 'FSY', S729); newly identified phosphorylation sites, yellow (S234, S316, S368).
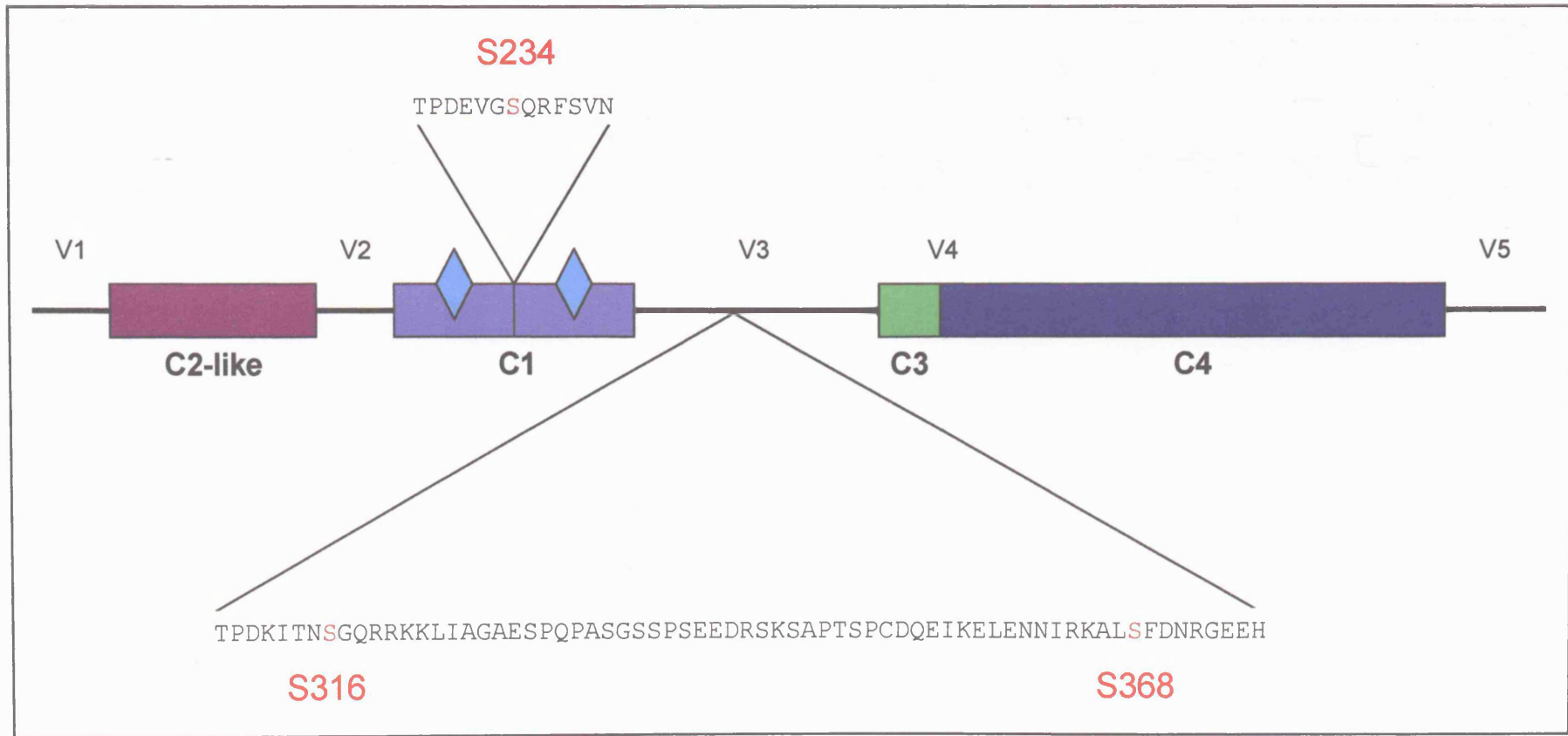
Figure 5.9 PKC-ε Domain Structure & Positioning of Phosphorylation Sites S234, S316 & S368. The domain structure of PKC-ε is represented diagrammatically, with the positioning of the newly identified phosphorylation sites highlighted (red text), and the surrounding sequences shown. Conserved (C1, C2-like, C3, C4) and variable regions (V1, V2, V3, V4,V5) are indicated.

Figure 5.10 PKC-ε S234, S316 & S368 Conservation. Alignments were performed using ClustalX software between a) PKC-ε amino acid sequences from different species, and b) human amino acids sequences for PKC-ε and the related nPKC-η, to investigate the conservation of human PKC-ε residues S234, S316 and S368, three newly identified phosphorylation sites. C1a/b domains are highlighted (green lines) and an actin binding motif {Prekeris, 1998 #674} is indicated (blue bracket).

5.2.1.2 PKC-δ *In Vitro* Phosphorylation & Phosphopeptide Mapping

PKC-δ phosphopeptide mapping was performed using the same approach that successfully identified novel PKC-ε phosphorylation sites. The full length PKC-δ sequence is shown in Figure 5.17, and an *in silico* tryptic digest is provided for reference (Appendix A2.2). Tryptic digests, reverse HPLC, mass spectrometry and Edman degradation were performed by the Protein Analysis Laboratory (CR-UK).

5.2.1.2.1 PKC-δ *In Vitro* Phosphorylation

In vitro kinase assays were performed using recombinant human PKC-δ purified from baculovirus. As was the case for PKC-ε, increased PKC-δ phosphorylation was detected over time (Figure 5.11). There was also a slight PKC-δ band shift apparent from the Coomassie stained gel following *in vitro* kinase assay incubation, consistent with a phosphorylation event. The stoichiometry of phosphorylation was calculated from 2 separate experiments at 0.74 ± 0.07pmol PO_4/pmol PKC-δ.
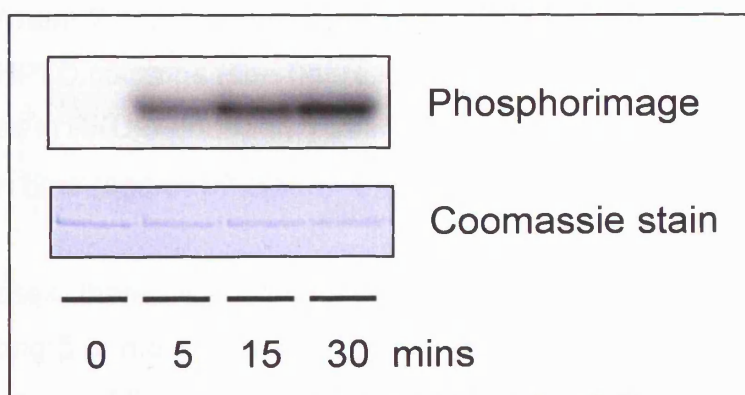
Figure 5.11 Phosphorylation of PKC-δ *In Vitro*. PKC-δ phosphorylation was assayed by *in vitro* kinase assay. 300ng of purified recombinant human PKC-δ was prepared in kinase assay buffer. Reactions were started with $[\gamma^{32}P]$-ATP (50μM ATP, 5μCi; 40Ci/mmol), incubated for 0-30mins at 30°C with shaking, and stopped with the addition of sample buffer. Samples were resolved by SDS-PAGE, stained with Coomassie and scanned; phoshorylation was visualised using the Storm 860 PhosphorImaging System. Data is representative of three separate experiments.

5.2.1.2.2 PKC-δ Phosphopeptide mapping

In vitro phosphorylated PKC-δ was analysed by phosphopeptide mapping as described above (section 5.2.1). Two separate experiments were performed (1 and 2), generating different but overlapping data sets.

5.2.1.2.2.1 Generation and Fractionation of Phosphorylated PKC-δ Tryptic Peptides

Purified recombinant human PKC-δ was incubated in an *in vitro* kinase reaction with $[\gamma^{32}P]$-ATP, either for 30mins (1), or 2hrs (2). Phosphorylated PKC-δ was subjected to in-gel tryptic digestion, generating a set of peptides which were then fractionated by reverse phase HPLC; parallel digestion with an alternative protease, AspN, was also performed, but this provided no interpretable information on phosphorylation sites (data not shown). Each tryptic fraction was counted in order to locate ^{32}P-labelled phosphopeptides. As shown in Figure 5.12, experiments 1 and 2 yielded products with the same patterns of fractionation, but with slightly different profiles; the most striking differences being the relative depletion of peak e and enrichment of peak f in experiment 2. This variation is in part explained by the use of different HPLC columns (see figure legend). It may also reflect differences in PKC-δ phosphorylation status due to altered kinase assay incubation time, and/or efficiency of tryptic digestion.

In both cases, there were 5 major peaks in ^{32}P detection (a-e), representing 5 or more different phosphopeptide populations. Mass spectrometry and Edman degradation were performed on the fractions corresponding to each peak, from each experiment. The data obtained is summarised in Tables 5.2 and 5.3. In the following sections, mass spectra and Edman degradation results are shown for those sites that could be positively identified; data regarding additional candidate sites is also described.
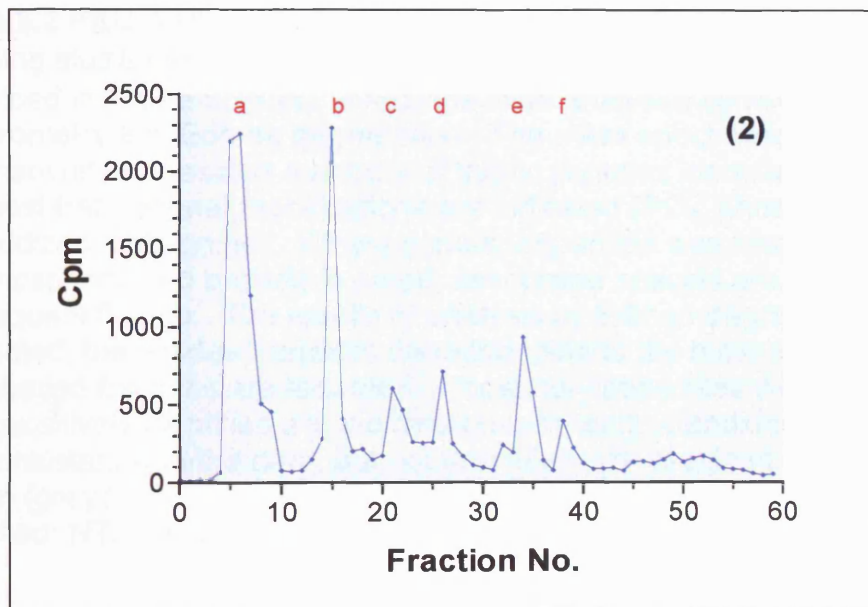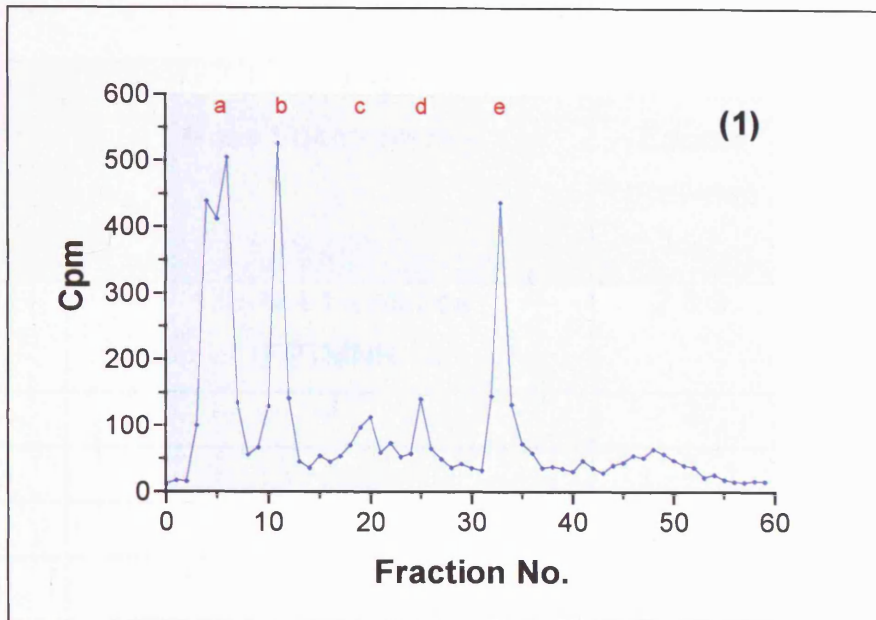
Figure 5.12 Phosphorylated PKC-δ Tryptic Peptide Fractionations.
In vitro kinase assays were performed using 500ng of purified
recombinant human PKC-δ. The reaction was started with $[\gamma^{32}P]$-ATP
(50μM ATP, 5μCi; 40Ci/mmol), incubated for 30mins (1) or 2hrs (2) at
30°C with shaking, and stopped with sample buffer. Following resolution
by SDS-PAGE and staining by Coomassie, PKC-δwas excised and
subjected to in-gel tryptic digestion at 37°C for 4hrs. Peptides were
extracted and fractionated by reverse phase HPLC, using an ABI 130A
Separation System, with a Vydac 1mm x 150mm C8 reverse phase
column at 50μl/min. Fractions were counted and those containing $[\gamma^{32}P]$-
labelled phosphopeptides were retained for further analysis.

Experiment 1			
Fraction	Mass Spectrometry	Edman (Residue No)	Site(s) Identified
a	139-144 1 x Met-ox FPTMNR	2 & 3	T-141?
b	-	2	x
c	-	3	x
d	NT	NT	x
e	298-318 + 2 x PO$_4$ ASRRSDSASSEPVGIYQGFEK	2 & 5	S-299 S-302

Table 5.2 PKC-δ Phosphopeptide Mapping (1). Phosphopeptide mapping studies were performed on *in vitro* phosphorylated PKC-δ as described in Figure 5.11 (1). Fractions were analysed by MALDI mass spectrometry and Edman degradation. The mass spectrometric data is summarised; the residue numbers of tryptic peptides identified are given, and post-translational modifications are indicated (PO$_4$, phosphate; Met-ox, oxidized methionine). Where a phosphopeptide was identified, only the phosphorylated peptide is noted; associated species are shown in subsequent figures. The results of analysis by Edman degradation are presented; the residue numbers corresponding to the most significantly ^{32}P-labelled fractions are recorded. Phosphorylation sites which have been positively identified are indicated (black text). Candidate sites which are consistent with the data, but not unequivocally assigned, are also shown (grey text). -, no phosphopeptide/candidate phosphopeptide identified; NT, not tested; x no site assigned.

Experiment 2			
Fraction	Mass Spectrometry	Edman (Residue No)	Site(s) Identified
a	-	1 & 2	x
b	-	2	x
c	-	NT	x
d	133-144 1 x Met-ox SEDEAKFPTMNR 133-145 1 x Met-ox SEDEAKFPTMNRR	9,10 & 11	T-141?
e	301-318 + 1 x PO₄ RSDSASSEPVGIYQGFEK 302-318 + 1 x PO₄ SDSASSEPVGIYQGFEK 298-318 + 2 x PO₄ ASRRSDSASSEPVGIYQGFEK	1-5, 10 & 11	S-304

Table 5.3 PKC-δ Phosphopeptide Mapping (2). Phosphopeptide mapping studies were performed on *in vitro* phosphorylated PKC-δ as described in Figure 5.11 (2). Fractions were analysed by MALDI mass spectrometry and Edman degradation. The mass spectrometric data is summarised; the residue numbers of tryptic peptides identified are given, and post-translational modifications indicated (PO₄, phosphate; Met-ox, oxidized methionine). Where a phosphopeptide was identified, only the phosphorylated peptide is noted; associated species are shown in subsequent figures. The results of analysis by Edman degradation are presented; the residue numbers corresponding to the most significantly ^{32}P-labelled fractions are recorded. Phosphorylation sites which have been positively identified are indicated (black text). Candidate sites which are consistent with the data, but not unequivocally assigned, are also shown (grey text). -, no phosphopeptide/candidate phosphopeptide identified; NT, not tested; x no site assigned.

5.2.1.2.2.2 Analysis of Phosphorylated PKC-δ Fraction 1e

An aliquot of fraction 34, representing peak 1e, was analysed by MALDI-TOF mass spectrometry. As shown in Figure 5.13a, a peptide corresponding in mass to PKC-δ residues 298-318, plus two phosphate moieties, was detected. An additional peak was observed at a mass 98Da less than this, representing post source decay of one phosphoric acid molecule from the doubly phosphorylated peptide.

Selected peptide ions from this first analysis were then subjected to high-energy collision to obtain fragment ions. The MALDI-TOF/TOF data recovered is shown in Figure 5.13b. Again, the doubly phosphorylated peptide, and its single site post source decay product, are evident from the spectrum. However, in this case, the product of double phospho-site decay is observed, as well as a singly phosphorylated peptide which has decayed in flight. Together, this data clearly demonstrates that two PKC-δ sites can be *in vitro* phosphorylated simultaneously, between residues 298-318; these could correspond to Ser-299, Ser-302, Ser-304, Ser-306 or Ser-307.

Fraction 33 from peak 1e was analysed by Edman degradation (Figure 5.13c). Two major increases in ^{32}P incorporation were detected at residues 2 and 5; these corresponding to Ser-299 and Ser-302 within the doubly phosphorylated peptide identified by mass spectrometry. Although the increase in counts above background is relatively small, the scintillation counting procedure was optimised to reduce standard error, such that this difference is meaningful; fractions were stored in the dark overnight and then subjected to a relatively long count, of 10mins.

Together, the data identify Ser-299 and Ser-302 as *in vitro* PKC-δ phosphorylation sites, which can be occupied simultaneously.

a)

Double Phosphopeptide,
one post source decay event
(298-318 + PO_4 - H_3PO_4)

Double Phosphopeptide
298-318 + $2PO_4$)

2335.4424

2430.6565

201.4

251

b)

Double Phosphopeptide,
two post source decay events
(298-318 - 2HPO$_3$)

Phosphopeptide,
post source decay
(298-318 - HPO$_3$)

Double Phosphopeptide,
one post source decay event
(298-318 + 1PO$_4$ - HPO$_3$)

Double Phosphopeptide
(298-318 + 2PO$_4$)

2234.8484
2252.7986
2335.3848
2431.7622
2334.9541
2238.6011
2240.87
2239.886
2333.2212
2221.562
2224.06
2258.0864
2339.6140
2318.3398
2307.5
2193.7900

167.4

Figure 5.13 Analysis of Phosphorylated PKC-δ Fraction 1e by Mass Spectrometry and Edman Degradation. PKC-δ was *in vitro* phosphorylated in the presence of [γ^{32}P]-ATP (50μM ATP, 5μCi; 40Ci/mmol) for 30mins, isolated and digested with trypsin. Tryptic peptides were fractionated by reverse phase HPLC and counted. ^{32}P-labelled phosphopeptides were detected in Fractions 33/34 and analysed by mass spectrometry and Edman degradation. a) An aliquot of fraction 34 was analysed by Matrix-Assisted Laser Desorption Ionization Time-Of-Flight (MALDI-TOF) mass spectrometry using an Applied Biosystems 4700. Peptide masses were searched ag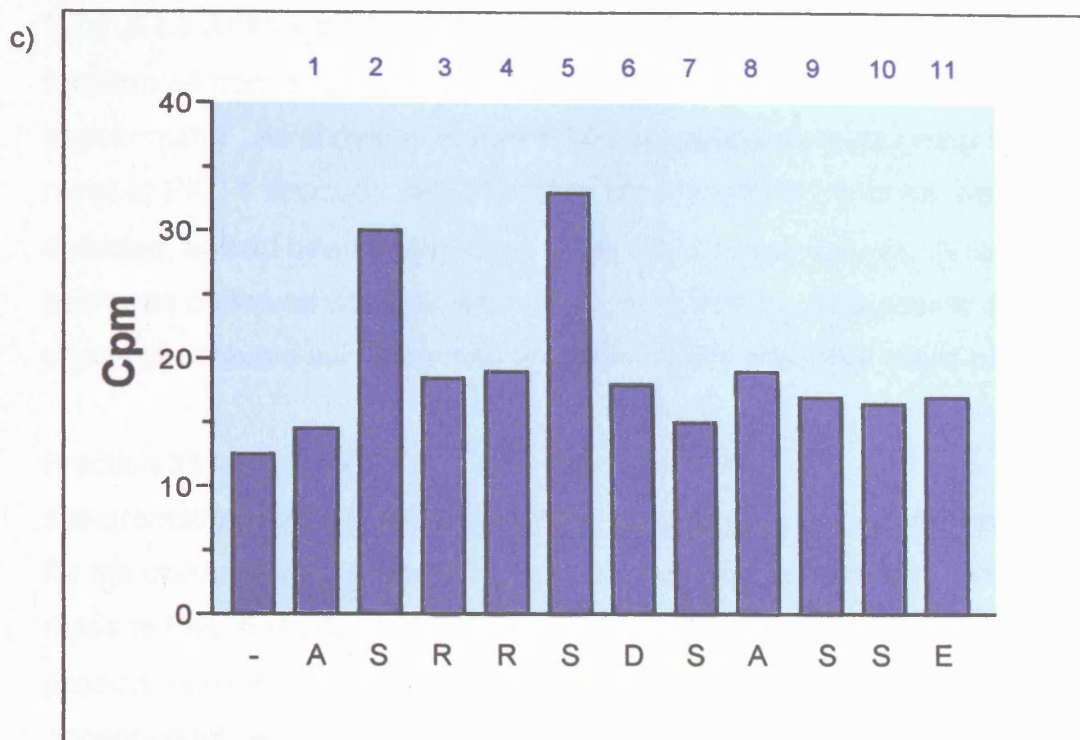ainst an 'in silico' digest (Protein Prospector, UCSF) and assigned as indicated. Phosphorylation increases peptide mass by 80Da (+PO$_4$) for each phosphorylated residue and phosphopeptide post source decay decreases this mass by 98Da, detected as a broad peak (-H$_3$PO$_4$). b) Phosphopeptide ions selected from analysis (a) were subjected to high energy collision to obtain fragment ions. MALDI-TOF/TOF data is presented with the phosphopeptide species indicated. c) Fraction 33 was subjected to solid-phase Edman degradation using an ABI Procise Sequencer. Residue number is shown (in blue) and the sequence of the peptide identified by mass spectroscopy is indicated. Fractions corresponding to individual residues were scintillation counted.

5.2.1.2.2.3 Analysis of Phosphorylated PKC-δ Fraction 2e

Fraction 34 from peak 2e was analysed by MALDI-TOF mass spectrometry. As shown in Figure 5.14a, a peptide corresponding in mass to PKC-δ residues 298-318, plus two phosphate moieties, was detected, as had been observed in experiment 1 (see above). A related peak was observed 98Da less than this, representing post source decay of one phosphoric acid molecule from the doubly phosphorylated peptide.

Fraction 35 from peak 2e was also analysed by MALDI-TOF mass spectrometry (Figure 5.14b). From this spectrum, evidence was obtained for the occurrence of a singly phosphorylated peptide corresponding in mass to PKC-δ residues 301-318, and for an alternative digestion product, from residues 302-318. In each case, the corresponding de-phosphopeptide, phosphopeptide and phosphopeptide decay product were all apparent.

Together, these data suggested that at least two PKC-δ sites could be *in vitro* phosphorylated, either independently, or simultaneously, between residues 298-318; these could correspond to Ser-299 and Ser-302, as identified in the previous section, and/or Ser-304, Ser-306 or Ser-307.

Fractions corresponding to peak 2e were further investigated by Edman degradation (Figure 5.14c). ^{32}P incorporation above background was evident in multiple fractions, namely 1-5 and 10/11. This is consistent with the identification of multiple phosphopeptide species by mass spectrometry, and with the presence of multiple candidate phospho-acceptor residues within them. Ser-299, already identified as an *in vitro* PKC-δ phosphorylation site, could contribute to the elevated radioactivity detected at residue 2, where the peptide represents 298-318. Phosphorylation of Ser-302, which has also been shown to be occupied *in vitro*, could account for ^{32}P incorporation at residue 1 where the peptide is 302-318 (although tryptic cleavage adjacent to a phosphorylated amino acid is unusual), position 2 in peptide 301-318, and position 5 in peptide

298-318. However, the most significant level of phosphorylation detected here is at residues 3 and 4, and these can only correspond to S304, in peptides 302-318 and 301-318 respectively. It is not clear whether the elevated counts at positions 10/11 derive from phosphorylation of peptide 298-318 at an additional serine, or from a separate phospho-peptide, not identified by mass spectrometric analysis of these fractions.

Together, these data reinforce the finding that Ser-299 and Ser-302 represent *in vitro* PKC-δ phosphorylation sites, and identify an additional site within the same region, Ser-304.

a)

Double Phosphopeptide,
one post source decay event
(298-318 + 1PO$_4$ - HPO$_3$)

Double
Phosphopeptide
(298-318 + 2PO4)

b)

De-phosphopeptide
(302-318)
1800.8416

Phosphopeptide
(302-318)
1880.8322

Post Source Decay
(301-318 - H_3PO_4)
1928.9347
1942.8224

De-phosphopeptide
(301-318)
1956.9514

1998.9355

Phosphopeptide
(301-318 + PO_4)
2036.9524

3.7E+4

% Intensity

Mass (m/z)

257

c)
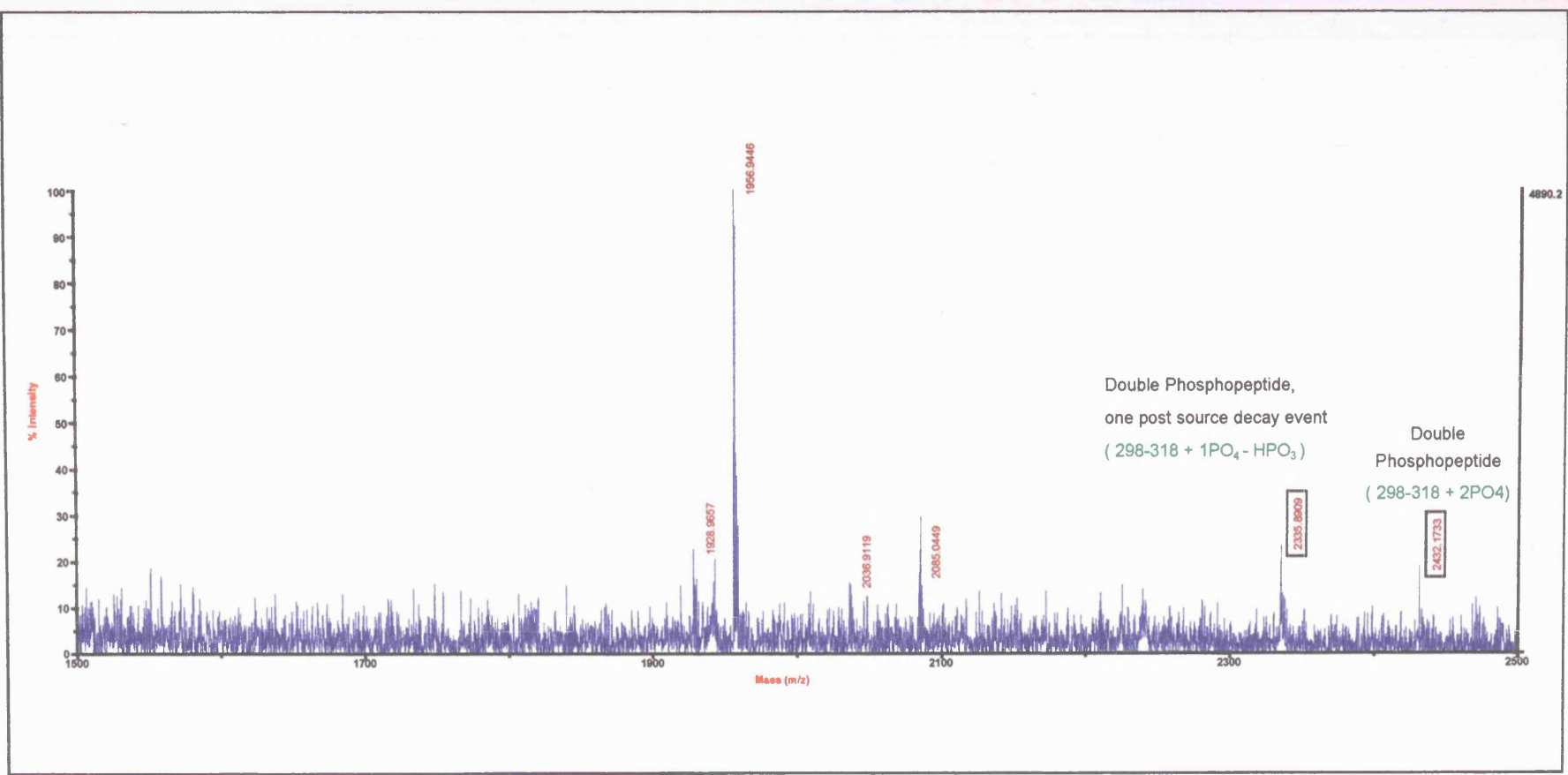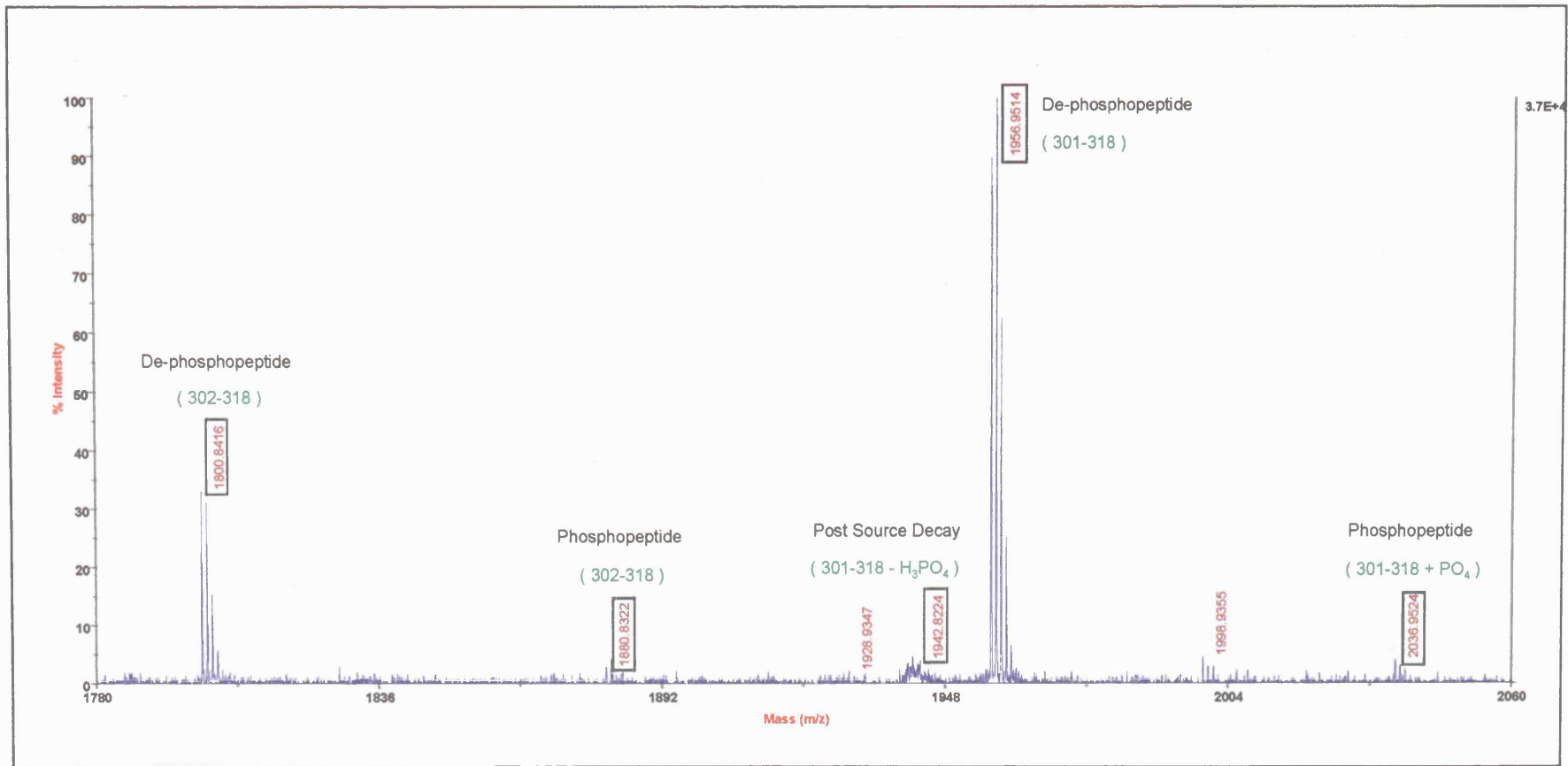
Figure 5.14 Analysis of Phosphorylated PKC-δ Fraction 2e by Mass Spectrometry and Edman Degradation. PKC-δ was *in vitro* phosphorylated in the presence of $[\gamma^{32}P]$-ATP (50µM ATP, 5µCi; 40Ci/mmol) for 2hrs, isolated and digested with trypsin. Tryptic peptides were fractionated by reverse phase HPLC and counted. ^{32}P-labelled phosphopeptides were detected in Fraction 34/35 and a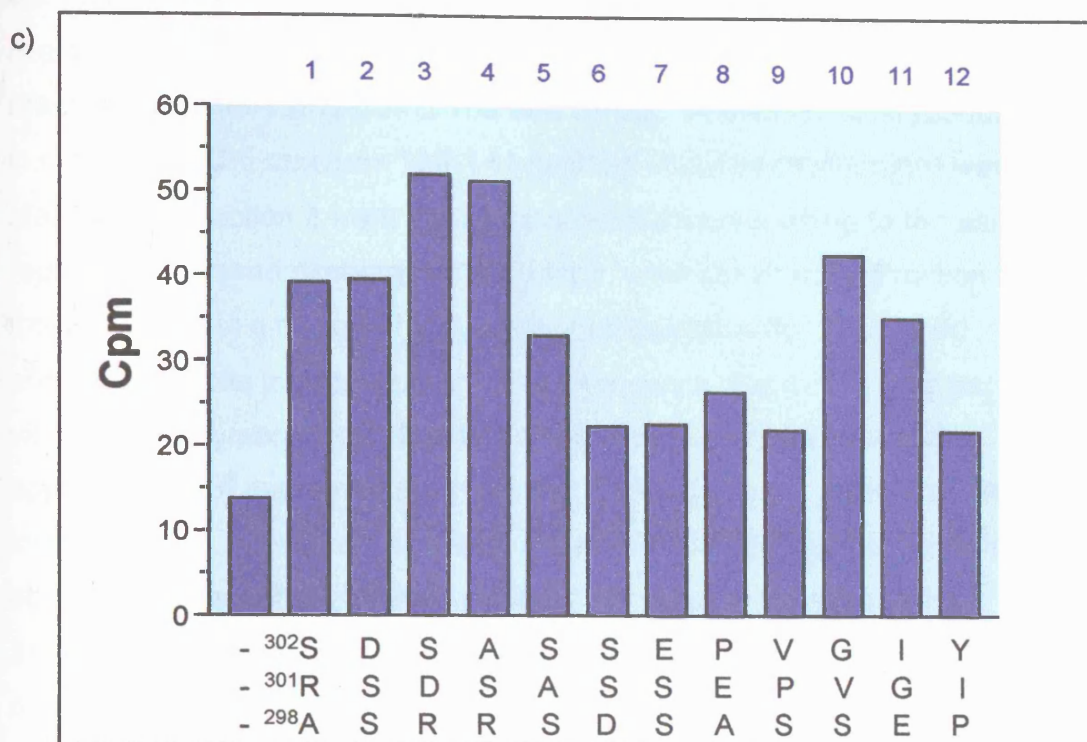nalysed by mass spectrometry and Edman degradation. Aliquots of a) Fraction 34 and b) Fraction 35 were analysed by Matrix-Assisted Laser Desorption Ionization Time-Of-Flight (MALDI-TOF) mass spectrometry using an Applied Biosystems 4700. Peptide masses were searched against an *'in silico'* digest (Protein Prospector, UCSF) and assigned as indicated. Phosphorylation increases peptide mass by 80Da (+PO$_4$) and phosphopeptide post source decay decreases this mass by 98Da, detected as a broad peak (-H$_3$PO$_4$). c) Fraction 35 was subjected to solid-phase Edman degradation using an ABI Procise Sequencer. Residue number is shown (in blue) and the sequences of the peptides identified by mass spectroscopy are indicated. Fractions corresponding to individual residues were scintillation counted.
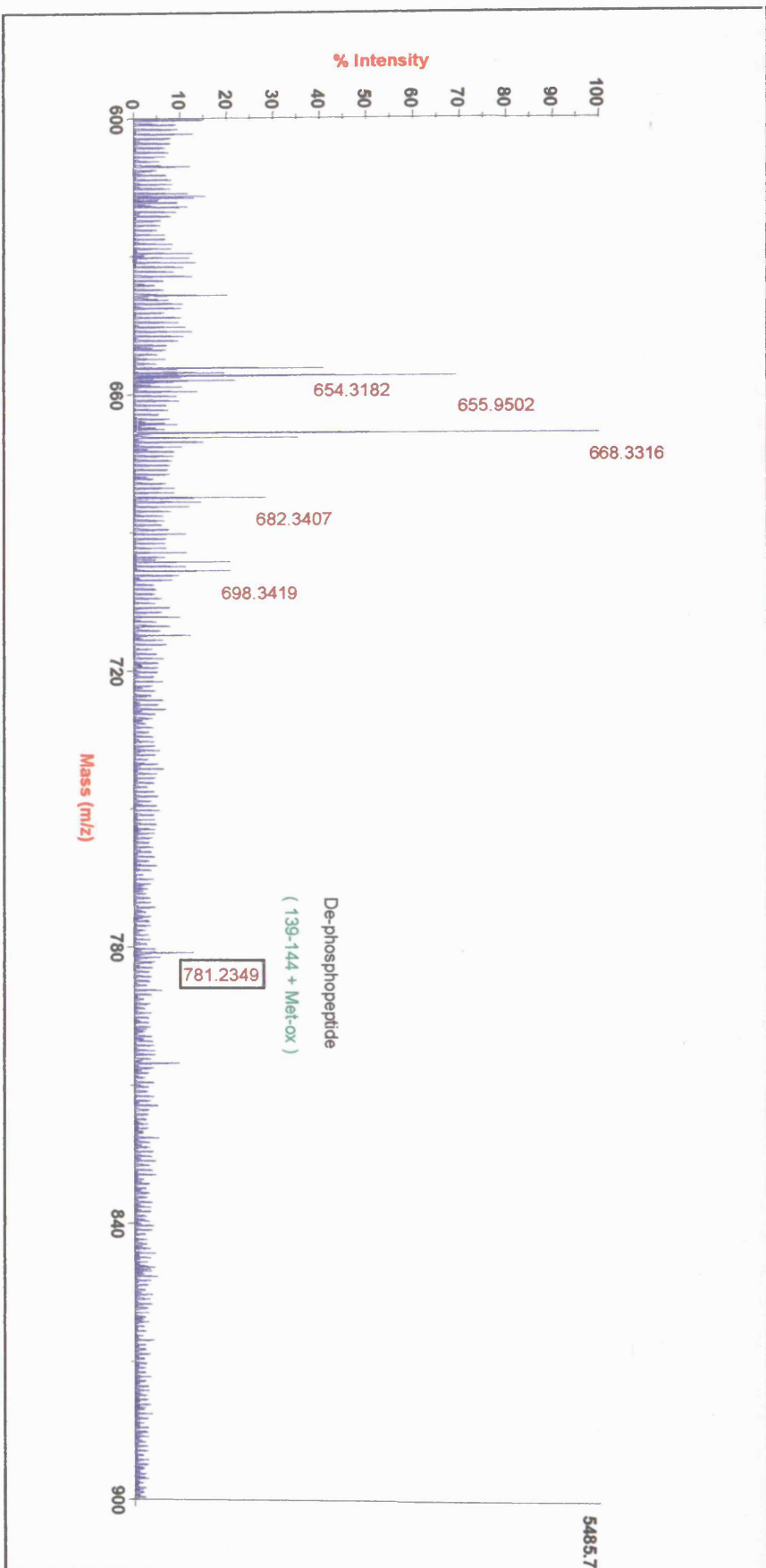
5.2.1.2.2.4 Analysis of Phosphorylated PKC-δ Fractions 1a & 2d

Fractions representing peaks 1a and 2d were analysed by MALDI-TOF mass spectrometry (Figures 5.15a and 5.16a). A peptide corresponding in mass to PKC-δ residues 139-144 (with an oxidized methionine) was identified in Fraction 8 from 1a, and peptides corresponding to the same region, with missed cleavages, 133-144/5, were identified in Fraction 27 from 2d. That this region of PKC-δ co-fractionates with ^{32}P-labelled phosphopeptides in two separate forms suggests that it may bear an *in vitro* phosphorylation site. Thr-141 is the only Ser/Thr residue which appears in all of the candidate peptides; Ser-133 is also present in the longer peptide. However, no direct mass spectrometric evidence was obtained for phosphorylation of either site, neither a phosphopeptide, nor an associated decay product, were observed related to any of the de-phosphopeptides detected. The data is thus consistent with, but not proof for, phosphorylation at Thr-141.

These fractions were also investigated by Edman degradation (Figures 5.15b and 5.16b). The major peaks in ^{32}P detection from peak 1a occur at residue 2 (Fractions 4/5) and residue 3 (Fractions 7/8); the latter would correspond to Thr-141 in the peptide 139-144, the former cannot relate to this peptide. The most significant elevation in counts detected following Edman degradation of Fractions 26/7 from 2d was found between residues 9-11. Thr-141 would be positioned at residue 9 in the peptides 133-144/5; the increased radioactivity detected at positions 10-11 could result from the inefficient removal of Pro-138 by Edman degradation, which would cause staggering of ^{32}P-Thr-141 detection. However, an analysis of the PKC-δ sequence reveals an alternative scenario which could theoretically account for this result: if Ser-57 and Thr-58 were both phosphorylated (either independently or together), these could account for phosphate incorporation detected at residues 9 and 10 in the peptides 49-67, and residues 10-11 in the peptide 48-67.

These data cannot unambiguously identify the phosphorylation site(s) present within Fractions 1a and 2d. The data is most compelling for Thr-141 as a candidate, but the lack of direct mass spectrometric evidence for phosphorylation, and the fact that the Edman degradation data is also consistent with at least one alternative interpretation, prevent a definitive conclusion being drawn.

Figure 5.15 Analysis of Phosphorylated PKC-δ Fraction 1a by Mass Spectrometry and Edman Degradation. PKC-δ was *in vitro* phosphorylated in the presence of $[\gamma^{32}P]$-ATP (50μM ATP, 5μCi; 40Ci/mmol) for 30mins, isolated and digested with trypsin. Tryptic peptides were fractionated by HPLC and counted. ^{32}P-labelled phosphopeptides were detected in Fractions 5-8 and analysed by mass spectrometry and Edman degradation. a) An aliquot of Fraction 8 was analysed by MALDI-TOF mass spectrometry using an Applied Biosystems 4700. Peptide masses were searched against an 'in silico' digest (Protein Prospector, UCSF) and assigned as indicated. Met-ox, oxidised methionine. Fractions b) 4/5 and c) 7/8 were subjected to solid-phase Edman degradation using an ABI Procise Sequencer. Residue number is shown (in blue) and the sequence of a candidate peptide identified by mass spectroscopy is indicated. Fractions corresponding to individual residues were scintillation counted.

a)

De-phosphopeptide
(133-144 + Met-ox)

1296.6854

De-phosphopeptide
(133-145 + Met-ox)

1596.7559

% Intensity

Mass (m/z)

2.6E+4

1217.6552
1233.6201
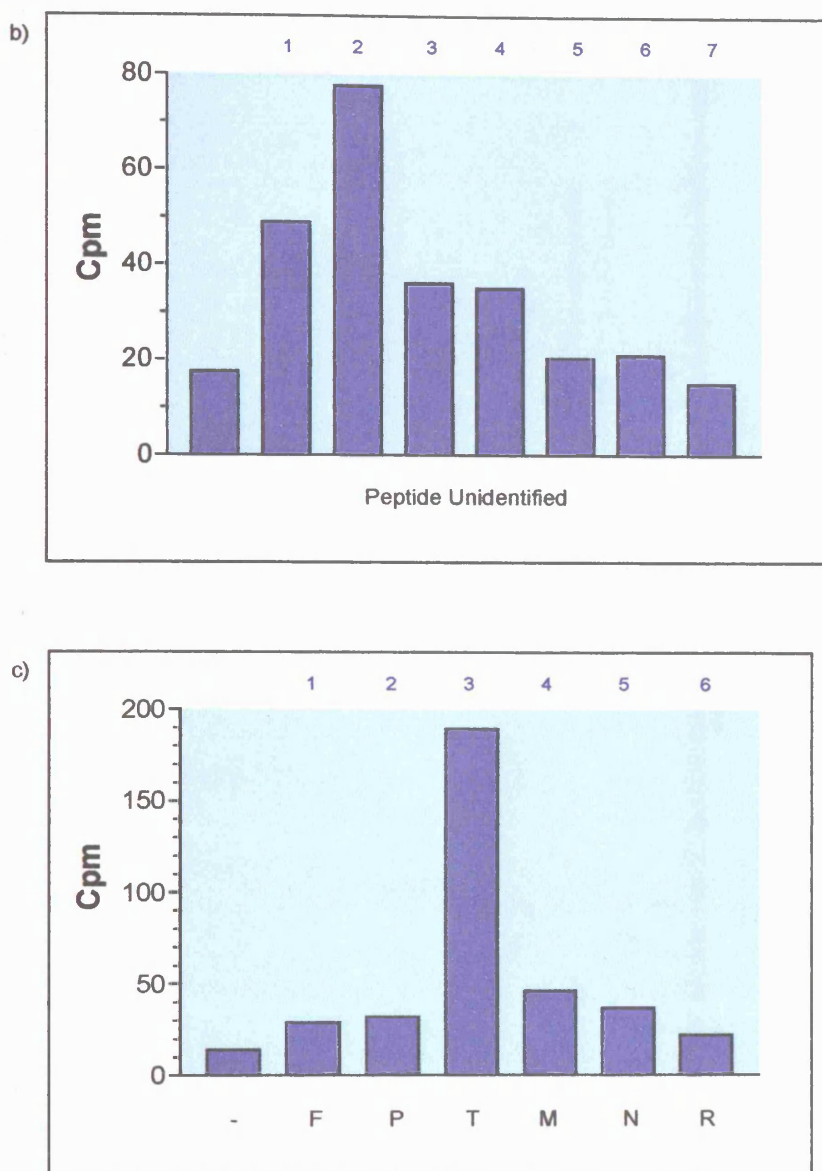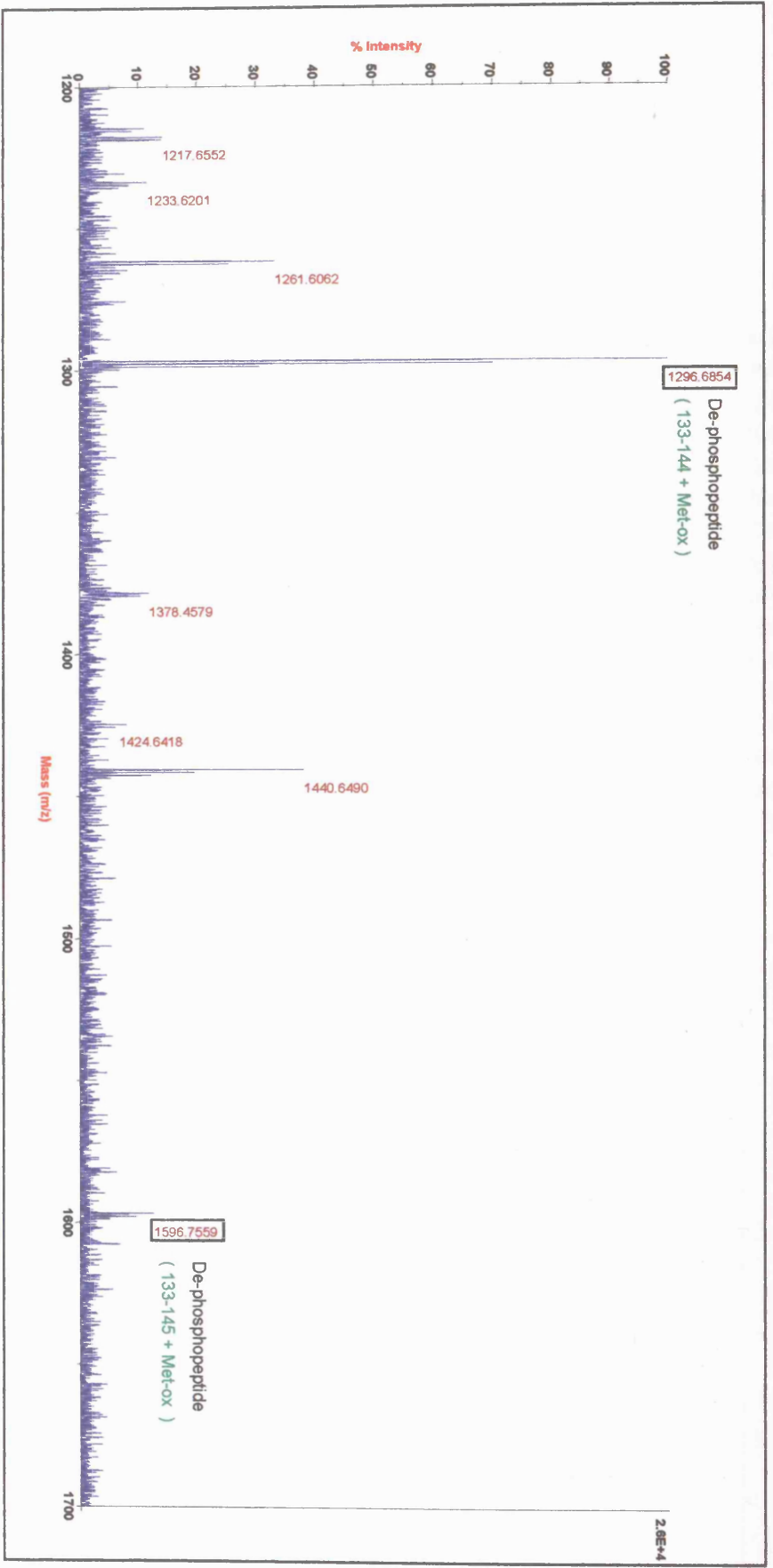1261.6062
1378.4579
1424.6418
1440.6490

b)

Figure 5.16 Analysis of Phosphorylated PKC-δ Fraction 2d by Mass Spectrometry and Edman Degradation. PKC-δ was *in vitro* phosphorylated in the presence of [γ^{32}P]-ATP (50µM ATP, 5µCi; 40Ci/mmol) for 2hrs, isolated and digested with trypsin. Tryptic peptides were fractionated by reverse phase HPLC and counted. ^{32}P-labelled phosphopeptides were detected in Fraction 26/27 and analysed by mass spectrometry and Edman degradation. a) An aliquot of Fraction 27 was analysed by Matrix-Assisted Laser Desorption Ionization Time-Of-Flight (MALDI-TOF) mass spectrometry using an Applied Biosystems 4700. Peptide masses were searched against an *'in silico'* digest (Protein Prospector, UCSF) and assigned as indicated. Met-ox, oxidised methionine. b) Fractions 26/27 were subjected to solid-phase Edman degradation using an ABI Procise Sequencer. Residue number is shown (in blue) and the sequence of a candidate peptide identified by mass spectroscopy is indicated. Fractions corresponding to individual residues were scintillation counted.
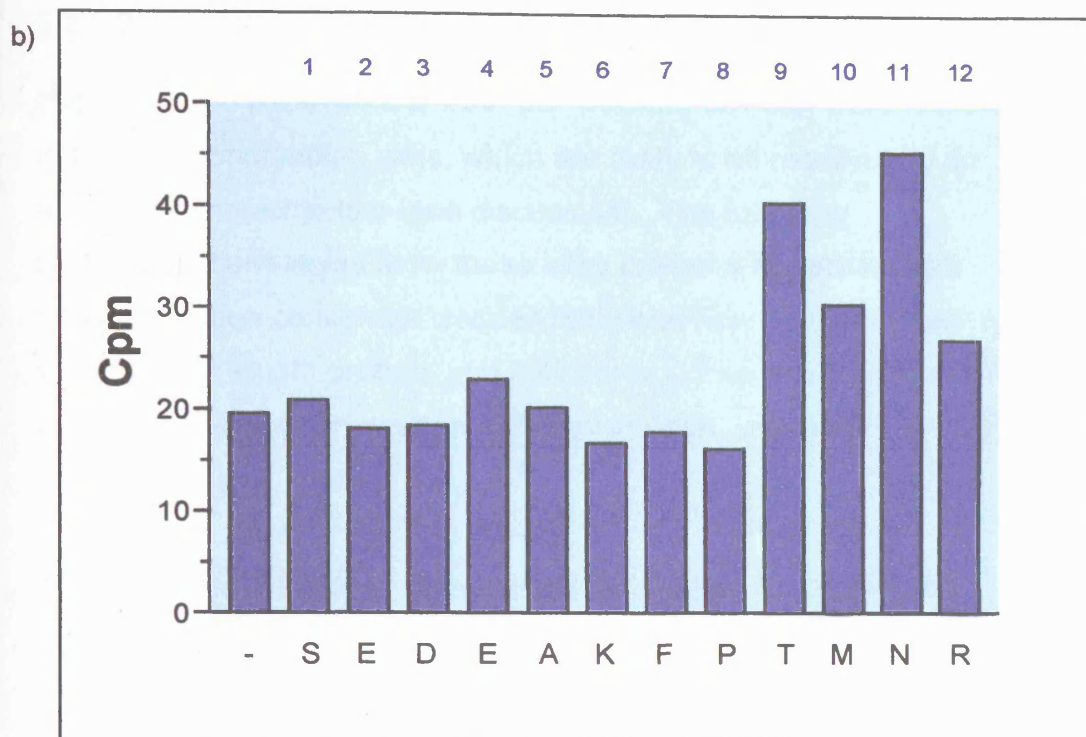
5.2.1.2.3 Novel PKC-δ *In Vitro* Phosphorylation Sites

Human PKC-δ residues Ser-299, Ser-302 and Ser-304 were identified as *in vitro* phosphorylation sites, which are likely to be modified by an autocatalytic mechanism (see discussion). The following characterisations reveal how these sites compare to optimal PKC phosphorylation consensus sequences, show how they are positioned within the full length protein, and indicate how they are conserved, both among PKC-δ sequences from different species, and among different PKC isoforms.

5.2.1.2.3.1 Novel PKC-δ Phosphorylation Sites as Consensus Sequences

The newly identified PKC-δ candidate autophosphorylation sites were analysed using a predictive database to test their potential as phospho-acceptors in relation to established PKC-δ substrates (Table 5.4). An additional candidate residue, Thr-141, was also screened. With the exception of Ser-299, these sites score relatively poorly, however, this is also the case for the 'TP' autophosphorylation site Ser-645.

Phospho-Site	Protein Scan Score	Percentile
Thr-141	24	Bottom 95
Ser-299	4	Top 5
Ser-302	17	Bottom 95
Ser-304	18	Bottom 95
Ser-645	17	Bottom 95

Table 5.4 Predicted PKC Phosphorylation Sites in PKC-δ. The amino acid sequence of human PKC-δ was searched against the Mammalian Phosphorylation Resource database for prediction of PKC phosphorylation sites. The scores obtained for selected phosphorylation sites (as PKC-δ phospho-acceptors) are shown, and the percentile in which this score falls is indicated. Residues scoring below the fifth percentile have been classed as unlikely to represent substrates (Fujii et al., 2004).

265

5.2.1.2.3.2 Positioning of Novel PKC-δ Phosphorylation Sites

Figures 5.17 and 5.18 illustrate the positioning of the *in vitro* phospho-residues within the full length protein. As was the case for two of the three PKC-ε sites mapped, Ser-299, Ser-302 and Ser-304 are all located within the variable V3 region. Thr-141, which was assigned as an additional candidate phospho-site, lies just N-terminal to the PKC-δ pseudosubstrate sequence.

5.2.1.2.3.3 Conservation of Novel PKC-δ Phosphorylation Sites

Alignments were performed to investigate the conservation of phosphorylation sites Ser-299, Ser-302 and Ser-304 among PKC-δ sequences from different species. (Figure 5.19a). Human PKC-δ Ser-299 is shown to be well conserved; a Ser/Thr occurs at the equivalent site among all of the species represented, flanked by basic residues at the -2 and +2/3 positions. The two other sites, however, are more divergent. Serine residues corresponding to human PKC-δ Ser-302 are apparent from chicken and dog sequences, while equivalents to Ser-304 are evident from chicken and rabbit sequences. This analysis is complicated somewhat by the fact that the number of amino acids within this part of the V3 region is variable. If the alignments are configured differently, additional similarities can be drawn. For instance, in the sequences from rat, mouse and dog, Thr residues lie C-terminal to acidic Asp-303 equivalents; these could be thus be considered to relate to Ser-304. Similarly, all three sites are conserved in xenopus PKC-δ if the alignment is shifted by one reside (xenopus has a single amino acid insertion after the residue corresponding to Ser-299). No homology was detected between any of the sites and the δ-type PKCs from Drosophila (PKCdelta), Aplysia (Apl II) or Caenorhabditis (tpa-1).

The sequence surrounding human PKC-δ amino acids 299-304 was also aligned against other members of the PKC superfamily. No homology was detected, even in comparison with PKC-θ, the most closely related isoform. Intriguingly, a certain degree of similarity was detected between

this sequence and part of pck2, one of the two PKC isoforms in *S.pombe*, although some of the basic context, likely to be important in directing PKC activity, is lost from the latter. Nevertheless, it is noteworthy that this loosely conserved, putative consensus sequence for phosphorylation is located between the two C1 domains of pck2, in an equivalent position to the newly identified PKC-ε Ser-234 phosphorylation site.

Figure 5.17 Annotated PKC-δ Amino Acid Sequence. The amino acid sequence of human PKC-δ (NP_006245) is presented with the following features highlighted: C2-like domain, pink; pseudosubstrate sequence, red; C1 domains, turquoise; V3, underlined; ATP binding site, green; kinase domain, blue; priming phosphorylation sites, grey (T-loop, 'TP', 'FSY'); newly identified phosphorylation sites, yellow (S299, S302, S304); candidate phosphorylation site (T141), yellow box.
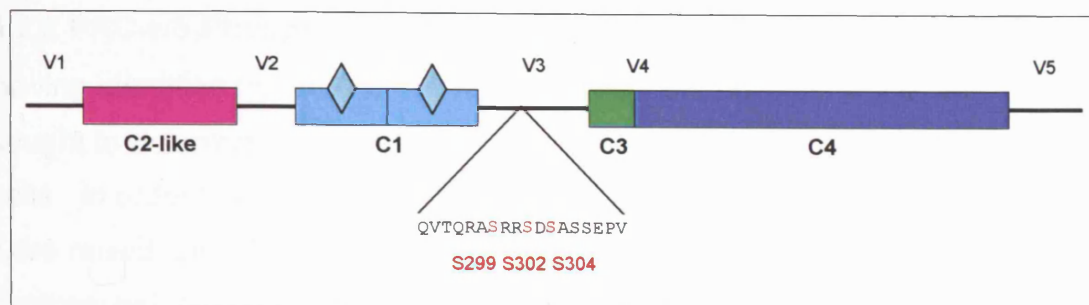
Figure 5.18 PKC-δ Phosphorylation Sites S299, S302 & S304. Three novel phosphorylation sites within human PKC-δ were identified by phosphopeptide mapping: S299, S302 & S304. The domain structure of PKC-δ is represented diagrammatically, with the positioning of the newly identified phosphorylation sites highlighted (red text), and the surrounding sequence shown. Conserved (C1, C2-like, C3, C4) and variable regions (V1, V2, V3, V4,V5) are indicated.
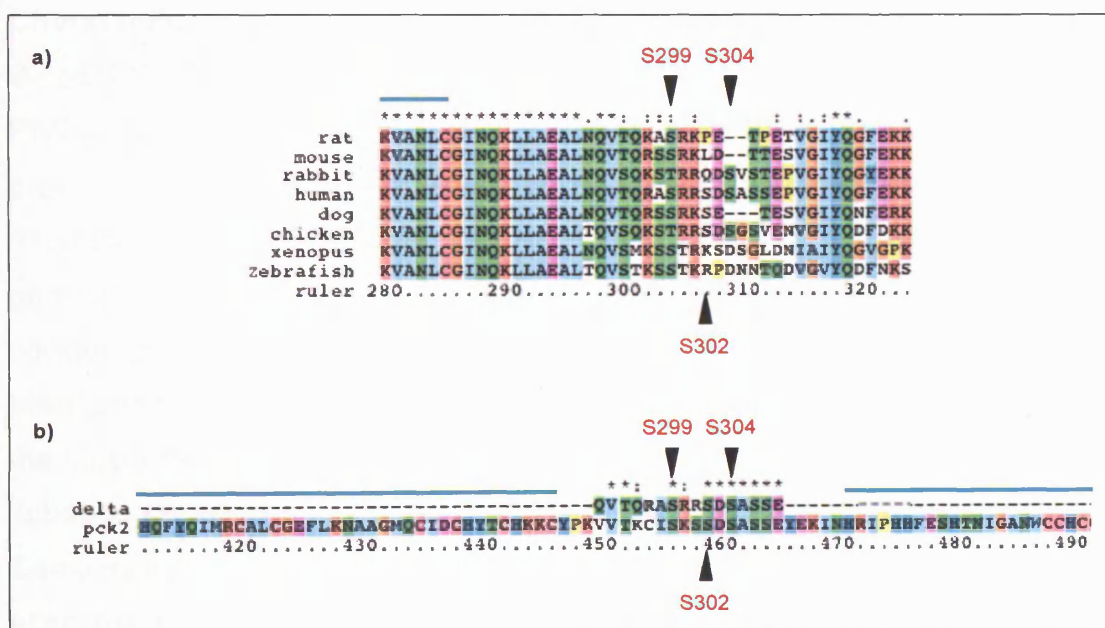
Figure 5.19 PKC-δ S299, S302 & S304 Conservation. Alignments were performed using ClustalX software between a) PKC-δ amino acid sequences from different species, and b) amino acids sequences for human PKC-δ 293-308 and *S.pombe* pck2, to investigate the conservation of human PKC-δ residues S299, S302 and S304, three newly identified phosphorylation sites. C1a/b domains are highlighted (green lines).

5.2.2 PKC-ε/δ Phosphorylation in Mammalian Cells

Having identified novel PKC-ε/δ *in vitro* phosphorylation sites, we next sought to determine whether they could be phosphorylated in mammalian cells. In order to investigate this possibility, phosphospecific antibodies were raised (see Chapter 2). Briefly, 9-mer phosphopeptides were synthesized, based on the sequences surrounding the phospho-sites, for immunisation; equivalent dephosphopeptides were also produced to use as blocking reagents. Three rabbits were immunized with each phosphopeptide and test bleeds were harvested. Sera were analysed by Western blotting for site and phospho-specificity as described below.

5.2.2.1 PKC-ε Phosphorylation in Mammalian Cells

5.2.2.1.1 PKC-ε Phospho-specific Antibody Generation & Characterisation

Since S234/S316/S368 phosphorylation sites were mapped from purified PKC-ε incubated in an *in vitro* kinase assay, we reasoned that this would provide an appropriate sample with which to test the antibodies raised. Aliquots of PKC-ε were taken prior to the assay, from a control assay performed in the absence of ATP, and from a test assay carried out under normal conditions. Western blotting was performed using the second test bleeds from immunized rabbits; the blots shown in Figure 5.20a represent the most effective of the three sera raised for each phospho-site; all subsequent western blotting analyses were performed using these sera. Samples were also probed for phosphorylation of the three PKC priming sites: the T-loop site, 'TP' site and FSY site (Figure 5.20b).
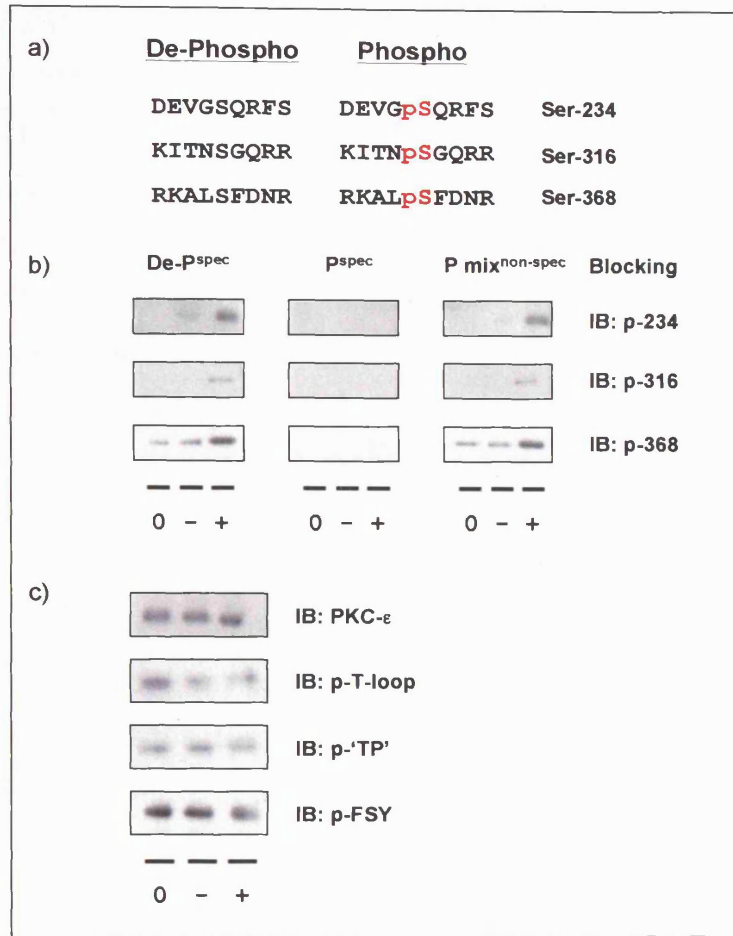
Figure 5.20 *In Vitro* **Phosphorylation of PKC-ε** .
S234, S316, S368 & Priming Site Phospho-Specific Antibodies. a)
Phospho/de-phosphopeptides were synthesized based on the sequences
surrounding PKC-ε phospho-sites Ser-234, Ser-316 and Ser-368;
antibodies were raised against the phosphopeptides. b) *In vitro* kinase
assays were performed using 25ng of purified human PKC-ε. An aliquot
of the starting material was harvested prior to incubation (0) and the
assays were started in the presence (+) or absence (-) of 100µM ATP.
Reactions were incubated at 30°C with shaking for 30mins, and stopped
with sample buffer. Samples were resolved by SDS-PAGE and analysed
by western blotting using the phospho-specific antibodies raised: p-S234
(PPA-501), p-S316 (PPA-503) and p-S368 (PPA-505). These sera were
used to probe samples in the presence or absence of 1µg/ml of different
blocking peptides: De-P^{spec}, de-phosphopeptide specific for
corresponding site (eg. S234 de-phosphopeptide for p-S234 serum);
P^{spec}, phosphopeptide specific for corresponding site (eg. 234
phosphopeptide for p-S234 serum); P mix$^{non-spec}$, two non-specific
phosphopeptides (eg. 316 and 368 phosphopeptides for p-S234 serum).
c) The same samples were probed for total protein (sc-214) and PKC-ε
priming phosphorylation sites: T-loop (PPA-204), 'TP' (PPA-218) and FSY
(anti p-S729). These results are representative of 2 separate
experiments.

The anti p-S234/p-S316/p-S368 sera were tested in the presence or absence of blocking peptides to assess specificity. The appropriate de-phosphopeptide was included to reduce non-specific signals, the corresponding phosphopeptide was tested for its ability to compete against specific phospho-signals, and a mixture of alternative phosphopeptides was employed to establish whether antibodies were site, or merely phospho-serine, specific. In each case an increased signal was detected following incubation with *in vitro* kinase assay mix, but only in the presence of ATP; there was a certain level of basal phosphorylation apparent at the S368 site. Signals could be competed with the corresponding phosphopeptide, indicating phospho-specificity, but not with a mixture of other phospho-serine containing phosphopeptides, confirming sequence specificity also. Phosphorylation at the PKC priming sites, the T-loop, the 'TP' and the 'FSY', did not increase over the course of the *in vitro* kinase assay.

In a similar experiment, PKC-ε aliquots were removed over a timecourse of *in vitro* phosphorylation, and probed for p-S234/p-S316/p-S368 in the presence of the de-phosphopeptide. Phosphorylation at each site increased over time; again a basal occupation of Ser-368 was detected (Figure 5.21).

Phospho/sequence-specific antibodies were thus obtained for all three novel PKC-ε *in vitro* phosphorylation sites: S234, S316 and S368.
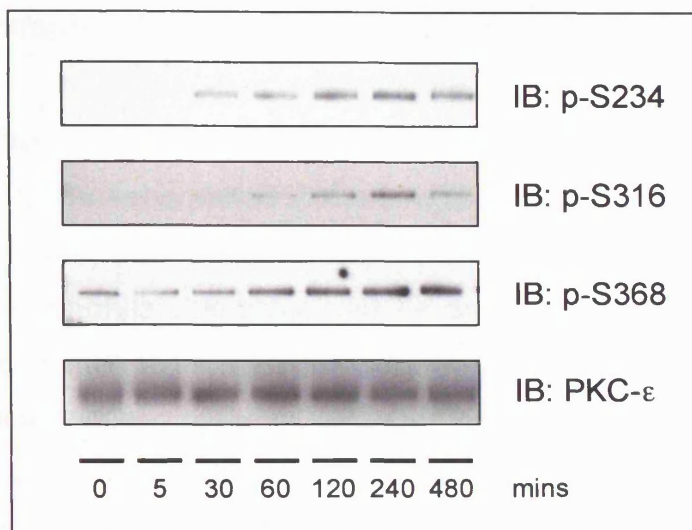
Figure 5.21 Timecourse of *In Vitro* Phosphorylation of PKC-ε
Purified recombinant human PKC-ε was prepared in kinase assay buffer
in the presence of 10μM okadaic acid. Reactions were started with
100μM ATP, incubated for 0-480mins at 30°C with shaking, and
terminated with sample buffer. 25ng samples were resolved by SDS-
PAGE and analysed by western blotting using phospho-specific
antibodies p-S234 (PPA-501), p-S316 (PPA-503) and p-S368 (PPA-505)
in the presence of 1μg/ml de-phosphopeptide. A parallel blot was run to
probe for total protein (sc-214).

5.2.2.1.2 Phosphorylation of PKC-ε S234/S316/S368 in Mammalian Cells

We first wished to establish whether PKC-ε residues S234, S316 and S368 could be phosphorylated in mammalian cells. To this end, GFP-tagged PKC-ε was over-expressed in COS7 cells to provide an abundant source of phosphorylatable protein which could be partially purified by immunoprecipitation to facilitate detection with crude test bleeds. Since *in vitro* phosphorylation of these sites was predicted to occur by an autocatalytic mechanism, cells were stimulated with a phorbol ester PKC activator, TPA, in the presence or absence of a cPKC/nPKC inhibitor, BIM1. The phosphospecific antibodies raised against the novel PKC-ε sites were used for western analysis. Although the phospho-specificity of the sera had been established *in vitro*, alanine mutants of the corresponding sites were employed as a negative controls (S234A for p-S234 analysis, S316A for p-S316 analysis, and S368A for p-S368 analysis).

As shown in Figure 5.22, an increased signal is detectable at all three sites in response to TPA, suggesting that S234, S316 and S368 are phosphorylated in mammalian cells in upon PKC activation. Such signals are not observed from the corresponding alanine mutant samples, further confirming the phosphospecificity of the antibodies. TPA induced phosphorylation of the wild type protein is largely inhibited by BIM1, which again, is consistent with a requirement for PKC activity.
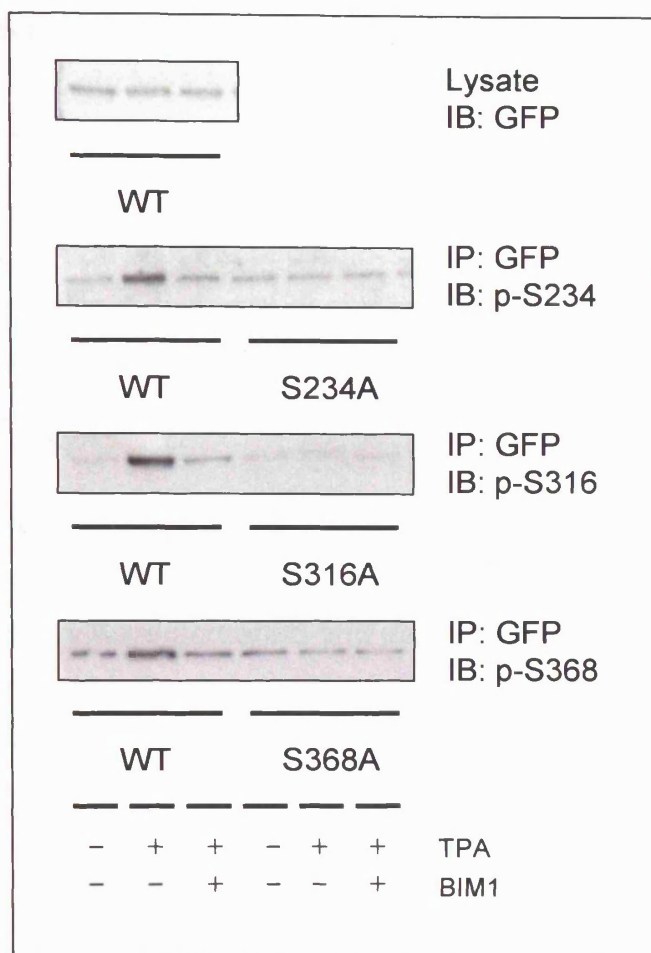
Figure 5.22 Phosphorylation of PKC-ε S234/S316/S368 in Mammalian Cells. COS7 cells were seeded on 6-well plates and transfected with GFP-PKC-ε (WT) or one of a panel of GFP-PKC-ε mutants (S234A/S316A/S368A). 24hrs post-transfection, cells were pre-treated +/- 1μM BIM1 for 15mins and stimulated +/- 400nM TPA for a further 45mins. Lysates were prepared and subjected to immunoprecipitation with anti GFP 4E12/8. Samples were analysed by Western blotting using phospho-specific antibodies: p-S234 (PPA-501), p-S316 (PPA-503) and p-S368 (PPA-505) in the presence of blocking de-phosphopeptide, or anti GFP 3E1. Each serum was tested using the alanine mutant of the corresponding site as a negative control. These results are representative of 2 separate experiments.

A similar experiment was carried out using Clone 5, a cell line derived from PKC-ε knock-out MEFS which stably re-express untagged PKC-ε to high levels (Figure 5.23). Cells were treated in the presence or absence of TPA, PKC-ε was recovered by denaturing immunoprecipitation and samples were probed with the phospho-specific antibodies. Phosphorylation was detected at each site in response to TPA, confirming that the apparent phosphorylation described above is not artefactually dependent on the GFP-tag.

The immunoprecipitation protocol employed to isolate PKC-ε from Clone 5 cells was the most effective of several approaches tested. A number of different antibodies were screened and protocols based on the affinity of PKC for heparin sulphate and protamine sulphate were explored as alternative means of partial purification; the efficiency of PKC-ε recovery was poor under all conditions tested. Consequently, although sufficient material was obtained from Clone 5 cells for analysis with the phospho-antibodies, it was not possible to recover enough endogenous PKC-ε from other cell lines to test phosphorylation under more physiological conditions.
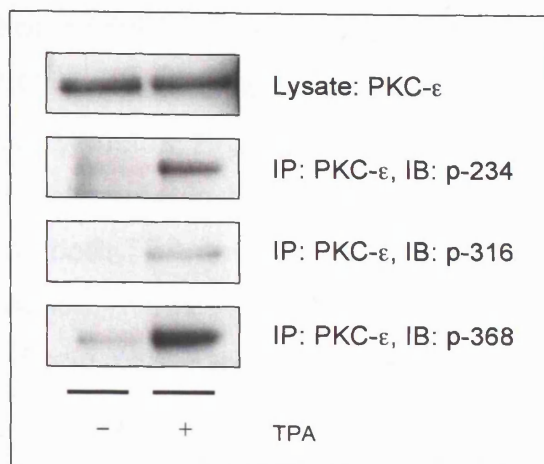
Figure 5.23 Phosphorylation of untagged PKC-ε S234/S316/S368.
Clone 5 cells were seeded on 15cm dishes. Confluent cells were
stimulated +/- 400nM TPA and incubated for 45mins. Lysates were
prepared and subjected to denaturing immunoprecipitation with anti PKC-
ε. Samples were analysed by Western blotting using phospho-specific
antibodies: p-S234 (PPA-501), p-S316 (PPA-503) and p-S368 (PPA-505)
in the presence of blocking de-phosphopeptide, or anti PKC-ε.
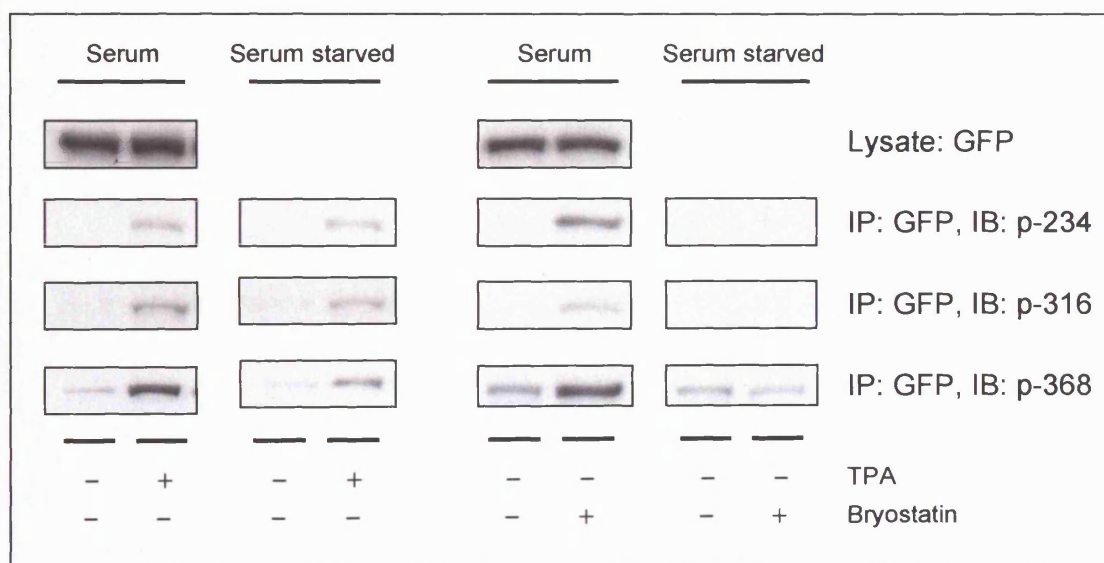
**Figure 5.24 Activation of PKC-ε Phosphorylation by TPA/Bryostatin
+/- serum.** COS7 cells were seeded on 6-well plates and transfected with
GFP-PKC-ε. 32hrs post-transfection, cells were either serum starved
(0.1% E4) or incubated with fresh 10% E4 (serum) for a further 16hrs.
Cells were treated +/- 400nM TPA or 1µM Bryostatin for 45mins. Lysates
were prepared and subjected to immunoprecipitation with anti GFP
4E12/8. Samples were analysed by Western blotting using phospho-
specific antibodies: p-S234 (PPA-501), p-S316 (PPA-503) and p-S368
(PPA-505) in the presence of blocking de-phosphopeptide, or anti GFP
3E1. These results are representative of 2 separate experiments.

5.2.2.1.3 Activation of PKC-ε Phosphorylation in Mammalian Cells

The process of PKC-ε phosphorylation was further analysed through the use of an additional stimulus, Bryostatin 1 (Figure 5.24); these experiments were performed in the presence or absence of serum. In the presence of serum, both TPA and Bryostatin 1 were shown to induce PKC-ε phosphorylation. However, in samples from serum starved cells, while TPA induced phosphorylation was observed, Bryostatin 1 had no effect.

5.2.2.1.4 Inhibition of PKC-ε Phosphorylation in Mammalian Cells

An additional inhibitor was also tested to gain further insight into the mechanism of PKC-ε phosphorylation. The inhibitor Gö6976, which shows relative specificity for cPKCs, was tested alongside BIM1 (Figure 5.25). TPA induced phosphorylation at all three sites proved insensitive to Gö6976, suggesting that catalysis is mediated by an nPKC.
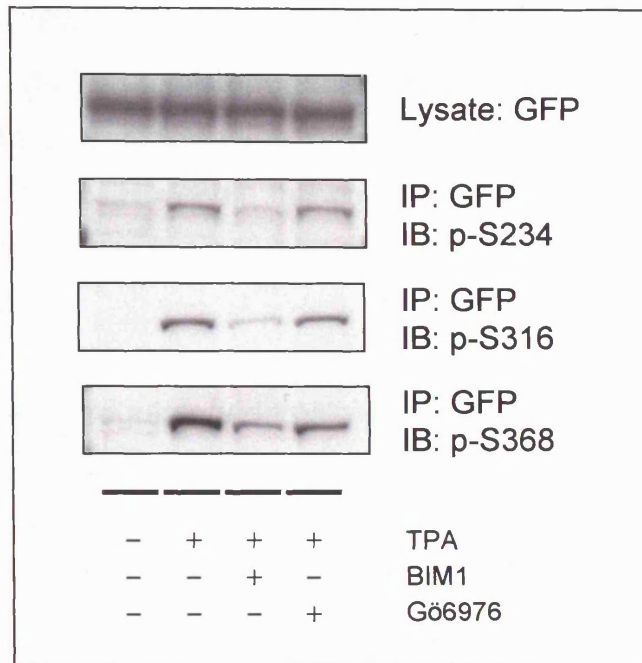
Figure 5.25 Inhibition of PKC-ε S234/S316/S368 Phosphorylation.
COS7 cells were seeded on 6-well plates and transfected with GFP-PKC-
ε (WT). 24hrs post-transfection, cells were pre-treated +/- 1μM Gö6976
or 1μM BIM1 for 15mins and stimulated +/- 400nM TPA for a further
45mins. Lysates were prepared and subjected to immunoprecipitation
with anti-GFP 4E12/8. Samples were analysed by Western blotting using
phospho-specific antibodies: p-S234 (PPA-501), p-S316 (PPA-503) and
p-S368 (PPA-505) in the presence of blocking de-phosphopeptide, or anti
GFP 3E1.

5.2.2.1.5 PKC-ε Phosphorylation in Mammalian Cells: Cis/Trans?

The data presented is consistent with the hypothesis that PKC-ε phosphorylation is catalysed by an nPKC, possibly by autophosphorylation. However, this could be mediated through either an intra- or inter-molecular event; preliminary work was undertaken to address this issue.

GFP-tagged PKC-ε regulatory domain was expressed in COS7 cells, this construct bears all three potential phospho-sites, but lacks a kinase domain with which to perform intra-molecular phosphorylation. Cells were treated with TPA, +/- Calyculin A to inhibit dephosphorylation, or Bryostatin 1, in the presence or absence of serum (Figure 5.26a). In the presence of serum, increased phosphorylation was detected at all sites in response to PKC activation, as had been observed in the full length protein; the signal was augmented by co-treatment with Calyculin A suggesting that these sites are subject to dephosphorylation. In the absence of serum, TPA + Calyculin A was the only treatment which facilitated increased phosphorylation of the PKC-ε regulatory domain. Additionally, a fast migrating PKC-ε species was detected by all antisera in the absence, but not presence, of serum. This species could correspond to either a dephosphorylated or a proteolytically cleaved form of the protein, since it is detectable even in the presence of Calyculin A, the latter seems more likely.

Phosphorylation of a kinase dead mutant was also investigated; S368 did not show an increase in phosphorylation in response to TPA (Figure 5.26b).
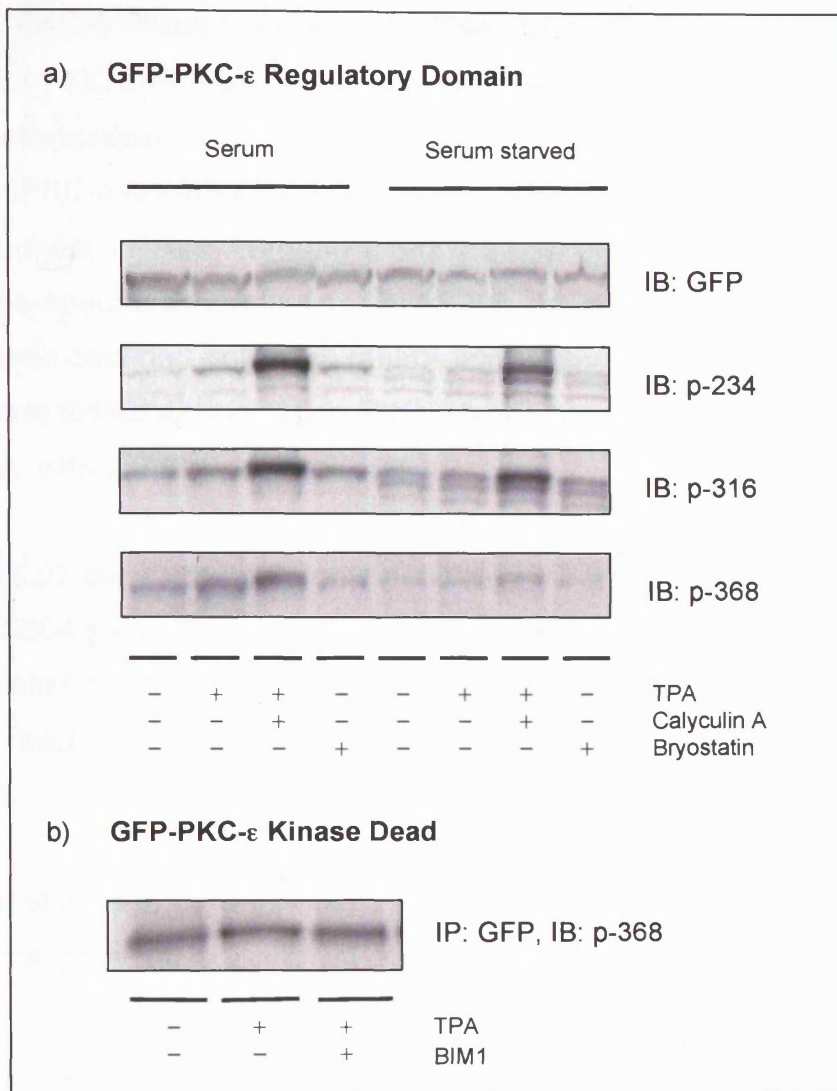
Figure 5.26 PKC-ε Regulatory Domain & PKC-ε Kinase Dead S234/S316/S368 Phosphorylation. a) COS7 cells were seeded on 6-well plates and transfected with GFP-PKC-ε regulatory domain. 32hrs post-transfection, cells were either serum starved (0.1% E4) or incubated with fresh 10% E4 (serum) for a further 16hrs. Cells were treated +/- 400nM TPA +/- 100nM Calyculin A or 1μM Bryostatin 1 for a further 45mins. Lysates were prepared and analysed by Western blotting using phospho-specific antibodies: p-S234 (PPA-501), p-S316 (PPA-503) and p-S368 (PPA-505) in the presence of blocking de-phosphopeptide, or anti GFP 3E1. b) COS7 cells were seeded on 6-well plates and transfected with GFP-PKC-ε kinase dead. 24hrs post-transfection, cells were pre-treated +/- 1μM BIM1 for 15mins and then stimulated +/- 400nM TPA for a further 45mins. Lysates were prepared and analysed by Western blotting using the phospho-specific antibody against p-S368 (PPA-505) in the presence of blocking de-phosphopeptide.

5.2.2.2 PKC-δ Phosphorylation in Mammalian Cells

5.2.2.2.1 PKC-δ Phospho-specific Antibody Generation & Characterisation

Human PKC-δ residues S299, S302 and S304 were identified as *in vitro* phosphorylation sites. Immunizations are now underway to raise phospho-specific antibodies against S299, however, to date, test bleeds have been obtained only from rabbits immunized with p-S304. These sera were tested directly using PKC-δ overexpressed in mammalian cells +/- TPA, with a S304A control.

Figure 5.27 shows the data obtained using the most effective of the three anti p-S304 sera. This figure reveals that S304 is phosphorylated in mammalian cells in response to TPA. Antibody specificity is evidenced by the fact that no signal is detected in cells transfected with a S304A mutant.

Further studies of PKC-δ phosphorylation await the production of additional phospho-specific antibodies.
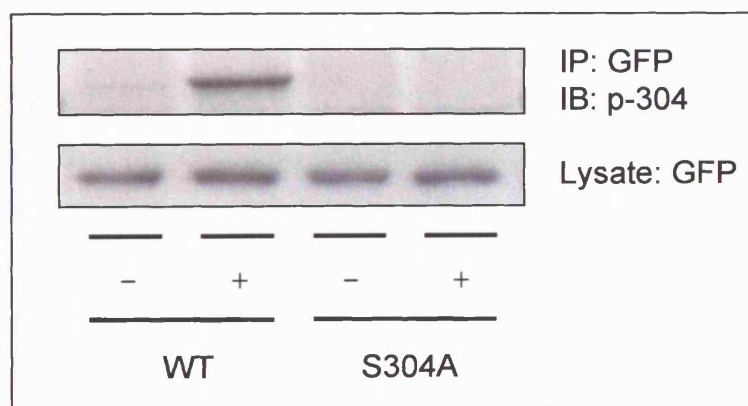
Figure 5.27 Phosphorylation of PKC-δ S304 in Mammalian Cells. COS7 cells were seeded on 6-well plates and transfected with GFP-PKC-δ (WT) or GFP-PKC-δ S304A. 24hrs post-transfection, cells were stimulated +/- 400nM TPA for 45mins. Lysates were prepared and subjected to anti GFP 4E12/8 immunoprecipitation. Samples were analysed by Western blotting using a phospho-specific antibody, p-S304 (PPA-514), in the presence of blocking de-phosphopeptide, and anti GFP 3E1. These results are representative of 2 separate experiments.

5.3 Discussion

PKC activity and PKC phosphorylation have been shown to play critical roles in regulating TPA-induced PKC degradation, but the details of this process remain to be fully characterised. We hypothesized that the identification of PKC phosphorylation sites induced upon PKC activation may therefore provide insights into the pathway(s) of down-regulation. Phosphopeptide mapping studies were undertaken, first focused on phosphorylated PKC-ε, and later, using the same approach, on phosphorylated PKC-δ.

Our preliminary experiments confirmed that phosphorylation of PKC-ε/δ increased with increasing enzyme concentration and incubation time *in vitro*. In each case, phosphorylation was calculated to occur with significant stoichiometry. However, once phosphorylation sites were mapped it became apparent that this figure actually reflects the sum of phosphate incorporation across multiple sites. No further quantitative studies have been undertaken to date to investigate the stoichiometry to which individual sites are occupied.

Since *in vitro* kinase assays were performed using purified PKC-ε/δ, we hypothesized that the detected phosphorylation was mediated by an autocatalytic mechanism, either in cis or trans. However, although the purity of the preparations used was ≥95% (Calbiochem), we could not exclude the possibility that a small amount of a contaminating kinase could be responsible for the PKC phosphorylation detected. Therefore, further *in vitro* kinase assays were performed to investigate the requirements of PKC-ε phosphorylation.

In vitro PKC-ε phosphorylation was demonstrated to occur more efficiently in the presence than absence of phosphatidylserine/TPA mixed micelles. Since PKC is a lipid-dependent kinase, this is consistent with, but not proof of, a requirement for PKC activity. *In vitro* phosphorylation

was also shown to be inhibited by BIM1, a cPKC/nPKC inhibitor, in a dose dependent fashion. This is more compelling as evidence for autophosphorylation, however, the possibility remains that an alternative cPKC/nPKC co-purified with PKC-ε. Although BIM1 is shown to be inhibitory towards PKC-ε phosphorylation, a relatively high concentration (10-50μM) is required to detect a significant 50% inhibition (IC_{50} with respect to PKC-ε: 0.132μM, Calbiochem). This could suggest that a contaminating kinase, partially and non-specifically inhibited by BIM1, is functioning here. However, this observation may in fact be indicative of an autophosphorylation event. cPKC autophosphorylation has a K_m for ATP (1.5μM) approximately 10-fold lower than that for phosphorylation of exogenous substrates (Huang et al., 1986); as such, a higher concentration of an ATP competitive inhibitor such as BIM1 would be expected to be required to achieve a comparable level of inhibition.

Phosphopeptide mapping was undertaken to identify the sites of nPKC phosphorylation in vitro, first focussing on PKC-ε. Counting of fractionated, ^{32}P-labelled phospho-PKC-ε tryptic peptides revealed the existence of at least four phosphopeptide populations of differing hydrophobicity. Analysis of three of these fractions facilitated the identification of three novel PKC-ε phosphorylation sites: S234, S316 and S368. In each case, the data obtained allowed the phosphorylation site to be assigned unequivocally. Mass spectrometry not only identified the relevant de-phosphopeptide, but provided direct evidence of phosphorylation, detecting both the corresponding phosphopeptide and its post source decay product. Edman degradation provided complementary data, with ^{32}P detected specifically in a fraction corresponding to a Ser residue within the identified peptide. The only species which was not detected during the analysis of PKC-ε was the de-phosphopeptide containing Ser-234. Stoichiometric analysis would suggest that this phosphorylation event did not proceed to completion; we therefore assume that the de-phosphopeptide eluted in a shifted fraction with respect to the phosphopeptide, due to a difference in hydrophobicity.

The fourth of the ^{32}P-labelled fractions detected from the phospho-PKC-ε tryptic digest comprised the breakthrough volume from the reverse phase HPLC column, and was considered unsuitable for further analysis. The counts detected in this fraction could have derived either from free phosphate, released by hydrolysis during peptide processing, or from small, hydrophilic phosphopeptides that passed directly through the column. It is possible that there are further PKC-ε residues, in addition to those successfully mapped, which are phosphorylated *in vitro*. Alternatively, the phosphopeptides present in these early fractions may represent distinct digestion products of sequences surrounding already identified sites. The phosphopeptides from which p-S316 (302-319) and p-S368 (365-377) were identified both contain missed sites for cleavage by trypsin (K312 and R372 respectively); if digested to completion these would yield smaller, more hydrophilic peptides, with lower column retention times. Analysis of the breakthrough volume by Edman degradation would have been informative in this respect, as the positioning of S316/S368 within alternative tryptic peptides would be predictable.

Phosphopeptide mapping of *in vitro* phosphorylated PKC-δ was undertaken using the same approach. The data obtained after the first experiment was not complete; it was possible to match comprehensive mass spectrometric data with Edman degradation results from only one fraction. The experiment was therefore repeated, using slightly different conditions, and phospho-PKC-δ was analysed by digestion with both trypsin and AspN, an alternative protease that would generate a different set of peptides, to provide complementary data. We obtained no mass spectrometric evidence of phosphorylation from any of the AspN derived samples, even when the protocol was repeated with a fresh sample; it appears that these peptides are not amenable to mass spectrometry. Certain peptides do not 'fly' effectively in a mass spectrometer flight tube as a result of inherent sequence properties which can influence the

efficiency of ionization and/or ion suppression phenomena; it is perhaps unusual though that none of the phosphopeptides yielded mass spectrometric data. The second experiment using trypsin yielded a different, but overlapping data set, to the first. This variation is likely to be accounted for by differences in kinase assay incubation time and efficiency of tryptic digestion. Both experiments revealed the existence of at least five phosphopeptide populations which were studied further.

PKC-δ residues Ser-299 and Ser-302 were identified as *in vitro* phosphorylations sites which could be occupied simultaneously; evidence relating to these sites was obtained from both experiments with trypsin. Ser-304 was also detected as a phospho-site, however, this observation was made only in the second experiment. It is possible that this reflects the increased kinase assay incubation time employed in experiment two; we could speculate that Ser-304 represents a minor site which can become phosphorylated over time, perhaps by virtue of its proximity to a preferred site such as Ser-299/302. We have not investigated whether these phosphorylation events proceed in a specific order; this could be tested over a timecourse once phospho-specific antibodies have been produced against all three sites, and/or by using alanine mutants. Neither have we explored further whether a population of PKC-δ can occur which is triply phosphorylated in this region, or whether certain combinations of phosphorylation events are mutually exclusive. These questions could be readily addressed in the future using de-phosphorylated, phosphorylated and doubly phosphorylated peptides based on this region as PKC- δ *in vitro* kinase assay substrates.

An additional PKC-δ residue, Thr-141, was identified as a candidate phosphorylation site, but the related data was somewhat ambiguous. Two different dephosphopeptides containing this residue were shown to co-fractionate with phosphopeptides, and Edman degradation data placed the ^{32}P-labelled residue in the position which would correspond to Thr-141 in both cases. However, no mass spectrometric evidence of

phosphorylation was obtained regarding either peptide. It is possible that these phosphorylated peptides do not fly effectively in the mass spectrometer flight tube. Alternatively, this co-fractionation may be merely coincidental. In order to test this hypothesis further, it would be worthwhile to repeat the phosphopeptide mapping process using wild type PKC-δ in comparison with a T141A mutant.

Certain of the other PKC-δ derived phosphopeptides, which could be detected by counting post-fractionation, were completely unaccounted for due to an absence of any corresponding mass spectrometric data. Those unidentified species present within the early HPLC fractions, representing small/hydrophilic peptides, may well bear established phospho-sites within alternatively digested peptides. For instance where counts were detected at residue 2 of the breakthrough volume by Edman degradation, S-299 would represent a strong candidate, since complete digestion would place this residue within a very short peptide (ASR(R)). However, it is also feasible that additional phosphorylation sites remain undetected. To address this issue, we plan to re-examine phospho-PKC-δ derived peptides using an alternative mass spectrometer, the 4000 Q TRAP LC/MS/MS System (Applied Biosystems). This system provides an alternative means of phosphopeptide mapping in a single LC/MS/MS run. Briefly, initial precursor ion and neutral loss scans are employed to identify which peptide ions are releasing a phosphate ion, these are then automatically selected for high sensitivity ion trap MS/MS scanning, to determine the sequence of, and phosphorylation site on, the phosphopeptide.

Since the issue of nPKC autophosphorylation is somewhat contentious, we were interested to determine whether we could observe in this system the phosphorylation of either the 'TP' site, which is well documented to be autophosphorylated (Parekh et al., 2000), or the hydrophobic motif, which is reported to be autophosphorylated in mammalian cells under some conditions (Cenni et al., 2002). We obtained no evidence for *in vitro*

phosphorylation of either residue; however, we cannot exclude either event as a possibility. Firstly, we may have overlooked phosphorylation of these sites in our studies. In the case of PKC-ε, it seems unlikely that either site falls within a tryptic fragment hydrophilic enough to elute in the breakthrough volume (TP: EEPVLpTLVDEAIV; FSY: GFpSYFGEDLMP), and all other phosphopeptides were accounted for. However, in the case of PKC-δ, there were clearly phosphopeptides which remained unidentified. One phosophopeptide was detected in the breakthrough volume with a ^{32}P-labelled residue at position 2; this could conceivably correspond to the PKC-δ 'TP' site, which is predicted to fall within a short peptide (LpSYSDK). Alternatively, these sites may already have been occupied in the purified, recombinant PKC preparations used in these assays, such that no further phosphorylation would be possible. This latter notion is supported by Western blotting performed with phospho-specific PKC-ε anti-sera, which detected 'TP' and 'FSY' site phosphorylation in the starting material, and showed no increase at either site over the course of the *in vitro* kinase assay. Alternative studies are now underway in our laboratory to investigate phosphorylation of the PKC-ε hydrophobic motif (S729); an RNAi library will be employed to systematically knock-down all kinases, and the effects on phosphorylation of S729 will be monitored. As such, the remainder of this work was focussed upon the characterisation of the novel nPKC phosphorylation sites which were identified.

The characteristics of the novel *in vitro* PKC-ε/δ phosphorylation sites were examined. Since PKC is a basophilic kinase, it followed that all of the sites detected display a degree of basic context. This was reflected experimentally by the fact that a number of the phospho-residues occurred within alternatively digested peptides; there were multiple Lys/Arg residues flanking some of these sites at which trypsin could cut. However, none of the assigned phosphorylated motifs comprised a highly optimal consensus sequence. In the previous chapter, a database predictive for PKC phosphorylation sites was exploited to screen for

potential substrates *in silico* (Fujii et al., 2004). If the PKC-ε /δ sequences themselves are searched using this tool, the *in vitro* phosphorylation sites score poorly in general. However, this is also the case for the established 'TP' autophosphorylation sites, PKC is in fact biased against phosphorylating residues immediately N-terminal to proline (Zhu et al., 2005). These observations reflect the fact that phosphorylation is determined both by the sequence specificity of the kinase, and by the accessibility of the substrate. As such, a favoured consensus will not be phosphorylated if inaccessible, and conversely, a less optimal sequence may be modified if appropriately positioned. The process of autophosphorylation (intramolecular) clearly presents a unique scenario in this respect, in which the candidate site is inherently juxtaposed with the kinase; this in part explains the propensity for PKC to phosphorylate sub-optimal motifs within its own sequence.

With the exception of PKC-ε residue Ser-234, all of the PKC-ε/δ *in vitro* phosphorylation sites distinguished occur within the variable V3 domain, between the regulatory and catalytic domains. The V3 region is one of the most divergent regions of the PKC sequence, and consistent with this, none of the sites located in this domain were conserved in other PKC family members. Post-translational modification of these unique residues may thus be postulated to contribute to PKC isoform specificity.

PKC-ε residue Ser-234, in contrast, is located between the C1a and C1b diacylglycerol/phorbol ester binding sites. Although not conserved among other PKC isoforms, it is notable that PKC-η, the most closely related family member to PKC-ε, bears a glutamate residue in the equivalent position, which may be predicted to behave as a phospho-mimic. Interestingly, a motif within *S.pombe* pck2, which shows homology to the region surrounding the PKC-δ V3 domain phosphorylation sites, also falls between the C1 domains. We could speculate that the PKC-δ phosphorylation consensus sequence, and PKC-ε S-234 phospho-residue location, have been conserved to a certain extent over evolution.

However, this proposition is confounded by the fact that equivalent sites are not apparent in sequences from Caenorhabditis or Drosophila as discussed below.

The conservation of an amino acid sequence through evolution is indicative that it may play an important functional role. As such, PKC sequences from other organisms were examined for homology with the *in vitro* phosphorylation sites identified in human PKC-ε/δ. All three PKC-ε sites were retained among mammalian species but were not detected in lower organisms. The analysis of PKC-δ sites was somewhat complicated by the variability of amino acid number as well as sequence, within this region. However, Ser-299 appeared to be conserved among a number of species, from xenopus to mammals, and residues corresponding to Ser-302 and Ser-304 were evident in a number of other organisms. In contrast, no homology was detected between this region of PKC-δ and sequences from Drosophila, Aplysia or Caenorhabditis. Since these sites are conserved among higher organisms, we could speculate that they may be functionally relevant, but less critical than the three established priming sites, which are largely conserved across all organisms and isoforms.

Having identified novel PKC-ε/δ phosphorylation sites *in vitro*, we next sought to characterise their modification in cells. To this end, we raised phospho-specific antibodies against the following sites in PKC-ε: p-S234, p-S316 and p-S368, and PKC-δ p-S304; we are awaiting the production of phospho-sera recognising PKC-δ p-S299. The anti PKC-ε antibodies were first used to probe *in vitro* phosphorylated material; consistent with the fact that these sites had been mapped from such samples, occupation of all three sites could be detected, increasing over the timecourse of the kinase assay. The phospho- and sequence specificities of these antibodies were validated by using different blocking peptides; the signals detected could be effectively competed using the appropriate blocking phosphopeptides. Subsequently, the antibodies

were also tested using alanine mutants of the corresponding sites in cells as negative controls, a degree of non-specific binding was encountered under these conditions, with a low level signal detected in alanine mutant samples, however, differences between wild type and mutant phospho-recognition were apparent post-stimulation.

The PKC-ε antibodies were utilized to investigate the process of PKC-ε phosphorylation in mammalian cells; equivalent studies remain to be performed for PKC-δ. Phosphorylation of overexpressed GFP-PKC-ε at sites S234, S316 and S368 was observed in cells in response to the phorbol ester PKC activator, TPA. Phosphorylation could also be detected from untagged PKC-ε expressed to high levels in a MEF cell line, Clone 5, proving that this process is not artefactually dependent on the N-terminal GFP. To date it has not been possible to establish a protocol for PKC-ε enrichment sufficiently effective to facilitate the analysis of the endogenous protein; further methods remain to be tested. Additionally, the phospho-sera will be affinity purified; a more concentrated and specific population of antibodies may be amenable to probing a whole cell lysate. Once conditions have been established with which to visualise phosphorylation of the endogenous protein, it will be of interest to assay these sites in response to more physiological stimuli (eg. growth factors for fibroblasts, LPS for macrophages).

TPA induced PKC-ε phosphorylation was shown to occur in a manner that was inhibited by BIM1, a cPKC/nPKC inhbitior, but not by Gö6976, an inhibitor more selective cPKC (IC_{50} for PKC-α = 2.3nM; PKC-ε, no inhibition (Martiny-Baron et al., 1993)), indicating a requirement for nPKC activity. Combined with the *in vitro* data discussed earlier, this strongly suggests that phosphorylation is mediated by autocatalysis. However, this data does not definitively exclude the possibility that another nPKC is responsible, and does not address whether the putative autophosphorylation of PKC-ε occurs in cis or trans.

Preliminary experiments were undertaken in order to explore whether PKC-ε undergoes intra- or inter-autophosphorylation. Firstly, phosphorylation of the GFP-PKC-ε regulatory domain was analysed; this construct bears all three potential phospho-sites, but lacks a kinase domain with which to perform intra-molecular catalysis. Increased signal was detected at each site in response to PKC activation, suggesting that phosphorylation can be performed in trans (by an endogenous PKC). It would be of interest to determine whether overexpression of the regulatory domain can competitively inhibit phosphorylation of a co-expressed wild type protein; this would also be indicative of trans-autophosphorylation. Autophosphorylation was next explored in the context of the full length protein using a kinase dead PKC-ε construct; a low level signal was detected, which could constitute either basal phosphorylation, or some non-specific recognition by the antibody, but elevated phosphorylation was not detected at S234, S316 or S368 in response to TPA. This data can be interpreted in a number of ways. It would be consistent either with a dominance of intra-molecular phosphorylation, or with a trans-autophosphorylation event, where PKC-ε dimerisation may be required. However, it is also plausible that the conformation of the kinase dead PKC-ε may be disrupted, such that these sites are less accessible to the relevant kinase, or more accessible to the antagonistic phosphatase. An unlikely, but nevertheless possible, alternative is that the site is already fully occupied under basal conditions; this could be checked by treating parallel samples +/- phosphatase prior to western analysis.

In order to try to address this issue in a more tractable system, we have obtained a PKC-ε mutant (M486A) that has been modified to facilitate its inhibition by a specific compound (1-Na), which has no effect on the wild type protein (provided by Dr. Bob Messing). The PKC-ε M486A mutant bears a FLAG-tag, such that there is a convenient difference in size between it and GFP-wild type PKC-ε. We designed an experiment in

which FLAG-PKC-ε M486A would be co-expressed with GFP-PKC-ε, and cells would be stimulated with TPA in the presence or absence of BIM1 or 1-Na. We reasoned that should cis-autophosphorylation predominate, phosphorylation of PKC-ε M486A at S234, S316 and S368 would be inhibited using 1-Na, despite the presence of the wild type protein. However, if autophosphorylation occurs in trans, PKC-ε M486A phosphorylation should be inhibited by BIM1 but not by 1-Na. Unfortunately, preliminary work has indicated that TPA-induced phosphorylation of this mutant is not readily detectable. It seems that the mutation incorporated may influence properties of the enzyme other than its inhibition profile; this awaits further investigation. In the meantime, the issue of intra-/inter- molecular autophosphorylation remains in question. An alternative possibility would be to characterise the autophosphorylation process kinetically. The initial rate of an intra-molecular autophosphorylation is first order with respect to enzyme concentration, while that of an inter-molecular autophosphorylation is second order (Wang and Wu, 2002). As such, initial rates of PKC-ε autophosphorylation could be measured at different enzyme concentrations, and should initial rate be shown to increase with concentration, we could conclude an inter-molecular process occurs. However, the use of this approach may be complicated by the nature of the PKC *in vitro* kinase assay system. The requirement for lipid micelles to activate the enzyme would need to be considered, establishing conditions under which the number of micelles exceeds the number of PKC molecules at all concentrations; this could be accomplished by using a physically defined, homogenous micelle system, such as that described by Hannun and colleagues (Hannun et al., 1985). To aid interpretation, it would also be worthwhile to explore the possibility of trans-phosphorylation by investigating whether PKC undergoes dimerisation; this could be achieved by measuring Fluorescence Resonance Energy Transfer (FRET) between GFP-PKC-ε and RFP-PKC-ε by Fluorescence Lifetime Imaging Microscopy (Peter et al., 2005).

The phosphorylation of both full length PKC-ε and its regulatory domain were examined in response to an alternative stimulus, Bryostatin 1. Although Bryostatin 1 is a potent PKC activator, it induces only a subset of the effects observed in response to TPA and often inhibits those which it does not promote (Szallasi et al., 1994). The mode of action of Bryostatin 1 is of particular interest, since it has demonstrated potential therapeutic value and is the subject of numerous clinical trials (Mutter and Wills, 2000). In comparison with TPA, Bryostatin 1 has been shown to render PKC more susceptible to dephosphorylation (Lee et al., 1996), to facilitate a differential pattern of localisation (Leontieva and Black, 2004; Wang et al., 1999), and significantly, to cause the down-regulation of some isoforms but the protection of others (Szallasi et al., 1994); these effects are clearly inter-related but the mechanism of action remains to be fully characterised. In this context, it is noteworthy that there was a dichotomy between the induction of full length PKC-ε phosphorylation in response to TPA and Bryostatin 1; while both activators induced phosphorylation in the presence of serum, only TPA mediated this effect in serum starved cells. It will be of interest to determine the basis of this difference. Given the propensity of Bryostatin 1 to encourage dephosphorylation, it would be worthwhile to perform the same experiments in the presence of Calyculin A, and also to monitor the occupation of the priming sites; if these sites are dephosphorylated, PKC will lack the catalytic competence to mediate autophosphorylation. The fact that this difference manifests only under serum starved conditions is also intriguing, suggesting that protection from dephosphorylation can be conferred.

The phosphorylation of the PKC-ε regulatory domain was also affected by the presence of serum. Under standard conditions, PKC activation was shown to induce phosphorylation, and this was augmented by Calyculin A, implying that S234, S316 and S368 are subject to dephosphorylation. In the absence of serum, however, only Calyculin A detectably increased phosphorylation; again this may suggest that serum imparts some

protection from dephosphorylation. That this effect is more pronounced with respect to the regulatory domain than the full length protein may reflect its more open and accessible conformation.

Since the novel PKC-ε and PKC-δ sites identified *in vitro* have proven to be phosphorylated in mammalian cells, it is of interest next to explore their functional relevance. The addition of a phosphate group can affect many properties of a protein, from its activity to protein-protein interactions, and significantly here, its down-regulation. Some specific predictions could be made regarding the potential influences of certain of the novel PKC-ε/δ sites by virtue of their positioning. For example PKC-ε residue S234 lies within the C1 domain, its phosphorylation could therefore be postulated to influence lipid binding and/or association with actin. The candidate PKC-δ phospho-site T141 falls close to the pseudosubstrate sequence, we could speculate that incorporation of a bulky negative charge so close to this autoinhibitory motif could affect PKC-δ conformation and activity. These hypotheses remain to be tested.

Using S234, S316 and S368 mutant constructs, the influence of these phosphorylation events on PKC down-regulation, as well as on other properties, was tested. The following chapter describes the functional analysis of these novel PKC-ε phosphorylation sites.

CHAPTER 6

Characterisation of PKC-ε

Phospho-Site Mutants

6.1 Introduction

Reversible protein phosphorylation is one of the most common forms of post-translational modification, with approximately one third of all cellular proteins estimated to be phosphorylated at any one time (Mann et al., 2002). The introduction of a phosphate moiety to a specific amino acid residue can have profound effects on the modified protein, both in terms of conformation and function; phosphorylation is known to regulate many aspects of protein behaviour, including activity, down-regulation, localisation and binding partner interactions.

It is well established that PKC is regulated at the level of phosphorylation. PKC activity is dependent upon the phosphorylation of three conserved priming sites (T-loop, 'TP' and 'FSY'), which provide permissive signals for subsequent allosteric activation (Parekh et al., 2000). Significantly, these priming site phosphorylation events are inter-related; for PKC-α, 'FSY' phosphorylation is the rate-limiting step for modification at the other sites, and subsequently, in combination with 'TP' site phosphorylation, influences phosphatase sensitivity (Bornancin and Parker, 1996; Bornancin and Parker, 1997). An intimate association also exists between PKC phosphorylation and down-regulation; however, this relationship is cell type/context dependent (Lee et al., 1996; Srivastava et al., 2002). It has been demonstrated that at least two pathways of PKC degradation operate, with different requirements for phosphorylation; one involves the ubiquitination and proteasomal degradation of the mature, fully phosphorylated enzyme, the second, a proteasome-independent mechanism, requires caveolar trafficking and dephosphorylation

(Leontieva and Black, 2004). The localisation of PKC too can be regulated by phosphorylation, for instance, autophosphorylation of PKC-α priming sites affects its carbachol induced membrane occupancy in neuroblastoma cells, by determining sensitivity to DAG (Stensman et al., 2004). In addition, phosphorylation is also known to effect PKC protein-protein interactions, for example, phosphorylation of PKC-δ at Tyr-332 creates a docking site for the SH2 domain of Shc, mediating an interaction relevant to mast cell degranulation (Leitges et al., 2002).

In the previous chapter, three residues were identified within human PKC-ε, S234, S316 and S368, which become phosphorylated, probably via an autocatalytic mechanism, upon PKC activation. This chapter describes the investigation of the functional consequences of phosphorylation at these sites. This work was carried out using the phospho-specific antibodies detailed in the previous chapter, and a set of phosphorylation site mutants. Single S234, S316 and S368 alanine mutants were cloned to abolish each site individually, alongside a triple alanine mutant lacking all three potential phospho-acceptors, and single aspartate mutants were generated to mimic some of the properties of the phosphorylated residues with negative charge. These tools were used to explore the effects of phosphorylation on PKC-ε down-regulation, and on other properties including priming site phosphorylation, activity, localisation and protein-protein interactions.

6.2 Results

6.2.1 Phosphorylation of Other Sites

The phosphorylation of one residue within a protein can influence the subsequent phosphorylation of other sites, and/or its susceptibility to dephosphorylation. Therefore, PKC-ε phosphorylation sites S234, S316 and S368 were investigated with respect to their effects on each other, and on the phosphorylation of the priming T-loop, 'TP' and 'FSY' sites. A panel of single alanine and aspartate mutants were expressed in COS7 cells, treated in the presence or absence of TPA, enriched by

immunoprecipitation and tested with an array of phospho-specific antibodies. Figure 6.1 shows that in each case, mutation of a particular phospho-acceptor residue affects only phosphorylation at that site. Consistent with previous results, S234, S316 and S368 are phosphorylated upon TPA treatment, while phosphorylation of the priming sites is detectable basally, and is not responsive to TPA.

A PKC-ε construct lacking all three newly identified phosphorylation sites, S234A/S316A/S368A (ε^{3A}), was tested in the same way, to determine whether their combined occupation can affect priming site phosphorylation. All of the priming sites were phosphorylated similarly in the wild type and the mutant proteins (Figure 6.2).
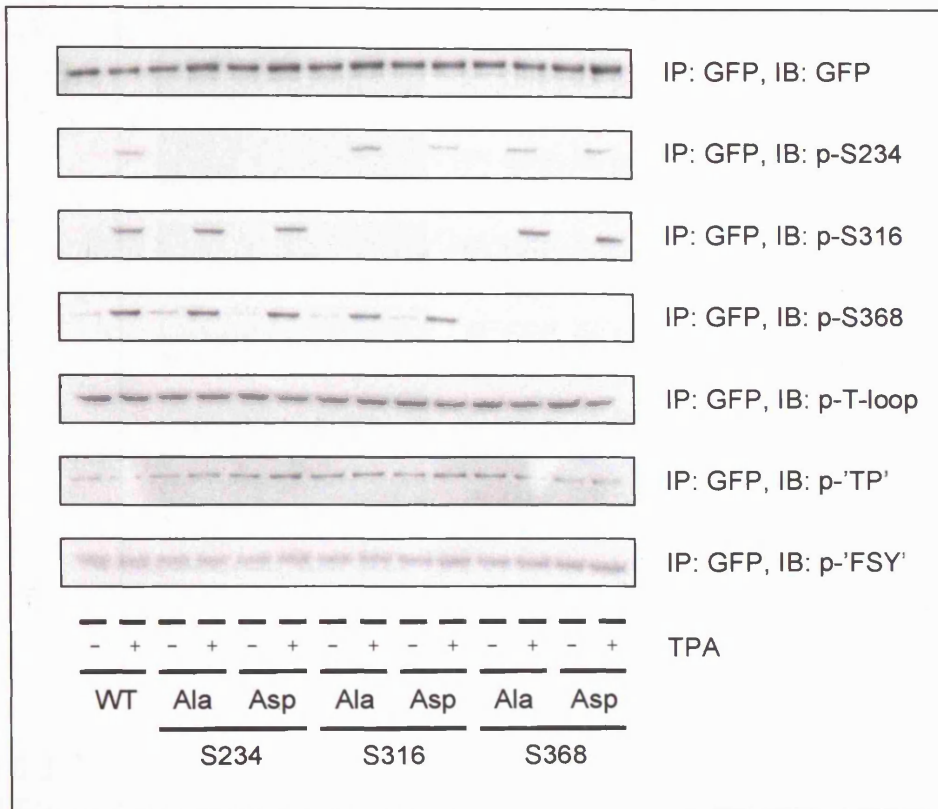
Figure 6.1 Priming Site & Autophosphorylation Site Phosphorylation of wild type, S234A/D, S316A/D & S368A/D PKC-ε. COS7 cells were seeded on 6-well plates and transfected with wild type (WT) PKC-ε and a panel of autophosphorylation site (S234, S316, S368) alanine mutants (Ala) and phosphomimetics (Asp). 24hrs post-transfection cells were treated +/- 400nM TPA for 1hr. Lysates were prepared and subjected to immunoprecipitation with anti-GFP 4E12/8. Samples were analysed by Western blotting using anti-GFP 3E1 and phospho-specific antibodies raised against the T-loop (T566), 'TP' (T710), 'FSY' (S729), S234, S316 and S368 sites (+1μg/ml corresponding dephosphopeptide). Data is representative of two separate experiments.
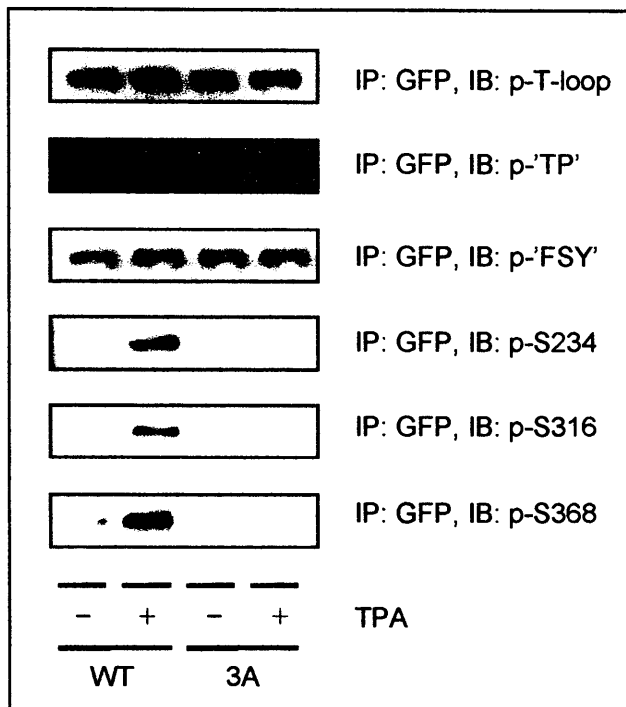
Figure 6.2 Priming Site & Autophosphorylation Site Phosphorylation of wild type PKC-ε & PKC-ε^{3A}. COS7 cells were seeded on 6-well plates and transfected wild type (WT) PKC-ε and a triple alanine mutant (S234A/S316A/S368A; PKC-ε^{3A}). 24hrs post-transfection cells were treated +/- 400nM TPA for 1hr. Lysates were prepared and subjected to immunoprecipitation with anti-GFP 4E12/8. Samples were analysed by Western blotting using phospho-specific antibodies raised against the T-loop (T566), 'TP' (T710), 'FSY' (S729), S234, S316 and S368 sites (+1μg/ml corresponding dephosphopeptide). Data is representative of 3 independent experiments.

6.2.2 Enzyme Activity

Modification by phosphorylation can influence enzyme activity, for example, the PKCα T-loop site must be phosphorylated in order for the protein to be catalytically competent (Cazaubon and Parker, 1993), and the 'TP' site, which is subsequently autophosphorylated, also influences activation state (Bornancin and Parker, 1996). As such, we sought to explore whether phosphorylation of residues S234, S316 and/or S368 affected PKC-ε activity.

COS7 cells were transfected with a panel of PKC-ε wild type and mutant constructs and treated with TPA to induce autophosphorylation. PKC-ε

species were isolated by immunoprecipitation and employed on beads in a series of *in vitro* kinase assays.

Firstly, phosphorylation of MBP was assessed. As shown in Figure 6.3, although some subtle variations were detected in activity between different PKC-ε mutants, there was not a profound loss or gain of activity associated with any particular phospho-residue alteration. We also explored whether autophosphorylation site occupation could affect lipid independent PKC activity. Protamine sulphate is a PKC substrate which directly activates the enzyme through charge effects associated with its binding (Chauhan and Chauhan, 1992). We speculated that changes in PKC phosphorylation status may either negate or enhance the activating effect of protamine, thereby influencing its phosphorylation; however, again, no significant difference was observed between wild type and mutant proteins (Figure 6.4). Finally lipid dependence was tested with respect to the phosphorylation of an optimised PKC substrate, a peptide based upon the pseudosubstrate sequence of PKC-ζ, in which the alanine residue has been replaced with a phosphorylatable serine (Figure 6.5). In these assays, all PKC-ε species were shown to be responsive to lipid activation, and once more, there were no striking differences in activity associated with phospho-site mutation.

Figure 6.3 MBP Phosphorylation Catalysed by Wild Type, S234A/D, S316A/D & S368A/D PKC-ε. COS7 cells were seeded on 6-well plates and transfected with wild type (WT) PKC-ε and a panel of autophosphorylation site (S234, S316, S368) alanine mutants (Ala) and phosphomimetics (Asp). 24hrs post-transfection cells were treated +/- 400nM TPA for 1hr. Lysates were prepared and subjected to immunoprecipitation with anti-GFP 4E12/8. Immunoprecipitated material was washed and incubated in kinase assay buffer with 5μg MBP substrate. Assays were started with $[\gamma^{32}P]$-ATP, incubated at 30°C for 10mins and stopped with the additon of kinase assay sample buffer. Samples were resolved by SDS-PAGE and a) Coomassie stained, exposed to a Phosporimager and counted; or b) analysed by Western blotting using anti-GFP 3E1. Relative activity was determined as a function of PKC-ε immunoreactivity. Data is representative of 2 separate experiments; error bars denote the range of specific activities observed.
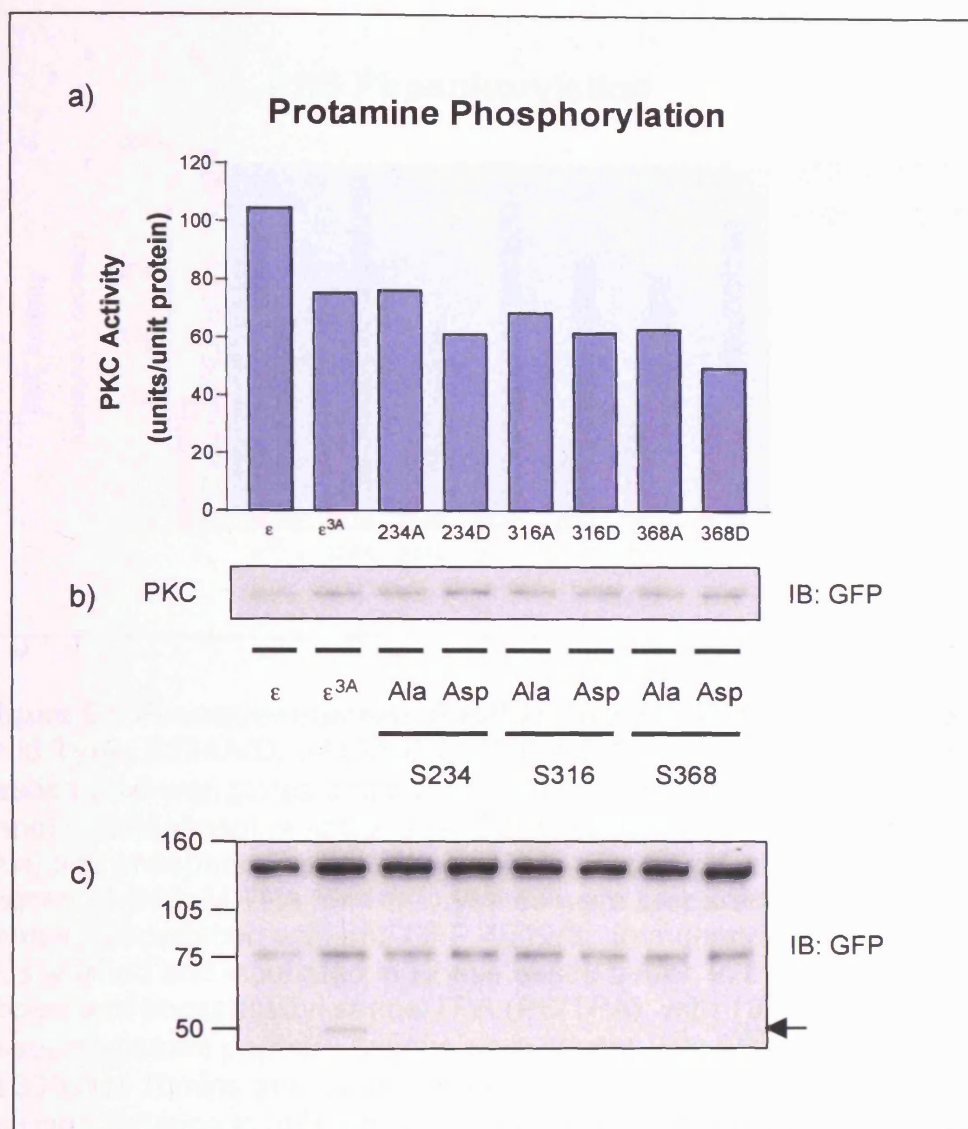
Figure 6.4 Protamine Phosphorylation Catalysed by Wild Type, S234A/D, S316A/D & S368A/D PKC-ε. COS7 cells were seeded on 6-well plates and transfected with wild type (WT) PKC-ε and a panel of autophosphorylation site (S234, S316, S368) alanine mutants (Ala) and phosphomimetics (Asp). 24hrs post-transfection cells were treated +/- 400nM TPA for 1hr. Lysates were prepared and subjected to immunoprecipitation with anti-GFP 4E12/8. Immunoprecipitated material was washed and incubated in kinase assay buffer (-PS/TPA) with 10μg protamine sulphate. Assays were started with $[\gamma^{32}P]$-ATP, incubated at 30°C for 10mins and stopped by a) spotting 15μl onto P81 paper and washing 3x5mins in 30% acetic acid. P81 strips were then counted; or b) adding sample buffer. Samples were resolved by SDS-PAGE and analysed by Western blotting using anti-GFP 3E1. c) represents a longer exposure of the same blot, to highlight the presence of a proteolytic fragment in the ε³ᴬ sample (indicated by arrow). Relative activity was determined as a function of PKC-ε immunoreactivity.
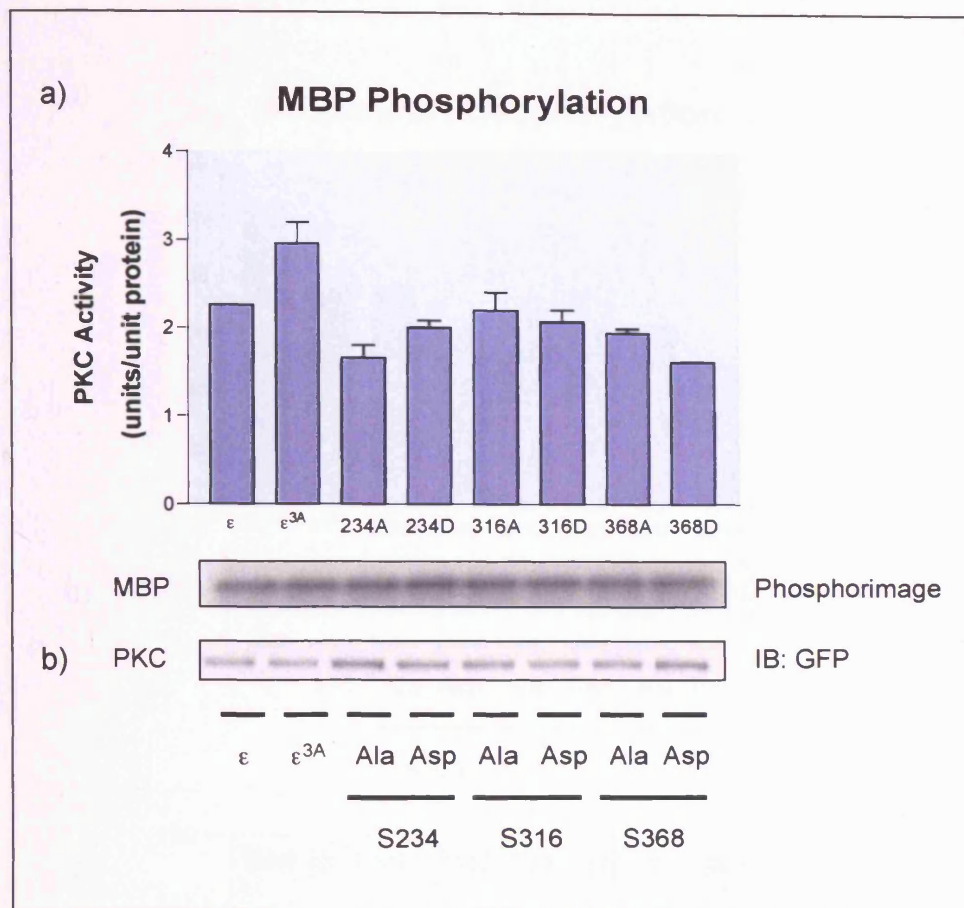
303
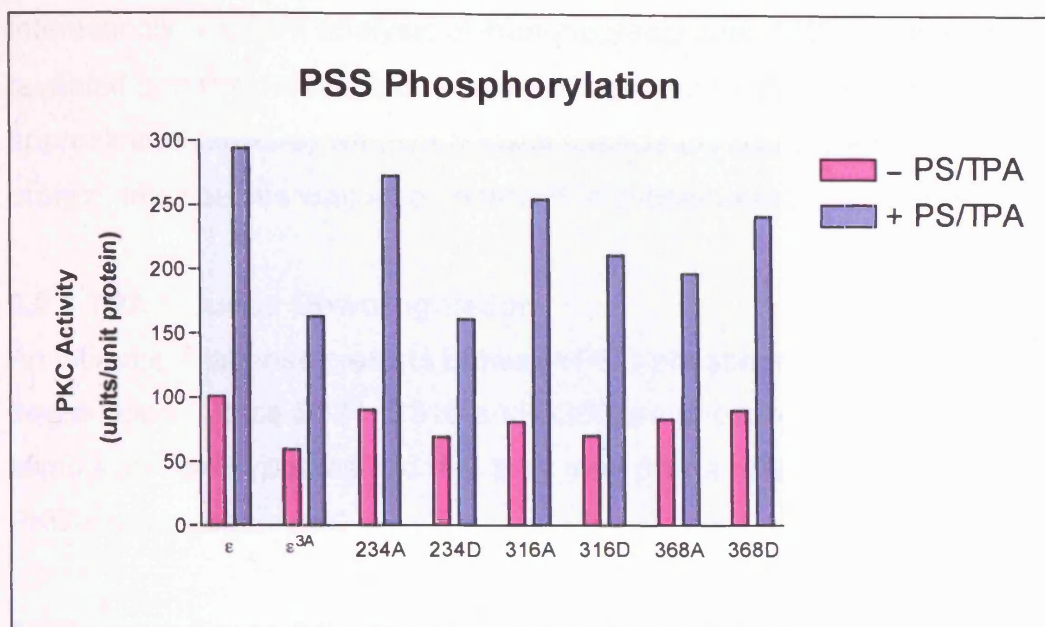
Figure 6.5 Pseuodosubstrate Peptide Phosphorylation Catalysed by Wild Type, S234A/D, S316A/D & S368A/D PKC-ε. COS7 cells were seeded on 6-well plates and transfected with wild type (WT) PKC-ε and a panel of autophosphorylation site (S234, S316, S368) alanine mutants (Ala) and phosphomimetics (Asp). 24hrs post-transfection cells were treated +/- 400nM TPA for 1hr. Lysates were prepared and subjected to immunoprecipitation with anti-GFP 4E12/8. Immunoprecipitated material was washed and incubated in kinase assay buffer, in the presence or absence of phosphatidyl serine/TPA (PS/TPA), with 10μg pseudosubstrate peptide. Assays were started with $[\gamma^{32}P]$-ATP, incubated at 30°C for 10mins and stopped by spotting 15μl onto P81 paper and washing 3x5mins in 30% acetic acid; P81 strips were then counted. Parallel samples were resolved by SDS-PAGE and analysed by Western blotting using anti-GFP 3E1; relative activity was determined as a function of PKC-ε immunoreactivity.

Interestingly, western analysis of immunoprecipitated PKC-ε constructs revealed that the presence of a particular proteolytic product (of approximately 50kDa) was specifically associated with the PKC-ε^{3A} protein; this species was also observed in subsequent experiments.

6.2.3 TPA Induced Downregulation

An intimate relationship exists between PKC phosphorylation and degradation. Since S234, S316 and S368 are phosphorylated upon TPA stimulation, we hypothesised that they may play a role in TPA-induced PKC-ε down-regulation.

As shown in Figure 6.6, TPA induces degradation of PKC-ε in a manner that is inhibited by BIM1 in RCC cells; a parallel blot for actin indicates that TPA and BIM1 have some effects on total protein levels, but that these are less pronounced and occur at later timepoints than the specific depletion of PKC-ε. S234A, S316A and S368A mutants are down-regulated with the same profile as wild type PKC-ε under these conditions.
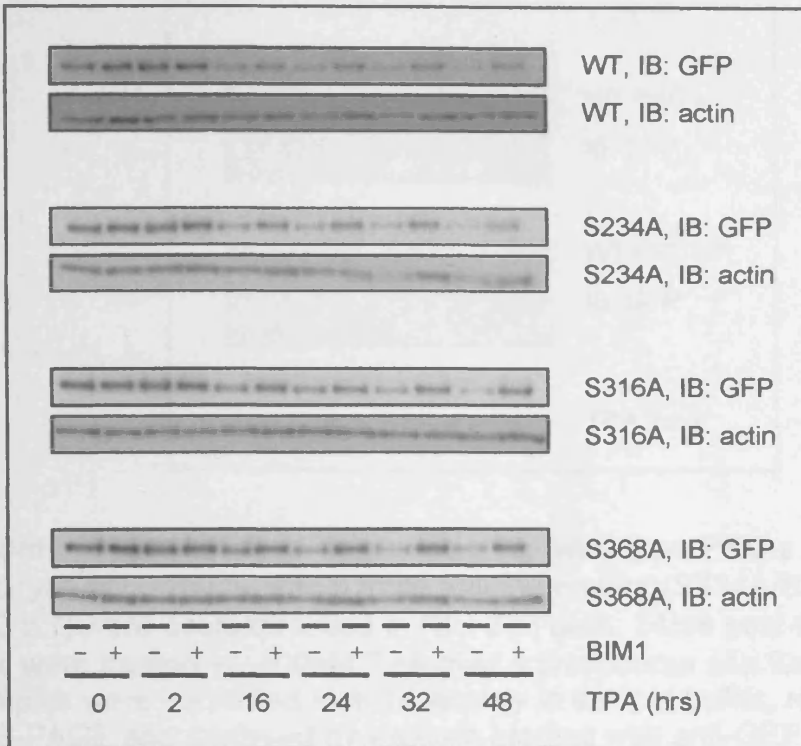
Figure 6.6 TPA-induced degradation of wild type, S234A, S316A & S368A PKC-ε. RCC cells were seeded on 24-well plates and transfected with wild type (WT) PKC-ε and a panel of autophosphorylation site alanine mutants (S234A, S316A, S368A). 24hrs post-transfection cells were pre-treated +/- 1μM BIM1 for 15 mins and incubated +/- 400nM TPA over a timecourse of a further 48hrs. Samples were harvested simultaneously in sample buffer, resolved by SDS-PAGE and analysed by western blotting with anti-GFP 3E1 and anti-actin antibodies.

The combined effects of phosphorylation at S234, S316 and S368 were also investigated by comparing the degradation of wild type PKC-ε and PKC-ε^{3A}, again, no significant difference was detected between wild type and mutant degradation profiles (Figure 6.7).
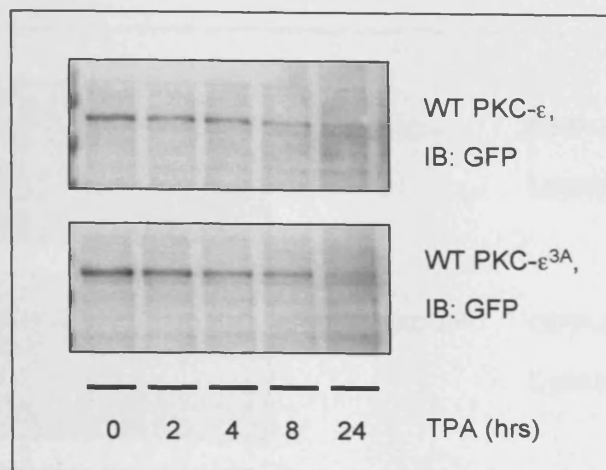
Figure 6.7 TPA-induced degradation of wild type PKC-ε and PKC-ε^{3A}.
Wild type (WT) PKC-ε and a triple alanine mutant (S234A/S316A/S368A; PKC-ε^{3A}) were overexpressed in NIH 3T3 cells. 24hrs post-transfection cells were treated +/- 400nM TPA over a timecourse of a further 24hrs. Samples were harvested simultaneously in sample buffer, resolved by SDS-PAGE and analysed by western blotting with anti-GFP 3E. Data is representative of 2 separate experiments.

PKC-ε and PKC-ε^{3A} polyclonal, stable cell lines were generated by Dr. Angus Cameron, in order to investigate the differences between wild type and mutant proteins more readily. PKC-ε knock out MEFs were stably transfected with either GFP-ε or GFP-ε^{3A}, and subpopulations expressing similar levels of GFP were isolated, through 3 successive rounds of Fluorescence Activated Cell Sorting (FACS), to facilitate comparative analyses.

As shown in Figure 6.8, a relatively long timecourse of TPA treatment was required in order to detect a depletion of GFP-ε proteins under these conditions. The profiles of wild type and mutant degradation were again broadly similar, however basal levels of GFP-ε^{3A} were consistently high in relation to GFP-ε in these cells, despite multiple rounds of FACS sorting to normalise GFP-PKC content, and in some experiments appeared to be slightly more persistent (perhaps as a result of its relative overexpression; see Figure 6.8b).
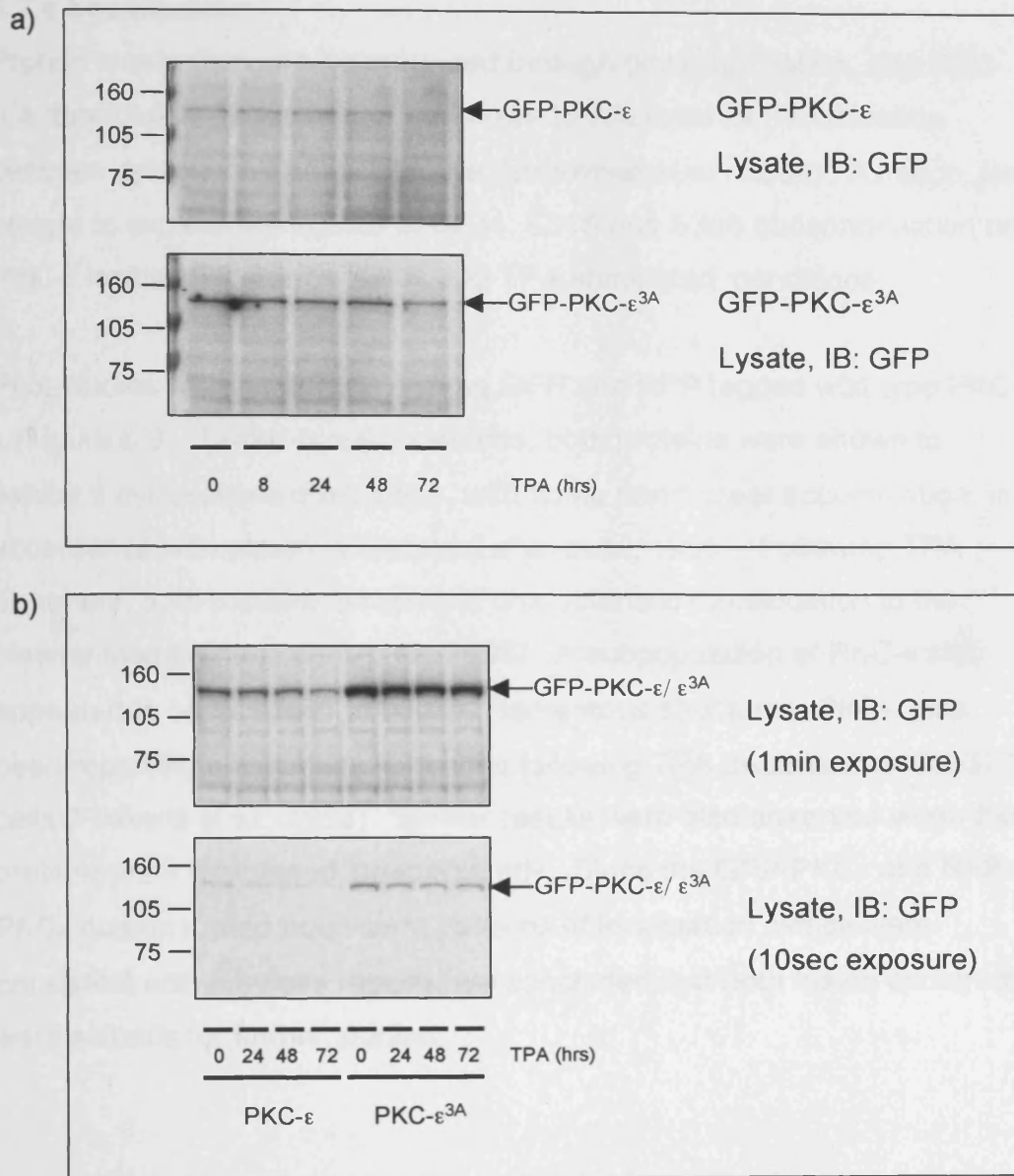
Figure 6.8 TPA-induced degradation of wild type PKC-ε and PKC-ε^3A in MEFs. PKC^-ε/-ε MEF cells stably re-expressing either GFP-PKC-ε or GFP-PKC-ε^3A were seeded on 24-well plates and incubated overnight. Cells were treated +/- 400nM TPA over a 72hr timecourse and harvested simultaneously in sample buffer. Samples were resolved by SDS-PAGE and analysed by western blotting with anti-GFP 3E. Data is representative of at least 3 similarly configured experiments.

6.2.4 Localisation

Protein localisation can be regulated through phosphorylation, and PKC-α autophosphorylation has been shown to influence its translocation between cytoplasm and membrane (Stensman et al., 2004). As such, we sought to explore the effects of S234, S316 and S368 phosphorylation on PKC-ε localisation under basal, and TPA stimulated, conditions.

Pilot studies were undertaken using GFP and RFP tagged wild type PKC-ε (Figure 6.9). Under basal conditions, both proteins were shown to exhibit a cytoplasmic distribution, with some perinuclear accumulation, in accordance with previous reports (Lehel et al., 1995). Following TPA treatment, both proteins underwent characteristic translocation to the plasma membrane (Lehel et al., 1996). A subpopulation of PKC-ε also appeared to be localised to certain filamentous structures; PKC-ε has been reported to associate with actin following TPA treatment in NIH 3T3 cells (Prekeris et al., 1998). Similar results were also observed when the proteins were expressed independently. Since the GFP-PKCε and RFP-PKCε demonstrated equivalent patterns of localisation, which were consistent with previous reports, we concluded that both fusion constructs were suitable for further studies.

Figure 6.9 GFP-PKCε and RFP-PKCε Colocalise Under Basal Conditions & Following TPA Stimulation in HeLa Cells. HeLa cells were seeded on coverslips and co-tranfected with GFP-PKCε and RFP-PKCε. 24hrs post-transfection cells were treated +/- 400nM TPA for 45mins. Cells were fixed and coverslips were mounted and analysed by confocal microscopy (LSM 510, Carl Zeiss Jena). All images comprise representative single 1.0μm 'Z' optical sections. The scale bar is equivalent to 10μm.

Preliminary work was undertaken to try to characterise the filamentous structures to which some of the PKC-ε protein was localising following TPA treatment. We hypothesised that the actin cytoskeleton was a likely candidate, since PKC-ε bears a functional actin binding motif (Prekeris et al., 1996). As shown in Figure 6.10, at least a partial colocalisation was demonstrated between PKC-ε and actin following TPA treatment. Interestingly, this colocalisation occurs in a cytoplasmic compartment, rather than at the membrane; there is clear cortical actin staining which is not positive for PKC-ε.

Since residue 234 lies in close proximity to the actin binding motif (LKKQET, 223-228), we predicted that its phosphorylation in particular might influence PKC-ε localisation. Aspartate mutants were investigated in this context, to try to mimic constitutive phosphorylation. Under basal conditions, all 3 mutants were localised as the wild type protein, and following TPA treatment, all translocated in the same fashion too (Figure 6.11); thus the addition of a negative charge at any of these sites has no discernable effect on localisation under these conditions.
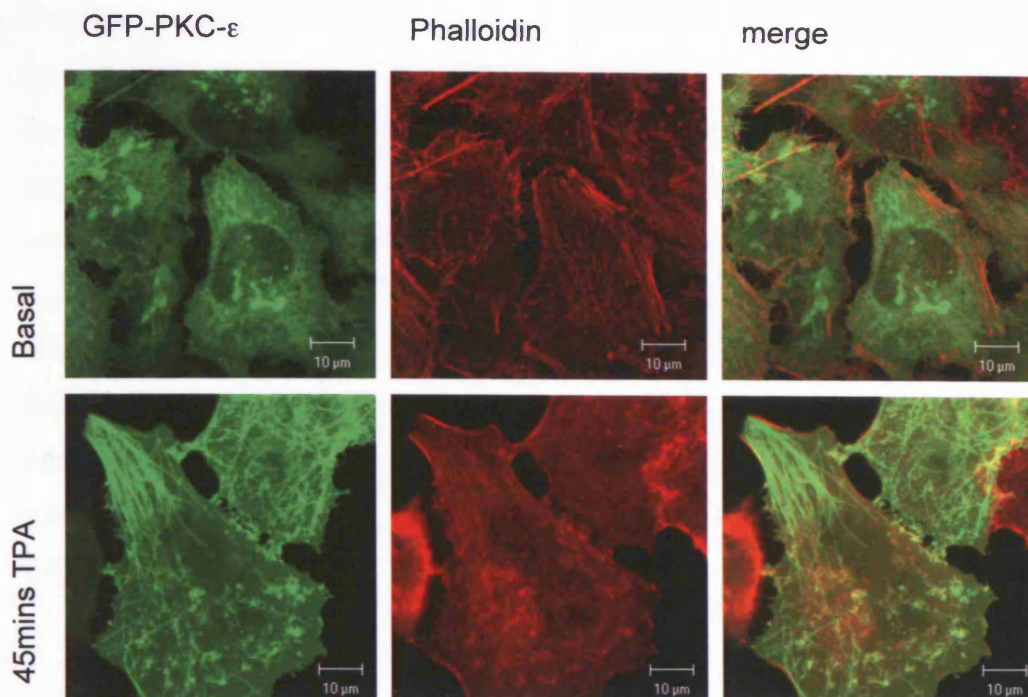
Figure 6.10 GFP-PKCε and Actin Partially Colocalise Following TPA Stimulation in HeLa cells. HeLa cells were seeded on coverslips and tranfected with GFP-PKCε. 24hrs post-transfection cells were treated +/- 400nM TPA for 45mins. Cells were fixed, permeablised, blocked and stained with Alexa Fluor 546 Phalloidin. Coverslips were mounted and analysed by confocal microscopy (LSM 510, Carl Zeiss Jena). All images comprise representative single 1.0μm 'Z' optical sections. The scale bar is equivalent to 10μm.
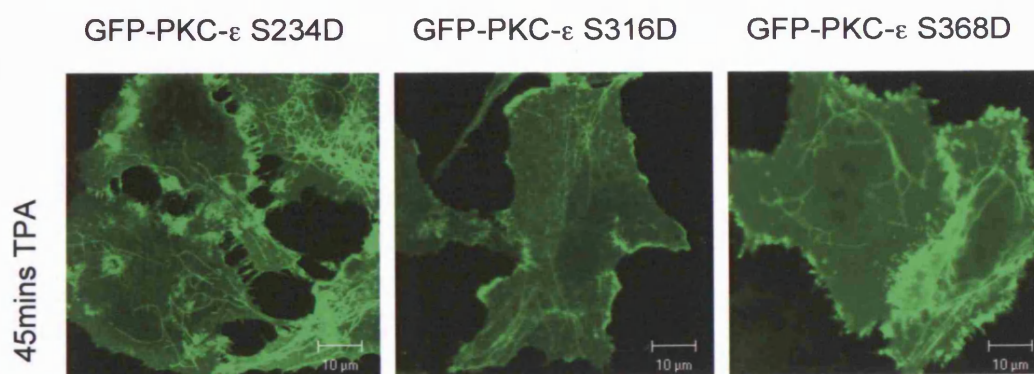
Figure 6.11 GFP-PKCε S234D, S316D and S368D Mutants are Similarly Localised Following TPA Stimulation in HeLa cells. HeLa cells were seeded on coverslips and tranfected with GFP-PKCε mutant constructs. 24hrs post-transfection cells were treated with 400nM TPA for 45mins. Cells were fixed and coverslips were mounted and analysed by confocal microscopy (LSM 510, Carl Zeiss Jena). All images comprise representative single 1.0μm 'Z' optical sections. The scale bar is equivalent to 10μm. The scale bar is equivalent to 10μm.

312

In order to explore whether the combined charge effects of pS234, pS316 and pS368 may influence localisation, the PKC-ε^{3A} mutant was investigated. RFP-PKCε^{3A} was co-expressed in HeLa cells with GFP-tagged wild type protein, in the presence or absence of TPA, and confocal images were collected. Colocalisation was observed under all conditions (Figure 6.12); similar patterns of behaviour were also detected when the constructs were expressed independently. Two fields of view are shown to represent the different compartments to which PKC-ε can localise post-TPA treatment; the central panel demonstrates predominate translocation to the membrane, while the lower panel exemplifies putative actin colocalisation.
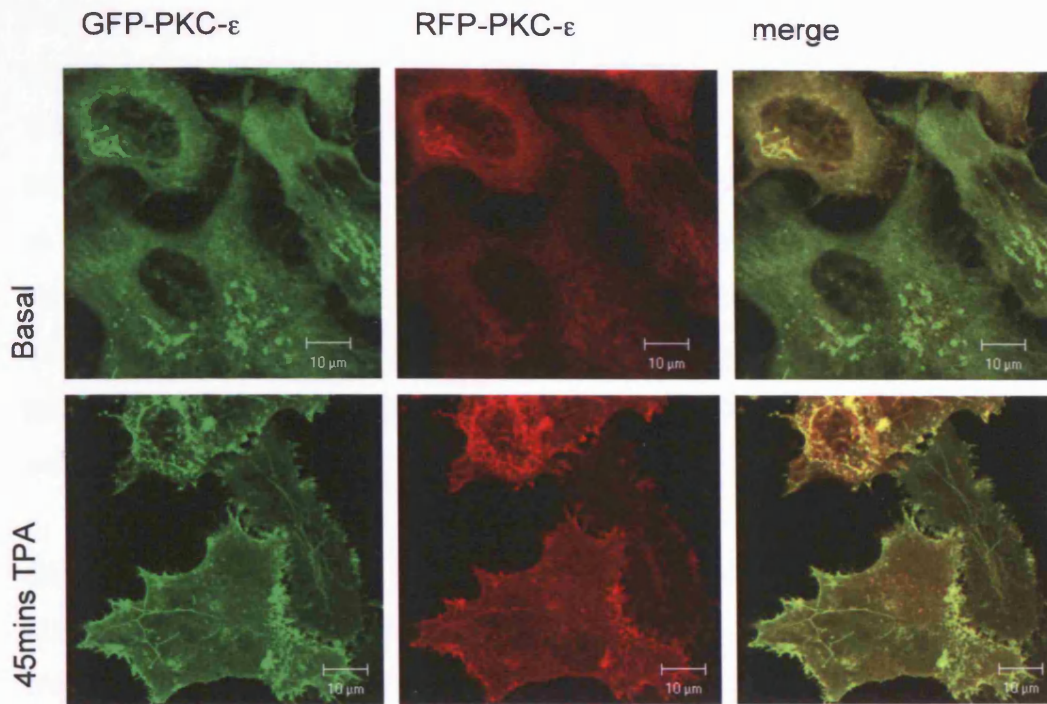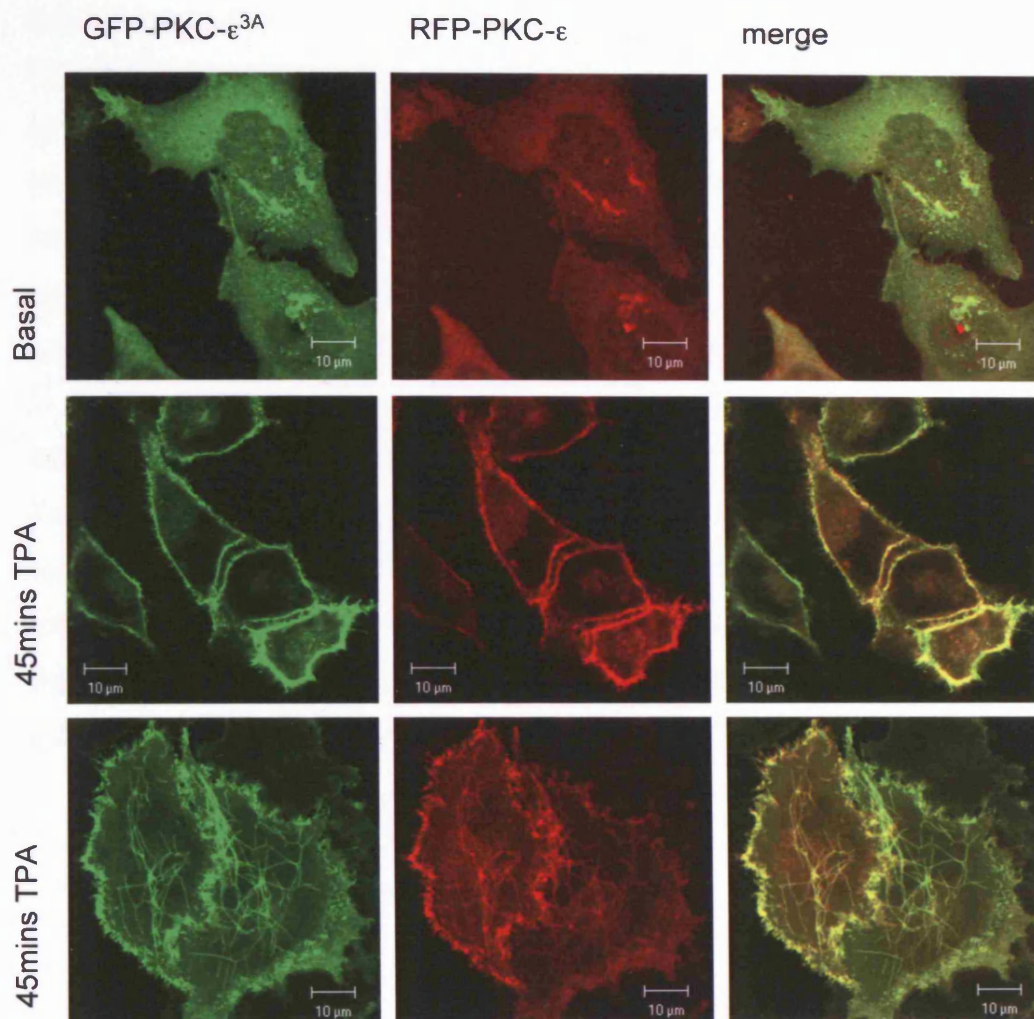
Figure 6.12 GFP-PKCε and RFP-PKCε^{3A} Colocalise Under Basal Conditions & Following TPA Stimulation. HeLa cells were seeded on coverslips and co-tranfected with GFP-PKCε and RFP-PKCε^{3A}. 24hrs post-transfection cells were treated +/- 400nM TPA for 45mins. Cells were fixed and coverslips were mounted and analysed by confocal microscopy (LSM 510, Carl Zeiss Jena). All images comprise representative single 1.0μM 'Z' optical sections. The scale bar is equivalent to 10μM.

6.2.5 Protein-Protein Interactions

Reversible phosphorylation can influence protein-protein interactions, either stimulating association or dissociation. We therefore sought to investigate the impact of phosphorylation at S234, S316 and S368 on the interactions between PKC-ε and some of the binding partners identified by yeast 2-hybrid screening in Chapter 3, VBP1, Fbw7 and 14-3-3β (isolated in a parallel screen by Dr. Adrian Saurin).

6.2.5.1 VBP1 & Fbw7

The interactions between PKC-ε and VBP1/Fbw7 were not found to be responsive to TPA, as such our prediction was that they would not be influenced by mutation at S234, S316 or S368. As shown in Figure 6.13, this hypothesis proved to be correct, with the wild type protein and triple alanine mutant interacting with equal efficiency with both partners.
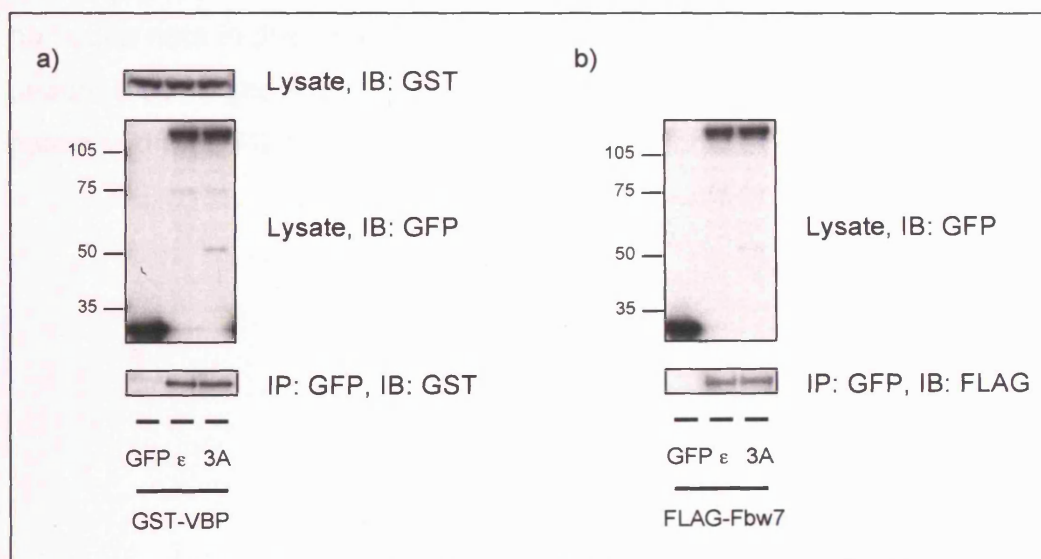
Figure 6.13 Interactions between wild type PKC-ε/PKC-ε^{3A} & VBP1/Fbw7 Detected by Coimmunoprecipitation. COS7 cells were seeded on 6-well plates and transfected with either GFP, GFP tagged PKC-ε (ε) or PKC-ε^{3A} (3A) and a) GST-VBP1 or b) FLAG-Fbw7. 24hrs post-transfection, cells were treated +/- 400nM TPA for 1hr. Cell lysates were prepared and coimmunoprecipitation was performed using anti-GFP 4E12/8. Samples were resolved by SDS-PAGE and analysed by Western blotting with anti-GFP 3E1 and a) anti-GST or b) anti-FLAG antibodies. Data is representative of 2 separate experiments.

6.2.5.2 14-3-3β

14-3-3β was isolated from a yeast 2-hybrid screen, using a PKC-ε regulatory domain bait and a human cardiac cDNA library, by Dr. Adrian Saurin in our laboratory. Dr. Saurin's subsequent work has demonstrated the existence of a well conserved Mode I 14-3-3 binding site in the PKC-ε V3 domain, centred at residue S346. As summarised in Figure 6.14, it has been shown that upon UV induced stress, p38 MAPK phosphorylates PKC-ε residue S350, creating a consensus sequence which permits GSK3 catalysed phosphorylation of S346; phospho-S346 and adjacent residues comprise the 14-3-3 binding site (unpublished data).

Since 14-3-3 proteins typically exist as dimers, and frequently bind to two phospho-residues within the same protein (Bridges and Moorhead, 2005), it was of particular interest to investigate the effects of S234, S316 and S368 phosphorylation on the interaction between 14-3-3β and PKC-ε. Of particular note in this regard is the fact that sequence alignments reveal phospho-S368 and surrounding residues to constitute a loosely conserved Mode II 14-3-3 binding site (see Figure 6.14c).
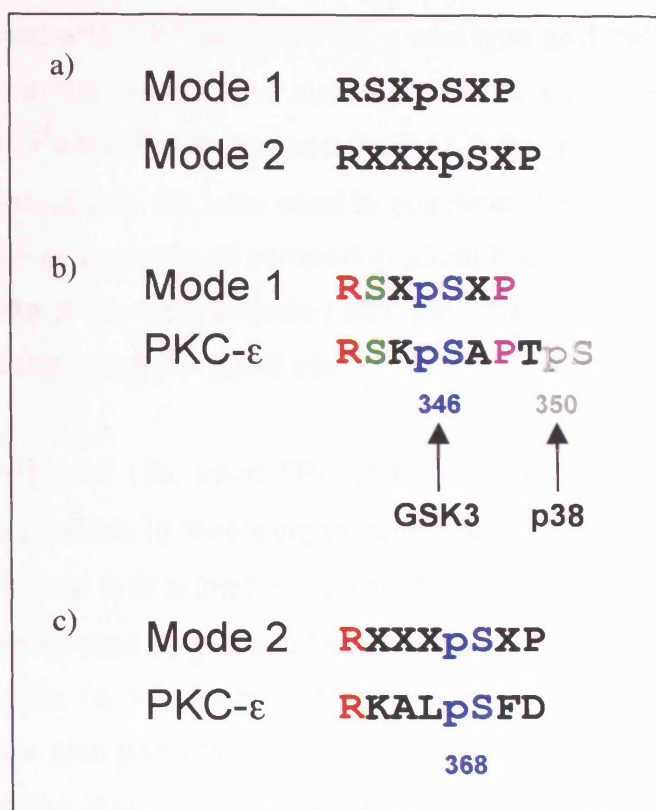
Figure 6.14 14-3-3 Consensus Binding Sites and PKC-ε V3 Domain Phosphorylation Sites. a) Structural analyses, and studies employing an orientated peptide library, have defined two major consensus motifs for 14-3-3 binding: Mode I and Mode II (Yaffe et al., 1997). b) Upon treatment with UV, PKC-ε is subject to phosphorylation by p38 at residue S350. This creates a consensus sequence permitting GSK3 catalysed phosphorylation of residue S346. Phospho-S346 and adjacent residues comprise a well conserved Mode I binding site for 14-3-3 (Dr. Adrain Saurin, unpublished data). c) Autophosphorylated PKC-ε S368 and adjacent residues comprise a loosely conserved Mode II 14-3-3 binding site.

PKC-ε/14-3-3β interactions were explored by GST-pull down. COS7 cells were transfected with GFP-tagged PKC-ε wild type and mutant constructs and incubated in the presence or absence of TPA, with or without a BIM1 pre-treatment. Bacterially expressed GST-14-3-3β, immobilised on Glutathione Sepharose 4B, was used to pull down from these cell lysates, in the presence or absence of competing phosphopeptide; one phosphopeptide comprised a Mode I site, the other represented a 9-mer based around the phospho-S368 site.

As shown in Figure 6.15a, upon TPA treatment, PKC-ε is recovered using 14-3-3β bearing beads to levels significantly above background (GST alone), in a manner that is inhibited by BIM1. This inducible 14-3-3β pull down is fully competed by a Mode I consensus sequence peptide, indicating that the 14-3-3 phospho-binding pocket represents the site of interaction. It is also partially competed by a phospho-S368 based peptide, indicating that this site may play a role in binding. That phosphorylation of S368 is necessary for 14-3-3β binding under these conditions is confirmed through the use of the alanine mutants. While S234A and S316A mutants, like wild type PKC-ε, exhibit basal interaction with 14-3-3β, which is enhanced following TPA treatment, the interaction between 14-3-3β and PKC-ε is completely abrogated in the S368A mutant, in the absence and presence of TPA (Figure 6.15b). It is important to note that Dr. Saurin's work has demonstrated that residue S346 is not phosphorylated under these conditions, and also that mutation of the S368 site does not affect the stress induced phosphorylation of S346. As such, we conclude that the requirement for S368 phosphorylation relates to a direct role for this residue in the *in vitro* binding of 14-3-3β.

a)

Lysate, IB: GFP

Lysate: Coomassie
(GST/GST-14-3-3)

14-3-3 GST PD, IB: GFP

−	+	+	−	+	+	+	+	TPA
−	−	+	−	−	+	−	−	BIM1
−	−	−	−	−	−	+	−	Mode 1 phosphopeptide
−	−	−	−	−	−	−	+	PKC-ε pS368 phosphopeptide

GST   GST-14-3-3

GFP-PKC-ε

b)

Lysate, IB: GFP

Lysate: Coomassie (GST-14-3-3)

GST PD, IB: GFP

| − | + | − | + | − | + | TPA |

GFP- S234A   S316A   S368A

GST-14-3-3
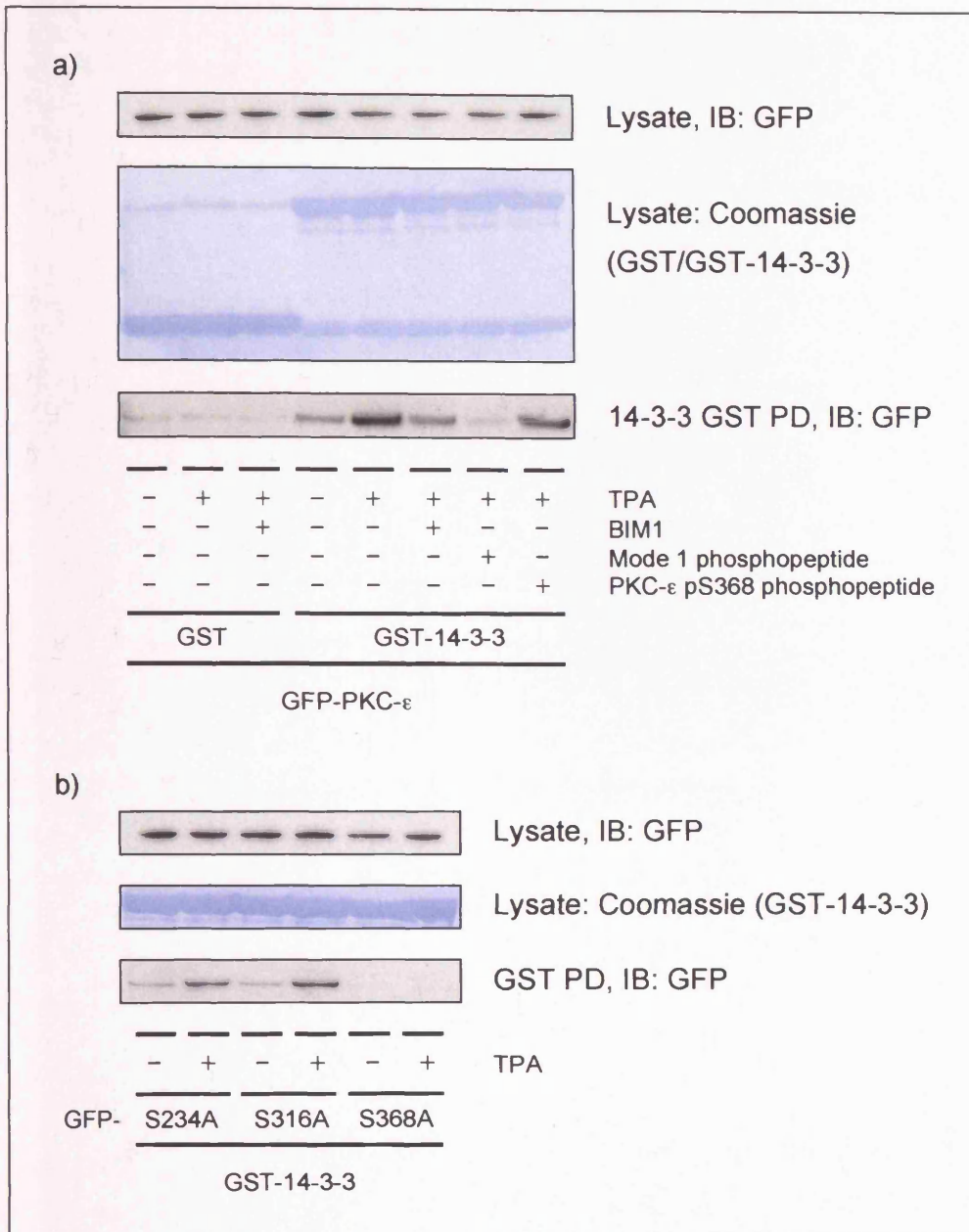
Figure 6.15 Wild type PKC-ε and S234A, S316A and S368A 14-3-3β Binding. COS7 cells were seeded on 6-well plates and transfected with a) GFP-ε or b) GFP-ε S234A, S316A or S368A mutants. 24hr post-transfection, cells were pre-treated +/- 1μM BIM1 for 15mins and stimulated +/- 400nM TPA for a further 45mins. Cell lysates were prepared and incubated with Glutathione Sepharose 4B beads, bearing bacterially expressed GST or GST-14-3-3β, overnight at 4°C with tumbling, +/- 1μg/ml competing phosphopeptide (Mode I: EDRSKpSAPTSP; p368: RKALpSFDN). Samples were washed, harvested in lysis buffer, resolved by SDS-PAGE and analysed by Western blotting using anti-GFP 3E1. Blots were subsequently stained with Coomassie and scanned. Data is representative of 2 separate experiments.

We predict that S346 and S368 comprise a pair of binding sites, which facilitate the recruitment of a 14-3-3β dimer to a single PKC-ε molecule. This working model is summarised in Figure 6.16.
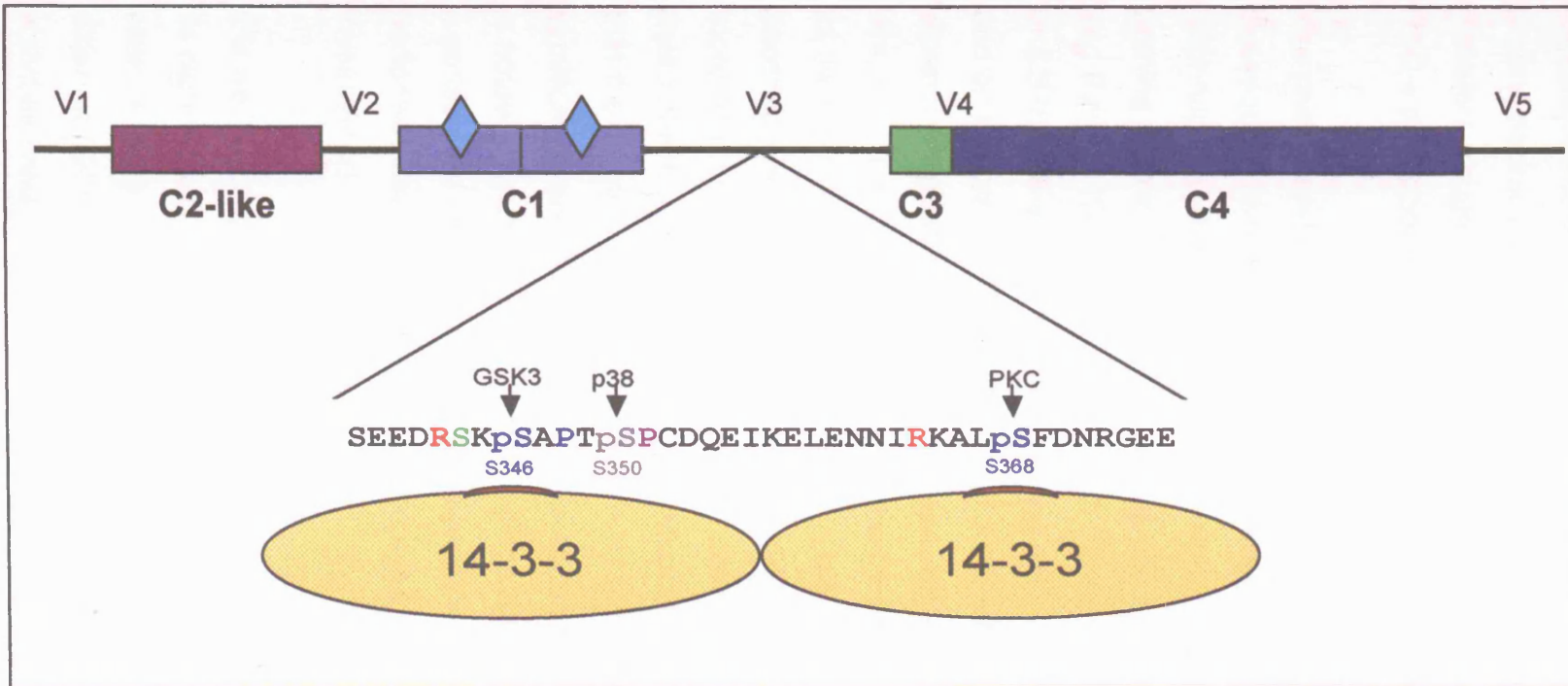
Figure 6.16 Working Model of the Interaction between PKC-ε and 14-3-3β. Phosphorylation of PKC-ε at S350 is catalysed by p38 MAPK. This creates a consensus sequence which permits GSK3 to mediate phosphorylation of S346. Phospho-S346 forms the basis of a Mode I 14-3-3 binding site. S368 phosphorylation is catalysed by PKC itself; phospho-S368 and surrounding residues comprise a loosely conserved Mode II 14-3-3 binding site. Simultaneously phosphorylated S346 and S368 constitute a pair of 14-3-3 binding sites, which facilitate the stable recruitment of a 14-3-3 dimer to a single PKC-ε molecule.

321

6.3 Discussion

The reversible phosphorylation of a protein can mediate significant regulatory effects, influencing a range of properties including activity, protein degradation, localisation and binding partner interactions. We therefore sought to investigate the functional consequences of the novel PKC-ε phosphorylation sites S234, S316 and S368.

The phosphorylation of one residue within a protein can influence the subsequent phosphorylation of other sites, and/or its susceptibility to dephosphorylation; for instance, phosphorylation events at the PKC priming sites are inter-related (Bornancin and Parker, 1996; Bornancin and Parker, 1997). Therefore, PKC-ε phosphorylation sites S234, S316 and S368 were investigated with respect to their effects on each other, and on the priming T-loop, 'TP' and 'FSY' sites. In each case, mutation of a particular phospho-acceptor residue, either to alanine to abolish the site, or to aspartate to mimic its phosphorylation, was shown only to affect its own phosphorylation. Additionally, the removal of all three phosphorylation sites in combination, which would be expected to have more profound effects on the protein post-TPA treatment, yielded no detectable change in priming site occupation. As such, we concluded that the phosphorylation of PKC-ε at S234, S316 and S368 does not significantly alter its phosphorylation status at other established sites. It is noteworthy that phosphorylation of residue S234 is predicted to create a consensus sequence for the phosphorylation of S238 by CK1 (analysis performed using Phosphobase database); this possibility remains to be investigated.

It is well established that an enzyme's phosphorylation status can affect its catalytic competence, for instance, the T-loop, 'TP' and 'FSY' priming sites serve to 'fine tune' PKC activity (Parekh et al., 2000). A panel of different S234, S316 and S368 mutants were tested with respect to their activities towards different classes of PKC substrate *in vitro*, in the presence and absence of lipid cofactors. Despite some subtle variability,

no significant effect of phosphorylation at any of these sites was detected. It would have been worthwhile to also investigate potential effects of these phospho-residues on the process of PKC autophosphorylation, although assays performed in mammalian cells, using phospho-specific antibodies, would suggest that autophosphorylation is neither enhanced nor impaired in any of the mutants (see above).

The kinase assays described are adequate for the investigation of the inherent catalytic competence of these different PKC-ε mutants, however, they are of limited physiological relevance given that the PKC is immobilised, the lipids are represented by artificially prepared micelles rather than membranes, and no additional cellular proteins, which might participate in the regulation of catalysis, are present. It would perhaps have been more informative to investigate PKC-ε wild type/mutant activity in a cell based system, using either a cellular substrate (e.g. PKD (Waldron and Rozengurt, 2003)), or a reporter gene engineered to be regulated downstream of PKC activity. Such a system may have permitted the investigation of more subtle features of the different PKC-ε species, such as the duration, rather than the gross level, of downstream signalling.

A secondary observation made during these *in vitro* kinase assay studies was that the PKC-ε^{3A} mutant appeared to be uniquely susceptible to a proteolytic event, resulting in the detection of a fragment of approximately 50kDa. Since this product was detected from an immunoprecipitation, we must assume either that it represents an N-terminal fragment, with an intact GFP-tag for recovery, or that it interacts and coimmunoprecipitates with, full length PKC-ε. Since it is also detected by western blotting with the GFP antibody, the former possibility seems most likely. Its altered susceptibility to cleavage suggests that the 3A mutant may be conformationally different to the wild type protein, and also to the single mutants; this would appear to represent an effect of the combined charge properties of S234, S316 and S368. It would be of interest to explore this

323

possibility further by investigating PKC-ε³ᴬ thermal stability and susceptibility to oxidation, tryptic digestion and/or phosphatase treatment, which are other markers of conformational alteration (Bornancin and Parker, 1997).

A primary aim of this work was to investigate the process of PKC down-regulation. Previous work has distinguished an association between PKC phosphorylation and degradation, but this relationship appears to be cell type/context dependent. Dephosphorylation has been shown to precede the degradation of PKC-α in LLC-MK2 renal epithelial cells (Lee et al., 1996), PKC-α and PKC-ε in non-immortalised human fibroblasts (Lee et al., 1997), PKC-α in COS7 cells (Hansra et al., 1999) and of PKC-α in MCF7 cells, via a pathway requiring the caveolar trafficking of the protein (Prevostel et al., 2000). Conversely, Srivastava *et al* determined that phosphorylation of PKC-δ was required for its TPA-induced down-regulation in NIH 3T3 cells (Srivastava et al., 2002). Recently, two pathways of PKC-α have been demonstrated to co-exist in IEC-18 rat intestinal epithelial cells, one dependent on phosphorylation, the other on dephosphorylation (Leontieva and Black, 2004). Significantly, PKC activity has also been shown to be necessary for its degradation in numerous studies (Goode et al., 1995; Hansra et al., 1999; Junoy et al., 2002; Kang et al., 2000; Lu et al., 1998; Ohno et al., 1990; Prevostel et al., 2000), with some indications that this input can operate in trans. Against this background, it was of particular interest to investigate the effects of S234, S316 and S368 phosphorylation with respect to PKC-ε degradation.

Experiments performed in RCC cells revealed that PKC-ε could be detectably depleted over a timecourse of TPA treatment, in a manner inhibited by BIM1. Since this mirrors the pattern of S234, S316 and S368 phosphorylation, alanine mutants were assayed in the same way, to examine whether any of the phospho-sites are involved in PKC-ε degradation. The profiles of wild type and mutant down-regulation were

comparable, suggesting that no single site either triggers or impedes PKC-ε this process. To reinforce this finding, it would have been worthwhile to perform a complementary analysis of phospho-site occupation in the wild type protein, over a corresponding timecourse. It would also have informative to test the triple alanine mutant in this system too, to investigate whether the combined removal of the phospho-sites may mediate a more pronounced effect. This possibility, however, was explored in NIH 3T3 cells, and once more, wild type and mutant PKC-ε were shown to be down-regulated in a similar manner.

PKC-ε degradation was further tested using polyclonal, stable cell lines, derived from PKC-ε knock out MEFs, which had been manipulated to express either GFP-PKC-ε or GFP-PKC-ε^{3A} at comparable levels. Again the profiles of wild type and mutant TPA-induced degradation were broadly similar. However, it was noteworthy that basal levels of GFP-PKC-ε^{3A} were consistently high in comparison to GFP-PKC-ε, despite the fact that these cell lines were subjected to multiple rounds of sorting by FACS to normalise the GFP-PKC content. It remains to be determined whether this represents an artefact of the protocol used to derive these cell lines, or a meaningful influence of S234/S316/S368 on PKC-ε turnover in this cell line.

Subcellular localisation comprises another protein property that can be modulated by phosphorylation. GFP- and RFP-tagged PKC-ε constructs were employed in order to determine whether S234, S316 or S368 phosphorylation influences localisation, as visualised by scanning confocal microscopy. Pilot studies confirmed that both proteins localised in accordance with previous reports, demonstrating cytoplasmic and perinuclear distribution under basal conditions (Lehel et al., 1995), and translocation to the membrane following TPA treatment (Lehel et al., 1996). PKC-ε also appeared to colocalise with some filamentous structures; we hypothesised that this might relate to the fact that PKC-ε contains an actin binding motif (Prekeris et al., 1996), and has been

325

shown to associate with the actin cytoskeleton following TPA treatment in NIH3T3 cells (Prekeris et al., 1998). We were able to discern that the TPA induced pattern of PKC-ε distribution at least partially colocalised with actin using a phalloidin stain. Interestingly, this colocalisation was detected along filamentous structures, rather than at the cell periphery, where membrane bound PKC-ε may be juxtaposed with cortical actin. Staining with further markers will enable a more definitive characterisation of this compartment, and further studies will be required in order to determine whether PKC-ε has any morphological influence on actin under these conditions.

Neither phosphomimetic S234, S316 or S368 aspartate mutants, nor an alanine mutant lacking all three phospho-acceptor residues, displayed differential localisation/translocation properties in the experiments performed here; however, a number of other conditions remain to be explored. Firstly, it would be worthwhile to explore localisation patterns in response to other stimuli. Notably, one pathway of PKC-α down-regulation involves caveolar-dependent trafficking to an endosomal compartment; an investigation of PKC-ε in this context would be of interest in terms of both its down-regulation and localisation. Also, PKC-ε inhibition can result in its accumulation in tetraspanin (CD81)-positive, β1 integrin containing, vesicular structures (Ivaska et al., 2002); we could speculate that PKC-ε autophosphorylation may influence this pattern of localisation and explore the distribution of mutant proteins accordingly. Secondly, it would be of interest to directly visualise the S234/S316/S368 phosphorylation sites within the wild type protein, alongside examining the behaviours of mutants lacking them. This would allow us to analyse whether the phosphorylation of a particular site is associated with residency in a particular compartment, and also to mark a subpopulation of active PKC-ε within the cell. Currently, the phospho-specific antibodies produced are not of sufficient purity for use in immunofluorescence studies; however, affinity purification may facilitate their application. Alternatively, a Fluorescent Resonance Energy Transfer (FRET) based

approach could be employed to attain the required specificity, if appropriately conjugated combinations of anti-PKCε and anti-phospho site antibodies were prepared. Finally, all of these studies would benefit from the application of live imaging, as well as standard confocal microscopy on fixed cells. This would permit the investigation of more subtle PKC-ε changes, for instance, in duration of translocation.

It is well established that reversible phosphorylation can affect protein-protein interactions. In some cases, phosphorylation is required to facilitate binding partner recruitment, in other cases it causes dissociation. Phosphorylation of residues S234, S316 and S368 were therefore investigated with respect to their effects on PKC-ε protein-protein interactions; the binding partners which were identified by yeast 2-hybrid analysis in Chapter 3 were tested for interaction with wild type and phospho-mutant proteins. The interactions between PKC-ε and VBP1/Fbw7 were not responsive to TPA, consequently, it would not be expected that their interactions would be affected by PKC-ε autophosphorylation. Consistent with this, wild type PKC-ε and the PKC-ε^{3A} mutant were shown to bind both proteins with equal efficiency. Contrastingly, 14-3-3β, which was identified by Dr Adrian Saurin as a PKC-ε regulatory domain binding partner in a parallel yeast 2-hybrid screen, was found to bind to PKC-ε, *in vitro*, in a TPA responsive manner, which was inhibited by BIM1; this pattern of behaviour reflects that of the autophosphorylation process defined in Chapter 5. The use of a competing peptides revealed firstly that the 14-3-3 phospho-binding pocket was the interface required for this interaction, and secondly, that p-S368 may comprise a point of contact within PKC-ε; notably phosphorylated S368 conforms loosely to the Mode II 14-3-3 binding consensus sequence. The role of S368 in binding 14-3-3β was confirmed using the corresponding alanine mutant; interaction with 14-3-3β was completely abolished in this protein. Recent work in the laboratory has revealed that phosphorylation of residue S368 has no influence on the phosphorylation of S346 (Dr Adrian Saurin, unpublished data);

consequently, we suggest that phospho-S368 plays a direct role in 14-3-3β binding.

Dr Saurin has demonstrated the existence of a well conserved Mode I 14-3-3 binding site centred at PKC-ε residue S346; phosphorylation at this site is mediated by the sequential activities of p38 MAPK and GSK3. It is well established that 14-3-3 dimers often bind to two sites within the same protein (Bridges and Moorhead, 2005), as such, we could hypothesise that both S346 and S368 represent functional 14-3-3 binding sites. Commonly, one binding motif within the target protein conforms to a high affinity Mode I site and interacts with the first 14-3-3 subunit; this is referred to as the 'gatekeeper'. The second site is often less well conserved, but will interact with the remaining 14-3-3 monomer by virtue of its close proximity, thereby stabilising the complex; its lower affinity may be physiologically relevant, permitting a degree of dissocation (Yaffe, 2002).

Our current working model proposes that the Mode I 14-3-3 binding motif at residue S346 constitutes the gatekeeper site under physiological conditions. Secondary interaction with autophosphorylated S368 is likely to stabilise the PKC-ε/14-3-3β complex. Since both of these sites are unique to PKC-ε among the PKC superfamily, this interaction may contribute to isoform specificity.

14-3-3 dimers can generally elicit three distinct effects on binding partners: conformational change, steric hindrance and dimerisation (Bridges and Moorhead, 2005). Preliminary work from Dr Saurin suggests that 14-3-3 binding confers lipid independent activity upon PKC-ε, this would be consistent with a conformational change in which 14-3-3 binding within the V3 hinge region holds PKC-ε in an open conformation, such that the kinase domain is inaccessible to the inhibitory pseudosubstrate motif. It will be of interest to explore the cellular changes associated with this complex formation and change in PKC

activity. It may also be of value to test whether 14-3-3β is able to mediate any other effects on PKC-ε. For example, perhaps under certain conditions each 14-3-3 dimer may bind to just one site per PKC-ε molecule; in this way it could facilitate dimerisation between two PKC-ε molecules, or trans-dimerisation, between PKC-ε and other 14-3-3 targets.

Previous studies have reported on physical and functional interactions between different 14-3-3 and PKC isoforms. There have been conflicting findings with respect to the functional consequences of the PKC and 14-3-3 interaction. Some studies have determined that 14-3-3 is inhibitory towards PKC (Matto-Yelin et al., 1997; Meller et al., 1996; Toker et al., 1992), while others have demonstrated PKC activation associated with 14-3-3 binding (Acs et al., 1995; Tanji et al., 1994). This disparity is likely to result in part from the use of different PKC isoforms, cell types and assay systems.

None of the published investigations regarding the interactions between 14-3-3 and PKC have described a phosphorylation dependent mechanism. In fact, Dai and colleagues identified PKC-ε S346 as a candidate Mode I site, and excluded its involvement in binding under their conditions through the use of a corresponding competing phosphopeptide (Dai and Murakami, 2003). A phosphorylation independent 14-3-3 binding site has been mapped to the PKC C1 domain (Matto-Yelin et al., 1997). It is of note, however, that in those studies which detected a degree of PKC isoform specificity, it was always the PKC-ε isotype which was implicated; we could speculate that in these studies, the phosphorylation dependent interaction between PKC-ε and 14-3-3 was in operation in parallel to less specific, C1 domain mediated binding. For instance, Acs et al demonstrated that recombinant 14-3-3ζ was able to activate various PKC isoforms by approximately two-fold, but had a 5-fold effect on PKC-ε; significantly, these assays were performed in the absence of lipid, and therefore agree with Dr Saurin's observations that

14-3-3 can confer lipid independent activity upon PKC-ε (Acs et al., 1995). Another study revealed that PKC-α and PKC-ε become associated with 14-3-3ζ in PC12 cells, following neuronal differentiation triggered by NGF. Intriguingly, while both isoforms were recovered by immunoprecipitation, only PKC-ε was shown to be constitutively activated as a result (Gannon-Murakami and Murakami, 2002). It would be of interest to determine whether S346 and/or S368 residues are phosphorylated in these cells following NGF treatment, as a means of exploring the nature of the 14-3-3ζ/PKC-ε interaction under these conditions.

In conclusion, the consequences of phosphorylation at residues S234, S316 and S368 were explored with respect to a broad panel of PKC-ε properties. Autophosphorylation was judged to have no significant effect on the phosphorylation of other PKC-ε sites, on enzyme activity targeted towards a number of different substrates, or on localisation under the conditions tested. Phosphorylation at these sites also appeared not to be involved in the pathway of TPA-induced degradation; this elusive process remains to be characterised. However, phosphorylation of PKC-ε at residue S368 was shown to influence the binding of 14-3-3β; thereby linking a phosphorylation site identified in Chapter 5, to one of the binding partners identified through work described in Chapter 3. It is likely that pS368 operates in combination with a second phospho-site at residue S346, to facilitate the recruitment of a 14-3-3β dimer. This complex would appear to bear constitutive PKC-ε activity, and it will be of considerable interest to determine the cellular responses which it mediates.

CHAPTER 7

Discussion

7.1 Overview

The work presented in this thesis was motivated by the theme of PKC down-regulation. It is well established that the chronic activation of the cPKCs/nPKCs frequently leads to their inactivation (Ballester and Rosen, 1985; Stabel et al., 1987), through an increase in rate of degradation (Young et al., 1987). It has been suggested that the ability to induce a particular profile of PKC isoform degradation is inherent to the tumour promoting effects of the phorbol esters (Young et al., 1987). Significantly, the ability of Bryostatin 1, an alternative PKC activator, to inhibit TPA-induced tumour promotion, correlates with the differential down-regulation of various PKC isoforms (Szallasi et al., 1994).

The ubiquitin/proteasome system has been clearly implicated in the agonist-induced down-regulation of PKC (Lee et al., 1996), but to date, only one E3 ubiquitin ligase, VHL/Elongin C/Elongin B/Cullin 2 (VCB-Cul2), has been demonstrated to target PKC (Okuda et al., 2001). Studies were therefore undertaken to try to identify PKC specific E3 ubiquitin ligases by yeast 2-hybrid analysis.

PKC activity is required for its agonist induced degradation (Goode et al., 1995; Kang et al., 2000; Srivastava et al., 2002). Additionally, its phosphorylation status is influential with respect to this process; 2 pathways have been identified, one involving the ubiquitination and subsequent proteasomal degradation of the mature, fully phosphorylated enzyme, the second, a proteasome-independent mechanism, requires caveolar trafficking and dephosphorylation (Leontieva and Black, 2004). Together, these observations led us to predict that PKC

331

autophosphorylation may serve to target the enzyme for ubiquitin-mediated degradation at the proteasome, and so we sought to map sites which may behave as phospho-degrons.

Although yeast 2-hybrid analysis successfully identified PKC-ε binding partners with associations to the ubiquitin/proteasome system, including VBP1 and Fbw7, no evidence was obtained to implicate these proteins in PKC down-regulation; the potential role of Fbxl15 remains to be tested. Similarly, while novel phosphorylation sites for both PKC-ε and PKC-δ were mapped, and validated in mammalian cells, there was no evidence that they played critical roles as phospho-degrons. Thus, the mechanism(s) of agonist induced PKC down-regulation remain to be elucidated.

Nevertheless, these studies catalysed the exploration of some fundamental properties of PKC-ε, and have proved informative with respect to further defining aspects of PKC regulation and function. The analysis of Fbw7 as a candidate PKC E3 ligase was followed by its investigation as a potential substrate. This led to the identification of a novel phosphorylation site, specific to the Fbw7α isoform, with a potential role in the post-translational regulation of this key tumour suppressor. Additionally, the newly identified phosphorylation sites within PKC-ε and PKC-δ constitute useful markers of PKC activation status, and may have important functional consequences. Most significantly, a relationship has been established between regulation of PKC-ε at the level of phosphorylation and protein-protein interaction, linking the two branches of this project, with the finding that phosphorylation at residue S368 is required for the recruitment of 14-3-3β.

7.2 PKC Degradation

The work undertaken in this project was not successful in identifying either a PKC specific E3 ligase, or a phospho-degron implicated in its targeting for degradation. As such, the intriguing mechanism(s) of agonist induced PKC down-regulation remain to be determined. Since the rather broad methodologies employed here provided such limited insight into the process, it seems reasonable to suggest that future investigations may benefit from a more focussed approach. By building a functional criterion into a screen for E3 ligases, it might be possible to target proteins involved in PKC down-regulation more directly. For instance, the propensity of mammalian PKCs to be down-regulated in *S.pombe* following chronic phorbol ester treatment could be exploited as the basis for a genetic screen (Goode et al., 1994); mutants lacking the capacity to degrade PKC would be immediately implicated in the process of agonist-induced degradation. Alternatively, the pathway(s) operating in mammalian cells in response to TPA could be partially dissected through the use of dominant negative ubiquitin/proteasome associated constructs; for example, the Cul1 mutant (Cul1^{DN}) lacks an Rbx1 binding site, and therefore sequesters Skp1/F-box protein complexes, and stabilises SCF targets (Ye et al., 2004). If Cul1^{DN} were to protect PKC from TPA induced degradation, the SCF complex would be implicated, and more directed studies could be exploited to define the specific F-box protein involved; for instance, RNAi could be used to knock-down the F-box protein complement.

The further characterisation of the mechanism of PKC down-regulation through such studies will be of considerable interest, providing insight into both the regulation of PKC, and the tumour promotion process.

7.3 PKC Binding Partners

The yeast 2-hybrid system established as part of this project proved to be effective for identifying PKC-ε binding partners. This is evidenced both by the fact that a known interacting protein, NELL2, was isolated by the screen, and also by the validation of Fbw7 and VBP1 interactions with PKC-ε, by coimmunoprecipitation in mammalian cells. A number of other proteins were classified as candidate PKC-ε binding partners using this approach, and it may be informative to explore these further. For instance, the receptor-type protein tyrosine phosphatase-σ (PTPσ, clone 104) represents an intriguing example. It has been shown previously that PKC-δ can regulate the activity of PTPα (Brandt et al., 2003), and PKN 2 has been associated with PTP-BL (Gross et al., 2001); as such, it would be interesting to establish whether PKC-ε may also participate in the control this class of proteins, which play a significant role in modulating signal transduction pathways.

Although positive results were obtained using this 2-hybrid system, it is important to acknowledge that there were a number of limitations to the approach. Some of these problems were specifically associated with this particular screen, and could be improved upon in future studies of PKC protein-protein interactions. Others are inherent to the yeast 2-hybrid system itself.

It could be argued that one disadvantage of the screen employed in this work is the nature of the PKC-ε bait itself. The full length protein is likely to exist in an inactive state under basal conditions in yeast, and may therefore be limited in its capacity to interact with partners that require an open conformation. One way to address this issue would be to employ a constitutively active bait, mutated at the inhibitory pseudosubstrate site. Alternatively, isolated regulatory and catalytic domains, which are conformationally more exposed than the full length protein, may be used. This latter strategy was exploited by Dr Adrian Saurin in our laboratory.

Using the PKC-ε regulatory domain bait described in Chapter 3 Dr. Saurin identified 14-3-3β as a binding partner. Interestingly, the interaction between PKC-ε and 14-3-3β which was subsequently characterised in mammalian cells required the phosphorylation of two isoform-specific sites within the PKC-ε hinge region, S346 and S368. We have not retrospectively tested whether these sites are occupied in yeast. Since 14-3-3 proteins are also known to interact, less selectively, with the PKC C1 domain (Dai and Murakami, 2003; Matto-Yelin et al., 1997), it is possible that this binding partner was identified by virtue of one mode of interaction, which fortuitously led to elucidation of another.

A further issue relating to the study of PKC by yeast 2-hybrid analysis is the localisation of the system to the yeast nucleus. Since PKC is activated at the membrane, it follows that many functionally significant interaction partners may occur in this compartment, and in fact depend upon this localisation for binding. One way to circumvent this issue in future work would be to exploit a modified 2-hybrid protocol; for instance, the split-ubiquitin system is specifically designed to enable the detection of binding partners at the membrane (Iyer et al., 2005).

Another profound problem associated with the yeast 2-hybrid screen undertaken was the poor reproducibility achieved. It is well documented that results obtained using this approach can be variable, only 141 interactions have been detected in common between two large scale 2-hybrid screens performed in yeast (Ito et al., 2001). However, it would appear that this inherent variability is exacerbated by the negative influence of PKC on yeast proliferation rates (Goode et al., 1994). In addition, the yeast 2-hybrid system also tends to generate numerous false positive and false negative results (Zhu et al., 2003).

Given the limitations discussed above, as well as the significant advances which have been made in the field of proteomics in recent years, it would be worthwhile to investigate PKC protein-protein interactions using a

more sophisticated approach. An effective high-throughput system has recently been described by Barrios-Rodiles and colleagues, which has facilitated the dynamic analysis of the TGFβ signalling network (Barrios-Rodiles et al., 2005). It would be of interest to explore PKC signalling in a similar way. As noted with respect to studies of degradation, it would also be preferable to build a layer of functional relevance into the primary screen, for example, by exploring differential interactions before and after a physiologically relevant stimulus.

7.4 Fbw7 Phosphorylation

The Fbw7 protein was identified as a PKC interacting protein by yeast 2-hybrid analysis and subsequently shown to represent an efficient substrate *in vitro*. A novel phosphorylation site was identified in the isoform specific N-terminus of Fbw7α at S18, and this site was shown to be phosphorylated in cells treated with Calyculin A. It will be critical next to establish whether Fbw7α S10 is also phosphorylated; the simultaneous occupation of both of sites could have even more profound functional consequences. This will be readily testable *in vitro* using the peptides which we have synthesised, corresponding to this region.

It will also be significant to explore whether PKC can catalyse the phosphorylation of S18 in cells. Inhibitor studies have excluded a role for cPKC/nPKCs in response to Calyculin A, but aPKC and PKN selective inhibitors remain to be tested; notably aPKC-ζ was recovered with particularly high efficiency from an Fbw7 immunoprecipitation. Other stimuli should also be screened for their ability to induce Fbw7α S18 phosphorylation. It would be worthwhile to focus pilot studies towards conditions which are known to induce PKC nuclear translocation, since Fbw7α is localised to this compartment. For instance, apoptotic stimuli (DeVries et al., 2002), hypoxia (Mizukami et al., 2000) and treatment with NGF (Wooten et al., 1997) have all been shown to induce the nuclear localisation of various isoforms. Given the inhibitor profile described

above, it is intriguing that the aPKCs have been shown to shuttle between cytoplasm and nucleus (Perander et al., 2001). Also, bearing in mind the association between Fbw7 and cell cycle control, it is noteworthy that PKC-δ translocation to the nucleus occurs specifically in S-phase in BL6T melanoma cells (Perego et al., 2002).

It will be of considerable interest to explore the functional consequences of Fbw7α phosphorylation. The phospho-acceptor residue S18 lies within a particularly significant part of the Fbw7α protein; this unique N-terminal region is responsible for isoform specific properties. Importantly, it contains one of two nuclear localisation signals (NLS 11-14), which can mediate Fbw7α nuclear localisation (Welcker et al., 2004). It is tempting to speculate that phosphorylation of Fbw7α at nearby S18 (and perhaps S10 too) may disrupt its nuclear localisation, under conditions where NLS 11-14 predominates. This would be consistent with the effects of PKC phosphorylation close to NLSs in numerous other proteins, including LIMK2 (Goyal et al., 2005) and the aryl hydrocarbon receptor (Ikuta et al., 2004). This hypothesis may be tested using a mutant construct which lacks the second NLS, and is therefore dependent upon NLS 11-14 for nuclear localisation. This mutant could be treated in the presence or absence of Calyculin A and studied by immunofluorescence, and/or modified further with the incorporation of a mutagenic alanine or phosphomimetic aspartate at S18 (and/or S10).

The regulation of E3 ligase activity through localisation is an emerging theme. For instance, SV40 large T antigen binding causes the mislocalisation of Fbw7γ, and interferes with the down-regulation of the client protein cyclin E (Welcker and Clurman, 2005). Similarly, the nucleolar architecture has been shown to detain MDM2 and VHL in response to regulatory cues, permitting the accumulation of their substrates elsewhere (Mekhail et al., 2005). If phosphorylation of Fbw7α proves to modulate localisation, it will be significant to determine the downstream effect on Fbw7α mediated substrate degradation.

7.5 PKC Autophosphorylation

In addition to identifying a novel PKC substrate, the work presented also defined previously unrecognised sites of autophosphorylation within PKC-ε (S234, S316, S368) and PKC-δ (S299, S302, S304). The PKC-ε sites were most thoroughly studied; PKC-δ awaits similar investigation.

The PKC-ε phosphorylation sites were identified from purified PKC-ε, phosphorylated *in vitro,* and were subsequently detected upon TPA stimulation in mammalian cells, using phospho-specific antibodies. We did not prove exhaustively that S234, S316 and S368 were the only sites of autophosphorylation under these conditions. For completion, it would be valuable to determine whether radiolabelled phosphate incorporation can be detected in the PKC-ε S234A/S316A/S368A triple alanine mutant, as a means of checking for additional sites; the mutant exhibits a similar level of activity as the wild type, such that this is achievable. If evidence is obtained for the phosphorylation of additional sites under these conditions, it may be necessary to devise an alternative phosphopeptide mapping strategy with which to map them. A different protease, such as AspN, could be employed to generate a modified selection of peptides, and/or an alternative mass spectrometry system could be tested.

The studies undertaken to date have focussed on overexpressed PKC-ε in response to phorbol ester treatment. As the PKC-ε knock-out phenotype includes defects in innate immunity, it is potentially significant that Dr. Amir Faisal in our laboratory has also observed elevated phosphorylation of S368 in response to lipopolysaccharide stimulation of RAW264.7 cells. However, again, this observation was made using cells overexpressing PKC-ε. Ideally, we would hope to investigate the phosphorylation of endogenous PKC-ε in response to physiological stimuli. In order to achieve this, it will be necessary to optimise an

338

immunoprecipitation protocol to allow the enrichment of sufficient PKC-ε for detection, and/or to affinity purify the antisera.

The catalytic mechanism responsible for the phosphorylation of PKC-ε at PKC-ε S234, S316 and S368 remains to be fully characterised. Several lines of evidence support the notion that these sites can be autophosphorylated, but it is not yet clear whether this involves an intra- or inter- molecular process. This may relate to another interesting question regarding the nature of PKC activity, namely whether PKC undergoes dimerisation, and if so, whether this is of functional significance. It would be productive to exploit the GFP/RFP-tagged PKC-ε constructs generated during this project, to explore these possibilities through Fluorescent Resonance Energy Transfer (FRET) studies.

Work was carried out to establish the functional consequences of phosphorylation at these sites. No significant effect was detected with respect to activity, down-regulation or localisation, but a requirement was established for S368 phosphorylation in 14-3-3β recruitment. We could speculate that autophosphorylation may participate in feedback control of PKC activity, mediating 'fine-tuning' rather than gross effects, on signal duration or localisation. As such, it will be important to follow these relatively crude analyses with more subtle studies, for example using live imaging to analyse the timecourse of mutant versus wild type PKC translocation.

A consideration of the placement of the phosphorylation sites leads to further hypotheses regarding the properties that they may influence. For example, S234 lies between the C1a and C1b domains, and so it is reasonable to suggest that it may therefore influence actin binding or membrane association. It is also juxtaposed to a sequence critical for the induction of neurite outgrowth by PKC-ε, and it will be interesting to explore, for example, whether an aspartate mutant at S234 is altered in its capacity to induce this process (Ling et al., 2005).

339

Regardless of the functional significance of these sites, they have important implications as markers of PKC activation. They can be detected using the phospho-specific antibodies raised, and exploited both experimentally, allowing the detection of a specific subpopulation of the enzyme, and clinically, facilitating the analysis of disease tissues for aberrant PKC activation (Ng et al., 1999). Since PKC comprises an enzyme activity subject to acute allosteric regulation, it may well be more informative to analyse its activation state than its protein concentration in addressing its the potential involvement in disease (Parker, 1999). This strategy was pioneered by Ng and colleagues, who employed a autophosphorylation site marker of PKC-α activation, pT250, to screen breast tumour samples. To obtain the necessary specificity, FRET between appropriately conjugated anti phospho-T250 and anti total PKC-α was measured by Fluorescence Lifetime Imaging Microscopy (FLIM). Activated PKC-α was identified in 11 out of 23 specimens, and notably, activation was not shown to correlate with overexpression in all cases (Ng et al., 1999). It will be of interest to employ a similar approach in order to analyse the roles of PKC-ε and PKC-δ isoforms in disease.

7.6 PKC & 14-3-3

14-3-3β was identified as a PKC-ε regulatory domain binding partner by yeast 2-hybrid analysis performed by Dr. Adrian Saurin. Dr Saurin subsequently defined a phosphorylated, Mode 1 14-3-3 binding site at PKC-ε S346, which is implicated in this interaction. We have also determined that autophosphorylation of PKC-ε at residue S368 is required for the recruitment of a 14-3-3β dimer. Consistent with an important functional role, both S346 and S368 are conserved among mammalian PKC-ε species; they are also both unique to PKC-ε. As such, the further characterisation of this regulatory mechanism may provide important insights into PKC-ε isoform specific functions.

Preliminary work from Dr Saurin demonstrates that 14-3-3β binding confers lipid independent activity to PKC-ε. It will be of great interest to explore the downstream consequences of this signalling complex. In order to address this question, either wild type or S346A/S368A PKC-ε could be re-expressed against a PKC-ε$^{-/-}$ background, and the effects on phenotypes associated with PKC-ε activity, such as cell spreading (Chun et al., 1996) or HGF-induced migration (Kermorgant et al., 2004), screened.

To a certain extent, such studies would be best directed by a consideration of the stimuli which permit S346/S368 phosphorylation, and thereby herald the recruitment of 14-3-3. For instance, since UV stress has been shown to initiate S346 phosphorylation, it may be pertinent to analyse mutant versus wild type PKC-ε function in the context of UV-induced apoptosis. Conversely, it would also be worthwhile to determine whether, under conditions where 14-3-3 is known to regulate PKC-ε, these phosphorylation sites have been induced; for instance, perhaps the association between 14-3-3ζ and PKC-ε which is stimulated in PC12 cells following NGF treatment involves S346/S368 phosphorylation (Gannon-Murakami and Murakami, 2002).

It will also be significant to determine whether 14-3-3 association mediates any other effects on PKC-ε. The fact that 14-3-3 binding confers constitutive activation strongly suggests that it brings about a conformational change. By virtue of its more open conformation, the population of PKC-ε complexed to 14-3-3 may be more sensitive to proteolytic cleavage, for example by caspases (Leverrier et al., 2002). Caspase cleavage of PKC-δ results in the nuclear import of the catalytic fragment, with important functional implications in apoptosis (DeVries et al., 2002). The PKC-δ NLS that is exposed to facilitate nuclear translocation is shared with PKC-ε, thus we could speculate that, either

directly or indirectly, conformational change mediated by 14-3-3 may influence PKC-ε/PKC-ε catalytic fragment nuclear localisation.

Our current working model, which incorporates the newly defined phosphorylation sites, the interaction between 14-3-3 and PKC-ε and the downstream effects on candidate substrates is summarised in Figure 7.1. Further elucidation of this pathway will provide valuable insights into the regulation and function of PKC-ε.
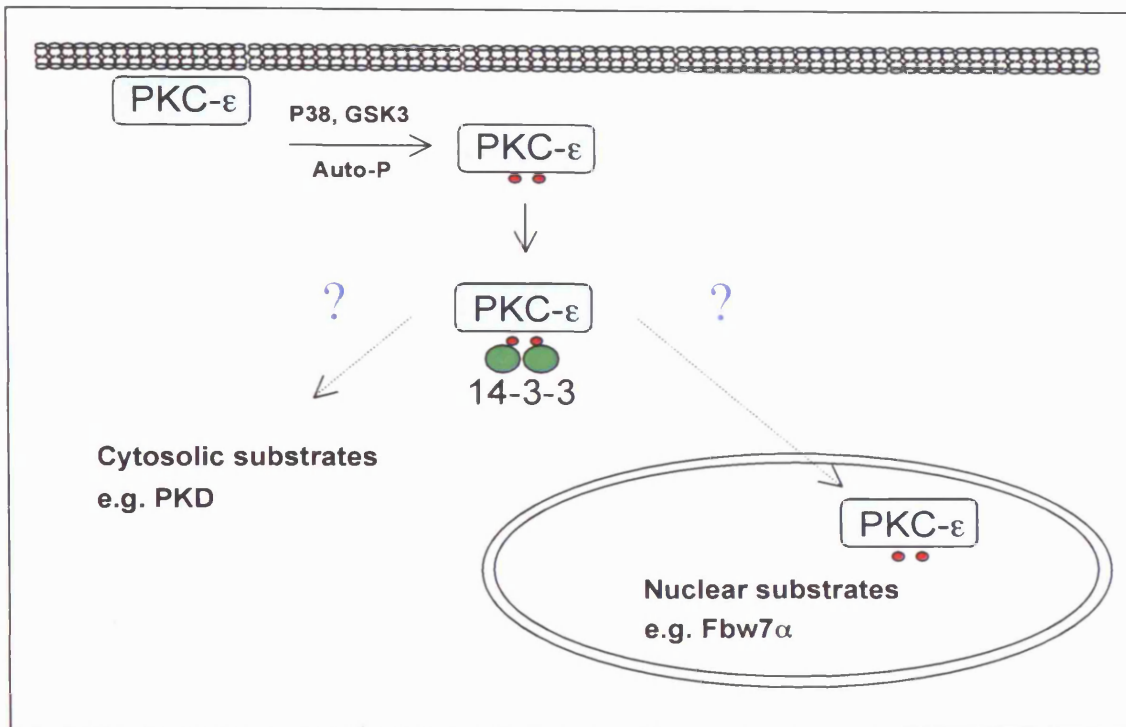
Figure 7.1 Working Model of the PKC-ε/14-3-3β Signalling Complex.
PKC-ε is phosphorylated at Ser-346 through the sequential activities of
p38 MAPK and GSK3; Ser-368 is autophosphorylated. p346/p368
represent binding sites for the recruitment of a 14-3-3β dimer.
Association with 14-3-3 confers constitutive activity to PKC-ε, which is
likely to result in the phosphorylation of cytosolic substrates. In addition,
14-3-3 mediates a conformational change, which may render PKC-ε more
susceptible to caspase cleavage and/or expose an NLS, ultimately
leading to PKC-ε/PKC-ε catalytic fragment nuclear translocation.
Phosphorylation of nuclear substrates, such as Fbw7α, may thereby be
effected.

APPENDICES

A1 Yeast 2-Hybrid Analysis

The yeast 2-hybrid screen described in Chapter 3 was performed using a full length PKC-ε bait and a mouse brain MATCHMAKER cDNA library (Clontech). The features of the library vector, pACT2, and the sequencing data obtained from the putative positive clones following the screen are compiled below.

A1.1 pACT2

The Mouse Brain MATCHMAKER cDNA Library (Clontech) utilized in the yeast 2-hybrid screen was constructed in pACT2; the vector map is shown in Figure A1 and the multiple cloning site in Figure A2.

A1.2 Mouse Brain MATCHMAKER cDNA Library Adaptor Sequence

The library was cloned into pACT2 between the EcoR I and Xho I restriction sites using the following adaptor sequence (overhang, compatible with EcoR I sticky end): 5'-AATTCGCGGCCGCGTCGAC-3', and Xho I-(dT)$_{15}$ priming. An illustration of the pACT2 multiple cloning site, which shows the incorporation of a library insert, is given in Figure A3. The library insert ORF begins directly after the adaptor sequence and is in frame with the GAL4 Activation Domain and the HA tag.
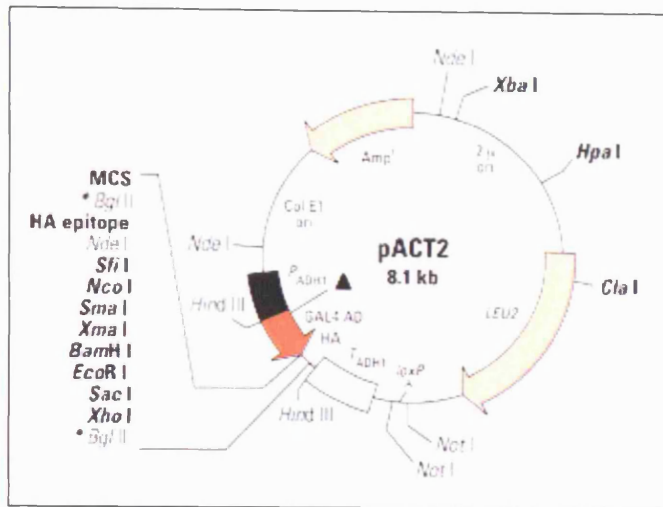
Figure A1.1 pACT2 Vector Map. The pACT2 vector map is represented, with unique restriction sites shown in bold.
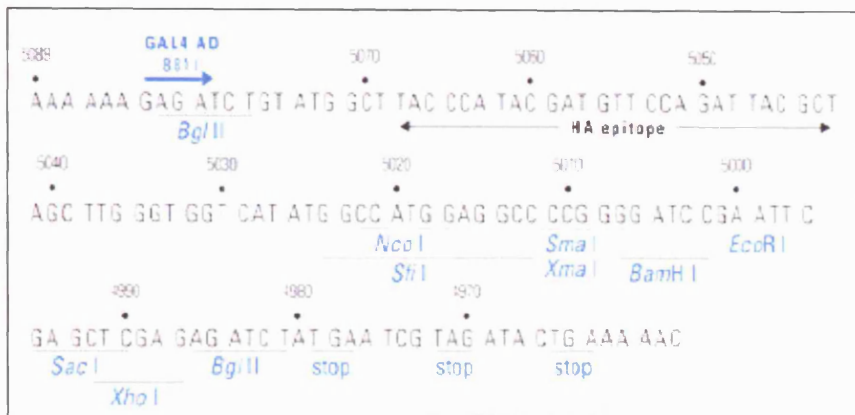
Figure A1.2 pACT2 Multiple Cloning Site (MCS). The pACT2 MCS is shown. Codons are in frame with respect to the GAL4 activation domain and HA epitope. Unique restriction sites and stop codons are shown in blue.
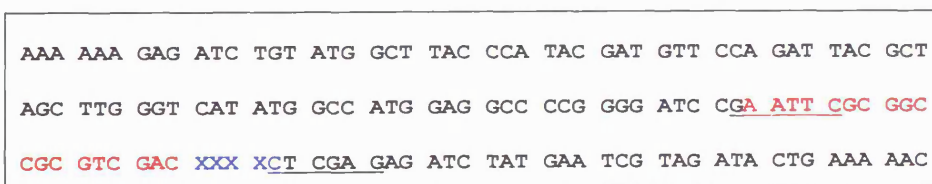
Figure A1.3 pACT2 Multiple Cloning Site with Library Insert. The multiple cloning site of pACT2, which corresponds to the sequence shown in Figure A1.2, is indicated in black. The EcoR I and Xho I sites are underlined. The adaptor sequence used for library construction is shown in red, the library insert is represented in blue. XXXX represents the library insert.

345

A1.3 Yeast 2-Hybrid Clone Sequences: Forward Sequence

The sequences obtained from the 129 positive yeast 2-hybrid clones using the forward sequencing primer are archived on the accompanying CD (Appendix1.3.doc). Sequences are shown in FASTA format and labelled by clone number. The adaptor sequence is underlined to facilitate orientation.

A1.4 Yeast 2-Hybrid Clone Sequences: Reverse Sequence

The sequences obtained from the 129 positive yeast 2-hybrid clones using the reverse sequencing primer are archived on the accompanying CD (Appendix 1.4.doc). Sequences are shown in FASTA format and labelled by clone number. The Xho site is underlined to facilitate orientation.

A2 Phosphopeptide Mapping

Phosphopeptide mapping was carried out as described in Chapter 5. Mass spectrometric data was interpreted by comparing the detected peptide masses against an *'in silico'* tryptic digest of the whole protein.

A2.1 PKC-ε *In Silico* Tryptic Digest

In Silico digestion was performed on the human PKC-ε sequence using the MS-Digest tool from the ProteinProspector database (http://prospector.ucsf.edu/); 3 missed cleavages were permitted. See file A2.1 on the accompanying CD, which can be viewed using an internet browser.

A2.2 PKC-δ *In Silico* Tryptic Digest

In Silico digestion was performed on the human PKC-δ sequence using the MS-Digest tool from the ProteinProspector database (http://prospector.ucsf.edu/); 3 missed cleavages were permitted. See file A2.2 on the accompanying CD, which can be viewed using an internet browser.

REFERENCES

Abeliovich, A., Chen, C., Goda, Y., Silva, A.J., Stevens, C.F. and Tonegawa, S. (1993) Modified hippocampal long-term potentiation in PKC gamma-mutant mice. *Cell*, **75**, 1253-1262.

Acs, P., Szallasi, Z., Kazanietz, M.G. and Blumberg, P.M. (1995) Differential activation of PKC isozymes by 14-3-3 zeta protein. *Biochem Biophys Res Commun*, **216**, 103-109.

Adjei, A.A. and Hidalgo, M. (2005) Intracellular signal transduction pathway proteins as targets for cancer therapy. *J Clin Oncol*, **23**, 5386-5403.

Agarwal-Mawal, A., Qureshi, H.Y., Cafferty, P.W., Yuan, Z., Han, D., Lin, R. and Paudel, H.K. (2003) 14-3-3 connects glycogen synthase kinase-3 beta to tau within a brain microtubule-associated tau phosphorylation complex. *J Biol Chem*, **278**, 12722-12728.

Agatep, R., RD, K., DL, P., RA, W. and RD, G. (1998) Transformation of Saccharomyces cerevisiae by the lithium acetate/single-stranded carrier DNA/polyethylene glycol (LiAc/ss-DNA/PEG) protocol. *Technical Tips Online*.

Alonso, A., Sasin, J., Bottini, N., Friedberg, I., Friedberg, I., Osterman, A., Godzik, A., Hunter, T., Dixon, J. and Mustelin, T. (2004) Protein tyrosine phosphatases in the human genome. *Cell*, **117**, 699-711.

Altschul, S.F., Madden, T.L., Schaffer, A.A., Zhang, J., Zhang, Z., Miller, W. and Lipman, D.J. (1997) Gapped BLAST and PSI-BLAST: a new generation of protein database search programs. *Nucleic Acids Res*, **25**, 3389-3402.

Alvaro, V., Levy, L., Dubray, C., Roche, A., Peillon, F., Querat, B. and Joubert, D. (1993) Invasive human pituitary tumors express a point-mutated alpha-protein kinase-C. *J Clin Endocrinol Metab*, **77**, 1125-1129.

Amano, M., Mukai, H., Ono, Y., Chihara, K., Matsui, T., Hamajima, Y., Okawa, K., Iwamatsu, A. and Kaibuchi, K. (1996) Identification of a putative target for Rho as the serine-threonine kinase protein kinase N. *Science*, **271**, 648-650.

Ananthanarayanan, B., Stahelin, R.V., Digman, M.A. and Cho, W. (2003) Activation mechanisms of conventional protein kinase C isoforms are determined by the ligand affinity and conformational flexibility of their C1 domains. *J Biol Chem*, **278**, 46886-46894.

Arellano, M., Valdivieso, M.H., Calonge, T.M., Coll, P.M., Duran, A. and Perez, P. (1999) Schizosaccharomyces pombe protein kinase C homologues, pck1p and pck2p, are targets of rho1p and rho2p and differentially regulate cell integrity. *J Cell Sci*, **112 (Pt 20)**, 3569-3578.

Ashman, K., Moran, M.F., Sicheri, F., Pawson, T. and Tyers, M.p.-p.i. (2001) Cell signalling - the proteomics of it all. *Sci STKE*, **2001**, PE33.

Atorino, L., Silvestri, L., Koppen, M., Cassina, L., Ballabio, A., Marconi, R., Langer, T. and Casari, G. (2003) Loss of m-AAA protease in mitochondria causes complex I deficiency and increased sensitivity to oxidative stress in hereditary spastic paraplegia. *J Cell Biol*, **163**, 777-787.

Aviezer, D., Golembo, M. and Yayon, A. (2003) Fibroblast growth factor receptor-3 as a therapeutic target for Achondroplasia--genetic short limbed dwarfism. *Curr Drug Targets*, **4**, 353-365.

Bai, C., Sen, P., Hofmann, K., Ma, L., Goebl, M., Harper, J.W. and Elledge, S.J. (1996) SKP1 connects cell cycle regulators to the ubiquitin proteolysis machinery through a novel motif, the F-box. *Cell*, **86**, 263-274.

Balendran, A., Biondi, R.M., Cheung, P.C., Casamayor, A., Deak, M. and Alessi, D.R. (2000) A 3-phosphoinositide-dependent protein kinase-1 (PDK1) docking site is required for the phosphorylation of protein kinase Czeta (PKCzeta) and PKC-related kinase 2 by PDK1. *J Biol Chem*, **275**, 20806-20813.

Ballester, R. and Rosen, O.M. (1985) Fate of immunoprecipitable protein kinase C in GH3 cells treated with phorbol 12-myristate 13-acetate. *J Biol Chem*, **260**, 15194-15199.

Barrios-Rodiles, M., Brown, K.R., Ozdamar, B., Bose, R., Liu, Z., Donovan, R.S., Shinjo, F., Liu, Y., Dembowy, J., Taylor, I.W., Luga, V., Przulj, N., Robinson, M., Suzuki, H., Hayashizaki, Y., Jurisica, I. and Wrana, J.L. (2005) High-throughput mapping of a dynamic signaling network in mammalian cells. *Science*, **307**, 1621-1625.

Baselga, J. and Arribas, J. (2004) Treating cancer's kinase 'addiction'. *Nat Med*, **10**, 786-787.

Behn-Krappa, A. and Newton, A.C. (1999) The hydrophobic phosphorylation motif of conventional protein kinase C is regulated by autophosphorylation. *Curr Biol*, **9**, 728-737.

Benes, C.H., Wu, N., Elia, A.E., Dharia, T., Cantley, L.C. and Soltoff, S.P. (2005) The C2 domain of PKCdelta is a phosphotyrosine binding domain. *Cell*, **121**, 271-280.

Birnbaum, S.G., Yuan, P.X., Wang, M., Vijayraghavan, S., Bloom, A.K., Davis, D.J., Gobeske, K.T., Sweatt, J.D., Manji, H.K. and Arnsten, A.F.

(2004) Protein kinase C overactivity impairs prefrontal cortical regulation of working memory. *Science*, **306**, 882-884.

Bittova, L., Stahelin, R.V. and Cho, W. (2001) Roles of ionic residues of the C1 domain in protein kinase C-alpha activation and the origin of phosphatidylserine specificity. *J Biol Chem*, **276**, 4218-4226.

Blobe, G.C., Stribling, D.S., Fabbro, D., Stabel, S. and Hannun, Y.A. (1996) Protein kinase C beta II specifically binds to and is activated by F-actin. *J Biol Chem*, **271**, 15823-15830.

Blume-Jensen, P. and Hunter, T. (2001) Oncogenic kinase signalling. *Nature*, **411**, 355-365.

Bornancin, F. and Parker, P.J. (1996) Phosphorylation of threonine 638 critically controls the dephosphorylation and inactivation of protein kinase Calpha. *Curr Biol*, **6**, 1114-1123.

Bornancin, F. and Parker, P.J. (1997) Phosphorylation of protein kinase C-alpha on serine 657 controls the accumulation of active enzyme and contributes to its phosphatase-resistant state. *J Biol Chem*, **272**, 3544-3549.

Bos, J.L. (1989) ras oncogenes in human cancer: a review. *Cancer Res*, **49**, 4682-4689.

Brandt, D.T., Goerke, A., Heuer, M., Gimona, M., Leitges, M., Kremmer, E., Lammers, R., Haller, H. and Mischak, H. (2003) Protein kinase C delta induces Src kinase activity via activation of the protein tyrosine phosphatase PTP alpha. *J Biol Chem*, **278**, 34073-34078.

Bridges, D. and Moorhead, G.B. (2005) 14-3-3 proteins: a number of functions for a numbered protein. *Sci STKE*, **2005**, re10.

Brinke, A., Green, P.M. and Giannelli, F. (1997) Characterization of the gene (VBP1) and transcript for the von Hippel-Lindau binding protein and isolation of the highly conserved murine homologue. *Genomics*, **45**, 105-112.

Brose, N. and Rosenmund, C. (2002) Move over protein kinase C, you've got company: alternative cellular effectors of diacylglycerol and phorbol esters. *J Cell Sci*, **115**, 4399-4411.

Buckley, C.D., Rainger, G.E., Bradfield, P.F., Nash, G.B. and Simmons, D.L. (1998) Cell adhesion: more than just glue (review). *Mol Membr Biol*, **15**, 167-176.

Campbell, R.E., Tour, O., Palmer, A.E., Steinbach, P.A., Baird, G.S., Zacharias, D.A. and Tsien, R.Y. (2002) A monomeric red fluorescent protein. *Proc Natl Acad Sci U S A*, **99**, 7877-7882.

Castagna, M., Takai, Y., Kaibuchi, K., Sano, K., Kikkawa, U. and Nishizuka, Y. (1982) Direct activation of calcium-activated, phospholipid-dependent protein kinase by tumor-promoting phorbol esters. *J Biol Chem*, **257**, 7847-7851.

Castrillo, A., Pennington, D.J., Otto, F., Parker, P.J., Owen, M.J. and Bosca, L. (2001) Protein kinase Cepsilon is required for macrophage activation and defense against bacterial infection. *J Exp Med*, **194**, 1231-1242.

Cazaubon, S., Bornancin, F. and Parker, P.J. (1994) Threonine-497 is a critical site for permissive activation of protein kinase C alpha. *Biochem J*, **301 (Pt 2)**, 443-448.

Cazaubon, S.M. and Parker, P.J. (1993) Identification of the phosphorylated region responsible for the permissive activation of protein kinase C. *J Biol Chem*, **268**, 17559-17563.

Cenni, V., Doppler, H., Sonnenburg, E.D., Maraldi, N., Newton, A.C. and Toker, A. (2002) Regulation of novel protein kinase C epsilon by phosphorylation. *Biochem J*, **363**, 537-545.

Chapline, C., Ramsay, K., Klauck, T. and Jaken, S. (1993) Interaction cloning of protein kinase C substrates. *J Biol Chem*, **268**, 6858-6861.

Chauhan, V.P. and Chauhan, A. (1992) Protamine induces autophosphorylation of protein kinase C: stimulation of protein kinase C-mediated protamine phosphorylation by histone. *Life Sci*, **51**, 537-544.

Chien, C.T., Bartel, P.L., Sternglanz, R. and Fields, S. (1991) The two-hybrid system: a method to identify and clone genes for proteins that interact with a protein of interest. *Proc Natl Acad Sci U S A*, **88**, 9578-9582.

Chou, M.M., Hou, W., Johnson, J., Graham, L.K., Lee, M.H., Chen, C.S., Newton, A.C., Schaffhausen, B.S. and Toker, A. (1998) Regulation of protein kinase C zeta by PI 3-kinase and PDK-1. *Curr Biol*, **8**, 1069-1077.

Chun, J.S., Ha, M.J. and Jacobson, B.S. (1996) Differential translocation of protein kinase C epsilon during HeLa cell adhesion to a gelatin substratum. *J Biol Chem*, **271**, 13008-13012.

Clague, M.J. and Urbe, S. (2001) The interface of receptor trafficking and signalling. *J Cell Sci*, **114**, 3075-3081.

Clontech. (1999) MATCHMAKER GAL4 Two-Hybrid System 3 & Libraries User Manual.

Cockman, M.E., Masson, N., Mole, D.R., Jaakkola, P., Chang, G.W., Clifford, S.C., Maher, E.R., Pugh, C.W., Ratcliffe, P.J. and Maxwell, P.H. (2000) Hypoxia inducible factor-alpha binding and ubiquitylation by the

von Hippel-Lindau tumor suppressor protein. *J Biol Chem*, **275**, 25733-25741.

Coussens, L., Parker, P.J., Rhee, L., Yang-Feng, T.L., Chen, E., Waterfield, M.D., Francke, U. and Ullrich, A. (1986) Multiple, distinct forms of bovine and human protein kinase C suggest diversity in cellular signaling pathways. *Science*, **233**, 859-866.

Csukai, M., Chen, C.H., De Matteis, M.A. and Mochly-Rosen, D. (1997) The coatomer protein beta'-COP, a selective binding protein (RACK) for protein kinase Cepsilon. *J Biol Chem*, **272**, 29200-29206.

Cuervo, A.M. and Dice, J.F. (1998) Lysosomes, a meeting point of proteins, chaperones, and proteases. *J Mol Med*, **76**, 6-12.

Czerwinski, R., Aulabaugh, A., Greco, R.M., Olland, S., Malakian, K., Wolfrom, S., Lin, L., Kriz, R., Stahl, M., Huang, Y., Liu, L. and Chaudhary, D. (2005) Characterization of Protein Kinase C theta Activation Loop Autophosphorylation and the Kinase Domain Catalytic Mechanism. *Biochemistry*, **44**, 9563-9573.

d'Azzo, A., Bongiovanni, A. and Nastasi, T. (2005) E3 ubiquitin ligases as regulators of membrane protein trafficking and degradation. *Traffic*, **6**, 429-441.

Dai, J.G. and Murakami, K. (2003) Constitutively and autonomously active protein kinase C associated with 14-3-3 zeta in the rodent brain. *J Neurochem*, **84**, 23-34.

Datta, S.R., Brunet, A. and Greenberg, M.E. (1999) Cellular survival: a play in three Akts. *Genes Dev*, **13**, 2905-2927.

Dekker, L.V. and Parker, P.J. (1994) Protein kinase C--a question of specificity. *Trends Biochem Sci*, **19**, 73-77.

Dekker, L.V. and Parker, P.J. (1997) Regulated binding of the protein kinase C substrate GAP-43 to the V0/C2 region of protein kinase C-delta. *J Biol Chem*, **272**, 12747-12753.

DeLange, R.J., Kemp, R.G., Riley, W.D., Cooper, R.A. and Krebs, E.G. (1968) Activation of skeletal muscle phosphorylase kinase by adenosine triphosphate and adenosine 3',5'-monophosphate. *J Biol Chem*, **243**, 2200-2208.

Deshaies, R.J. (1999) SCF and Cullin/Ring H2-based ubiquitin ligases. *Annu Rev Cell Dev Biol*, **15**, 435-467.

DeVries, T.A., Neville, M.C. and Reyland, M.E. (2002) Nuclear import of PKCdelta is required for apoptosis: identification of a novel nuclear import sequence. *Embo J*, **21**, 6050-6060.

Dikic, I. and Giordano, S. (2003) Negative receptor signalling. *Curr Opin Cell Biol*, **15**, 128-135.

Dlugosz, A.A., Cheng, C., Williams, E.K., Dharia, A.G., Denning, M.F. and Yuspa, S.H. (1994) Alterations in murine keratinocyte differentiation induced by activated rasHa genes are mediated by protein kinase C-alpha. *Cancer Res*, **54**, 6413-6420.

Dodge, K.L., Khouangsathiene, S., Kapiloff, M.S., Mouton, R., Hill, E.V., Houslay, M.D., Langeberg, L.K. and Scott, J.D. (2001) mAKAP assembles a protein kinase A/PDE4 phosphodiesterase cAMP signaling module. *Embo J*, **20**, 1921-1930.

Downward, J. (2001) The ins and outs of signalling. *Nature*, **411**, 759-762.

Druker, B.J. (2004) Imatinib as a paradigm of targeted therapies. *Adv Cancer Res*, **91**, 1-30.

Dutil, E.M., Keranen, L.M., DePaoli-Roach, A.A. and Newton, A.C. (1994) In vivo regulation of protein kinase C by trans-phosphorylation followed by autophosphorylation. *J Biol Chem*, **269**, 29359-29362.

Dutil, E.M., Toker, A. and Newton, A.C. (1998) Regulation of conventional protein kinase C isozymes by phosphoinositide-dependent kinase 1 (PDK-1). *Curr Biol*, **8**, 1366-1375.

Earnshaw, W.C., Martins, L.M. and Kaufmann, S.H. (1999) Mammalian caspases: structure, activation, substrates, and functions during apoptosis. *Annu Rev Biochem*, **68**, 383-424.

Esplugues, J.V. (2002) NO as a signalling molecule in the nervous system. *Br J Pharmacol*, **135**, 1079-1095.

Faux, M.C. and Scott, J.D. (1996a) Molecular glue: kinase anchoring and scaffold proteins. *Cell*, **85**, 9-12.

Faux, M.C. and Scott, J.D. (1996b) More on target with protein phosphorylation: conferring specificity by location. *Trends Biochem Sci*, **21**, 312-315.

Feldman, D.E., Thulasiraman, V., Ferreyra, R.G. and Frydman, J. (1999) Formation of the VHL-elongin BC tumor suppressor complex is mediated by the chaperonin TRiC. *Mol Cell*, **4**, 1051-1061.

Feldman, R.M., Correll, C.C., Kaplan, K.B. and Deshaies, R.J. (1997) A complex of Cdc4p, Skp1p, and Cdc53p/cullin catalyzes ubiquitination of the phosphorylated CDK inhibitor Sic1p. *Cell*, **91**, 221-230.

Ferrara, N., Hillan, K.J. and Novotny, W. (2005) Bevacizumab (Avastin), a humanized anti-VEGF monoclonal antibody for cancer therapy. *Biochem Biophys Res Commun*, **333**, 328-335.

Fields, S. and Song, O. (1989) A novel genetic system to detect protein-protein interactions. *Nature*, **340**, 245-246.

Flint, A.J., Paladini, R.D. and Koshland, D.E., Jr. (1990) Autophosphorylation of protein kinase C at three separated regions of its primary sequence. *Science*, **249**, 408-411.

Flynn, P., Mellor, H., Palmer, R., Panayotou, G. and Parker, P.J. (1998) Multiple interactions of PRK1 with RhoA. Functional assignment of the Hr1 repeat motif. *J Biol Chem*, **273**, 2698-2705.

Franco, S.J. and Huttenlocher, A. (2005) Regulating cell migration: calpains make the cut. *J Cell Sci*, **118**, 3829-3838.

Fredriksson, R., Lagerstrom, M.C., Lundin, L.G. and Schioth, H.B. (2003) The G-protein-coupled receptors in the human genome form five main families. Phylogenetic analysis, paralogon groups, and fingerprints. *Mol Pharmacol*, **63**, 1256-1272.

Fujii, K., Zhu, G., Liu, Y., Hallam, J., Chen, L., Herrero, J. and Shaw, S. (2004) Kinase peptide specificity: improved determination and relevance to protein phosphorylation. *Proc Natl Acad Sci U S A*, **101**, 13744-13749.

Gannon-Murakami, L. and Murakami, K. (2002) Selective association of protein kinase C with 14-3-3 zeta in neuronally differentiated PC12 Cells. Stimulatory and inhibitory effect of 14-3-3 zeta in vivo. *J Biol Chem*, **277**, 23116-23122.

Geissler, S., Siegers, K. and Schiebel, E. (1998) A novel protein complex promoting formation of functional alpha- and gamma-tubulin. *Embo J*, **17**, 952-966.

Gelperin, D., Weigle, J., Nelson, K., Roseboom, P., Irie, K., Matsumoto, K. and Lemmon, S. (1995) 14-3-3 proteins: potential roles in vesicular transport and Ras signaling in Saccharomyces cerevisiae. *Proc Natl Acad Sci U S A*, **92**, 11539-11543.

Gennarini, G., Cibelli, G., Rougon, G., Mattei, M.G. and Goridis, C. (1989) The mouse neuronal cell surface protein F3: a phosphatidylinositol-anchored member of the immunoglobulin superfamily related to chicken contactin. *J Cell Biol*, **109**, 775-788.

Glickman, M.H. (2000) Getting in and out of the proteasome. *Semin Cell Dev Biol*, **11**, 149-158.

Goode, N.T., Hajibagheri, M.A. and Parker, P.J. (1995) Protein kinase C (PKC)-induced PKC down-regulation. Association with up-regulation of vesicle traffic. *J Biol Chem*, **270**, 2669-2673.

Goode, N.T., Hajibagheri, M.A., Warren, G. and Parker, P.J. (1994) Expression of mammalian protein kinase C in Schizosaccharomyces

pombe: isotype-specific induction of growth arrest, vesicle formation, and endocytosis. *Mol Biol Cell*, **5**, 907-920.

Goyal, P., Pandey, D., Behring, A. and Siess, W. (2005) Inhibition of nuclear import of LIMK2 in endothelial cells by protein kinase C-dependent phosphorylation at Ser-283. *J Biol Chem*, **280**, 27569-27577.

Gross, C., Heumann, R. and Erdmann, K.S. (2001) The protein kinase C-related kinase PRK2 interacts with the protein tyrosine phosphatase PTP-BL via a novel PDZ domain binding motif. *FEBS Lett*, **496**, 101-104.

Gupta-Rossi, N., Le Bail, O., Gonen, H., Brou, C., Logeat, F., Six, E., Ciechanover, A. and Israel, A. (2001) Functional interaction between SEL-10, an F-box protein, and the nuclear form of activated Notch1 receptor. *J Biol Chem*, **276**, 34371-34378.

Haj, F.G., Verveer, P.J., Squire, A., Neel, B.G. and Bastiaens, P.I. (2002) Imaging sites of receptor dephosphorylation by PTP1B on the surface of the endoplasmic reticulum. *Science*, **295**, 1708-1711.

Hale, K.J., Hummersone, M.G., Manaviazar, S. and Frigerio, M. (2002) The chemistry and biology of the bryostatin antitumour macrolides. *Nat Prod Rep*, **19**, 413-453.

Hanafusa, H., Torii, S., Yasunaga, T. and Nishida, E. (2002) Sprouty1 and Sprouty2 provide a control mechanism for the Ras/MAPK signalling pathway. *Nat Cell Biol*, **4**, 850-858.

Hanks, S.K. and Hunter, T. (1995) Protein kinases 6. The eukaryotic protein kinase superfamily: kinase (catalytic) domain structure and classification. *Faseb J*, **9**, 576-596.

Hannun, Y.A., Loomis, C.R. and Bell, R.M. (1985) Activation of protein kinase C by Triton X-100 mixed micelles containing diacylglycerol and phosphatidylserine. *J Biol Chem*, **260**, 10039-10043.

Hansra, G., Garcia-Paramio, P., Prevostel, C., Whelan, R.D., Bornancin, F. and Parker, P.J. (1999) Multisite dephosphorylation and desensitization of conventional protein kinase C isotypes. *Biochem J*, **342** **(Pt 2)**, 337-344.

Hatakeyama, S. and Nakayama, K.I. (2003) U-box proteins as a new family of ubiquitin ligases. *Biochem Biophys Res Commun*, **302**, 635-645.

Hennings, H., Blumberg, P.M., Pettit, G.R., Herald, C.L., Shores, R. and Yuspa, S.H. (1987) Bryostatin 1, an activator of protein kinase C, inhibits tumor promotion by phorbol esters in SENCAR mouse skin. *Carcinogenesis*, **8**, 1343-1346.

Her, C., Wu, X., Griswold, M.D. and Zhou, F. (2003) Human MutS homologue MSH4 physically interacts with von Hippel-Lindau tumor suppressor-binding protein 1. *Cancer Res*, **63**, 865-872.

Hernandez, A.I., Blace, N., Crary, J.F., Serrano, P.A., Leitges, M., Libien, J.M., Weinstein, G., Tcherapanov, A. and Sacktor, T.C. (2003) Protein kinase M zeta synthesis from a brain mRNA encoding an independent protein kinase C zeta catalytic domain. Implications for the molecular mechanism of memory. *J Biol Chem*, **278**, 40305-40316.

Hernandez, R.M., Wescott, G.G., Mayhew, M.W., McJilton, M.A. and Terrian, D.M. (2001) Biochemical and morphogenic effects of the interaction between protein kinase C-epsilon and actin in vitro and in cultured NIH3T3 cells. *J Cell Biochem*, **83**, 532-546.

Hershko, A. and Ciechanover, A. (1998) The ubiquitin system. *Annu Rev Biochem*, **67**, 425-479.

Hodge, C.W., Mehmert, K.K., Kelley, S.P., McMahon, T., Haywood, A., Olive, M.F., Wang, D., Sanchez-Perez, A.M. and Messing, R.O. (1999) Supersensitivity to allosteric GABA(A) receptor modulators and alcohol in mice lacking PKCepsilon. *Nat Neurosci*, **2**, 997-1002.

Hofmann, J. (1997) The potential for isoenzyme-selective modulation of protein kinase C. *Faseb J*, **11**, 649-669.

Hommel, U., Zurini, M. and Luyten, M. (1994) Solution structure of a cysteine rich domain of rat protein kinase C. *Nat Struct Biol*, **1**, 383-387.

Hon, W.C., Wilson, M.I., Harlos, K., Claridge, T.D., Schofield, C.J., Pugh, C.W., Maxwell, P.H., Ratcliffe, P.J., Stuart, D.I. and Jones, E.Y. (2002) Structural basis for the recognition of hydroxyproline in HIF-1 alpha by pVHL. *Nature*, **417**, 975-978.

House, C. and Kemp, B.E. (1987) Protein kinase C contains a pseudosubstrate prototope in its regulatory domain. *Science*, **238**, 1726-1728.

Huang, K.P., Chan, K.F., Singh, T.J., Nakabayashi, H. and Huang, F.L. (1986) Autophosphorylation of rat brain Ca2+-activated and phospholipid-dependent protein kinase. *J Biol Chem*, **261**, 12134-12140.

Hug, H. and Sarre, T.F. (1993) Protein kinase C isoenzymes: divergence in signal transduction? *Biochem J*, **291 (Pt 2)**, 329-343.

Hyatt, S.L., Liao, L., Aderem, A., Nairn, A.C. and Jaken, S. (1994) Correlation between protein kinase C binding proteins and substrates in REF52 cells. *Cell Growth Differ*, **5**, 495-502.

Hynes, R.O. (2002) Integrins: bidirectional, allosteric signaling machines. *Cell*, **110**, 673-687.

Ihle, J.N. and Kerr, I.M. (1995) Jaks and Stats in signaling by the cytokine receptor superfamily. *Trends Genet*, **11**, 69-74.

Ikuta, T., Kobayashi, Y. and Kawajiri, K. (2004) Phosphorylation of nuclear localization signal inhibits the ligand-dependent nuclear import of aryl hydrocarbon receptor. *Biochem Biophys Res Commun*, **317**, 545-550.

Inoue, M., Kishimoto, A., Takai, Y. and Nishizuka, Y. (1977) Studies on a cyclic nucleotide-independent protein kinase and its proenzyme in mammalian tissues. II. Proenzyme and its activation by calcium-dependent protease from rat brain. *J Biol Chem*, **252**, 7610-7616.

Ito, T., Chiba, T., Ozawa, R., Yoshida, M., Hattori, M. and Sakaki, Y. (2001) A comprehensive two-hybrid analysis to explore the yeast protein interactome. *Proc Natl Acad Sci U S A*, **98**, 4569-4574.

Ivan, M. and Kaelin, W.G., Jr. (2001) The von Hippel-Lindau tumor suppressor protein. *Curr Opin Genet Dev*, **11**, 27-34.

Ivan, M., Kondo, K., Yang, H., Kim, W., Valiando, J., Ohh, M., Salic, A., Asara, J.M., Lane, W.S. and Kaelin, W.G., Jr. (2001) HIFalpha targeted for VHL-mediated destruction by proline hydroxylation: implications for O2 sensing. *Science*, **292**, 464-468.

Ivaska, J., Kermorgant, S., Whelan, R., Parsons, M., Ng, T. and Parker, P.J. (2003) Integrin-protein kinase C relationships. *Biochem Soc Trans*, **31**, 90-93.

Ivaska, J., Whelan, R.D., Watson, R. and Parker, P.J. (2002) PKC epsilon controls the traffic of beta1 integrins in motile cells. *Embo J*, **21**, 3608-3619.

Iyer, K., Burkle, L., Auerbach, D., Thaminy, S., Dinkel, M., Engels, K. and Stagljar, I. (2005) Utilizing the split-ubiquitin membrane yeast two-hybrid system to identify protein-protein interactions of integral membrane proteins. *Sci STKE*, **2005**, pl3.

Jaakkola, P., Mole, D.R., Tian, Y.M., Wilson, M.I., Gielbert, J., Gaskell, S.J., Kriegsheim, A., Hebestreit, H.F., Mukherji, M., Schofield, C.J., Maxwell, P.H., Pugh, C.W. and Ratcliffe, P.J. (2001) Targeting of HIF-alpha to the von Hippel-Lindau ubiquitylation complex by O2-regulated prolyl hydroxylation. *Science*, **292**, 468-472.

Joazeiro, C.A. and Weissman, A.M. (2000) RING finger proteins: mediators of ubiquitin ligase activity. *Cell*, **102**, 549-552.

Joy, S.V., Scates, A.C., Bearelly, S., Dar, M., Taulien, C.A., Goebel, J.A. and Cooney, M.J. (2005) Ruboxistaurin, a Protein Kinase C {beta} Inhibitor, as an Emerging Treatment for Diabetes Microvascular Complications (October). *Ann Pharmacother*.

Junco, M., Webster, C., Crawford, C., Bosca, L. and Parker, P.J. (1994) Protein kinase C V3 domain mutants with differential sensitivities to m-

calpain are not resistant to phorbol-ester-induced down-regulation. *Eur J Biochem*, **223**, 259-263.

Junoy, B., Maccario, H., Mas, J.L., Enjalbert, A. and Drouva, S.V. (2002) Proteasome implication in phorbol ester- and GnRH-induced selective down-regulation of PKC (alpha, epsilon, zeta) in alpha T(3)-1 and L beta T(2) gonadotrope cell lines. *Endocrinology*, **143**, 1386-1403.

Kang, B.S., French, O.G., Sando, J.J. and Hahn, C.S. (2000) Activation-dependent degradation of protein kinase C eta. *Oncogene*, **19**, 4263-4272.

Kashiwagi, M., Ohba, M., Chida, K. and Kuroki, T. (2002) Protein kinase C eta (PKC eta): its involvement in keratinocyte differentiation. *J Biochem (Tokyo)*, **132**, 853-857.

Keranen, L.M. and Newton, A.C. (1997) Ca2+ differentially regulates conventional protein kinase Cs' membrane interaction and activation. *J Biol Chem*, **272**, 25959-25967.

Kermorgant, S. and Parker, P.J. (2005) c-Met signalling: spatio-temporal decisions. *Cell Cycle*, **4**, 352-355.

Kermorgant, S., Zicha, D. and Parker, P.J. (2004) PKC controls HGF-dependent c-Met traffic, signalling and cell migration. *Embo J*, **23**, 3721-3734.

Kiley, S.C. and Parker, P.J. (1995) Differential localization of protein kinase C isozymes in U937 cells: evidence for distinct isozyme functions during monocyte differentiation. *J Cell Sci*, **108 (Pt 3)**, 1003-1016.

Kiley, S.C., Parker, P.J., Fabbro, D. and Jaken, S. (1991) Differential regulation of protein kinase C isozymes by thyrotropin-releasing hormone in GH4C1 cells. *J Biol Chem*, **266**, 23761-23768.

King, R.W., Deshaies, R.J., Peters, J.M. and Kirschner, M.W. (1996a) How proteolysis drives the cell cycle. *Science*, **274**, 1652-1659.

King, R.W., Glotzer, M. and Kirschner, M.W. (1996b) Mutagenic analysis of the destruction signal of mitotic cyclins and structural characterization of ubiquitinated intermediates. *Mol Biol Cell*, **7**, 1343-1357.

Kishimoto, A., Mikawa, K., Hashimoto, K., Yasuda, I., Tanaka, S., Tominaga, M., Kuroda, T. and Nishizuka, Y. (1989) Limited proteolysis of protein kinase C subspecies by calcium-dependent neutral protease (calpain). *J Biol Chem*, **264**, 4088-4092.

Kmiecik, T.E. and Shalloway, D. (1987) Activation and suppression of pp60c-src transforming ability by mutation of its primary sites of tyrosine phosphorylation. *Cell*, **49**, 65-73.

Knauf, J.A., Elisei, R., Mochly-Rosen, D., Liron, T., Chen, X.N., Gonsky, R., Korenberg, J.R. and Fagin, J.A. (1999) Involvement of protein kinase Cepsilon (PKCepsilon) in thyroid cell death. A truncated chimeric PKCepsilon cloned from a thyroid cancer cell line protects thyroid cells from apoptosis. *J Biol Chem*, **274**, 23414-23425.

Knauf, J.A., Ward, L.S., Nikiforov, Y.E., Nikiforova, M., Puxeddu, E., Medvedovic, M., Liron, T., Mochly-Rosen, D. and Fagin, J.A. (2002) Isozyme-specific abnormalities of PKC in thyroid cancer: evidence for post-transcriptional changes in PKC epsilon. *J Clin Endocrinol Metab*, **87**, 2150-2159.

Knighton, D.R., Zheng, J.H., Ten Eyck, L.F., Ashford, V.A., Xuong, N.H., Taylor, S.S. and Sowadski, J.M. (1991) Crystal structure of the catalytic subunit of cyclic adenosine monophosphate-dependent protein kinase. *Science*, **253**, 407-414.

Kolibaba, K.S. and Druker, B.J. (1997) Protein tyrosine kinases and cancer. *Biochim Biophys Acta*, **1333**, F217-248.

Koriyama, H., Kouchi, Z., Umeda, T., Saido, T.C., Momoi, T., Ishiura, S. and Suzuki, K. (1999) Proteolytic activation of protein kinase C delta and epsilon by caspase-3 in U937 cells during chemotherapeutic agent-induced apoptosis. *Cell Signal*, **11**, 831-838.

Kotsonis, P., Funk, L., Prountzos, C., Iannazzo, L. and Majewski, H. (2001) Differential abilities of phorbol esters in inducing protein kinase C (PKC) down-regulation in noradrenergic neurones. *Br J Pharmacol*, **132**, 489-499.

Kuroda, S., Oyasu, M., Kawakami, M., Kanayama, N., Tanizawa, K., Saito, N., Abe, T., Matsuhashi, S. and Ting, K. (1999) Biochemical characterization and expression analysis of neural thrombospondin-1-like proteins NELL1 and NELL2. *Biochem Biophys Res Commun*, **265**, 79-86.

Kuroda, S. and Tanizawa, K. (1999) Involvement of epidermal growth factor-like domain of NELL proteins in the novel protein-protein interaction with protein kinase C. *Biochem Biophys Res Commun*, **265**, 752-757.

Lammer, D., Mathias, N., Laplaza, J.M., Jiang, W., Liu, Y., Callis, J., Goebl, M. and Estelle, M. (1998) Modification of yeast Cdc53p by the ubiquitin-related protein rub1p affects function of the SCFCdc4 complex. *Genes Dev*, **12**, 914-926.

Lander, E.S., Linton, L.M., Birren, B., Nusbaum, C., Zody, M.C., Baldwin, J., Devon, K., Dewar, K., Doyle, M., FitzHugh, W., Funke, R., Gage, D., Harris, K., Heaford, A., Howland, J., Kann, L., Lehoczky, J., LeVine, R., McEwan, P., McKernan, K., Meldrim, J., Mesirov, J.P., Miranda, C., Morris, W., Naylor, J., Raymond, C., Rosetti, M., Santos, R., Sheridan, A., Sougnez, C., Stange-Thomann, N., Stojanovic, N., Subramanian, A., Wyman, D., Rogers, J., Sulston, J., Ainscough, R., Beck, S., Bentley, D.,

Burton, J., Clee, C., Carter, N., Coulson, A., Deadman, R., Deloukas, P., Dunham, A., Dunham, I., Durbin, R., French, L., Grafham, D., Gregory, S., Hubbard, T., Humphray, S., Hunt, A., Jones, M., Lloyd, C., McMurray, A., Matthews, L., Mercer, S., Milne, S., Mullikin, J.C., Mungall, A., Plumb, R., Ross, M., Shownkeen, R., Sims, S., Waterston, R.H., Wilson, R.K., Hillier, L.W., McPherson, J.D., Marra, M.A., Mardis, E.R., Fulton, L.A., Chinwalla, A.T., Pepin, K.H., Gish, W.R., Chissoe, S.L., Wendl, M.C., Delehaunty, K.D., Miner, T.L., Delehaunty, A., Kramer, J.B., Cook, L.L., Fulton, R.S., Johnson, D.L., Minx, P.J., Clifton, S.W., Hawkins, T., Branscomb, E., Predki, P., Richardson, P., Wenning, S., Slezak, T., Doggett, N., Cheng, J.F., Olsen, A., Lucas, S., Elkin, C., Uberbacher, E., Frazier, M., Gibbs, R.A., Muzny, D.M., Scherer, S.E., Bouck, J.B., Sodergren, E.J., Worley, K.C., Rives, C.M., Gorrell, J.H., Metzker, M.L., Naylor, S.L., Kucherlapati, R.S., Nelson, D.L., Weinstock, G.M., Sakaki, Y., Fujiyama, A., Hattori, M., Yada, T., Toyoda, A., Itoh, T., Kawagoe, C., Watanabe, H., Totoki, Y., Taylor, T., Weissenbach, J., Heilig, R., Saurin, W., Artiguenave, F., Brottier, P., Bruls, T., Pelletier, E., Robert, C., Wincker, P., Smith, D.R., Doucette-Stamm, L., Rubenfield, M., Weinstock, K., Lee, H.M., Dubois, J., Rosenthal, A., Platzer, M., Nyakatura, G., Taudien, S., Rump, A., Yang, H., Yu, J., Wang, J., Huang, G., Gu, J., Hood, L., Rowen, L., Madan, A., Qin, S., Davis, R.W., Federspiel, N.A., Abola, A.P., Proctor, M.J., Myers, R.M., Schmutz, J., Dickson, M., Grimwood, J., Cox, D.R., Olson, M.V., Kaul, R., Raymond, C., Shimizu, N., Kawasaki, K., Minoshima, S., Evans, G.A., Athanasiou, M., Schultz, R., Roe, B.A., Chen, F., Pan, H., Ramser, J., Lehrach, H., Reinhardt, R., McCombie, W.R., de la Bastide, M., Dedhia, N., Blocker, H., Hornischer, K., Nordsiek, G., Agarwala, R., Aravind, L., Bailey, J.A., Bateman, A., Batzoglou, S., Birney, E., Bork, P., Brown, D.G., Burge, C.B., Cerutti, L., Chen, H.C., Church, D., Clamp, M., Copley, R.R., Doerks, T., Eddy, S.R., Eichler, E.E., Furey, T.S., Galagan, J., Gilbert, J.G., Harmon, C., Hayashizaki, Y., Haussler, D., Hermjakob, H., Hokamp, K., Jang, W., Johnson, L.S., Jones, T.A., Kasif, S., Kaspryzk, A., Kennedy, S., Kent, W.J., Kitts, P., Koonin, E.V., Korf, I., Kulp, D., Lancet, D., Lowe, T.M., McLysaght, A., Mikkelsen, T., Moran, J.V., Mulder, N., Pollara, V.J., Ponting, C.P., Schuler, G., Schultz, J., Slater, G., Smit, A.F., Stupka, E., Szustakowski, J., Thierry-Mieg, D., Thierry-Mieg, J., Wagner, L., Wallis, J., Wheeler, R., Williams, A., Wolf, Y.I., Wolfe, K.H., Yang, S.P., Yeh, R.F., Collins, F., Guyer, M.S., Peterson, J., Felsenfeld, A., Wetterstrand, K.A., Patrinos, A., Morgan, M.J., de Jong, P., Catanese, J.J., Osoegawa, K., Shizuya, H., Choi, S. and Chen, Y.J. (2001) Initial sequencing and analysis of the human genome. *Nature*, **409**, 860-921.

Larsson, C. (2005) Protein kinase C and the regulation of the actin cytoskeleton. *Cell Signal.*

Latif, F., Tory, K., Gnarra, J., Yao, M., Duh, F.M., Orcutt, M.L., Stackhouse, T., Kuzmin, I., Modi, W., Geil, L. and et al. (1993) Identification of the von Hippel-Lindau disease tumor suppressor gene. *Science*, **260**, 1317-1320.

Le Good, J.A., Ziegler, W.H., Parekh, D.B., Alessi, D.R., Cohen, P. and Parker, P.J. (1998) Protein kinase C isotypes controlled by phosphoinositide 3-kinase through the protein kinase PDK1. *Science*, **281**, 2042-2045.

Lee, D.H. and Goldberg, A.L. (1998) Proteasome inhibitors: valuable new tools for cell biologists. *Trends Cell Biol*, **8**, 397-403.

Lee, H.W., Smith, L., Pettit, G.R. and Bingham Smith, J. (1996a) Dephosphorylation of activated protein kinase C contributes to downregulation by bryostatin. *Am J Physiol*, **271**, C304-311.

Lee, H.W., Smith, L., Pettit, G.R. and Smith, J.B. (1997) Bryostatin 1 and phorbol ester down-modulate protein kinase C-alpha and -epsilon via the ubiquitin/proteasome pathway in human fibroblasts. *Mol Pharmacol*, **51**, 439-447.

Lee, H.W., Smith, L., Pettit, G.R., Vinitsky, A. and Smith, J.B. (1996b) Ubiquitination of protein kinase C-alpha and degradation by the proteasome. *J Biol Chem*, **271**, 20973-20976.

Legrain, P., Wojcik, J. and Gauthier, J.M. (2001) Protein--protein interaction maps: a lead towards cellular functions. *Trends Genet*, **17**, 346-352.

Lehel, C., Olah, Z., Jakab, G. and Anderson, W.B. (1995) Protein kinase C epsilon is localized to the Golgi via its zinc-finger domain and modulates Golgi function. *Proc Natl Acad Sci U S A*, **92**, 1406-1410.

Lehel, C., Olah, Z., Petrovics, G., Jakab, G. and Anderson, W.B. (1996) Influence of various domains of protein kinase C epsilon on its PMA-induced translocation from the Golgi to the plasma membrane. *Biochem Biophys Res Commun*, **223**, 98-103.

Leitges, M., Gimborn, K., Elis, W., Kalesnikoff, J., Hughes, M.R., Krystal, G. and Huber, M. (2002) Protein kinase C-delta is a negative regulator of antigen-induced mast cell degranulation. *Mol Cell Biol*, **22**, 3970-3980.

Leitges, M., Sanz, L., Martin, P., Duran, A., Braun, U., Garcia, J.F., Camacho, F., Diaz-Meco, M.T., Rennert, P.D. and Moscat, J. (2001) Targeted disruption of the zetaPKC gene results in the impairment of the NF-kappaB pathway. *Mol Cell*, **8**, 771-780.

Leitges, M., Schmedt, C., Guinamard, R., Davoust, J., Schaal, S., Stabel, S. and Tarakhovsky, A. (1996) Immunodeficiency in protein kinase cbeta-deficient mice. *Science*, **273**, 788-791.

Leontieva, O.V. and Black, J.D. (2004) Identification of two distinct pathways of protein kinase Calpha down-regulation in intestinal epithelial cells. *J Biol Chem*, **279**, 5788-5801.

Leverrier, S., Vallentin, A. and Joubert, D. (2002) Positive feedback of protein kinase C proteolytic activation during apoptosis. *Biochem J*, **368**, 905-913.

Levkowitz, G., Waterman, H., Zamir, E., Kam, Z., Oved, S., Langdon, W.Y., Beguinot, L., Geiger, B. and Yarden, Y. (1998) c-Cbl/Sli-1 regulates endocytic sorting and ubiquitination of the epidermal growth factor receptor. *Genes Dev*, **12**, 3663-3674.

Li, B. and Fields, S. (1993) Identification of mutations in p53 that affect its binding to SV40 large T antigen by using the yeast two-hybrid system. *Faseb J*, **7**, 957-963.

Li, C., Ullrich, B., Zhang, J.Z., Anderson, R.G., Brose, N. and Sudhof, T.C. (1995) Ca(2+)-dependent and -independent activities of neural and non-neural synaptotagmins. *Nature*, **375**, 594-599.

Li, J., Pauley, A.M., Myers, R.L., Shuang, R., Brashler, J.R., Yan, R., Buhl, A.E., Ruble, C. and Gurney, M.E. (2002) SEL-10 interacts with presenilin 1, facilitates its ubiquitination, and alters A-beta peptide production. *J Neurochem*, **82**, 1540-1548.

Li, S., Armstrong, C.M., Bertin, N., Ge, H., Milstein, S., Boxem, M., Vidalain, P.O., Han, J.D., Chesneau, A., Hao, T., Goldberg, D.S., Li, N., Martinez, M., Rual, J.F., Lamesch, P., Xu, L., Tewari, M., Wong, S.L., Zhang, L.V., Berriz, G.F., Jacotot, L., Vaglio, P., Reboul, J., Hirozane-Kishikawa, T., Li, Q., Gabel, H.W., Elewa, A., Baumgartner, B., Rose, D.J., Yu, H., Bosak, S., Sequerra, R., Fraser, A., Mango, S.E., Saxton, W.M., Strome, S., Van Den Heuvel, S., Piano, F., Vandenhaute, J., Sardet, C., Gerstein, M., Doucette-Stamm, L., Gunsalus, K.C., Harper, J.W., Cusick, M.E., Roth, F.P., Hill, D.E. and Vidal, M. (2004) A map of the interactome network of the metazoan C. elegans. *Science*, **303**, 540-543.

Ling, M., Troller, U., Zeidman, R., Stensman, H., Schultz, A. and Larsson, C. (2005) Identification of conserved amino acids N-terminal of the PKCepsilonC1b domain crucial for protein kinase Cepsilon-mediated induction of neurite outgrowth. *J Biol Chem*, **280**, 17910-17919.

Liu, Y., Graham, C., Li, A., Fisher, R.J. and Shaw, S. (2002) Phosphorylation of the protein kinase C-theta activation loop and hydrophobic motif regulates its kinase activity, but only activation loop phosphorylation is critical to in vivo nuclear-factor-kappaB induction. *Biochem J*, **361**, 255-265.

Lopez-Lluch, G., Bird, M.M., Canas, B., Godovac-Zimmerman, J., Ridley, A., Segal, A.W. and Dekker, L.V. (2001) Protein kinase C-delta C2-like domain is a binding site for actin and enables actin redistribution in neutrophils. *Biochem J*, **357**, 39-47.

Lu, Z., Liu, D., Hornia, A., Devonish, W., Pagano, M. and Foster, D.A. (1998) Activation of protein kinase C triggers its ubiquitination and degradation. *Mol Cell Biol*, **18**, 839-845.

Luo, J., Manning, B.D. and Cantley, L.C. (2003) Targeting the PI3K-Akt pathway in human cancer: rationale and promise. *Cancer Cell*, **4**, 257-262.

Mackay, H.J. and Twelves, C.J. (2003) Protein kinase C: a target for anticancer drugs? *Endocr Relat Cancer*, **10**, 389-396.

Mandil, R., Ashkenazi, E., Blass, M., Kronfeld, I., Kazimirsky, G., Rosenthal, G., Umansky, F., Lorenzo, P.S., Blumberg, P.M. and Brodie, C. (2001) Protein kinase Calpha and protein kinase Cdelta play opposite roles in the proliferation and apoptosis of glioma cells. *Cancer Res*, **61**, 4612-4619.

Mangelsdorf, D.J., Thummel, C., Beato, M., Herrlich, P., Schutz, G., Umesono, K., Blumberg, B., Kastner, P., Mark, M., Chambon, P. and Evans, R.M. (1995) The nuclear receptor superfamily: the second decade. *Cell*, **83**, 835-839.

Mann, M. and Jensen, O.N. (2003) Proteomic analysis of post-translational modifications. *Nat Biotechnol*, **21**, 255-261.

Mann, M., Ong, S.E., Gronborg, M., Steen, H., Jensen, O.N. and Pandey, A. (2002) Analysis of protein phosphorylation using mass spectrometry: deciphering the phosphoproteome. *Trends Biotechnol*, **20**, 261-268.

Manning, G., Whyte, D.B., Martinez, R., Hunter, T. and Sudarsanam, S. (2002) The protein kinase complement of the human genome. *Science*, **298**, 1912-1934.

Mao, J.H., Perez-Losada, J., Wu, D., Delrosario, R., Tsunematsu, R., Nakayama, K.I., Brown, K., Bryson, S. and Balmain, A. (2004) Fbxw7/Cdc4 is a p53-dependent, haploinsufficient tumour suppressor gene. *Nature*, **432**, 775-779.

Margolis, B., Li, N., Koch, A., Mohammadi, M., Hurwitz, D.R., Zilberstein, A., Ullrich, A., Pawson, T. and Schlessinger, J. (1990) The tyrosine phosphorylated carboxyterminus of the EGF receptor is a binding site for GAP and PLC-gamma. *Embo J*, **9**, 4375-4380.

Marshall, C.J. (1995) Specificity of receptor tyrosine kinase signaling: transient versus sustained extracellular signal-regulated kinase activation. *Cell*, **80**, 179-185.

Maruyama, S., Hatakeyama, S., Nakayama, K., Ishida, N., Kawakami, K. and Nakayama, K. (2001) Characterization of a mouse gene (Fbxw6) that encodes a homologue of Caenorhabditis elegans SEL-10. *Genomics*, **78**, 214-222.

Massague, J. (1998) TGF-beta signal transduction. *Annu Rev Biochem*, **67**, 753-791.

Matthews, S.A., Rozengurt, E. and Cantrell, D. (2000) Protein kinase D. A selective target for antigen receptors and a downstream target for protein kinase C in lymphocytes. *J Exp Med*, **191**, 2075-2082.

Matto-Yelin, M., Aitken, A. and Ravid, S. (1997) 14-3-3 inhibits the Dictyostelium myosin II heavy-chain-specific protein kinase C activity by a direct interaction: identification of the 14-3-3 binding domain. *Mol Biol Cell*, **8**, 1889-1899.

Maxwell, P.H., Wiesener, M.S., Chang, G.W., Clifford, S.C., Vaux, E.C., Cockman, M.E., Wykoff, C.C., Pugh, C.W., Maher, E.R. and Ratcliffe, P.J. (1999) The tumour suppressor protein VHL targets hypoxia-inducible factors for oxygen-dependent proteolysis. *Nature*, **399**, 271-275.

McGehee, D.S. (1999) Molecular diversity of neuronal nicotinic acetylcholine receptors. *Ann N Y Acad Sci*, **868**, 565-577.

Mecklenbrauker, I., Saijo, K., Zheng, N.Y., Leitges, M. and Tarakhovsky, A. (2002) Protein kinase Cdelta controls self-antigen-induced B-cell tolerance. *Nature*, **416**, 860-865.

Medkova, M. and Cho, W. (1999) Interplay of C1 and C2 domains of protein kinase C-alpha in its membrane binding and activation. *J Biol Chem*, **274**, 19852-19861.

Meijer, A.J. and Dubbelhuis, P.F. (2004) Amino acid signalling and the integration of metabolism. *Biochem Biophys Res Commun*, **313**, 397-403.

Mekhail, K., Khacho, M., Carrigan, A., Hache, R.R., Gunaratnam, L. and Lee, S. (2005) Regulation of ubiquitin ligase dynamics by the nucleolus. *J Cell Biol*, **170**, 733-744.

Meller, N., Liu, Y.C., Collins, T.L., Bonnefoy-Berard, N., Baier, G., Isakov, N. and Altman, A. (1996) Direct interaction between protein kinase C theta (PKC theta) and 14-3-3 tau in T cells: 14-3-3 overexpression results in inhibition of PKC theta translocation and function. *Mol Cell Biol*, **16**, 5782-5791.

Mellor, H. and Parker, P.J. (1998) The extended protein kinase C superfamily. *Biochem J*, **332 (Pt 2)**, 281-292.

Messerschmidt, A., Macieira, S., Velarde, M., Badeker, M., Benda, C., Jestel, A., Brandstetter, H., Neuefeind, T. and Blaesse, M. (2005) Crystal Structure of the Catalytic Domain of Human Atypical Protein Kinase C-iota Reveals Interaction Mode of Phosphorylation Site in Turn Motif. *J Mol Biol*, **352**, 918-931.

Miura, M., Hatakeyama, S., Hattori, K. and Nakayama, K. (1999) Structure and expression of the gene encoding mouse F-box protein, Fwd2. *Genomics*, **62**, 50-58.

Miyamoto, A., Nakayama, K., Imaki, H., Hirose, S., Jiang, Y., Abe, M., Tsukiyama, T., Nagahama, H., Ohno, S., Hatakeyama, S. and Nakayama, K.I. (2002) Increased proliferation of B cells and auto-immunity in mice lacking protein kinase Cdelta. *Nature*, **416**, 865-869.

Mizukami, Y., Kobayashi, S., Uberall, F., Hellbert, K., Kobayashi, N. and Yoshida, K. (2000) Nuclear mitogen-activated protein kinase activation by protein kinase czeta during reoxygenation after ischemic hypoxia. *J Biol Chem*, **275**, 19921-19927.

Moberg, K.H., Bell, D.W., Wahrer, D.C., Haber, D.A. and Hariharan, I.K. (2001) Archipelago regulates Cyclin E levels in Drosophila and is mutated in human cancer cell lines. *Nature*, **413**, 311-316.

Moberg, K.H., Mukherjee, A., Veraksa, A., Artavanis-Tsakonas, S. and Hariharan, I.K. (2004) The Drosophila F box protein archipelago regulates dMyc protein levels in vivo. *Curr Biol*, **14**, 965-974.

Mochly-Rosen, D. (1995) Localization of protein kinases by anchoring proteins: a theme in signal transduction. *Science*, **268**, 247-251.

Mochly-Rosen, D. and Gordon, A.S. (1998) Anchoring proteins for protein kinase C: a means for isozyme selectivity. *Faseb J*, **12**, 35-42.

Mukai, H. and Ono, Y. (1994) A novel protein kinase with leucine zipper-like sequences: its catalytic domain is highly homologous to that of protein kinase C. *Biochem Biophys Res Commun*, **199**, 897-904.

Nakhost, A., Forscher, P. and Sossin, W.S. (1998) Binding of protein kinase C isoforms to actin in Aplysia. *J Neurochem*, **71**, 1221-1231.

Nash, P., Tang, X., Orlicky, S., Chen, Q., Gertler, F.B., Mendenhall, M.D., Sicheri, F., Pawson, T. and Tyers, M. (2001) Multisite phosphorylation of a CDK inhibitor sets a threshold for the onset of DNA replication. *Nature*, **414**, 514-521.

Nateri, A.S., Riera-Sans, L., Da Costa, C. and Behrens, A. (2004) The ubiquitin ligase SCFFbw7 antagonizes apoptotic JNK signaling. *Science*, **303**, 1374-1378.

Nauert, J.B., Klauck, T.M., Langeberg, L.K. and Scott, J.D. (1997) Gravin, an autoantigen recognized by serum from myasthenia gravis patients, is a kinase scaffold protein. *Curr Biol*, **7**, 52-62.

Newton, A.C. (1997) Regulation of protein kinase C. *Curr Opin Cell Biol*, **9**, 161-167.

Ng, T., Squire, A., Hansra, G., Bornancin, F., Prevostel, C., Hanby, A., Harris, W., Barnes, D., Schmidt, S., Mellor, H., Bastiaens, P.I. and Parker, P.J. (1999) Imaging protein kinase Calpha activation in cells. *Science*, **283**, 2085-2089.

Nishizuka, Y. (1986) Studies and perspectives of protein kinase C. *Science*, **233**, 305-312.

Nishizuka, Y. (1995) Protein kinase C and lipid signaling for sustained cellular responses. *Faseb J*, **9**, 484-496.

O'Brian, C., Vogel, V.G., Singletary, S.E. and Ward, N.E. (1989) Elevated protein kinase C expression in human breast tumor biopsies relative to normal breast tissue. *Cancer Res*, **49**, 3215-3217.

Oberg, C., Li, J., Pauley, A., Wolf, E., Gurney, M. and Lendahl, U. (2001) The Notch intracellular domain is ubiquitinated and negatively regulated by the mammalian Sel-10 homolog. *J Biol Chem*, **276**, 35847-35853.

Obsil, T., Ghirlando, R., Klein, D.C., Ganguly, S. and Dyda, F. (2001) Crystal structure of the 14-3-3zeta:serotonin N-acetyltransferase complex. a role for scaffolding in enzyme regulation. *Cell*, **105**, 257-267.

Ohno, S. (2001) Intercellular junctions and cellular polarity: the PAR-aPKC complex, a conserved core cassette playing fundamental roles in cell polarity. *Curr Opin Cell Biol*, **13**, 641-648.

Ohno, S., Konno, Y., Akita, Y., Yano, A. and Suzuki, K. (1990) A point mutation at the putative ATP-binding site of protein kinase C alpha abolishes the kinase activity and renders it down-regulation-insensitive. A molecular link between autophosphorylation and down-regulation. *J Biol Chem*, **265**, 6296-6300.

Okuda, H., Hirai, S., Takaki, Y., Kamada, M., Baba, M., Sakai, N., Kishida, T., Kaneko, S., Yao, M., Ohno, S. and Shuin, T. (1999) Direct interaction of the beta-domain of VHL tumor suppressor protein with the regulatory domain of atypical PKC isotypes. *Biochem Biophys Res Commun*, **263**, 491-497.

Okuda, H., Saitoh, K., Hirai, S., Iwai, K., Takaki, Y., Baba, M., Minato, N., Ohno, S. and Shuin, T. (2001) The von Hippel-Lindau tumor suppressor protein mediates ubiquitination of activated atypical protein kinase C. *J Biol Chem*, **276**, 43611-43617.

Olivier, A.R., Hansra, G., Pettitt, T.R., Wakelam, M.J. and Parker, P.J. (1996) The co-mitogenic combination of transforming growth factor beta 1 and bombesin protects protein kinase C-delta from late-phase down-regulation, despite synergy in diacylglycerol accumulation. *Biochem J*, **318 (Pt 2)**, 519-525.

Ono, Y., Fujii, T., Igarashi, K., Kuno, T., Tanaka, C., Kikkawa, U. and Nishizuka, Y. (1989) Phorbol ester binding to protein kinase C requires a

cysteine-rich zinc-finger-like sequence. *Proc Natl Acad Sci U S A*, **86**, 4868-4871.

Ono, Y., Fujii, T., Ogita, K., Kikkawa, U., Igarashi, K. and Nishizuka, Y. (1987) Identification of three additional members of rat protein kinase C family: delta-, epsilon- and zeta-subspecies. *FEBS Lett*, **226**, 125-128.

Orlicky, S., Tang, X., Willems, A., Tyers, M. and Sicheri, F. (2003) Structural basis for phosphodependent substrate selection and orientation by the SCFCdc4 ubiquitin ligase. *Cell*, **112**, 243-256.

Orr, J.W., Keranen, L.M. and Newton, A.C. (1992) Reversible exposure of the pseudosubstrate domain of protein kinase C by phosphatidylserine and diacylglycerol. *J Biol Chem*, **267**, 15263-15266.

Orr, J.W. and Newton, A.C. (1994) Requirement for negative charge on "activation loop" of protein kinase C. *J Biol Chem*, **269**, 27715-27718.

Osada, S., Mizuno, K., Saido, T.C., Akita, Y., Suzuki, K., Kuroki, T. and Ohno, S. (1990) A phorbol ester receptor/protein kinase, nPKC eta, a new member of the protein kinase C family predominantly expressed in lung and skin. *J Biol Chem*, **265**, 22434-22440.

Osada, S., Mizuno, K., Saido, T.C., Suzuki, K., Kuroki, T. and Ohno, S. (1992) A new member of the protein kinase C family, nPKC theta, predominantly expressed in skeletal muscle. *Mol Cell Biol*, **12**, 3930-3938.

Otte, A.P., Kramer, I.M. and Durston, A.J. (1991) Protein kinase C and regulation of the local competence of Xenopus ectoderm. *Science*, **251**, 570-573.

Palmer, R.H., Ridden, J. and Parker, P.J. (1995) Cloning and expression patterns of two members of a novel protein-kinase-C-related kinase family. *Eur J Biochem*, **227**, 344-351.

Pan, Q., Bao, L.W., Kleer, C.G., Sabel, M.S., Griffith, K.A., Teknos, T.N. and Merajver, S.D. (2005) Protein kinase C epsilon is a predictive biomarker of aggressive breast cancer and a validated target for RNA interference anticancer therapy. *Cancer Res*, **65**, 8366-8371.

Pappa, H., Murray-Rust, J., Dekker, L.V., Parker, P.J. and McDonald, N.Q. (1998) Crystal structure of the C2 domain from protein kinase C-delta. *Structure*, **6**, 885-894.

Parekh, D., Ziegler, W., Yonezawa, K., Hara, K. and Parker, P.J. (1999) Mammalian TOR controls one of two kinase pathways acting upon nPKCdelta and nPKCepsilon. *J Biol Chem*, **274**, 34758-34764.

Parekh, D.B., Ziegler, W. and Parker, P.J. (2000) Multiple pathways control protein kinase C phosphorylation. *Embo J*, **19**, 496-503.

Parker, P.J. (1999) Inhibition of protein kinase C--do we, can we, and should we? *Pharmacol Ther*, **82**, 263-267.

Parker, P.J., Bosca, L., Dekker, L., Goode, N.T., Hajibagheri, N. and Hansra, G. (1995) Protein kinase C (PKC)-induced PKC degradation: a model for down-regulation. *Biochem Soc Trans*, **23**, 153-155.

Parker, P.J., Coussens, L., Totty, N., Rhee, L., Young, S., Chen, E., Stabel, S., Waterfield, M.D. and Ullrich, A. (1986) The complete primary structure of protein kinase C--the major phorbol ester receptor. *Science*, **233**, 853-859.

Parker, P.J., Durgan, J., Iturrioz, X. and Sipeki, S. (2003) Protein Kinase C Protein Interactions. *Handbook of Cell Signalling*, **2**, 389-395.

Parker, P.J. and Murray-Rust, J. (2004) PKC at a glance. *J Cell Sci*, **117**, 131-132.

Parker, P.J. and Parkinson, S.J. (2001) AGC protein kinase phosphorylation and protein kinase C. *Biochem Soc Trans*, **29**, 860-863.

Parkinson, S.J., Le Good, J.A., Whelan, R.D., Whitehead, P. and Parker, P.J. (2004) Identification of PKCzetaII: an endogenous inhibitor of cell polarity. *Embo J*, **23**, 77-88.

Pawson, T. (2002) Protein Interaction Domains. *Cell Signalling Technology Technical Reference*, 264-279.

Pawson, T. and Nash, P. (2000) Protein-protein interactions define specificity in signal transduction. *Genes Dev*, **14**, 1027-1047.

Pawson, T. and Nash, P. (2003) Assembly of cell regulatory systems through protein interaction domains. *Science*, **300**, 445-452.

Pawson, T., Raina, M. and Nash, P. (2002) Interaction domains: from simple binding events to complex cellular behavior. *FEBS Lett*, **513**, 2-10.

Pears, C.J., Kour, G., House, C., Kemp, B.E. and Parker, P.J. (1990) Mutagenesis of the pseudosubstrate site of protein kinase C leads to activation. *Eur J Biochem*, **194**, 89-94.

Perander, M., Bjorkoy, G. and Johansen, T. (2001) Nuclear import and export signals enable rapid nucleocytoplasmic shuttling of the atypical protein kinase C lambda. *J Biol Chem*, **276**, 13015-13024.

Perego, C., Porro, D. and La Porta, C.A. (2002) Differential localisation of nPKC delta during cell cycle progression. *Biochem Biophys Res Commun*, **294**, 127-131.

Perez, P. and Calonge, T.M. (2002) Yeast protein kinase C. *J Biochem (Tokyo)*, **132**, 513-517.

Perez-Losada, J., Mao, J.H. and Balmain, A. (2005) Control of genomic instability and epithelial tumor development by the p53-Fbxw7/Cdc4 pathway. *Cancer Res*, **65**, 6488-6492.

Peter, M., Ameer-Beg, S.M., Hughes, M.K., Keppler, M.D., Prag, S., Marsh, M., Vojnovic, B. and Ng, T. (2005) Multiphoton-FLIM quantification of the EGFP-mRFP1 FRET pair for localization of membrane receptor-kinase interactions. *Biophys J*, **88**, 1224-1237.

Pickart, C.M. (2001) Mechanisms underlying ubiquitination. *Annu Rev Biochem*, **70**, 503-533.

Ponting, C.P. and Parker, P.J. (1996) Extending the C2 domain family: C2s in PKCs delta, epsilon, eta, theta, phospholipases, GAPs, and perforin. *Protein Sci*, **5**, 162-166.

Prekeris, R., Hernandez, R.M., Mayhew, M.W., White, M.K. and Terrian, D.M. (1998) Molecular analysis of the interactions between protein kinase C-epsilon and filamentous actin. *J Biol Chem*, **273**, 26790-26798.

Prekeris, R., Mayhew, M.W., Cooper, J.B. and Terrian, D.M. (1996) Identification and localization of an actin-binding motif that is unique to the epsilon isoform of protein kinase C and participates in the regulation of synaptic function. *J Cell Biol*, **132**, 77-90.

Prevostel, C., Alice, V., Joubert, D. and Parker, P.J. (2000) Protein kinase C(alpha) actively downregulates through caveolae-dependent traffic to an endosomal compartment. *J Cell Sci*, **113 (Pt 14)**, 2575-2584.

Prevostel, C., Martin, A., Alvaro, V., Jaffiol, C. and Joubert, D. (1997) Protein kinase C alpha and tumorigenesis of the endocrine gland. *Horm Res*, **47**, 140-144.

Quest, A.F., Bloomenthal, J., Bardes, E.S. and Bell, R.M. (1992) The regulatory domain of protein kinase C coordinates four atoms of zinc. *J Biol Chem*, **267**, 10193-10197.

Rajagopalan, H., Jallepalli, P.V., Rago, C., Velculescu, V.E., Kinzler, K.W., Vogelstein, B. and Lengauer, C. (2004) Inactivation of hCDC4 can cause chromosomal instability. *Nature*, **428**, 77-81.

Rechsteiner, M. (1991) Natural substrates of the ubiquitin proteolytic pathway. *Cell*, **66**, 615-618.

Rechsteiner, M. and Rogers, S.W. (1996) PEST sequences and regulation by proteolysis. *Trends Biochem Sci*, **21**, 267-271.

Reddig, P.J., Dreckschmidt, N.E., Ahrens, H., Simsiman, R., Tseng, C.P., Zou, J., Oberley, T.D. and Verma, A.K. (1999) Transgenic mice overexpressing protein kinase Cdelta in the epidermis are resistant to skin tumor promotion by 12-O-tetradecanoylphorbol-13-acetate. *Cancer Res*, **59**, 5710-5718.

Reddig, P.J., Dreckschmidt, N.E., Zou, J., Bourguignon, S.E., Oberley, T.D. and Verma, A.K. (2000) Transgenic mice overexpressing protein kinase C epsilon in their epidermis exhibit reduced papilloma burden but enhanced carcinoma formation after tumor promotion. Cancer Res, 60, 595-602.

Rey, O., Young, S.H., Cantrell, D. and Rozengurt, E. (2001) Rapid protein kinase D translocation in response to G protein-coupled receptor activation. Dependence on protein kinase C. J Biol Chem, 276, 32616-32626.

Rhodes, D.R., Tomlins, S.A., Varambally, S., Mahavisno, V., Barrette, T., Kalyana-Sundaram, S., Ghosh, D., Pandey, A. and Chinnaiyan, A.M. (2005) Probabilistic model of the human protein-protein interaction network. Nat Biotechnol, 23, 951-959.

Riley, W.D., DeLange, R.J., Bratvold, G.E. and Krebs, E.G. (1968) Reversal of phosphorylase kinase activation. J Biol Chem, 243, 2209-2215.

Ron, D., Luo, J. and Mochly-Rosen, D. (1995) C2 region-derived peptides inhibit translocation and function of beta protein kinase C in vivo. J Biol Chem, 270, 24180-24187.

Rozengurt, E., Sinnett-Smith, J. and Zugaza, J.L. (1997) Protein kinase D: a novel target for diacylglycerol and phorbol esters. Biochem Soc Trans, 25, 565-571.

Sakurai, Y., Onishi, Y., Tanimoto, Y. and Kizaki, H. (2001) Novel protein kinase C delta isoform insensitive to caspase-3. Biol Pharm Bull, 24, 973-977.

Sambrook, J., Fritsch, E. and T, M. (1989) Molecular Cloning: A Laboratory Manual. Cold Spring Harbor Laboratory Press.

Saurin, A.T., Pennington, D.J., Raat, N.J., Latchman, D.S., Owen, M.J. and Marber, M.S. (2002) Targeted disruption of the protein kinase C epsilon gene abolishes the infarct size reduction that follows ischaemic preconditioning of isolated buffer-perfused mouse hearts. Cardiovasc Res, 55, 672-680.

Schimke, R.T. (1973) Control of enzyme levels in mammalian tissues. Adv Enzymol Relat Areas Mol Biol, 37, 135-187.

Schuster-Gossler, K., Bilinski, P., Sado, T., Ferguson-Smith, A. and Gossler, A. (1998) The mouse Gtl2 gene is differentially expressed during embryonic development, encodes multiple alternatively spliced transcripts, and may act as an RNA. Dev Dyn, 212, 214-228.

Selbie, L.A., Schmitz-Peiffer, C., Sheng, Y. and Biden, T.J. (1993) Molecular cloning and characterization of PKC iota, an atypical isoform of

protein kinase C derived from insulin-secreting cells. *J Biol Chem*, **268**, 24296-24302.

Shao, X., Davletov, B.A., Sutton, R.B., Sudhof, T.C. and Rizo, J. (1996) Bipartite Ca2+-binding motif in C2 domains of synaptotagmin and protein kinase C. *Science*, **273**, 248-251.

Sharkey, N.A., Leach, K.L. and Blumberg, P.M. (1984) Competitive inhibition by diacylglycerol of specific phorbol ester binding. *Proc Natl Acad Sci U S A*, **81**, 607-610.

Sherr, C.J. (1996) Cancer cell cycles. *Science*, **274**, 1672-1677.

Shuin, T., Kondo, K., Torigoe, S., Kishida, T., Kubota, Y., Hosaka, M., Nagashima, Y., Kitamura, H., Latif, F., Zbar, B. and et al. (1994) Frequent somatic mutations and loss of heterozygosity of the von Hippel-Lindau tumor suppressor gene in primary human renal cell carcinomas. *Cancer Res*, **54**, 2852-2855.

Simons, C.T., Staes, A., Rommelaere, H., Ampe, C., Lewis, S.A. and Cowan, N.J. (2004) Selective contribution of eukaryotic prefoldin subunits to actin and tubulin binding. *J Biol Chem*, **279**, 4196-4203.

Skowyra, D., Craig, K.L., Tyers, M., Elledge, S.J. and Harper, J.W. (1997) F-box proteins are receptors that recruit phosphorylated substrates to the SCF ubiquitin-ligase complex. *Cell*, **91**, 209-219.

Slamon, D.J., Leyland-Jones, B., Shak, S., Fuchs, H., Paton, V., Bajamonde, A., Fleming, T., Eiermann, W., Wolter, J., Pegram, M., Baselga, J. and Norton, L. (2001) Use of chemotherapy plus a monoclonal antibody against HER2 for metastatic breast cancer that overexpresses HER2. *N Engl J Med*, **344**, 783-792.

Smith, F.D. and Scott, J.D. (2002) Signaling complexes: junctions on the intracellular information super highway. *Curr Biol*, **12**, R32-40.

Smith, L., Chen, L., Reyland, M.E., DeVries, T.A., Talanian, R.V., Omura, S. and Smith, J.B. (2000) Activation of atypical protein kinase C zeta by caspase processing and degradation by the ubiquitin-proteasome system. *J Biol Chem*, **275**, 40620-40627.

Soh, J.W. and Weinstein, I.B. (2003) Roles of specific isoforms of protein kinase C in the transcriptional control of cyclin D1 and related genes. *J Biol Chem*, **278**, 34709-34716.

Sorimachi, H., Ishiura, S. and Suzuki, K. (1997) Structure and physiological function of calpains. *Biochem J*, **328 (Pt 3)**, 721-732.

Srivastava, J., Procyk, K.J., Iturrioz, X. and Parker, P.J. (2002) Phosphorylation is required for PMA- and cell-cycle-induced degradation of protein kinase Cdelta. *Biochem J*, **368**, 349-355.

Stabel, S., Rodriguez-Pena, A., Young, S., Rozengurt, E. and Parker, P.J. (1987) Quantitation of protein kinase C by immunoblot--expression in different cell lines and response to phorbol esters. J Cell Physiol, 130, 111-117.

Stahelin, R.V., Digman, M.A., Medkova, M., Ananthanarayanan, B., Melowic, H.R., Rafter, J.D. and Cho, W. (2005) Diacylglycerol-induced membrane targeting and activation of protein kinase Cepsilon: mechanistic differences between protein kinases Cdelta and Cepsilon. J Biol Chem, 280, 19784-19793.

Stahelin, R.V., Digman, M.A., Medkova, M., Ananthanarayanan, B., Rafter, J.D., Melowic, H.R. and Cho, W. (2004) Mechanism of diacylglycerol-induced membrane targeting and activation of protein kinase Cdelta. J Biol Chem, 279, 29501-29512.

Stamenkovic, I. (2003) Extracellular matrix remodelling: the role of matrix metalloproteinases. J Pathol, 200, 448-464.

Standaert, M.L., Bandyopadhyay, G., Kanoh, Y., Sajan, M.P. and Farese, R.V. (2001) Insulin and PIP3 activate PKC-zeta by mechanisms that are both dependent and independent of phosphorylation of activation loop (T410) and autophosphorylation (T560) sites. Biochemistry, 40, 249-255.

Staropoli, J.F., McDermott, C., Martinat, C., Schulman, B., Demireva, E. and Abeliovich, A. (2003) Parkin is a component of an SCF-like ubiquitin ligase complex and protects postmitotic neurons from kainate excitotoxicity. Neuron, 37, 735-749.

Stebbins, C.E., Kaelin, W.G., Jr. and Pavletich, N.P. (1999) Structure of the VHL-ElonginC-ElonginB complex: implications for VHL tumor suppressor function. Science, 284, 455-461.

Steinberg, S.F. (2004) Distinctive activation mechanisms and functions for protein kinase Cdelta. Biochem J, 384, 449-459.

Stensman, H., Raghunath, A. and Larsson, C. (2004) Autophosphorylation suppresses whereas kinase inhibition augments the translocation of protein kinase Calpha in response to diacylglycerol. J Biol Chem, 279, 40576-40583.

Strohmaier, H., Spruck, C.H., Kaiser, P., Won, K.A., Sangfelt, O. and Reed, S.I. (2001) Human F-box protein hCdc4 targets cyclin E for proteolysis and is mutated in a breast cancer cell line. Nature, 413, 316-322.

Strous, G.J. and Gent, J. (2002) Dimerization, ubiquitylation and endocytosis go together in growth hormone receptor function. FEBS Lett, 529, 102-109.

Stumpo, D.J., Graff, J.M., Albert, K.A., Greengard, P. and Blackshear, P.J. (1989) Molecular cloning, characterization, and expression of a

cDNA encoding the "80- to 87-kDa" myristoylated alanine-rich C kinase substrate: a major cellular substrate for protein kinase C. *Proc Natl Acad Sci U S A*, **86**, 4012-4016.

Szallasi, Z., Bogi, K., Gohari, S., Biro, T., Acs, P. and Blumberg, P.M. (1996) Non-equivalent roles for the first and second zinc fingers of protein kinase Cdelta. Effect of their mutation on phorbol ester-induced translocation in NIH 3T3 cells. *J Biol Chem*, **271**, 18299-18301.

Szallasi, Z., Smith, C.B., Pettit, G.R. and Blumberg, P.M. (1994) Differential regulation of protein kinase C isozymes by bryostatin 1 and phorbol 12-myristate 13-acetate in NIH 3T3 fibroblasts. *J Biol Chem*, **269**, 2118-2124.

Takai, Y., Kishimoto, A., Kikkawa, U., Mori, T. and Nishizuka, Y. (1979) Unsaturated diacylglycerol as a possible messenger for the activation of calcium-activated, phospholipid-dependent protein kinase system. *Biochem Biophys Res Commun*, **91**, 1218-1224.

Takenaga, K. and Takahashi, K. (1986) Effects of 12-O-tetradecanoylphorbol-13-acetate on adhesiveness and lung-colonizing ability of Lewis lung carcinoma cells. *Cancer Res*, **46**, 375-380.

Tanaka, M., Gunawan, F., Terry, R.D., Inagaki, K., Caffarelli, A.D., Hoyt, G., Tsao, P.S., Mochly-Rosen, D. and Robbins, R.C. (2005) Inhibition of heart transplant injury and graft coronary artery disease after prolonged organ ischemia by selective protein kinase C regulators. *J Thorac Cardiovasc Surg*, **129**, 1160-1167.

Tanaka, M., Terry, R.D., Mokhtari, G.K., Inagaki, K., Koyanagi, T., Kofidis, T., Mochly-Rosen, D. and Robbins, R.C. (2004) Suppression of graft coronary artery disease by a brief treatment with a selective epsilonPKC activator and a deltaPKC inhibitor in murine cardiac allografts. *Circulation*, **110**, II194-199.

Tanji, M., Horwitz, R., Rosenfeld, G. and Waymire, J.C. (1994) Activation of protein kinase C by purified bovine brain 14-3-3: comparison with tyrosine hydroxylase activation. *J Neurochem*, **63**, 1908-1916.

Tetzlaff, M.T., Yu, W., Li, M., Zhang, P., Finegold, M., Mahon, K., Harper, J.W., Schwartz, R.J. and Elledge, S.J. (2004) Defective cardiovascular development and elevated cyclin E and Notch proteins in mice lacking the Fbw7 F-box protein. *Proc Natl Acad Sci U S A*, **101**, 3338-3345.

Thelen, M., Rosen, A., Nairn, A.C. and Aderem, A. (1991) Regulation by phosphorylation of reversible association of a myristoylated protein kinase C substrate with the plasma membrane. *Nature*, **351**, 320-322.

Toker, A., Sellers, L.A., Amess, B., Patel, Y., Harris, A. and Aitken, A. (1992) Multiple isoforms of a protein kinase C inhibitor (KCIP-1/14-3-3)

from sheep brain. Amino acid sequence of phosphorylated forms. *Eur J Biochem*, **206**, 453-461.

Torbett, N.E., Casamassima, A. and Parker, P.J. (2003) Hyperosmotic-induced protein kinase N 1 activation in a vesicular compartment is dependent upon Rac1 and 3-phosphoinositide-dependent kinase 1. *J Biol Chem*, **278**, 32344-32351.

Tsuchiya, H., Iseda, T. and Hino, O. (1996) Identification of a novel protein (VBP-1) binding to the von Hippel-Lindau (VHL) tumor suppressor gene product. *Cancer Res*, **56**, 2881-2885.

Tsunoda, S., Sierralta, J., Sun, Y., Bodner, R., Suzuki, E., Becker, A., Socolich, M. and Zuker, C.S. (1997) A multivalent PDZ-domain protein assembles signalling complexes in a G-protein-coupled cascade. *Nature*, **388**, 243-249.

Vainberg, I.E., Lewis, S.A., Rommelaere, H., Ampe, C., Vandekerckhove, J., Klein, H.L. and Cowan, N.J. (1998) Prefoldin, a chaperone that delivers unfolded proteins to cytosolic chaperonin. *Cell*, **93**, 863-873.

Vallentin, A., Lo, T.C. and Joubert, D. (2001) A single point mutation in the V3 region affects protein kinase Calpha targeting and accumulation at cell-cell contacts. *Mol Cell Biol*, **21**, 3351-3363.

Van Der Hoeven, P.C., Van Der Wal, J.C., Ruurs, P. and Van Blitterswijk, W.J. (2000) Protein kinase C activation by acidic proteins including 14-3-3. *Biochem J*, **347 Pt 3**, 781-785.

Varshavsky, A. (1991) Naming a targeting signal. *Cell*, **64**, 13-15.

Varshavsky, A. (1996) The N-end rule: functions, mysteries, uses. *Proc Natl Acad Sci U S A*, **93**, 12142-12149.

Venter, J.C., Adams, M.D., Myers, E.W., Li, P.W., Mural, R.J., Sutton, G.G., Smith, H.O., Yandell, M., Evans, C.A., Holt, R.A., Gocayne, J.D., Amanatides, P., Ballew, R.M., Huson, D.H., Wortman, J.R., Zhang, Q., Kodira, C.D., Zheng, X.H., Chen, L., Skupski, M., Subramanian, G., Thomas, P.D., Zhang, J., Gabor Miklos, G.L., Nelson, C., Broder, S., Clark, A.G., Nadeau, J., McKusick, V.A., Zinder, N., Levine, A.J., Roberts, R.J., Simon, M., Slayman, C., Hunkapiller, M., Bolanos, R., Delcher, A., Dew, I., Fasulo, D., Flanigan, M., Florea, L., Halpern, A., Hannenhalli, S., Kravitz, S., Levy, S., Mobarry, C., Reinert, K., Remington, K., Abu-Threideh, J., Beasley, E., Biddick, K., Bonazzi, V., Brandon, R., Cargill, M., Chandramouliswaran, I., Charlab, R., Chaturvedi, K., Deng, Z., Di Francesco, V., Dunn, P., Eilbeck, K., Evangelista, C., Gabrielian, A.E., Gan, W., Ge, W., Gong, F., Gu, Z., Guan, P., Heiman, T.J., Higgins, M.E., Ji, R.R., Ke, Z., Ketchum, K.A., Lai, Z., Lei, Y., Li, Z., Li, J., Liang, Y., Lin, X., Lu, F., Merkulov, G.V., Milshina, N., Moore, H.M., Naik, A.K., Narayan, V.A., Neelam, B., Nusskern, D., Rusch, D.B., Salzberg, S., Shao, W., Shue, B., Sun, J., Wang, Z., Wang, A., Wang, X., Wang, J.,

Wei, M., Wides, R., Xiao, C., Yan, C., Yao, A., Ye, J., Zhan, M., Zhang, W., Zhang, H., Zhao, Q., Zheng, L., Zhong, F., Zhong, W., Zhu, S., Zhao, S., Gilbert, D., Baumhueter, S., Spier, G., Carter, C., Cravchik, A., Woodage, T., Ali, F., An, H., Awe, A., Baldwin, D., Baden, H., Barnstead, M., Barrow, I., Beeson, K., Busam, D., Carver, A., Center, A., Cheng, M.L., Curry, L., Danaher, S., Davenport, L., Desilets, R., Dietz, S., Dodson, K., Doup, L., Ferriera, S., Garg, N., Gluecksmann, A., Hart, B., Haynes, J., Haynes, C., Heiner, C., Hladun, S., Hostin, D., Houck, J., Howland, T., Ibegwam, C., Johnson, J., Kalush, F., Kline, L., Koduru, S., Love, A., Mann, F., May, D., McCawley, S., McIntosh, T., McMullen, I., Moy, M., Moy, L., Murphy, B., Nelson, K., Pfannkoch, C., Pratts, E., Puri, V., Qureshi, H., Reardon, M., Rodriguez, R., Rogers, Y.H., Romblad, D., Ruhfel, B., Scott, R., Sitter, C., Smallwood, M., Stewart, E., Strong, R., Suh, E., Thomas, R., Tint, N.N., Tse, S., Vech, C., Wang, G., Wetter, J., Williams, S., Williams, M., Windsor, S., Winn-Deen, E., Wolfe, K., Zaveri, J., Zaveri, K., Abril, J.F., Guigo, R., Campbell, M.J., Sjolander, K.V., Karlak, B., Kejariwal, A., Mi, H., Lazareva, B., Hatton, T., Narechania, A., Diemer, K., Muruganujan, A., Guo, N., Sato, S., Bafna, V., Istrail, S., Lippert, R., Schwartz, R., Walenz, B., Yooseph, S., Allen, D., Basu, A., Baxendale, J., Blick, L., Caminha, M., Carnes-Stine, J., Caulk, P., Chiang, Y.H., Coyne, M., Dahlke, C., Mays, A., Dombroski, M., Donnelly, M., Ely, D., Esparham, S., Fosler, C., Gire, H., Glanowski, S., Glasser, K., Glodek, A., Gorokhov, M., Graham, K., Gropman, B., Harris, M., Heil, J., Henderson, S., Hoover, J., Jennings, D., Jordan, C., Jordan, J., Kasha, J., Kagan, L., Kraft, C., Levitsky, A., Lewis, M., Liu, X., Lopez, J., Ma, D., Majoros, W., McDaniel, J., Murphy, S., Newman, M., Nguyen, T., Nguyen, N., Nodell, M., Pan, S., Peck, J., Peterson, M., Rowe, W., Sanders, R., Scott, J., Simpson, M., Smith, T., Sprague, A., Stockwell, T., Turner, R., Venter, E., Wang, M., Wen, M., Wu, D., Wu, M., Xia, A., Zandieh, A. and Zhu, X. (2001) The sequence of the human genome. *Science*, **291**, 1304-1351.

Vihinen, M., Mattsson, P.T. and Smith, C.I. (2000) Bruton tyrosine kinase (BTK) in X-linked agammaglobulinemia (XLA). *Front Biosci*, **5**, D917-928.

von Arnim, A.G. (2001) A hitchhiker's guide to the proteasome. *Sci STKE*, **2001**, PE2.

Waldron, R.T. and Rozengurt, E. (2003) Protein kinase C phosphorylates protein kinase D activation loop Ser744 and Ser748 and releases autoinhibition by the pleckstrin homology domain. *J Biol Chem*, **278**, 154-163.

Wang, Q.J., Bhattacharyya, D., Garfield, S., Nacro, K., Marquez, V.E. and Blumberg, P.M. (1999) Differential localization of protein kinase C delta by phorbol esters and related compounds using a fusion protein with green fluorescent protein. *J Biol Chem*, **274**, 37233-37239.

Wang, Z.X. and Wu, J.W. (2002) Autophosphorylation kinetics of protein kinases. *Biochem J*, **368**, 947-952.

374

Watanabe, G., Saito, Y., Madaule, P., Ishizaki, T., Fujisawa, K., Morii, N., Mukai, H., Ono, Y., Kakizuka, A. and Narumiya, S. (1996) Protein kinase N (PKN) and PKN-related protein rhophilin as targets of small GTPase Rho. *Science*, **271**, 645-648.

Webb, B.L., Hirst, S.J. and Giembycz, M.A. (2000) Protein kinase C isoenzymes: a review of their structure, regulation and role in regulating airways smooth muscle tone and mitogenesis. *Br J Pharmacol*, **130**, 1433-1452.

Wei, W., Jin, J., Schlisio, S., Harper, J.W. and Kaelin, W.G., Jr. (2005) The v-Jun point mutation allows c-Jun to escape GSK3-dependent recognition and destruction by the Fbw7 ubiquitin ligase. *Cancer Cell*, **8**, 25-33.

Welcker, M. and Clurman, B.E. (2005) The SV40 large T antigen contains a decoy phosphodegron that mediates its interactions with Fbw7/hCdc4. *J Biol Chem*, **280**, 7654-7658.

Welcker, M., Orian, A., Grim, J.A., Eisenman, R.N. and Clurman, B.E. (2004a) A nucleolar isoform of the Fbw7 ubiquitin ligase regulates c-Myc and cell size. *Curr Biol*, **14**, 1852-1857.

Welcker, M., Orian, A., Jin, J., Grim, J.A., Harper, J.W., Eisenman, R.N. and Clurman, B.E. (2004b) The Fbw7 tumor suppressor regulates glycogen synthase kinase 3 phosphorylation-dependent c-Myc protein degradation. *Proc Natl Acad Sci U S A*, **101**, 9085-9090.

Wellbrock, C., Karasarides, M. and Marais, R. (2004) The RAF proteins take centre stage. *Nat Rev Mol Cell Biol*, **5**, 875-885.

Wera, S. and Hemmings, B.A. (1995) Serine/threonine protein phosphatases. *Biochem J*, **311 (Pt 1)**, 17-29.

Winston, J.T., Koepp, D.M., Zhu, C., Elledge, S.J. and Harper, J.W. (1999) A family of mammalian F-box proteins. *Curr Biol*, **9**, 1180-1182.

Withers, D.J. and White, M. (2000) Perspective: The insulin signaling system--a common link in the pathogenesis of type 2 diabetes. *Endocrinology*, **141**, 1917-1921.

Wooten, M.W., Zhou, G., Wooten, M.C. and Seibenhener, M.L. (1997) Transport of protein kinase C isoforms to the nucleus of PC12 cells by nerve growth factor: association of atypical zeta-PKC with the nuclear matrix. *J Neurosci Res*, **49**, 393-403.

Wu, G., Hubbard, E.J., Kitajewski, J.K. and Greenwald, I. (1998) Evidence for functional and physical association between Caenorhabditis elegans SEL-10, a Cdc4p-related protein, and SEL-12 presenilin. *Proc Natl Acad Sci U S A*, **95**, 15787-15791.

Wu, G., Lyapina, S., Das, I., Li, J., Gurney, M., Pauley, A., Chui, I., Deshaies, R.J. and Kitajewski, J. (2001) SEL-10 is an inhibitor of notch signaling that targets notch for ubiquitin-mediated protein degradation. *Mol Cell Biol*, **21**, 7403-7415.

Xu, Z.B., Chaudhary, D., Olland, S., Wolfrom, S., Czerwinski, R., Malakian, K., Lin, L., Stahl, M.L., Joseph-McCarthy, D., Benander, C., Fitz, L., Greco, R., Somers, W.S. and Mosyak, L. (2004) Catalytic domain crystal structure of protein kinase C-theta (PKCtheta). *J Biol Chem*, **279**, 50401-50409.

Yada, M., Hatakeyama, S., Kamura, T., Nishiyama, M., Tsunematsu, R., Imaki, H., Ishida, N., Okumura, F., Nakayama, K. and Nakayama, K.I. (2004) Phosphorylation-dependent degradation of c-Myc is mediated by the F-box protein Fbw7. *Embo J*, **23**, 2116-2125.

Yaffe, M.B. (2002) How do 14-3-3 proteins work?-- Gatekeeper phosphorylation and the molecular anvil hypothesis. *FEBS Lett*, **513**, 53-57.

Yaffe, M.B., Rittinger, K., Volinia, S., Caron, P.R., Aitken, A., Leffers, H., Gamblin, S.J., Smerdon, S.J. and Cantley, L.C. (1997) The structural basis for 14-3-3:phosphopeptide binding specificity. *Cell*, **91**, 961-971.

Yang, J., Winkler, K., Yoshida, M. and Kornbluth, S. (1999) Maintenance of G2 arrest in the Xenopus oocyte: a role for 14-3-3-mediated inhibition of Cdc25 nuclear import. *Embo J*, **18**, 2174-2183.

Ye, J., Rawson, R.B., Komuro, R., Chen, X., Dave, U.P., Prywes, R., Brown, M.S. and Goldstein, J.L. (2000) ER stress induces cleavage of membrane-bound ATF6 by the same proteases that process SREBPs. *Mol Cell*, **6**, 1355-1364.

Ye, X., Nalepa, G., Welcker, M., Kessler, B.M., Spooner, E., Qin, J., Elledge, S.J., Clurman, B.E. and Harper, J.W. (2004) Recognition of phosphodegron motifs in human cyclin E by the SCF(Fbw7) ubiquitin ligase. *J Biol Chem*, **279**, 50110-50119.

Young, S., Parker, P.J., Ullrich, A. and Stabel, S. (1987) Down-regulation of protein kinase C is due to an increased rate of degradation. *Biochem J*, **244**, 775-779.

Yuan, J., Bae, D., Cantrell, D., Nel, A.E. and Rozengurt, E. (2002) Protein kinase D is a downstream target of protein kinase Ctheta. *Biochem Biophys Res Commun*, **291**, 444-452.

Yuspa, S.H. (1998) The pathogenesis of squamous cell cancer: lessons learned from studies of skin carcinogenesis. *J Dermatol Sci*, **17**, 1-7.

Zeidman, R., Troller, U., Raghunath, A., Pahlman, S. and Larsson, C. (2002) Protein kinase Cepsilon actin-binding site is important for neurite outgrowth during neuronal differentiation. *Mol Biol Cell*, **13**, 12-24.

Zhang, G., Kazanietz, M.G., Blumberg, P.M. and Hurley, J.H. (1995) Crystal structure of the cys2 activator-binding domain of protein kinase C delta in complex with phorbol ester. *Cell*, **81**, 917-924.

Zheng, Y., Liu, H., Coughlin, J., Zheng, J., Li, L. and Stone, J.C. (2005) Phosphorylation of RasGRP3 on threonine 133 provides a mechanistic link between PKC and Ras signaling systems in B cells. *Blood*, **105**, 3648-3654.

Zhu, G., Fujii, K., Belkina, N., Liu, Y., James, M., Herrero, J. and Shaw, S. (2005a) Exceptional disfavor for proline at the P + 1 position among AGC and CAMK kinases establishes reciprocal specificity between them and the proline-directed kinases. *J Biol Chem*, **280**, 10743-10748.

Zhu, H., Bilgin, M. and Snyder, M.p.-p.i. (2003) Proteomics. *Annu Rev Biochem*, **72**, 783-812.

Zhu, Y., Smith, D., Verma, C., Lim, W.G., Tan, B.J., Armstrong, J.S., Zhou, S., Chan, E., Tan, S.L., Zhu, Y.Z., Cheung, N.S. and Duan, W. (2005b) The very C-terminus of protein kinase Cvarepsilon is critical for the full catalytic competence but its hydrophobic motif is dispensable for the interaction with 3-phosphoinositide-dependent kinase-1. *Cell Signal*.

Ziegler, W.H., Parekh, D.B., Le Good, J.A., Whelan, R.D., Kelly, J.J., Frech, M., Hemmings, B.A. and Parker, P.J. (1999) Rapamycin-sensitive phosphorylation of PKC on a carboxy-terminal site by an atypical PKC complex. *Curr Biol*, **9**, 522-529.

Zugaza, J.L., Sinnett-Smith, J., Van Lint, J. and Rozengurt, E. (1996) Protein kinase D (PKD) activation in intact cells through a protein kinase C-dependent signal transduction pathway. *Embo J*, **15**, 6220-6230.